

# Engineering the tumor microenvironment of colorectal cancer

## Inauguraldissertation

zur  
Erlangung der Würde eines Dr.sc.med.  
vorgelegt der  
Medizinischen Fakultät  
der Universität Basel  
von

Christian Kurt Hirt

Birrhard, Aargau, Schweiz  
Basel, 2014

Originaldokument gespeichert auf dem Dokumentenserver der Universität Basel  
edoc.unibas.ch



Dieses Werk ist lizenziert unter einer Creative Commons Namensnennung-Nicht kommerziell –  
Keine Bearbeitungen 4.0 International Lizenz.



Genehmigt von der Medizinischen Fakultät  
Auf Antrag von

Prof. Dr. Ivan Martin (Fakultätsverantwortlicher)  
Prof. Dr. Giulio Spagnoli (Dissertationsleiter)  
Prof. Dr. Melody Swartz (Koreferent)

Basel den 21.05.2014

Prof. Ch. Beglinger

Dekan Med. Fakultät Basel



for my mother



## Acknowledgements

This thesis would not have been possible without the help and support of lot of people believing in the work which I'm doing and supporting me through the PhD-time in Basel:

Adam Papadimitropoulos, for his motivations and support in all - never tired to discuss about science and always interested in new fields

Giulio Spagnoli and Ivan Martin, which gave me the opportunity to perform this research in a stimulating and challenging environment

Prof. Michael Heberer, for his beliefs in the project and scientific support

Prof. Giandomenica Iezzi, for xenograft experiments and primary samples

Prof. Rachel Rosental, for her helping come true the change from a surgeon to a scientist

Prof. Daniel Speiser, EPFL Lausanne, for being an external mentor and advisor

Prof. Ton Schumacher, NKI Amsterdarm, for offering me the unique opportunity to work in one of the best lab's in the world

Prof. Primo Schär, DBM Basel, for his interests in the project and willing to contribute

Emmanuele Trella, for his cheering up in difficult time

Francesca Amicarella & Eleonora Cremonesi, for their time and motivation to contribute to the projects

Paul Zajac, which, with is outside view of the project and scientific experience, pointed out the relevant issues.

Raoul Droeser, for his insistence and continuous work in science as clinician.

Brynn Kvinlaug for her last minute English corrections and teaching in scientific writing.

Elke Schultz-Thater for her patience in improving Western-Blots.

People from Pathology: Serenella Eppenberger-Castori, Luigi Terracciano, Luigi Tornillo, for their help in stainings, statistics and samples

Atanas Todorov for contributing with his skills in data assesement and analysis

Waldemar Hoffman for his engineering support

My wife, who has always supported me, parents and family, my friends, which gave me power and strength to continue on the scientific way throughout the whole PhD.

## Summary

### *Introduction*

Colorectal Cancer (CRC) belongs to the three most common cancers in both men and women and arises mostly sporadically in elderly people. Environmental factors and long-standing inflammatory bowel diseases have been shown to contribute to its pathogenesis. Since clinical symptoms are unspecific the diagnosis is mostly made at already late stages, when the primary tumor has metastasized to local lymph nodes or distant organs. Surgical resection is the initial treatment of choice followed by a combination with standard chemotherapies. The response rate of adjuvant or palliative treatment is in late stages poor.

Recently, works of Galon and others clearly indicate, that the tumor microenvironment contributes significantly to the clinical prognosis, especially in CRC. Infiltration by cells from the adaptive immune system (e.g. CD8) has been linked to a better survival independently of TNM-stage. Meanwhile, immune-checkpoints like PD-1/PD-L1 have become attractive targets to further activate T-cells in the tumor microenvironment. The roles of several subpopulations of innate immune cells characterized by substantial plasticity have been less well describe . Importantly, features of the CRC microenvironment have also been shown to be different from other tumor entities like melanomas or breast cancer in regard to prognostic relevance of specific cell populations (e.g. Tregs).

The complex tumor microenvironment is not well mirrored by conventional in vitro tumor assays where response to drug or treatment is evaluated on tumor cell lines monolayers. It has been proposed that 3D tumor models could at least to some extent better represent the in-vivo tumor microenvironment. Tissue formation by spheroid-assay or static scaffold assays from established cell lines has been shown to be limited. Primary culture of freshly excised tumor specimens is even more difficult to achieve, with success rates ranging around 30% and poor expansion using organoid 3D cultures.

In this work we aimed therefore not only at the characterization of the CRC-microenvironment in regard to innate and adaptive immunity but also to engineer innovative in vitro models of CRC better reflecting in-vivo tumor response to treatment.

### *Studies/Methods*

During two retrospective studies using Tissue-Microarrays (TMA) with over 1'400 patient samples of CRC annotated with clinic-pathological data we evaluated the prognostic relevance of tumor infiltration by innate, myeloperoxidase (MPO) positive cells) and of the expression of PD-L1 expression in CRC cells. In this regard, we also analyzed several fresh tumor samples by FACS and gene expression. To mimic the complex tumor microenvironment of CRC we then evaluated a 3D perfused bioreactor, previously established for regenerative medicine purposes, to establish a new tumor model. Besides phenotypically and functional studies, drug responses were analyzed and compared to those observed in in-vivo xenografts. Finally, this 3D perfused tumor culture technique was adapted for primary CRC culture.

## **Results**

Using tumor microarray (TMA) technology we found that an infiltration by cells with neutrophil phenotype expressing high MPO positivity was associated with a favorable prognostic effect and correlated with CD8 infiltration. As tumoricidal activity of CD8-T-cells has been described to be influenced by immunological checkpoints engagement we evaluated in another TMA study the expression of PD-L1 on colorectal cancer specimens. PD-L1 expression on CRC correlated with CD8 infiltration but, interestingly, was associated with a good survival. We found a correlation with expression of IFN- $\gamma$  and could see that the CRC infiltrating CD8 were mostly negative for its receptor PD-1.

This intriguing role of the microenvironment composition on the survival of colorectal cancer patients lead us then to start working on an innovative perfused 3D tumor model to better mimic the complexity of cancer tissue in-vivo. By using cancer cell lines we could establish a model, which had phenotypical but as well functional properties similar to xenografted tumors. Most importantly the response to standard treatments, were also similar. The anti-apoptotic genes BCL-2, TRAF-1 and c-FLIP could represent new targets in 5-FU partial responsive CRC. Neoadjuvant treated patients with a partial tumor response had a high expression of BCL-2.

As this perfused tumor model only partially mimics the complex tumor microenvironment, an ultimate goal remains the culture of primary colorectal cancer specimens. By using the perfused u-tube-bioreactor and adaption of protocol using collagen-sandwich we could with a high efficiency keep tumor tissue alive and proliferating.

## **Discussion**

In our studies on CRC microenvironment we could observe that activated neutrophils, somehow unknown and unappreciated players in tumor immunology, contributed significantly to a better survival. As other studies claimed their tumor-promoting features, activation markers like MPO could help to elucidate mechanisms leading to an anti-tumoral phenotype. Compounds stimulating these potent phagocytes to infiltrate intratumoral and activate locally could therefore be of great interest for further treatments.

On the other hand the immune-regulatory checkpoint ligand PD-L1 has been associated with improved survival in CRC in contrast to melanoma or breast-cancer. This could be regarded as marker of an ongoing-immune response because we observed a correlation between CD8 cells and IFN- $\gamma$  gene expression. Additional studies are necessary to evaluate the use of checkpoint inhibitors in CRC.

Engineering the complex tumor microenvironment by a perfused 3D bioreactor able to generate large tumor-tissues in short time could be helpful as tool for further phenotypical and functional screenings. Additionally, we could observe a significant impact of perfusion on survival and proliferation of tumor cells within primary tumor fragments. Further studies will be necessary to elucidate the potential of this technology for drug screenings.



# Contents

|  |            |
|--|------------|
| <b>GENERAL INTRODUCTION</b> .....  | <b>12</b>  |
| A. COLORECTAL CANCER (CLINICS, DIAGNOSIS, TREATMENTS, SURVIVAL) .....  | 12         |
| B. CANCER MICROENVIRONMENT (STROMAL AND IMMUNE CELLS CONTRIBUTION) .....   | 15         |
| C. 3D TUMOR MODELLS (SPHEROIDS, ORGANIDS, 3D STAT, 3D PERFUSED SYSTEMS) .....  | 17         |
| D. IMPACT OF THIS THESIS AND CONTRIBUTIONS .....   | 19         |
| <b>CHAPTER 1</b> .....   | <b>26</b>  |
| HIGH MYELOPEROXIDASE POSITIVE CELL INFILTRATION IN COLORECTAL CANCER IS AN INDEPENDENT FAVORABLE PROGNOSTIC FACTOR ( <i>DROESER&amp;HIRT ET AL. PLOS ONE 2013</i> )  |            |
| <b>CHAPTER 2</b> .....   | <b>36</b>  |
| COLORECTAL CANCER INFILTRATION BY MYELOPEROXIDASE POSITIVE NEUTROPHIL GRANULOCYTES IS ASSOCIATED WITH FAVORABLE PROGNOSIS ( <i>DROESER&amp;HIRT ET AL. ONCOIMMUNOLOGY 2013</i> )                           |            |
| <b>CHAPTER 3</b> .....   | <b>39</b>  |
| ENHANCED PD-L1 EXPRESSION IS A FAVOURABLE PROGNOSTIC MARKER IN MMR-PROFICIENT COLORECTAL CANCER ( <i>DROESER&amp;HIRT ET AL. EUR J CANCER 2013</i> )   |            |
| <b>CHAPTER 4</b> .....   | <b>49</b>  |
| “IN VITRO” 3D MODELS OF TUMOR-IMMUNE SYSTEM INTERACTION ( <i>HIRT ET AL. ADVANCED DRUG DELIVERY SYSTEMS, IN PRESS 2014</i> ) .....   |            |
| <b>CHAPTER 5</b> .....   | <b>59</b>  |
| BIOREACTOR-ENGINEERED CANCER TISSUES MIMIC PHENOTYPES, GENE EXPRESSION PROFILES AND DRUG RESISTANCE PATTERNS OBSERVED IN XENOGRAFTS AND CLINICAL SPECIMENS ( <i>HIRT ET AL. IN SUBMISSION 2014</i> ) ..... |            |
| <b>CHAPTER 6</b> .....   | <b>85</b>  |
| PERFUSION CULTURE OF PRIMARY COLORECTAL CANCER SPECIMENS ( <i>HIRT ET AL. MANUSCRIPT</i> ) .....   |            |
| <b>DISCUSSION &amp; CONCLUSIONS</b> .....  | <b>114</b> |
| A. INNATE IMMUNITY IN THE MICROENVIRONMENT (MPO) .....   | 114        |
| B. ADAPTIVE IMMUNITY IN THE MICROENVIRONMENT (PD-L1) .....   | 115        |
| C. MICROENVIRONMENT ENGINEERING THROUGH PERFUSED TUMOR CULTURE .....   | 117        |
| <b>FUTURE PERSPECTIVES</b> .....   | <b>120</b> |
| <b>CV CHRISTIAN HIRT</b> .....   | <b>126</b> |

## Introduction

### A. Colorectal Cancer

Colorectal cancer (CRC) is the second most frequent cancer among women and the third among men in Switzerland. More than 10% of all cancer in both men and women are CRC and it is still the third leading cause of cancer death. CRC is a cancer of the elderly people with most cases occurring after the age of 70<sup>1</sup>.

The reason for this late appearance lays in the pathogenesis of CRC. It arises as a consequence of accumulation of genetic and epigenetic alterations, the so-called adenoma-carcinoma-sequence. These mutations create a clonal growth advantage that leads to the generation of progressively more malignant cells, which eventually lead to an invasive adenocarcinoma<sup>2</sup>. This process is a highly inefficient process, which takes years to decades until a full invasive carcinoma develops.

According to their molecular phenotype, CRC can be classified in specific subgroups. Whereas 85% of all CRC have chromosomal instability and chromosome amplification respond/or translocation, which lead to tumor aneuploidy, the remaining 15% have high-frequency microsatellite instability phenotypes<sup>3</sup>. Errors occurring during the DNA replication can because of this microsatellite instability not be correct. Several genes, like MLH1, MSH2, MSH6, are involved in the process. The resulting mutations or epigenetic alterations lead to more and more single nucleotide mutations in the repetitive microsatellite nucleotide sequences<sup>4</sup>.

CRC is in most cases sporadic. Traditional risk factors are increasing age, male sex, previous polyps and environmental factors (eg, red meat, high-fat diet, inadequate intake of fibers, obesity, sedentary lifestyle, diabetes mellitus, smoking and high consumption of alcohol)<sup>5</sup>. Additionally, patients suffering since years of ulcerative colitis and Crohn's disease are more prone to develop colorectal cancer. In these patients, the risk of CRC increases with longer duration and greater anatomic extent of colitis, the degree of inflammation, and the presence of primary sclerosing cholangitis. It has been shown that like sporadic CRC, colitis-associated CRC results from sequential episodes of somatic genetic mutation and clonal expansion, although additional factors may be responsible<sup>6</sup>.

Besides sporadically arising CRC, more than a fifth of patients will have a familial background. If two or more first-degree relatives have CRC, the risk is around two- to three-fold higher than in the normal population. The Lynch syndrome, also known as hereditary non-polyposis colorectal cancer, is the most common (3%), followed by familial adenomatous polyposis, which is much less common (<1%). In most cases however, the familial component remains elusive<sup>3,7</sup>.

CRC is mostly diagnosed in late stage after onset of unspecific symptoms or occult bleeding. Some symptoms/signs associated with CRC include hematochezia or melena, abdominal pain, otherwise unexplained iron related anemia, and/or a change in bowel habits. Less common presenting symptoms include abdominal distention, and/or nausea and vomiting, which may be indicators of already late stage tumor resulting in bowel obstruction<sup>8,9</sup>.

With the introduction of a colonoscopy screening there is the possibility of an immediate polypectomy, and adenomas can be directly removed. This approach, as it has been shown, reduces not only the incidence of CRC, but also cancer-related deaths<sup>10</sup>. Yet, few patients take the advantage of screening for CRC, which is

recommended from the age of 50 every 5 years. Another possible screening approach is fecal occult blood test, which screens for occult blood in the stool. Not-bleeding earlier lesions however, cannot be detected and, due to other bleeding sources, sensitivity is low but the test is less invasive and easier to perform than colonoscopy<sup>11</sup>.

Once CRC is detected, mostly following histopathological evaluation of a biopsy, it remains in most cases a “surgical disease”. An estimated 92% of colon cancer patients and 84% of rectal cancer patients undergo surgical resection as the primary modality of treatment; the procedure is most typically performed to be directly curative<sup>12</sup>. Neoadjuvant radiochemotherapy, is mostly performed in rectal cancer with lymph node positivity and in metastatic colorectal cancer to induce a down-staging prior to surgery<sup>13</sup>. Tumor regression is classified according to Dworak Regression Grading but is not included in standard staging<sup>14</sup>.

The most powerful clinical predictors are the pathologic features of the resection specimen. These are pathologic stage and stage-independent prognostic factors such as histologic grade, vascular invasion, perineural invasion, and tumor border features<sup>12</sup>. Pathological classification is traditionally performed according to the American Joint Committee on Cancer TNM Staging (s. Tab.1).

| <b>Primary Tumor (T)</b>  | <b>Regional Lymph Nodes (N)</b>  | <b>Distant Metastasis (M)</b>   |
|---|--|---|
| <b>TX</b> Primary tumor cannot be assessed<br><b>T0</b> No evidence of primary tumor<br><b>Tis</b> Carcinoma in situ: intraepithelial or invasion of lamina propria<br><b>T1</b> Tumor invades submucosa<br><b>T2</b> Tumor invades muscularis propria<br><b>T3</b> Tumor invades through the muscularis propria into pericolorectal tissues<br><b>T4a</b> Tumor penetrates to the surface of the visceralperitoneum<br><b>T4b</b> Tumordirectly invades or is adherent to other organs or structures | <b>NX</b> Regional lymph nodes cannot be assessed<br><b>N0</b> No regional lymph node metastasis<br><b>N1</b> Metastasis in 1–3 regional lymph nodes<br><b>N1a</b> Metastasis in one regional lymph node<br><b>N1b</b> Metastasis in 2–3 regional lymph nodes<br><b>N1c</b> Tumor deposit(s) in the subserosa, mesentery, or nonperitonealized pericolic or perirectal tissues without regional nodal metastasis<br><b>N2</b> Metastasis in 4 or more regional lymph nodes<br><b>N2a</b> Metastasis in 4–6 regional lymph nodes<br><b>N2b</b> Metastasis in 7 or more regional lymph nodes | <b>M0</b> No distant metastasis<br><b>M1</b> Distant metastasis<br><b>M1a</b> Metastasis confined to one organ or site (for example, liver, lung, ovary, nonregional node)<br><b>M1b</b> Metastases in more than one organ/site or the peritoneum |

Tab 1: **Definitions of TNM according to AJCC 7<sup>th</sup> Edition**

Stages are defined by the TNM status. Briefly, the lower Stages 0-2 correspond to tumors of different size (T-stadium) without any lymph node involvement. The intermediate stage 3 patients have metastatic spread to local or distant lymph nodes and the advanced stage 4 patients have distant metastatic lesions in one or more several organs<sup>15</sup>.

Adjuvant Chemotherapy is performed in stage 3-4 CRC. The efficacy has improved substantially over the last 10 years. While infusional 5-fluorouracil (5-FU) results in response rates of <25% and a median overall survival of about 12 months<sup>16</sup>, combination chemotherapy including infusional 5-FU plus irinotecan and

oxaliplatin, can result in a response rate in up to half of all patients<sup>17</sup>. Besides these standard cytotoxic chemotherapies newer biologicals or so called targeted treatment options have in the last year been introduced. They are used either as first- or second-line treatments. Bevacizumab, a humanized monoclonal antibody against vascular endothelial growth factor (VEGF), combined with fluoropyrimidine-based chemotherapy has become the standard first line treatment for metastatic colorectal cancer<sup>18</sup>. Cetuximab, a chimeric IgG1 monoclonal antibody against epidermal growth factor receptor (EGFR), has been shown to be effective as monotherapy and in combination with irinotecan in irinotecan-resistant patients<sup>19</sup>. Cetuximab effectiveness is depending on overexpression of EGFR and KRAS wild-type protein as it has been shown that KRAS mutation is predictive of unresponsiveness and shorter survival following treatment with an EGFR-mAb<sup>20</sup>.

In addition, several targeted agents are being explored in phase I-II clinical trials. In particular, mTOR inhibitors block several key pathways activated in response to growth stimuli and may lead to induction of apoptosis. Furthermore, protein kinase C antagonists target cell signaling cascades leading to tumor growth and promoting cancer cell survival. Other approaches more specifically target the tyrosine kinase Src, which was the first identified proto-oncogene, or mitotic kinesins, responsible for the mitotic spindle formation<sup>21</sup>.

Even though a variety of these agents has shown promising efficacy “in vitro” a number of them are ineffective or even toxic “in vivo” and possibly associated to poor survival as exemplified by KRAS-mutated cancers undergoing cetuximab treatment.

Indeed, preclinical cancer drug research has still the worst success rate of any therapeutic area with only a 5% of candidate compounds passing phase III clinical trials<sup>22,23</sup>. With the establishment of new preclinical cancer models, taking into account the complex tumor microenvironment and the heterogeneity of cancer tissue, discoveries could be facilitated.

The 5-year overall survival rate of patients with CRC in Switzerland<sup>1</sup> is stage independent and ranging around 60%. In advanced disease stage, large T and/or nodal positivity, survival rate drops to 30% and below 10% if the tumor has metastasized to distant sites<sup>24</sup>. As even following advances in screening methods and early diagnosis, 15-20% of CRC-patients present at diagnosis already with synchronous metastasis<sup>25</sup>, new treatment options, which could significantly improve clinical outcome in advanced stages, are needed and new screening tools could be helpful in this context.

## **B. Colorectal cancer microenvironment**

It is now well established that genetic changes of the tumor cell itself are insufficient to account for tumor progression and metastasis and that several epigenetic alteration can profoundly affect several features of cancer cells during their progression towards clinically relevant malignancies<sup>26</sup>. However, over the last decades it became more and more clear that tumor outgrowth is substantially influenced by the tumor microenvironment (TME). Therefore, to successful target cancer cells it is necessary to gain a better understanding of the influence of treatment on tumor microenvironment.

The TME consist of a variety of non-transformed cells (immune, stromal, endothelial etc.) and extracellular matrix (ECM) together with soluble factors and signaling molecules. Their interplay can substantially influence tumor outcome as suggested by studies taking advantage of systems biology approaches to evaluate signatures of tumor subtypes<sup>27,28</sup>. Fibroblasts are the most abundant cell type in connective tissues where they are responsible of secreting extracellular matrix (ECM) components. In the context of cancer they become activated which leads then to characteristically persistent fibrosis of the TME. They are therefore called cancer-associated-fibroblasts (CAFs)<sup>29</sup>. In early stages CAFs repress tumor progression, mainly due to contact inhibition over gap junctions on cancer cells, while in later stages they become tumor promoting<sup>30</sup>.

Immune infiltrate may be different in tumors of different histological origin and in different patients bearing tumors of similar histology. The analysis of the location, density and functional orientation of the different immune cell populations (“immune contexture”) has lead the identification of components that are beneficial or deleterious regarding patient outcome<sup>27</sup>. It has been suggested that the evaluation of the immune contexture has a higher prognostic significance than classical TNM-staging systems<sup>32</sup>. In particular, infiltration by CD8+ cytotoxic T cells and CD45RO+ memory T cells were found to be clearly associated with a longer disease-free survival after surgical resection of the primary tumour and/or overall survival. For other subpopulations, like Treg cells, data are more conflicting and dependent on the tumor type<sup>27</sup>. Regarding innate immune cells work from Bronte et al. indicates that myeloid-derived suppressor (MDSCs), a heterogeneous population of myeloid cells, might play a role in the suppression of host immune response<sup>33</sup>. However, myeloid cells might still have anti-tumor effects as proposed for macrophages (M1 phenotype) and neutrophils (N1 phenotype)<sup>34,35</sup>. Future work will help to identify factors attracting anti-tumoral immune subsets or re-educating pro-tumoral subsets, as there is quite some plasticity. In this context immune modulators have been recently developed and successful implemented in the clinics. Anti-CTLA-4 and anti-PD-1/anti-PD-L1 monoclonal antibodies, exemplify successful approaches, positively influencing immune contexture<sup>36-38</sup>.

Additional cellular players in the TME are endothelial cells, which are responsible for the formation of vascular and lymphatic structures. In tumors, the aggressive growth of the neoplastic cell population and associated overexpression of pro-angiogenic factors leads to the development of disorganized, immature blood vessel networks<sup>39</sup>. This imperfect vasculature architecture leads to the formation of large zones of hypoxic intratumoral areas next to normoxic tumor regions. Hypoxic cells are known to have higher resistance to apoptosis than normoxic<sup>40</sup>. Additionally, the leaky vessels generate elevated interstitial fluid pressure and flow, which

stimulates lymphatic endothelial cells<sup>41</sup>. By VEGF-C release, tumor itself promote lymph angiogenesis, which has been linked to tumor invasion and lymph node metastasis<sup>42,43</sup>.

An additional TME player is the extracellular matrix (ECM), which forms a mechanically stable support for epithelial cells. This allows for the diffusion of oxygen and nutrients between the microvasculature and adjacent tissues and guides freely moving cells<sup>26</sup>. The ECM is composed of a biopolymer fiber network of proteins, proteoglycans and glycosaminoglycans that is heterogenous in composition and structure among different locations<sup>44</sup>. In cancer, this composition is commonly deregulated and becomes disorganized. Tumor stroma is typically stiffer than normal stroma, which might contribute to the pathogenesis<sup>45</sup>. Studies in CRC have shown that increased stiffness of the tumor is associated with a more proliferative and invasive tumor phenotype<sup>46</sup>.

In the context of TME and CRC an additional player has to be introduced: the gut microbiota. Studies on mutant mice that are genetically susceptible to colorectal cancer (CRC) showed, that they develop significantly fewer tumours under germ-free conditions than when gut is colonized by conventional microbiota<sup>47</sup>. Deep-sequencing technology has allowed to explore the microbial composition of both healthy and diseased body sites, and there is now experimental data that proposes intestinal microorganisms be involved in the pathogenesis of CRC<sup>48,49</sup>. Similar to the genetic driver-passenger model a bacterial driver-passenger model has been introduced<sup>50</sup>. Future studies will help to better evaluate the contribution of dysbiosis to the CRC pathogenesis.

This overview of contributors to the TME leads to the conclusion that the physiology of solid tumors at the microenvironmental level is different from that of the normal tissues from which they arise. This could provide unique and selective targets for cancer treatment<sup>51</sup>. Therefore, complex in-vitro tumor models, incorporating specific aspects of the TME, are needed to better elaborate such differences and reveal potential treatment targets.

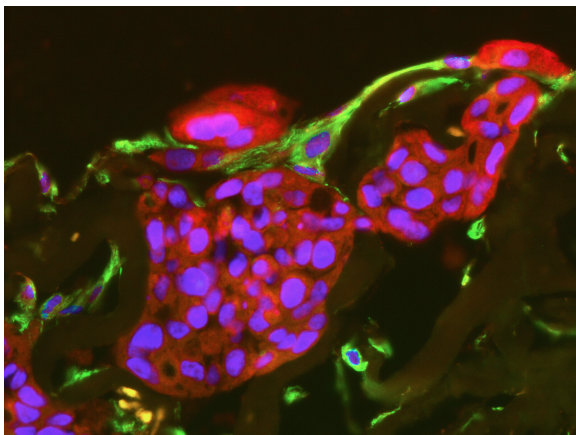


**Fig. 1: Engineering the tumor microenvironment in vitro: Co-culture of mesenchymal stromal cells and colorectal cancer cell lines under 3D perfusion**

Bone marrow derived mesenchymal stromal cells were cultured for 2 days before the addition of the HT29 colorectal cancer line in perfusion culture on a collagen scaffold. Immunofluorescence staining for EPCAM (red), Vimentin (green) and DAPI (blue) shows tumor nodules surrounded by stromal cells.

### ***C. 3D tumor models mimicking the tumor microenvironment***

Since the successful generation of the HeLa cell line by George Gey in 1952, cancer cell lines have been widely used as simple and cheap tool to explore biological mechanisms and characteristics of cancer tissues. Regarding CRC over the last decades 24 cell lines with different phenotype and genetic and epigenetic profile have been generated<sup>52</sup>. However, their long term adaptation to artificial culture conditions in vitro and the absence of any TME factor represent substantial limitations for the comparison to heterogeneous in-vivo tumors.

Nevertheless since the late 1980s until nowadays the US National Cancer Institute 60 human tumour cell line anticancer drug screen (NCI60) is in several academic and industrial laboratories used as in vitro drug screening tool. It consists of a panel of cancer cell lines representing nine distinct tumour entities: leukaemia, colon, lung, CNS, renal, melanoma, ovarian, breast and prostate cancer<sup>53</sup>. For selected, promising compounds, the hollow-fiber assay where cell lines are precultured in hollow-fibers and then implanted in nude mouse either s.c. or i.p was developed, for an additional fast in-vivo screening. Mice are then treated with the test compounds and the efficacy evaluated by MTT-assay after recovery of the constructs<sup>54</sup>. Only for compounds with in vivo activity in at least one-third of tested xenograft models, a correlation with ultimate activity in at least some Phase II trials could be observed<sup>55</sup>.

This approach has recently been questioned and new in-vitro models were proposed, which could better represent 3D structures and TME. This could dramatically improve upon the current low predictive value of preclinical drug screening by providing valuable information about drug efficacy early in the drug development process<sup>56</sup>.

3D tumor models can be classified based on their complexity. Simple models consist of tumor spheroids where tumor microtissue is generated either by culturing tumor cell lines as hanging drops or by preventing the attachment to the plastic dish. Simple 3D models like spheroids can be adapted to high throughput methods and studies have shown the better predictive value of such assays compared to standard 2D in vitro culture<sup>57,58</sup>. Nevertheless the formed spheroids are still heterogeneous in nature and assays must be standardized to improve read-out. Additionally, not all cell lines are suitable for this type of 3D culture, as some do not form spheroids.

For a better understanding of the interaction of tumors with the TME, cells can be cultured on soft or hard substrates to mimic the interaction with the extracellular matrix. An example of soft substrate is represented by hydrogel embedding of tumor cells, e.g. mammosphere assay, where cells are plated in gel-like substrates<sup>59,60</sup>. Another technique is to coat plastic dishes with matrigel, derived from ECM, as used in the organoid cell culture<sup>61</sup>. Matrigel could better represent factors from the ECM. Hard or more complex environment can be engineered using scaffold structure<sup>62-64</sup>. They can be based on natural substrate, e.g. collagen, silk, or synthetic substrates, e.g. polyethylene, polystyrene. The advantage of these scaffolds is that the cells can orientate and migrate similarly to in vivo behavior along collagen fibers. By changing properties of the scaffold (stiffness, porosity, coating) the phenotype of tumor cells is strongly influenced<sup>65</sup>.

As tumor tissue is highly perfused in-vivo and consists of “leaky” vessels, perfused tumor culture in vitro could enhance nutrient availability in the generation of

tissue-like structures and allow the formation of larger constructs. Additionally, flow could better mimic drug administration as compared to simple addition on static 2D or 3D culture where medium is simply overlaid. In most cases micro-bioreactors or micro-chips have been established where a 2D cell layer is overflowed with medium<sup>66–68</sup>. Direct perfusion of constructs has been less well characterized<sup>69</sup>. In the case of colorectal cancer only one publication using a microbio reactor and a polyethylene scaffold is available<sup>70</sup>.

In most of these cultures it is possible to introduce additional cellular partners for co-culture experiments. This tissue engineering approach could lead to improved understanding of biological mechanism governing the interaction of tumoral with non-tumoral cells in the TME. Standard migration assays as the Boyden chamber could be reproduced more precisely using 3D assays where cells may migrate on substrates and integrate into tissue-like structures. It remains more difficult to allow this infiltration in formed constructs as it has been shown for spheroids<sup>71</sup>.

Future studies based on techniques like the organoid cell culture or others, which were established for primary cell culture, would hopefully advance models to patient derived samples. The efficiency of keeping viable tumor cells from epithelial tumors in vitro is very low and in most cases it is simpler to keep non-tumoral cells alive than the tumor itself<sup>72</sup>. Studies have shown that retaining cell–cell contact enhances the viability of spheroids composed of pure primary cancer cells from CRC<sup>73</sup>. By injection in immunodeficient mice, after 1-2 months, patient-derived xenograft models can be generated more successfully, but still in 50% only of all CRC-cases<sup>74,75</sup>. Organoid cell cultures where tumor digest is cultured in vitro on matrigel coated plates can slightly increase this efficiency<sup>61</sup>. For both patient-derived xenografts and organoid cell cultures it is mainly possible to keep the tumoral part of the TME alive<sup>76</sup>. New methods allowing to maintain the initial TME composition could therefore help towards the final goal of developing personalized drug screening procedures.

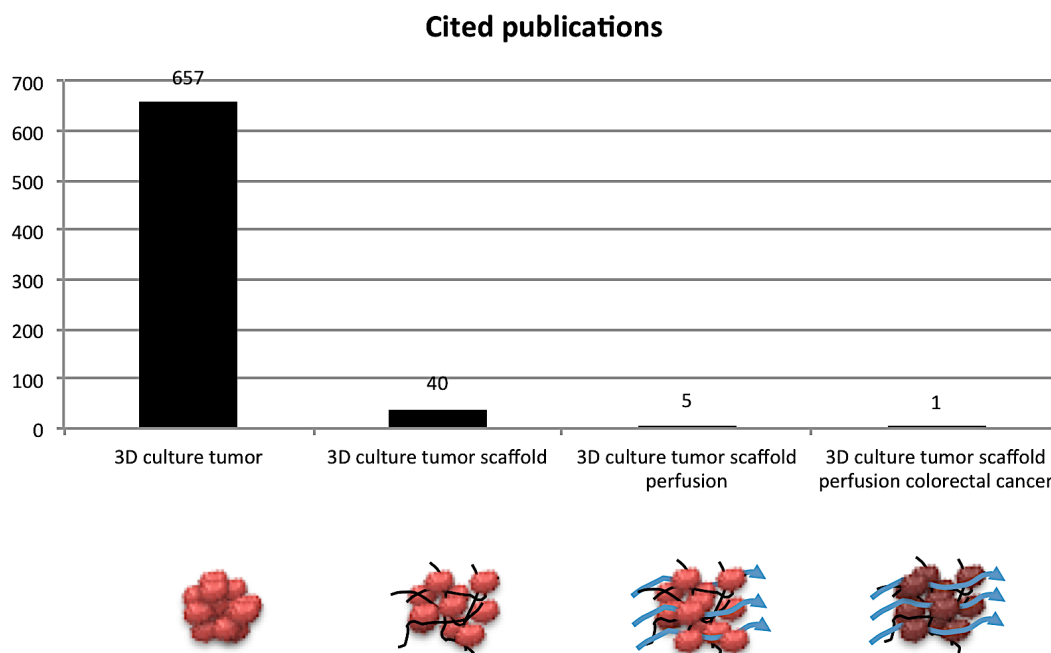


Fig. 2: Tumor models described in literature (NCBI Jan 2013)

## ***D. Impact of this thesis and contributions***

As part of the PhD program biomedical engineering of the University of Basel, this thesis focuses on the components of the tumor microenvironment in colorectal cancer. By studying not only factors contributing to clinical outcome (MPO and PD-L1 study) but as well trying to recapitulate phenotypical, and functional features of CRC tissue in vitro we could obtain additional insights in the field of tumor biology in regard of poorly understood contribution of the TME. Techniques used for perfused 3D cultures for cancer cell line could be successful implemented for patient-derived patient samples and are now under evaluation as new methods to allow the survival of tissue in vitro. Further studies are needed to evaluate its use not only for research purposes but for better prediction of tumor-sensitivity to standard and new drug components as well.

Additionally our findings on the MPO positive cell infiltration, probably neutrophil population, and its impact on survival, lead to a follow up PhD project where factors and mechanisms are carefully evaluated. Neutrophils and their contribution to tumor growth, after long neglect as bystanders, have now been re-addressed in several high impact publications<sup>77,78</sup>.

On the other side our findings for PD-L1 expression in colorectal cancer have led to a new collaboration with the Ton Schumacher lab in Amsterdam, the Netherlands. As we have seen that PD-L1 is associated with good survival, the aim is to sort PD-1 positive and negative T-cell populations and to study the TCR-specificity towards the initial tumors. Transduction of engineered TCRs into autologous peripheral blood lymphocytes cells, this could be implemented as possible approach to effective adoptive cell therapy of solid tumors.

Here I would like to give an overview of the contribution to the main chapters of this thesis to acknowledge the co-authors (major work):

Publication: High myeloperoxidase positive cell infiltration in colorectal cancer is an independent favorable prognostic factor.

*PLoSone 2013*

Droeser RA (RD,DC,DA,MP) & Hirt C (DC,DA,MP), Eppenberger-Castori S (DA), Zlobec I (RD), Amicarella F (DA), Sconocchia G (DC), Lugli A (DA), Tornillo L (DA), Terracciano L (RD, DA), Spagnoli GC (RD, DA, MP).

Review: Colorectal cancer infiltration by myeloperoxidase positive neutrophil granulocytes is associated with favorable prognosis

*Oncoimmunology 2013*

Hirt C (MP & Graphical Abstract), Spagnoli GC (MP), Droeser RA (MP).

Publication: Enhanced PD-L1 expression is a favourable prognostic marker in MMR-proficient colorectal cancer

*Eur J Cancer 2013.*

Droeser RA (RD,DC,DA,MP) & Hirt C (DC,DA,MP), Zlobec I (RD), Eppenberger-Castori S (DA), Muraro MG (DC), Amicarella F (DC), Cremonesi E (DC), Lugli A (DA), Terracciano L (DA), Sconocchia G (RD), Spagnoli GC (RD,DA,MP), Tornillo L (RD,DA,MP).

Review: “In vitro” 3D models of tumor-immune system interaction

*Advanced Drug Delivery Reviews 2014*

Hirt C (MP, Figures), Papadimitropoulos A (MP), Mele V (MP), Muraro MG (MP), Mengus C (Figures), Iezzi G (MP), Terracciano L (MP), Martin I (MP), Spagnoli GC (MP)

Publication: 5-FU treatment of perfused colorectal cancer cell cultures reveals BCL-2 as new potential target to overcome resistance

*Submitted Feb 2014*

Hirt C (RD, DC, DA, MP), Papadimitropoulos A (RD, DA, MP), Evangelos Panapoulos E (DC), Cremonesi E (DC), Mele V (DC), Muraro MG (DC), Eppenberger-Castori S (DA), Terracciano L (DA), Tronillo L (DA), Martin I (RD, DA, MP), Spagnoli GC (RD, DA, MP)

Draft/Patent: Perfusion Culture of primary colorectal cancer specimens.

Hirt C (RD, DC, DA, MP), Papadimitropoulos A (RD, DA, MP), Amicarella F (DC), Cremonesi E (DC), Iezzi G (RD, DA, DC, MP), Martin I (RD, DA, DC, MP), Spagnoli G (RD, DA, DC, MP)

RD=Research Design; DC=Data Collection; DA=Data Analysis; MP=Manuscript

## References Introduction

1. Cancer in Switzerland: 1983 - 2007. at <http://www.bfs.admin.ch/bfs/portal/en/index/themen/14/02/05/dos/01.html>>
2. Grady, W. M. & Carethers, J. M. Genomic and epigenetic instability in colorectal cancer pathogenesis. *Gastroenterology* **135**, 1079–99 (2008).
3. Cunningham, D. *et al.* Colorectal cancer. *Lancet* **375**, 1030–47 (2010).
4. Peltomaki, P. Role of DNA Mismatch Repair Defects in the Pathogenesis of Human Cancer. *J. Clin. Oncol.* **21**, 1174–1179 (2003).
5. CDC - Colorectal Cancer Risk Factors. at [http://www.cdc.gov/cancer/colorectal/basic\\_info/risk\\_factors.htm](http://www.cdc.gov/cancer/colorectal/basic_info/risk_factors.htm)>
6. Triantafillidis, J. K., Nasioulas, G. & Kosmidis, P. A. Colorectal cancer and inflammatory bowel disease: epidemiology, risk factors, mechanisms of carcinogenesis and prevention strategies. *Anticancer Res.* **29**, 2727–37 (2009).
7. Lynch, H. T. & de la Chapelle, A. Hereditary colorectal cancer. *N. Engl. J. Med.* **348**, 919–32 (2003).
8. Clinical presentation, diagnosis, and staging of colorectal cancer. at <http://www.uptodate.com/contents/clinical-presentation-diagnosis-and-staging-of-colorectal-cancer>>
9. Majumdar, S. R., Fletcher, R. H. & Evans, A. T. How does colorectal cancer present? Symptoms, duration, and clues to location. *Am. J. Gastroenterol.* **94**, 3039–45 (1999).
10. Manser, C. N. *et al.* Colonoscopy screening markedly reduces the occurrence of colon carcinomas and carcinoma-related death: a closed cohort study. *Gastrointest. Endosc.* **76**, 110–7 (2012).
11. Burch, J. A. *et al.* Diagnostic accuracy of faecal occult blood tests used in screening for colorectal cancer: a systematic review. *J. Med. Screen.* **14**, 132–7 (2007).
12. Compton, C. C. Colorectal carcinoma: diagnostic, prognostic, and molecular features. *Mod. Pathol.* **16**, 376–88 (2003).
13. Pozzo, C., Barone, C. & Kemeny, N. E. Advances in neoadjuvant therapy for colorectal cancer with liver metastases. *Cancer Treat. Rev.* **34**, 293–301 (2008).
14. Dworak, O., Keilholz, L. & Hoffmann, A. Pathological features of rectal cancer after preoperative radiochemotherapy. *Int. J. Colorectal Dis.* **12**, 19–23 (1997).
15. NCCN Clinical Practice Guidelines in Oncology. at [http://www.nccn.org/professionals/physician\\_gls/f\\_guidelines.asp](http://www.nccn.org/professionals/physician_gls/f_guidelines.asp)>
16. Efficacy of intravenous continuous infusion of fluorouracil compared with bolus administration in advanced colorectal cancer. Meta-analysis Group In Cancer. *J. Clin. Oncol.* **16**, 301–308 (1998).

17. Beppu, T. *et al.* FOLFOX enables high resectability and excellent prognosis for initially unresectable colorectal liver metastases. *Anticancer Res.* **30**, 1015–20 (2010).
18. Hurwitz, H. *et al.* Bevacizumab plus irinotecan, fluorouracil, and leucovorin for metastatic colorectal cancer. *N. Engl. J. Med.* **350**, 2335–42 (2004).
19. Jonker, D. J. *et al.* Cetuximab for the treatment of colorectal cancer. *N. Engl. J. Med.* **357**, 2040–8 (2007).
20. Laurent-Puig, P. *et al.* Analysis of PTEN, BRAF, and EGFR status in determining benefit from cetuximab therapy in wild-type KRAS metastatic colon cancer. *J. Clin. Oncol.* **27**, 5924–30 (2009).
21. El Zouhairi, M., Charabaty, A. & Pishvaian, M. J. Molecularly targeted therapy for metastatic colon cancer: proven treatments and promising new agents. *Gastrointest. Cancer Res.* **4**, 15–21 (2011).
22. Hutchinson, L. & Kirk, R. High drug attrition rates--where are we going wrong? *Nat. Rev. Clin. Oncol.* **8**, 189–90 (2011).
23. Begley, C. G. & Ellis, L. M. Drug development: Raise standards for preclinical cancer research. *Nature* **483**, 531–3 (2012).
24. Edge, S. B. & Compton, C. C. The American Joint Committee on Cancer: the 7th edition of the AJCC cancer staging manual and the future of TNM. *Ann. Surg. Oncol.* **17**, 1471–4 (2010).
25. Adam, R. Colorectal cancer with synchronous liver metastases. *Br. J. Surg.* **94**, 129–31 (2007).
26. Taddei, M. L., Giannoni, E., Comito, G. & Chiarugi, P. Microenvironment and tumor cell plasticity: an easy way out. *Cancer Lett.* **341**, 80–96 (2013).
27. Fridman, W. H., Pagès, F., Sautès-Fridman, C. & Galon, J. The immune contexture in human tumours: impact on clinical outcome. *Nat. Rev. Cancer* **12**, 298–306 (2012).
28. Kreeger, P. K. & Lauffenburger, D. A. Cancer systems biology: a network modeling perspective. *Carcinogenesis* **31**, 2–8 (2010).
29. Cirri, P. & Chiarugi, P. Cancer-associated-fibroblasts and tumour cells: a diabolic liaison driving cancer progression. *Cancer Metastasis Rev.* **31**, 195–208 (2012).
30. Ostman, A. & Augsten, M. Cancer-associated fibroblasts and tumor growth--bystanders turning into key players. *Curr. Opin. Genet. Dev.* **19**, 67–73 (2009).
31. Dvorak, H. F. Tumors: wounds that do not heal . Similarities between tumor stroma generation and wound healing. *N. Engl. J. Med.* **315**, 1650–9 (1986).
32. Galon, J. *et al.* Type, density, and location of immune cells within human colorectal tumors predict clinical outcome. *Science* **313**, 1960–4 (2006).

33. Marigo, I., Dolcetti, L., Serafini, P., Zanovello, P. & Bronte, V. Tumor-induced tolerance and immune suppression by myeloid derived suppressor cells. *Immunol. Rev.* **222**, 162–79 (2008).
34. Fridlender, Z. G. *et al.* Polarization of tumor-associated neutrophil phenotype by TGF-beta: “N1” versus “N2” TAN. *Cancer Cell* **16**, 183–94 (2009).
35. Sica, A. & Mantovani, A. Macrophage plasticity and polarization: in vivo veritas. *J. Clin. Invest.* **122**, 787–95 (2012).
36. Hodi, F. S. *et al.* Improved survival with ipilimumab in patients with metastatic melanoma. *N. Engl. J. Med.* **363**, 711–23 (2010).
37. Brahmer, J. R. *et al.* Safety and activity of anti-PD-L1 antibody in patients with advanced cancer. *N. Engl. J. Med.* **366**, 2455–65 (2012).
38. Topalian, S. L. *et al.* Safety, activity, and immune correlates of anti-PD-1 antibody in cancer. *N. Engl. J. Med.* **366**, 2443–54 (2012).
39. Siemann, D. W. The unique characteristics of tumor vasculature and preclinical evidence for its selective disruption by Tumor-Vascular Disrupting Agents. *Cancer Treat. Rev.* **37**, 63–74 (2011).
40. Wang, J. H., Wu, Q. Di, Bouchier-Hayes, D. & Redmond, H. P. Hypoxia upregulates Bcl-2 expression and suppresses interferon-gamma induced antiangiogenic activity in human tumor derived endothelial cells. *Cancer* **94**, 2745–55 (2002).
41. Shieh, A. C. & Swartz, M. A. Regulation of tumor invasion by interstitial fluid flow. *Phys. Biol.* **8**, 015012 (2011).
42. Issa, A., Le, T. X., Shoushtari, A. N., Shields, J. D. & Swartz, M. A. Vascular endothelial growth factor-C and C-C chemokine receptor 7 in tumor cell-lymphatic cross-talk promote invasive phenotype. *Cancer Res.* **69**, 349–57 (2009).
43. Skobe, M. *et al.* Induction of tumor lymphangiogenesis by VEGF-C promotes breast cancer metastasis. *Nat. Med.* **7**, 192–8 (2001).
44. Shoulders, M. D. & Raines, R. T. Collagen structure and stability. *Annu. Rev. Biochem.* **78**, 929–58 (2009).
45. Lu, P., Weaver, V. M. & Werb, Z. The extracellular matrix: a dynamic niche in cancer progression. *J. Cell Biol.* **196**, 395–406 (2012).
46. Baker, A.-M., Bird, D., Lang, G., Cox, T. R. & Erler, J. T. Lysyl oxidase enzymatic function increases stiffness to drive colorectal cancer progression through FAK. *Oncogene* **32**, 1863–8 (2013).
47. Uronis, J. M. *et al.* Modulation of the intestinal microbiota alters colitis-associated colorectal cancer susceptibility. *PLoS One* **4**, e6026 (2009).
48. Castellarin, M. *et al.* *Fusobacterium nucleatum* infection is prevalent in human colorectal carcinoma. *Genome Res.* **22**, 299–306 (2012).

49. Kostic, A. D. *et al.* Genomic analysis identifies association of Fusobacterium with colorectal carcinoma. *Genome Res.* **22**, 292–8 (2012).
50. Tjalsma, H., Boleij, A., Marchesi, J. R. & Dutilh, B. E. A bacterial driver-passenger model for colorectal cancer: beyond the usual suspects. *Nat. Rev. Microbiol.* **10**, 575–82 (2012).
51. Brown, J. M. & Giaccia, A. J. The Unique Physiology of Solid Tumors: Opportunities (and Problems) for Cancer Therapy. *Cancer Res.* **58**, 1408–1416 (1998).
52. Ahmed, D. *et al.* Epigenetic and genetic features of 24 colon cancer cell lines. *Oncogenesis* **2**, e71 (2013).
53. Shoemaker, R. H. The NCI60 human tumour cell line anticancer drug screen. *Nat. Rev. Cancer* **6**, 813–23 (2006).
54. Suggitt, M. & Bibby, M. C. 50 years of preclinical anticancer drug screening: empirical to target-driven approaches. *Clin. Cancer Res.* **11**, 971–81 (2005).
55. Johnson, J. I. *et al.* Relationships between drug activity in NCI preclinical in vitro and in vivo models and early clinical trials. *Br. J. Cancer* **84**, 1424–1431 (2001).
56. Burdett, E., Kasper, F. K., Mikos, A. G. & Ludwig, J. A. Engineering tumors: a tissue engineering perspective in cancer biology. *Tissue Eng. Part B. Rev.* **16**, 351–9 (2010).
57. Lee, J. M. *et al.* A three-dimensional microenvironment alters protein expression and chemosensitivity of epithelial ovarian cancer cells in vitro. *Lab. Invest.* **93**, 528–42 (2013).
58. Friedrich, J., Seidel, C., Ebner, R. & Kunz-Schughart, L. a. Spheroid-based drug screen: considerations and practical approach. *Nat. Protoc.* **4**, 309–24 (2009).
59. Shaw, F. L. *et al.* A detailed mammosphere assay protocol for the quantification of breast stem cell activity. *J. Mammary Gland Biol. Neoplasia* **17**, 111–7 (2012).
60. Liang, Y. *et al.* A cell-instructive hydrogel to regulate malignancy of 3D tumor spheroids with matrix rigidity. *Biomaterials* **32**, 9308–15 (2011).
61. Sato, T. *et al.* Long-term Expansion of Epithelial Organoids From Human Colon, Adenoma, Adenocarcinoma, and Barrett's Epithelium. *Gastroenterology* **141**, 1762–1772 (2011).
62. Fong, E. L. S. *et al.* Modeling Ewing sarcoma tumors in vitro with 3D scaffolds. *Proc. Natl. Acad. Sci. U. S. A.* **110**, 6500–5 (2013).
63. Chen, L. *et al.* The enhancement of cancer stem cell properties of MCF-7 cells in 3D collagen scaffolds for modeling of cancer and anti-cancer drugs. *Biomaterials* **33**, 1437–44 (2012).
64. Fischbach, C. *et al.* Engineering tumors with 3D scaffolds. *Nat. Methods* **4**, 855–60 (2007).

65. Fischbach, C. *et al.* Cancer cell angiogenic capability is regulated by 3D culture and integrin engagement. *Proc. Natl. Acad. Sci. U. S. A.* **106**, 399–404 (2009).
66. Agastin, S., Giang, U.-B. T., Geng, Y., Delouise, L. A. & King, M. R. Continuously perfused microbubble array for 3D tumor spheroid model. *Biomicrofluidics* **5**, 24110 (2011).
67. Lin, H.-Y. *et al.* Pharmacodynamic modeling of anti-cancer activity of tetraiodothyroacetic acid in a perfused cell culture system. *PLoS Comput. Biol.* **7**, e1001073 (2011).
68. Elliott, N. T. & Yuan, F. A microfluidic system for investigation of extravascular transport and cellular uptake of drugs in tumors. *Biotechnol. Bioeng.* **109**, 1326–35 (2012).
69. Ma, L. *et al.* Towards personalized medicine with a three-dimensional micro-scale perfusion-based two-chamber tissue model system. *Biomaterials* **33**, 4353–61 (2012).
70. Wen, Y., Zhang, X. & Yang, S.-T. Microplate-reader compatible perfusion microbioreactor array for modular tissue culture and cytotoxicity assays. *Biotechnol. Prog.* **26**, 1135–44
71. Feder-Mengus, C. *et al.* Multiple mechanisms underlie defective recognition of melanoma cells cultured in three-dimensional architectures by antigen-specific cytotoxic T lymphocytes. *Br. J. Cancer* **96**, 1072–82 (2007).
72. Masters, J. R. Human cancer cell lines: fact and fantasy. *Nat. Rev. Mol. Cell Biol.* **1**, 233–6 (2000).
73. Kondo, J. *et al.* Retaining cell-cell contact enables preparation and culture of spheroids composed of pure primary cancer cells from colorectal cancer. *Proc. Natl. Acad. Sci. U. S. A.* **108**, 6235–40 (2011).
74. Williams, S. A., Anderson, W. C., Santaguida, M. T. & Dylla, S. J. Patient-derived xenografts, the cancer stem cell paradigm, and cancer pathobiology in the 21st century. *Lab. Invest.* **93**, 970–82 (2013).
75. Jin, K. *et al.* Patient-derived human tumour tissue xenografts in immunodeficient mice: a systematic review. *Clin. Transl. Oncol.* **12**, 473–80 (2010).
76. Mattie, M. *et al.* Molecular characterization of patient-derived human pancreatic tumor xenograft models for preclinical and translational development of cancer therapeutics. *Neoplasia* **15**, 1138–50 (2013).
77. Granot, Z. *et al.* Tumor entrained neutrophils inhibit seeding in the premetastatic lung. *Cancer Cell* **20**, 300–14 (2011).
78. Mishalian, I. *et al.* Neutrophils recruit regulatory T-cells into tumors via secretion of CCL17 - a new mechanism of impaired anti-tumor immunity. *Int. J. Cancer* (2014). doi:10.1002/ijc.28770

# High Myeloperoxidase Positive Cell Infiltration in Colorectal Cancer Is an Independent Favorable Prognostic Factor

Raoul A. Droeser<sup>1,2,\*</sup>, Christian Hirt<sup>1,2,9</sup>, Serenella Eppenberger-Castori<sup>3</sup>, Inti Zlobec<sup>4</sup>, Carsten T. Viehl<sup>1</sup>, Daniel M. Frey<sup>1</sup>, Christian A. Nebiker<sup>1</sup>, Raffaele Rosso<sup>6</sup>, Markus Zuber<sup>7</sup>, Francesca Amicarella<sup>2</sup>, Giandomenica Iezzi<sup>2</sup>, Giuseppe Sconocchia<sup>5</sup>, Michael Heberer<sup>2</sup>, Alessandro Lugli<sup>4</sup>, Luigi Tornillo<sup>3</sup>, Daniel Oertli<sup>1</sup>, Luigi Terracciano<sup>3,9</sup>, Giulio C. Spagnoli<sup>2,9</sup>

**1** Department of Surgery, University Hospital Basel, Switzerland, **2** Institute of Surgical Research and Hospital Management (ICFS) and Department of Biomedicine, University of Basel, Switzerland, **3** Institute of Pathology, University Hospital Basel, Switzerland, **4** Institute for Pathology, University of Bern, Switzerland, **5** Institute of Translational Pharmacology, National Research Council, Rome, Italy, **6** Department of Surgery, Ospedale Regionale di Lugano, Switzerland, **7** Department of Surgery, Cantonal Hospital Olten, Switzerland

## Abstract

**Background:** Colorectal cancer (CRC) infiltration by adaptive immune system cells correlates with favorable prognosis. The role of the innate immune system is still debated. Here we addressed the prognostic impact of CRC infiltration by neutrophil granulocytes (NG).

**Methods:** A TMA including healthy mucosa and clinically annotated CRC specimens (n = 1491) was stained with MPO and CD15 specific antibodies. MPO+ and CD15+ positive immune cells were counted by three independent observers. Phenotypic profiles of CRC infiltrating MPO+ and CD15+ cells were validated by flow cytometry on cell suspensions derived from enzymatically digested surgical specimens. Survival analysis was performed by splitting randomized data in training and validation subsets.

**Results:** MPO+ and CD15+ cell infiltration were significantly correlated ( $p < 0.0001$ ;  $r = 0.76$ ). However, only high density of MPO+ cell infiltration was associated with significantly improved survival in training ( $P = 0.038$ ) and validation ( $P = 0.002$ ) sets. In multivariate analysis including T and N stage, vascular invasion, tumor border configuration and microsatellite instability status, MPO+ cell infiltration proved an independent prognostic marker overall ( $P = 0.004$ ; HR = 0.65; CI:  $\pm 0.15$ ) and in both training ( $P = 0.048$ ) and validation ( $P = 0.036$ ) sets. Flow-cytometry analysis of CRC cell suspensions derived from clinical specimens showed that while MPO+ cells were largely CD15+/CD66b+, sizeable percentages of CD15+ and CD66b+ cells were MPO-.

**Conclusions:** High density MPO+ cell infiltration is a novel independent favorable prognostic factor in CRC.

**Citation:** Droeser RA, Hirt C, Eppenberger-Castori S, Zlobec I, Viehl CT, et al. (2013) High Myeloperoxidase Positive Cell Infiltration in Colorectal Cancer Is an Independent Favorable Prognostic Factor. PLoS ONE 8(5): e64814. doi:10.1371/journal.pone.0064814

**Editor:** Syed A. Aziz, Health Canada, Canada

**Received:** January 18, 2013; **Accepted:** April 17, 2013; **Published:** May 29, 2013

**Copyright:** © 2013 Droeser et al. This is an open-access article distributed under the terms of the Creative Commons Attribution License, which permits unrestricted use, distribution, and reproduction in any medium, provided the original author and source are credited.

**Funding:** Financial support for this study was provided by the Swiss National Science Foundation (SNF) Grants Nr. PP00P3-133699, Nr. 31003A-122235 and Nr. 320030-120320, the Italian Association for Cancer Research (AIRC) IG Grant Nr. 10555, the Rainbow Association for Research in Pediatric Oncology-Hematology/The NANDO PERETTI Foundation, and Lazio Regional Agency for Transplantation and Related Diseases. The funders had no role in study design, data collection and analysis, decision to publish, or preparation of the manuscript.

**Competing Interests:** The authors have declared that no competing interests exist.

\* E-mail: rdroeser@uhbs.ch e-mail

<sup>9</sup> These authors contributed equally to this work.

## Introduction

Outgrowth and progression of human colorectal cancers (CRC) are driven by gene mutations and microsatellite instability tumor inherent characteristics [1,2], and by the interaction of cancer cells with microenvironmental stimuli provided by non-transformed cells [3,4]. In particular, cytokine and chemokine environment and infiltration by immunocompetent cells significantly influence CRC outcome [5–8].

Infiltration by activated CD8+ memory T cells and expression of IFN- $\gamma$  gene within CRC were convincingly shown to be associated with favorable prognosis [5,7]. Furthermore, we and others have shown that FOXP3+ immune cell infiltration independently predicts improved survival in CRC [9,10].

The role of innate immune system cells was not studied in comparable detail and controversial data were reported regarding CRC infiltration by NK cells [11–14] and macrophages [15–17].

Granulocytes have largely been disregarded by tumor immunologists [18]. However, recent studies, mainly performed in

experimental models, suggest that neutrophil granulocytes might prevent metastatic cancer progression [19]. Furthermore, they were suggested to undergo cytokine driven differentiation into N1 and N2 cells endowed with anti- and pro-tumor properties, respectively [20,21]. These findings have led to a resurgent interest in granulocyte infiltration in cancer [22–24].

In previous work, we showed that CRC infiltration by CD33+/HLA-DR–/CD16+ myeloid cells is associated with improved patient survival [13]. Based on these phenotypic features, we hypothesized that CRC could be infiltrated by granulocytes with a favorable prognostic significance.

Myeloperoxidase (MPO) is a lysosomal enzyme produced in high amounts by neutrophilic granulocytes (NG) [25], especially during their early maturation phase. MPO catalyzes the production of hypochlorous acid from hydrogen peroxide and chloride anion and oxidizes tyrosine to tyrosyl radicals. Both hypochlorous acid and tyrosyl radicals are cytotoxic to a variety of microorganisms. Notably, MPO is also involved in the induction of granulocyte apoptosis following activation [26,27].

In a small series of CRC samples (n = 67), it has been shown that MPO+ cell infiltration is significantly higher in CRC than in normal colon mucosa [28]. However, prognostic relevance of CRC infiltration by MPO+ cells has not been addressed so far.

CD15, also known as Lewis X and stage-specific embryonic antigen 1, is a carbohydrate adhesion molecule expressed on mature neutrophils, mediating phagocytosis and chemotaxis [29]. Importantly, CD15 expression has been detected in tumor cells and found to correlate with poor prognosis in head and neck, gastric and lung cancers [30–32]. In CRC, expression of CD15 on tumor cells was shown to occur during progression to metastatic stages [33] and to be associated with high incidence of recurrences and poor survival [34,35]. However, the prognostic value of CRC infiltration by CD15+ immune cells has not been explored.

Here we show for the first time that a subgroup of CRC is characterized by a high infiltration by MPO+ and CD15+ positive cells. Most importantly, high MPO+ cell density in CRC is independently associated with favorable prognosis.

## Materials and Methods

### Ethics Statement

Written consent has been given from the patients for their information to be stored in the hospital database and used for research. The use of this clinically annotated TMA for research was approved by the corresponding Ethics Committee of the University Hospital of Basel (Ethikkommission beider Basel) and the ex vivo analyses were approved by the Institutional Review Board (63/07). For freshly excised clinical specimens included in this study written consent has been given from the patients undergoing surgical treatment at Basel University Hospital.

### Tissue Microarray Construction

The TMA used in this work was constructed by using 1420 non-consecutive, primary CRCs, as previously described [36]. Briefly, formalin-fixed, paraffin-embedded CRC tissue blocks were obtained. Tissue cylinders with a diameter of 0.6 mm were punched from morphologically representative areas of each donor block and brought into one recipient paraffin block (30×25 mm), using a semiautomated tissue arrayer. Each punch was made from the center of the tumor so that each TMA spot consisted of at least a 50% of tumor cells. One core per case was used.

## Clinicopathological Features

Clinicopathological data for the 1420 CRC patients included in the TMA were collected retrospectively in a non-stratified and non-matched manner. Annotation included patient age, tumor diameter, location, pT/pN stage, grade, histologic subtype, vascular invasion, border configuration, presence of peritumoral lymphocytic inflammation at the invasive tumor front and disease-specific survival (table 1). Tumor border configuration and peritumoral lymphocytic inflammation were evaluated according to Jass using the original H&E slides of the resection specimens corresponding to each tissue microarray punch [37]. The number of lymph nodes evaluated ranged between 1 and 61 with mean and median of 12 and 11, respectively. MMR status was evaluated by IHC according to MLH1, MSH2 and MSH6 expression [38]. Based on this analysis, the TMA included 1031 MMR-proficient tumors and 194 MMR-deficient tumors.

Overall survival was defined as primary endpoint. Follow-up data were available for 1379 patients with mean/median and IQR event-free follow-up time of 67.7/68 and 45–97 months.

## Immunohistochemistry

Standard indirect immunoperoxidase procedures were used for immunohistochemistry (IHC; ABC-Elite, Vector Laboratories, Burlingame, CA). Briefly, slides were dewaxed and rehydrated in distilled water. Endogenous peroxidase activity was blocked using 0.5% H<sub>2</sub>O<sub>2</sub>. Sections were incubated with 10% normal goat serum (DakoCytomation, Carpinteria, CA) for 20 min and incubated with primary antibody at room temperature. Primary antibodies used were specific for MPO (clone 59A5 Novocastra, Newcastle, UK), CD15 (clone Carb-1, Leica Biosystems, Nussloch, Germany), CD16 (clone 2H7, Novocastra), CD68 (clone PG-M1, Dako, Glostrup, Denmark), FOXP3 (clone 236A/E7, Abcam, Cambridge, UK) and CD8 (clone C8/144B, DakoCytomation, Switzerland). Subsequently, sections were incubated with peroxidase-labelled secondary antibody (DakoCytomation) for 30 min at room temperature. For visualization of the antigen, sections were immersed in 3-amino-9-ethylcarbazole plus substrate-chromogen (DakoCytomation) for 30 min, and counterstained with Gill's hematoxylin.

## Evaluation of Immunohistochemistry

MPO+ and CD15+ tumor infiltrating cells were counted for each punch (approximately one high power [20x] field) by a trained research fellow [R.D.]. Data were independently validated by two additional investigators [L.To. and C.H.] and a high Spearman correlation coefficient (=0.82) and a highly significant (p<0.0001) correlation between measurements was observed. Evaluation of MLH1, MSH2, MSH6, CD16, CD68, CD8 and FOXP3 specific stainings in the CRC TMA under investigation was published previously [9,13,39].

## Flow Cytometry Analyses

Following Institutional Review Board approval (63/07), tissues from surgically removed CRC and adjacent normal mucosa were minced, centrifuged, and resuspended in RPMI 1640 medium supplemented with 5% foetal calf serum, 2 mg/ml collagenase IV, 0.1 mg/ml hyaluronidase V, and 0.2 mg/ml DNase I (Sigma Aldrich, Basel, Switzerland). Following a 1 hour digestion, cell suspensions were filtered and centrifuged. For phenotypic analysis of surface markers, cells were stained with mAbs for 15 minutes on ice in PBS, washed once with PBS 0.5% FCS, 0.5 M EDTA buffer and fixed in lysis buffer from BD Bioscience (1:10). Samples were then permeabilized in BD fixation/permeabilization buffer. For

**Table 1.** Characteristics of CRC patient cohort (n = 1420)\*.

| Characteristics                         | Number of cases or mean | Percentage or range |
|---|-------------------------|---------------------|
| <b>Age, years</b>                       | 71                      | (30–96)             |
| <b>Tumor size (mm)</b>                  | 75                      | (4–170)             |
| <b>Gender</b>                           |                         |                     |
| Female (%)                              | 741                     | (52.2)              |
| Male (%)                                | 673                     | (47.4)              |
| <b>Anatomic site of the tumor</b>       |                         |                     |
| Left-sided (%)                          | 912                     | (64.2)              |
| Right-sided (%)                         | 488                     | (34.4)              |
| <b>T stage</b>                          |                         |                     |
| T1 (%)                                  | 62                      | (4.4)               |
| T2 (%)                                  | 203                     | (14.3)              |
| T3 (%)                                  | 899                     | (63.3)              |
| T4 (%)                                  | 223                     | (15.7)              |
| <b>N stage</b>                          |                         |                     |
| N0 (%)                                  | 711                     | (50.1)              |
| N1 (%)                                  | 358                     | (25.2)              |
| N2 (%)                                  | 294                     | (20.7)              |
| <b>Tumor grade</b>                      |                         |                     |
| G1 (%)                                  | 31                      | (2.2)               |
| G2 (%)                                  | 1177                    | (82.9)              |
| G3 (%)                                  | 177                     | (12.5)              |
| <b>UICC</b>                             |                         |                     |
| Stage I (pN0 pT1 or 2) (%)              | 185                     | (13.6)              |
| Stage IIA (pN0 pT3)+IIB-C (pN0 pT4) (%) | 445+61                  | (37.2)              |
| Stage III (pN>0) (%)                    | 581                     | (42.7)              |
| Stage IV metastasis (%)                 | 88                      | (6.5)               |
| <b>Tumor border configuration</b>       |                         |                     |
| Infiltrative (%)                        | 871                     | (61.3)              |
| Pushing (%)                             | 513                     | (36.1)              |
| <b>Vascular invasion</b>                |                         |                     |
| No (%)                                  | 1002                    | (70.6)              |
| Yes (%)                                 | 383                     | (27)                |
| <b>Microsatellite Stability</b>         |                         |                     |
| Proficient (%)                          | 1031                    | (72.6)              |
| Deficient (%)                           | 194                     | (13.7)              |
| Rectal cancers (%)                      | 575                     | (40.5)              |
| <b>Overall survival time (months)</b>   | 67.7                    | (0–152)             |
| <b>5-years survival % (95%CI)</b>       | 56.4                    | (54–59)             |

\*percentage may not add to 100% due to missing values of some variables; age and tumor size were evaluated using the Kruskal-Wallis test. Gender, anatomical site, T stage, N stage, grade, vascular invasion, and tumor border configuration were analyzed using the  $\chi^2$  test. Survival analysis was performed using the Kaplan-Meier method.

doi:10.1371/journal.pone.0064814.t001

intracellular staining, an anti-MPO reagent or an isotype matched negative control antibody were added for a 15 min incubation at room temperature. After a PBS wash, cells were suspended in wash buffer and analyzed by flow cytometry using a 2-laser BD FACSCalibur (Becton Dickinson, San Jose, CA). Results were analyzed by Cell Quest (Becton Dickinson, San Jose, CA) and Flow Jo (Tree Star, Ashland, OR) softwares.

### Statistical Analysis

Cut-off scores used to classify CRC with low or high MPO+ or CD15+ infiltration were obtained by regression tree analysis, evaluating sensitivity and false positive rate for the discrimination of survivors and non-survivors, on all tumor samples [40]. Specific scores were set at 60 cells/TMA-punch for MPO+ and at 46 cells/TMA-punch for CD15+ infiltration. Chi-Square or Fisher's Exact tests were used to determine the association of MPO+ and CD15+

infiltration and clinicopathological features. Univariate survival analysis was carried out by the Kaplan-Meier method and log rank test. The assumption of proportional hazards was verified for both markers by analyzing the correlation of Schoenfeld residuals and the ranks of individual failure times. Any missing clinicopathological information was assumed to be missing at random. Subsequently, MPO+ and CD15+ cell infiltration data were entered into multivariate Cox regression analysis and hazard ratios (HR) and 95% confidence intervals (CI) were used to determine associations with survival time. The multivariate Cox regression analysis was performed with 975 cases since missing values were excluded from the model.

Spearman's rank correlation was used to analyze the correlation between MPO+, CD15+, CD16+, CD68+, CD8+ and FOXP3+ cell infiltration. Statistical analyses were performed using R i386 Version 2.15.2 (<http://www.R-project.org>). Data reporting was performed according to the REMARK criteria [41].

## Results

### CRC Infiltration by MPO+ and CD15+ Cells: Detection and Association with Clinicopathological Features

MPO+ and CD15+ cells could be successfully identified in the TMA under investigation by specific mAbs. Figure 1A–D shows

representative stainings of CRC with low and high MPO+ or CD15+ cell infiltration.

Out of 1420 CRC individual specimens, MPO expression could be evaluated in 1225 samples including 1031 MMR-proficient and 194 MMR-deficient CRC. CD15 expression was evaluable in 1191 CRC specimens, including 817 MMR proficient and 191 MMR deficient samples. Numbers of samples evaluated for each feature are indicated in absolute numbers and percentages in table 2. Dropouts were due to loss of punches during TMA staining preparation or missing information, and usually accounted for <15% of data (tables 1–2).

Normal colonic mucosa was indeed infiltrated by MPO+ and CD15+ cells (mean: 6.4, median: 2, range 0–59 cells/punch for MPO (n = 48) and mean: 4.3, median: 1, range 0–35 cells/punch for CD15 (n = 47), respectively). However, a significantly higher ( $P < 0.001$ ) infiltration by MPO+ and CD15+ cells was detectable in CRC samples (mean: 26.7, median: 23, range 0–150 cells/punch for MPO (n = 1225) and mean: 16.4, median: 7, range 0–125 cells/punch for CD15 (n = 1191), respectively; figure 1E–F).

MPO+ and CD15+ infiltration, as evaluated by absolute cell numbers, was significantly higher in MMR deficient than in MMR proficient CRC (median: 30 cells/punch in deficient vs. 21 cells/punch in proficient CRC  $P = 0.007$  and 9 cells/punch in deficient

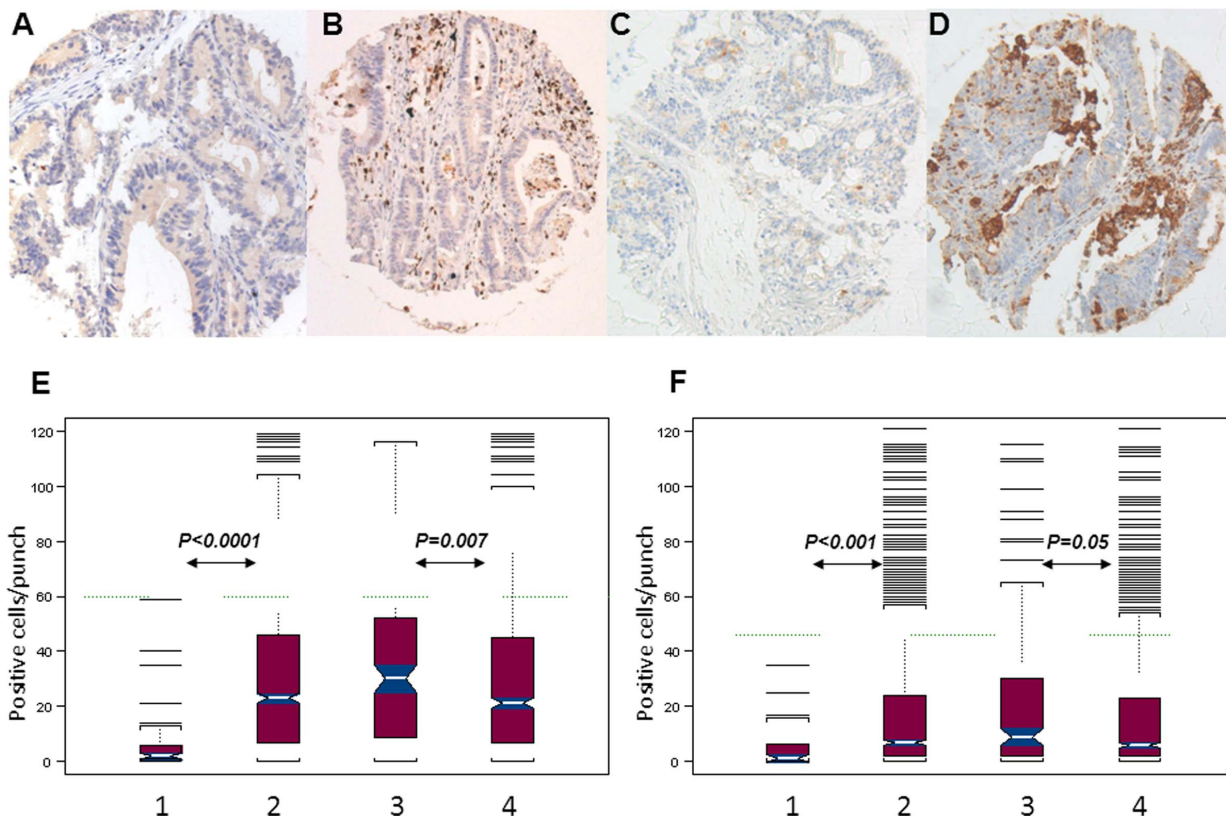


**Figure 1. MPO and CD15 specific staining in CRC.** CRC samples were stained with MPO and CD15 specific monoclonal antibodies (clone 59A5, Novocastra and clone Carb-1, Leica, respectively). Tumor punches are representative of low (panels A and C) and high (panels B and D) density of CRC infiltrating MPO+ (panels A–B) and CD15+ (panels C–D) cells, respectively. Magnification: 20x. Panel E reports the distribution of MPO+ cells in normal mucosa (E1), total CRC (E2), MMR-deficient CRC (E3) and MMR-proficient CRC (E4). The green line indicates the cut-off of 60 cells/punch as defined by regression tree analysis. Panel F reports the distribution of CD15+ cells in normal mucosa (F1), total CRC (F2), MMR-deficient CRC (F3) and MMR-proficient CRC (F4). The green line indicates the cut-off of 46 cells/punch as defined by regression tree analysis.  
doi:10.1371/journal.pone.0064814.g001

**Table 2.** Association of MPO+ and CD15+ low and high immune cell density with clinicopathological features in CRC.

|                                 |              | MPO–     |           | MPO+    |             | p-value       | CD15 –   |             | CD15+   |             | p-value       |
|---------------------------------|--------------|----------|-----------|---------|-------------|---------------|----------|-------------|---------|-------------|---------------|
|                                 |              | N = 1047 | (85.4%)   | N = 178 | (14.5%)     |               | N = 1062 | (89.2%)     | N = 129 | (10.8%)     |               |
| <b>Age</b>                      | years        | 71       | (30–96)   | 73      | (37–96)     | <b>0.04</b>   | 71       | (30–96)     | 71      | (38–96)     | 0.45          |
| <b>Tumor diameter</b>           | mm           | 49       | (8–120)   | 45      | (4–170)     | 0.84          | 45       | (4–160)     | 45      | (8–170)     | 0.99          |
| <b>Gender</b>                   | Female       | 546      | (52.1)    | 90      | (50.6)      |               | 558      | (52)        | 70      | (54.3)      | 0.64          |
|                                 | Male         | 501      | (47.9)    | 88      | (49.4)      | 0.75          | 515      | (48)        | 59      | (45.7)      |               |
| <b>Tumor location</b>           | Left-sided   | 674      | (64.4)    | 117     | (65.7)      | 0.86          | 677      | (63.1)      | 95      | (73.6)      | <b>0.018</b>  |
|                                 | Right-sided  | 361      | (34.5)    | 60      | (33.7)      |               | 385      | (35.9)      | 32      | (24.8)      |               |
| <b>Histologic subtype</b>       | Mucinous     | 86       | (8.2)     | 16      | (9)         | 0.66          | 97       | (9)         | 7       | (5.4)       | 0.19          |
|                                 | Non-mucinous | 955      | (91.2)    | 158     | (88.8)      |               | 965      | (89.9)      | 122     | (94.6)      |               |
| <b>pT stage</b>                 | pT1–2        | 182      | (17.4)    | 48      | (27)        | <b>0.007</b>  | 190      | (17.7)      | 41      | (31.8)      | <b>0.0004</b> |
|                                 | pT3–4        | 833      | (79.6)    | 129     | (72.5)      |               | 857      | (79.9)      | 87      | (67.4)      |               |
| <b>pN stage</b>                 | pN0          | 527      | (50.3)    | 101     | (56.7)      | 0.16          | 536      | (50)        | 72      | (55.8)      | 0.35          |
|                                 | pN1–2        | 479      | (45.7)    | 72      | (40.4)      |               | 494      | (46)        | 55      | (42.6)      |               |
| <b>Tumor grade</b>              | G1–2         | 894      | (85.4)    | 146     | (82)        | 0.224         | 907      | (84.5)      | 110     | (85.3)      | 0.68          |
|                                 | G3           | 129      | (12.3)    | 28      | (15.7)      |               | 138      | (12.9)      | 18      | (14)        |               |
| <b>Vascular invasion</b>        | Absent       | 740      | (70.7)    | 133     | (74.7)      | 0.27          | 754      | (70.3)      | 102     | (79.1)      | 0.07          |
|                                 | Present      | 283      | (27)      | 41      | (23)        |               | 291      | (27.1)      | 26      | (20.2)      |               |
| <b>Tumor border</b>             | Pushing      | 385      | (36.8)    | 75      | (42.1)      | 0.178         | 404      | (37.7)      | 45      | (34.9)      | 0.44          |
|                                 | Infiltrating | 637      | (60.8)    | 99      | (55.6)      |               | 640      | (59.6)      | 83      | (64.3)      |               |
| <b>PTL inflammation</b>         | Absent       | 819      | (78.2)    | 132     | (74.2)      | 0.224         | 835      | (77.8)      | 97      | (75.2)      | 0.3           |
|                                 | Present      | 205      | (19.6)    | 42      | (23.6)      |               | 211      | (19.7)      | 31      | (24)        |               |
| <b>Local recurrence</b>         | Absent       | 212      | (20.2)    | 54      | (30.3)      | <b>0.031</b>  | 241      | (22.5)      | 26      | (20.2)      | <b>0.03</b>   |
|                                 | Present      | 162      | (15.5)    | 23      | (12.9)      |               | 180      | (16.8)      | 8       | (6.2)       |               |
| <b>Distant metastasis</b>       | Absent       | 304      | (29)      | 69      | (38.8)      | 0.108         | 343      | (32)        | 32      | (24.8)      | 0.08          |
|                                 | Present      | 75       | (7.2)     | 9       | (5.1)       |               | 84       | (7.8)       | 2       | (1.6)       |               |
| <b>Microsatellite stability</b> | Deficient    | 159      | (15.2)    | 35      | (19.7)      | 0.161         | 167      | (15.6)      | 24      | (18.6)      | 0.45          |
|                                 | Proficient   | 888      | (86.1)    | 143     | (13.9)      |               | 729      | (67.9)      | 88      | (68.2)      |               |
| <b>5-year survival rate</b>     | (95%CI)      | 55.6     | (52.4–59) | 68.5    | (61.3–76.5) | <b>0.0009</b> | 56.8     | (53.6–60.2) | 63.6    | (55.1–73.4) | <b>0.033</b>  |

\*percentage may not add to 100% due to missing values of same variables; variables are indicated as absolute numbers, %, median or range; age and tumor size were evaluated using the Kruskal-Wallis test. Gender, anatomical site, T stage, N stage, grade, vascular invasion, and tumor border configuration were analyzed using the  $\chi^2$  test. Survival analysis was performed using the Kaplan-Meier method.  
doi:10.1371/journal.pone.0064814.t002

vs 6 cells/punch in proficient CRC  $P=0.05$ , for MPO and CD15 respectively; figures 2E–F).

Regression tree analysis defined cut-off scores for MPO+ and CD15+ CRC infiltrating cells detected in individual punch biopsies ( $n=60$  and  $n=46$ , respectively) were used to assess clinicopathological correlations.

Univariate Cox regression analysis revealed that high density MPO+ cell infiltration ( $\geq 60$  cells/punch), detectable in 14.5% of tumors, was significantly associated with older age of patients ( $P=0.04$ ). Most importantly, it was significantly associated with early (pT1–2) tumor stage ( $P=0.007$ ), absence of local recurrence ( $P=0.031$ ) and higher 5-year survival rate ( $P=0.0009$ ) (table 2).

High density of CD15+ infiltrating cells ( $\geq 46$  cells/punch), detectable in 10.8% of tumors, was significantly associated with left sided location ( $P=0.018$ ), early (pT1–2) stage ( $P=0.0004$ ), absence of local recurrence ( $P=0.03$ ) and higher 5-year survival rate ( $P=0.033$ ) (table 2).

### Correlation between MPO+, CD15+, CD16+ and CD68+ Tumor-infiltrating Myeloid Cells

To explore relationships between tumor infiltration by cells expressing MPO and other immune markers (CD15, CD16, CD68, CD8, FOXP3) expressed by immunocompetent cells infiltrating CRC, data from additional immune-histochemical stainings of the same TMA from previous studies were used [9,13,39]. The statistically strongest correlation was detectable between MPO+ and CD15+ cell infiltration ( $r=0.75$ ,  $P<0.0001$ ), whereas correlations of lesser significance were detectable with CD16+ ( $r=0.32$ ), CD68+ ( $r=0.35$ ), CD8+ ( $r=0.13$ ) and FOXP3+ ( $r=0.21$ ) cell infiltration.

### Ex vivo Characterization of MPO+ cells from Freshly Removed CRC

To assess in detail phenotypic characteristics of tissue infiltrating MPO+ cells, freshly excised CRC ( $n=8$ ) were enzymatically digested, and single cell suspensions were analyzed by flow cytometry. Examples of this phenotypic analysis are reported in figure 2a.

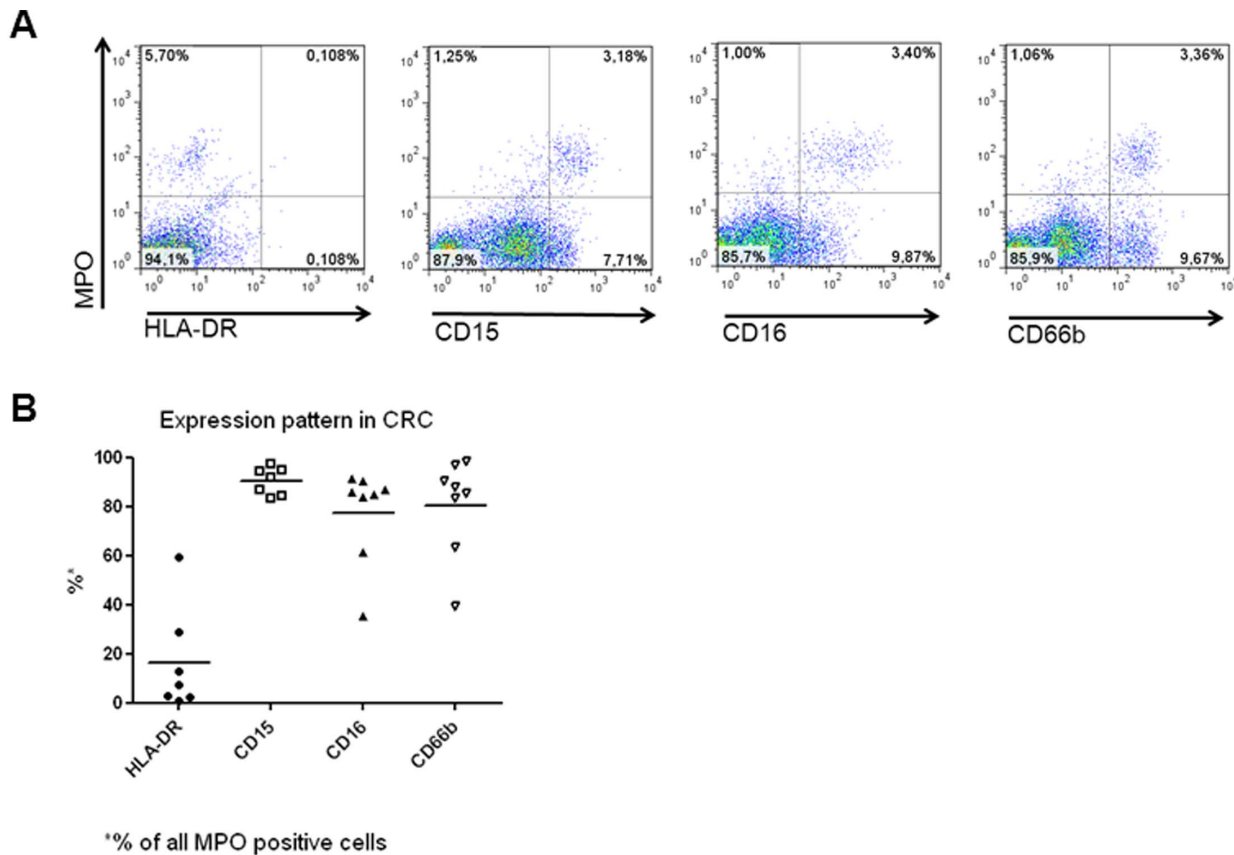


**Figure 2. Phenotypic characterization of CRC infiltrating MPO+ cells.** CRC surgical specimens were enzymatically digested and immediately stained with fluorochrome labeled mAbs recognizing MPO, HLA-DR, CD66b, CD15 and CD16, as indicated in “materials and methods”. Panel A reports one representative staining, whereas panel B summarizes results from freshly excised specimens (n=8) regarding the expression of the indicated markers in CRC infiltrating MPO+ cells.  
doi:10.1371/journal.pone.0064814.g002

The large majority of CRC infiltrating, MPO+ cells were CD15+ (90.3%±5.6%), CD16+, (77.6±19.4%), and CD66b+ (80.6±19.9%; figure 2b). Interestingly, MPO+ cells detectable in autologous normal mucosa displayed a similar (P>0.05) marker expression pattern (data not shown). Notably however, sizeable percentages of MPO-/CD66b+ cells (47.3±35.7%) and, more expectedly, of MPO-/CD15+ cells (78.0±17.7%) of possibly cancerous nature were also detectable in CRC derived cell suspensions.

### Prognostic Significance of MPO+ and CD15+ Cell Infiltration in the CRC Microenvironment

Median survival time was 50 and 46 months for patients with high or low MPO+ cell density, respectively. High MPO+ cell infiltration was significantly (P=0.0003) associated with better prognosis (0.59 HR, 95%CI: 0.45–0.74), as compared to tumors with low MPO+ cell infiltration in univariate Cox regression analysis. Upon splitting of the cohort in a test and a validation set, high score MPO+ cell infiltration was still associated with significantly improved survival (P=0.038 and P=0.002, respectively; figure 3A–B). Several randomizations of the overall cohort were tried and all results were found to be comparable.

In univariate analysis survival was also increased in case of high score CD15+ cell infiltration (P=0.051, figure 3C). A combination

analysis however, showed that MPO is the dominant marker associated with improved prognosis, without relevant additive benefit provided by CD15 positivity (figure 3D).

Most importantly, in multivariate analysis, high score MPO+, but not CD15+, cell infiltration was independently associated with favorable prognosis after adjusting for several known prognostic factors such as age, sex, T stage, N stage, tumor grade, vascular invasion, tumor border configuration and microsatellite stability (P=0.004; table 3). Also in the two stratified collectives the effect of MPO+ cell infiltration on survival of patients with CRC remained significant (P=0.048 and P=0.036 in the testing and validation set, respectively).

### Discussion

To the best of our knowledge, this is the first study identifying MPO+ neutrophil granulocyte tumor infiltration as an independent favorable prognostic factor in CRC.

Myeloid cell infiltration is known to promote tumor growth and to be associated with poor prognosis in a variety of human cancers [42]. In particular, tumor associated macrophages have been indicated as obligate partners for tumor progression and metastasis formation [43]. Granulocyte infiltration has also been found to be associated with poor prognosis in different tumors including lung cancers and renal and hepatocellular carcinoma [44–47]. In this

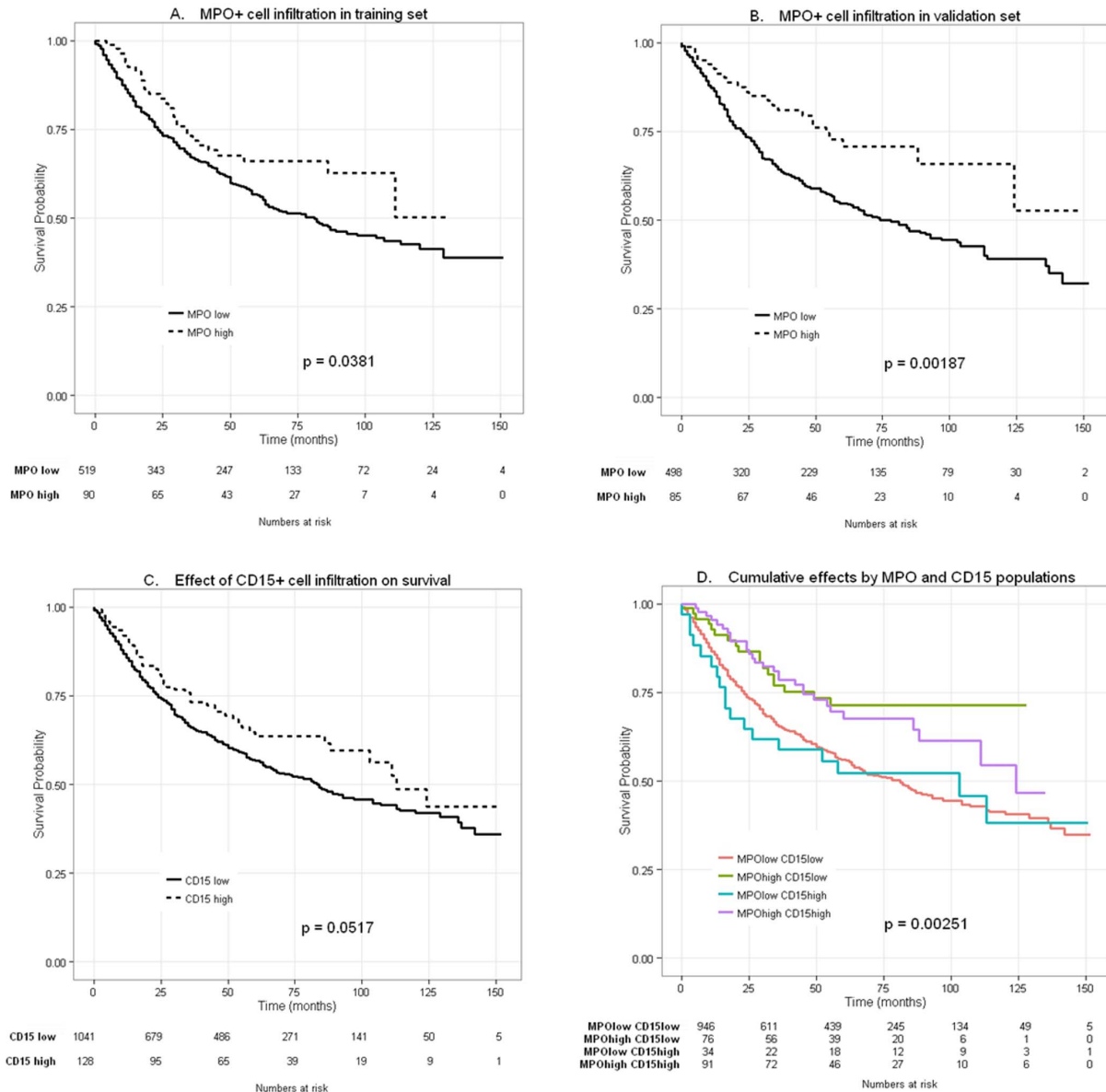


**Figure 3. Effects of MPO+ and CD15+ tumor infiltration on overall survival in patients with CRC.** Kaplan-Meier overall survival curves were designed according to MPO+ and CD15+ tumor infiltration in patients bearing CRC. In panels A–C, dotted lines refer to high density and black lines to low density infiltration according to cut-off values established by regression tree analysis (60 cells/punch for MPO+ and 46 cells/punch for CD15+ cell infiltration). Panels A and B report the effects of high MPO+ cell infiltration, as detected in the training ( $n = 609$ ; 255 deaths observed in 519 patients with low CRC infiltration by MPO+ cells and 28 deaths observed in 90 patients with tumors with high MPO+ cell infiltration,  $P = 0.038$ ) and in the validation set ( $n = 583$ ; 234 deaths observed in 498 patients with low CRC infiltration by MPO+ cells and 23 deaths observed in 85 patients with tumors with high MPO+ cell infiltration,  $P = 0.002$ ). Panel C reports the effect of high CD15+ CRC infiltration in the whole group of patients under investigation ( $n = 1169$ ; 458 deaths observed in 1041 patients with low CRC infiltration by CD15+ cells and 47 deaths observed in 128 patients with tumors with high CD15+ cell infiltration,  $P = 0.051$ ). In panel D cumulative effects of tumor infiltration by MPO+ and CD15+ cells were explored. Rosa line (430/946) refers to tumors with low MPO+/CD15+ cell infiltration. Light blue line (18/34) refers to tumors with low MPO+ and high CD15+ cell infiltration. Lila line (29/91) refers to tumors with high MPO+/CD15+ cell infiltration and green line (18/76) refers to CRC with high MPO+ and low CD15+ cell infiltration ( $n = 1147$ ; 430 deaths observed in 946 patients with low CRC infiltration by MPO+ and CD15+ cells; 18 deaths observed in 34 patients with tumors with high CD15+ and low MPO+ cell infiltration; 29 deaths observed in 91 patients with high CRC infiltration by MPO+ and CD15+ cells; 18 deaths observed in 76 patients with tumors with high MPO+ and low CD15+ cell infiltration,  $P = 0.002$ ). doi:10.1371/journal.pone.0064814.g003

context, CRC might represent an interesting exception [48,49]. Indeed, controversial data have been reported on the prognostic significance of macrophage infiltration in CRC [50–54].

Neutrophil infiltration has been found to be increased in the transition from normal to dysplastic and cancerous mucosa [55].

**Table 3.** Multivariate Hazard Cox regression survival analysis.

|  | HR (95% CI)             | P-Values           |
|--|-------------------------|--------------------|
| <b>MPO (low vs high)</b>                                   | <b>0.65</b> (0.5–0.8)   | <b>0.004</b>       |
| <b>Age (continuous)</b>                                    | <b>1.03</b> (1.02–1.03) | <b>&lt;0.0001</b>  |
| <b>Gender (men vs women)</b>                               | <b>1.21</b> (1.16–1.26) | <b>&lt;0.0001</b>  |
| <b>pT stage (1,2,3,4)</b>                                  | <b>1.79</b> (1.71–1.87) | <b>&lt;0.00001</b> |
| <b>pN stage (0,1,2)</b>                                    | <b>1.93</b> (1.87–1.99) | <b>&lt;0.0001</b>  |
| <b>Tumor Grade (1,2,3)</b>                                 | <b>1.23</b> (1.10–1.36) | <b>0.11</b>        |
| <b>Vascular invasion (0,1)*</b>                            | <b>1.43</b> (1.33–1.53) | <b>0.0006</b>      |
| <b>Tumor border configuration (0,1)**</b>                  | <b>1.52</b> (1.41–1.63) | <b>0.0003</b>      |
| <b>Microsatellite stability (deficient vs. proficient)</b> | <b>1.70</b> (1.56–1.84) | <b>0.0002</b>      |

Multivariate analyses showing Hazard Ratios and p-value for all CRC (n=975, due to missing values, see “materials and methods”) conferred by high MPO density, age, sex, tumor size, nodal status, tumor grade, vascular invasion, tumor border configuration and microsatellite stability.

\*0: absent, 1: present.

\*\*0: pushing, 1: infiltrating.

doi:10.1371/journal.pone.0064814.t003

Furthermore, CRC infiltration by CD66b+ cells has recently been proposed to be associated with adverse prognosis [56].

In previous work we showed that CRC infiltration by CD16+ cells correlates with improved survival [13]. This marker is expressed in neutrophils, in a subset of macrophages and in NK cells [57,58]. Indeed, NK cell infiltration in CRC is negligible [13,14] and devoid of prognostic significance [59]. Since CRC infiltrating CD16+ cells are also CD11b+/CD33+/HLA-DR-, in this study we focused on the analysis of cells expressing MPO and CD15 granulocyte markers.

In univariate analysis high density CRC infiltration by cells expressing either marker was associated with improved survival. However, following adjustment for multiple comparisons carried out to compensate for the exploratory nature of this analysis this favorable prognostic relevance was maintained for MPO+ but not for CD15+ cell infiltration.

Importantly, in accord with a previously published report [55] we observed that MPO+ and CD15+ cells preferentially colonized CRC tissues while they poorly infiltrated normal colon mucosa, suggesting that they might be specifically recruited to the tumor microenvironment. Interestingly, MPO+ cell infiltration was higher in MMR-deficient than in MMR-proficient CRC as previously suggested by a study conducted with 67 samples from a limited number of cancers (n = 35) [28].

Flow-cytometric analysis of digested paired normal and cancerous tissues indicates that in both healthy mucosa and CRC infiltrating MPO+ cells are CD15+/CD16+/CD66b+/HLA-DR-, consistent with a granulocytic lineage. Most importantly however, we observed substantial percentages of CD66b+/MPO- cells infiltrating CRC. These data might explain the discrepancies between our findings and a previous report focusing on CD66b+ CRC infiltrating cells [56]. Notably, neutrophils with similar phenotypic characteristics have also been found to infiltrate head and neck cancers [60].

Similarly, the presence of CD15+/MPO- cells in healthy mucosa and cancerous tissues might explain the differential prognostic relevance of these markers. Notably however, MPO gene expression was undetectable in CRC or normal mucosa specimens (data not shown) consistent with a mature granulocyte nature of MPO+ infiltrating cells [61].

MPO activity has been suggested to contribute to the pathogenesis of degenerative diseases, including atherosclerosis, multiple sclerosis and Alzheimer disease [62]. Furthermore, high

MPO activity or MPO+ cell infiltration have been detected in esophageal [63], and gynecological cancers [64,65] and in CRC [28,66,67], but their prognostic impact was not analyzed.

Despite early reports documenting their ability to mediate tumor cell cytotoxicity [68] granulocytes have largely been neglected by tumor immunologists [18]. However experimental models in the past have indicated that colorectal cancer cells transfected with G-CSF gene can be rejected by tumor infiltrating neutrophils upon interaction with IFN- $\gamma$  producing T cells [69]. Granulocytes were also shown to express co-stimulatory molecules and to be able to present antigens [70,71], thus suggesting the possibility of a role in the initiation of antigen specific antitumor responses.

More recently, evidence of the ability of granulocytes to inhibit lung metastasis formation in an experimental breast cancer model was provided [19]. Furthermore, the capacity of granulocytes to undergo TGF- $\beta$  dependent polarization into N1 and N2 functional profiles, characterized by anti- or pro-tumoral properties, respectively, similarly to macrophages, has also been documented [20].

The molecular background underlying CRC infiltration by MPO+ cells and its prognostic significance is unclear. These phenomena could reflect chemokine production by activated T cells, and therefore indirectly result from ongoing antitumoral adaptive responses. Alternatively, they might be related to the production of granulocyte attracting chemokines by tumor cells. At least CXCL8 (IL-8) is known to be produced by CRC cells. However, its production was suggested to be associated with increased angiogenesis and tumor dissemination [72]. On the other hand, we and others have previously shown that GM-CSF, promoting granulocyte maturation and survival, can also be produced by CRC cells [73,74].

Our results contribute to the characterization of the complex features inherent in gut microenvironment and with CRC-immune system interaction [75]. Further research is warranted to clarify molecular mechanisms underlying the independent prognostic impact of MPO+ cells in CRC. Importantly, here we show that CRC infiltrating MPO+ cells express CD16 Fc $\gamma$  intermediate affinity receptor. The ability of granulocytes to mediate antibody dependent cellular cytotoxicity (ADCC) is debated. However, the availability of novel therapeutic mAb with glycoengineered Fc fragments characterized by increased affinity

for Fcγ receptors [76] might lead to a reevaluation of the effector significance of granulocytes.

Within this framework, it is tempting to speculate that neutrophil infiltration should be included in current prognostic models for CRC [77] and that it might represent an important novel stratification factor for randomization in specific clinical trials.

## References

- Boland CR, Goel A (2010) Microsatellite instability in colorectal cancer. *Gastroenterology* 138: 2073–2087.
- Wood LD, Parsons DW, Jones S, Lin J, Sjoblom T et al. (2007) The genomic landscapes of human breast and colorectal cancers. *Science* 318: 1108–1113.
- Coussens LM, Werb Z (2002) Inflammation and cancer. *Nature* 420: 860–867.
- Hanahan D, Weinberg RA (2011) Hallmarks of cancer: the next generation. *Cell* 144: 646–674.
- Galon J, Costes A, Sanchez-Cabo F, Kirilovsky A, Mlecnik B et al. (2006) Type, density, and location of immune cells within human colorectal tumors predict clinical outcome. *Science* 313: 1960–1964.
- Mlecnik B, Tosolini M, Charoentong P, Kirilovsky A, Bindea G et al. (2010) Biomolecular network reconstruction identifies T-cell homing factors associated with survival in colorectal cancer. *Gastroenterology* 138: 1429–1440.
- Pages F, Berger A, Camus M, Sanchez-Cabo F, Costes A et al. (2005) Effector memory T cells, early metastasis, and survival in colorectal cancer. *N Engl J Med* 353: 2654–2666.
- Tosolini M, Kirilovsky A, Mlecnik B, Fredriksen T, Mauger S et al. (2011) Clinical impact of different classes of infiltrating T cytotoxic and helper cells (Th1, th2, treg, th17) in patients with colorectal cancer. *Cancer Res* 71: 1263–1271.
- Frey DM, Drosner RA, Viehl CT, Zlobec I, Lugli A et al. (2010) High frequency of tumor-infiltrating FOXP3(+) regulatory T cells predicts improved survival in mismatch repair-proficient colorectal cancer patients. *Int J Cancer* 126: 2635–2643.
- Salama P, Phillips M, Grieco F, Morris M, Zeps N et al. (2009) Tumor-infiltrating FOXP3+ T regulatory cells show strong prognostic significance in colorectal cancer. *J Clin Oncol* 27: 186–192.
- Coca S, Perez-Piqueras J, Martinez D, Colmenarejo A, Saez MA et al. (1997) The prognostic significance of intratumoral natural killer cells in patients with colorectal carcinoma. *Cancer* 79: 2320–2328.
- Halama N, Braun M, Kahlert C, Spille A, Quack C et al. (2011) Natural killer cells are scarce in colorectal carcinoma tissue despite high levels of chemokines and cytokines. *Clin Cancer Res* 17: 678–689.
- Sconocchia G, Zlobec I, Lugli A, Calabrese D, Iezzi G et al. (2011) Tumor infiltration by FcγRIIIb (CD16b) myeloid cells is associated with improved survival in patients with colorectal carcinoma. *Int J Cancer* 128: 2663–2672.
- Sconocchia G, Arriga R, Tornillo L, Terracciano L, Ferrone S et al. (2012) Melanoma cells inhibit NK cell functions—letter. *Cancer Res* 72: 5428–5429.
- Forsell J, Oberg A, Henriksson ML, Stenling R, Jung A et al. (2007) High macrophage infiltration along the tumor front correlates with improved survival in colon cancer. *Clin Cancer Res* 13: 1472–1479.
- Nagorsen D, Voigt S, Berg E, Stein H, Thiel E et al. (2007) Tumor-infiltrating macrophages and dendritic cells in human colorectal cancer: relation to local regulatory T cells, systemic T-cell response against tumor-associated antigens and survival. *J Transl Med* 5: 62.
- Pancione M, Forte N, Sabatino L, Tomaselli E, Parente D et al. (2009) Reduced beta-catenin and peroxisome proliferator-activated receptor-gamma expression levels are associated with colorectal cancer metastatic progression: correlation with tumor-associated macrophages, cyclooxygenase 2, and patient outcome. *Hum Pathol* 40: 714–725.
- Di CE, Forni G, Lollini P, Colombo MP, Modesti A et al. (2001) The intriguing role of polymorphonuclear neutrophils in antitumor reactions. *Blood* 97: 339–345.
- Granot Z, Henke E, Comen EA, King TA, Norton L et al. (2011) Tumor entrained neutrophils inhibit seeding in the premetastatic lung. *Cancer Cell* 20: 300–314.
- Fridlender ZG, Sun J, Kim S, Kapoor V, Cheng G et al. (2009) Polarization of tumor-associated neutrophil phenotype by TGF-beta: “N1” versus “N2” TAN. *Cancer Cell* 16: 183–194.
- Jablonska J, Leschner S, Westphal K, Lienenklaus S, Weiss S (2010) Neutrophils responsive to endogenous IFN-beta regulate tumor angiogenesis and growth in a mouse tumor model. *J Clin Invest* 120: 1151–1164.
- Fridlender ZG, Albelda SM (2012) Tumor-associated neutrophils: friend or foe? *Carcinogenesis* 33: 949–955.
- Mantovani A (2009) The yin-yang of tumor-associated neutrophils. *Cancer Cell* 16: 173–174.
- Mantovani A, Cassatella MA, Costantini C, Jaillon S (2011) Neutrophils in the activation and regulation of innate and adaptive immunity. *Nat Rev Immunol* 11: 519–531.

## Author Contributions

Conceived and designed the experiments: RAD CH L. Terracciano G. Spagnoli. Performed the experiments: FA GI G. Sconocchia IZ. Analyzed the data: L. Terracciano L. Tornillo G. Spagnoli MH SEC. Contributed reagents/materials/analysis tools: L. Terracciano L. Tornillo G. Spagnoli MH IZ SEC. Wrote the paper: RAD CH FA GI G. Sconocchia L. Terracciano L. Tornillo G. Spagnoli MH IZ SEC CTV DMF CAN RR MZ DO AL. Provided histopathological expertise: L. Tornillo AL.

- Krawisz JE, Sharon P, Stenson WF (1984) Quantitative assay for acute intestinal inflammation based on myeloperoxidase activity. Assessment of inflammation in rat and hamster models. *Gastroenterology* 87: 1344–1350.
- Heinecke JW, Li W, Francis GA, Goldstein JA (1993) Tyrosyl radical generated by myeloperoxidase catalyzes the oxidative cross-linking of proteins. *J Clin Invest* 91: 2866–2872.
- Kanayama A, Miyamoto Y (2007) Apoptosis triggered by phagocytosis-related oxidative stress through FLIPs down-regulation and JNK activation. *J Leukoc Biol* 82: 1344–1352.
- Roncucci L, Mora E, Mariani F, Bursi S, Pezzi A et al. (2008) Myeloperoxidase-positive cell infiltration in colorectal carcinogenesis as indicator of colorectal cancer risk. *Cancer Epidemiol Biomarkers Prev* 17: 2291–2297.
- Kerr MA, Stocks SC (1992) The role of CD15-(Le(X))-related carbohydrates in neutrophil adhesion. *Histochem J* 24: 811–826.
- Sittel C, Eckel HE, Damm M, von PE, Kvasnicka HM (2000) Ki-67 (MIB1), p53, and Lewis-X (LeuM1) as prognostic factors of recurrence in T1 and T2 laryngeal carcinoma. *Laryngoscope* 110: 1012–1017.
- Mayer B, Funke I, Schraut W, Johnson JP, Schildberg FW (1998) [Expression of Lewis blood group antigens in stomach carcinoma induces metastatic potential]. *Langenbecks Arch Chir Suppl Kongressbd* 115: 631–634.
- Kadota A, Masutani M, Takei M, Horie T (1999) Evaluation of expression of CD15 and sCD15 in non-small cell lung cancer. *Int J Oncol* 15: 1081–1089.
- Hoff SD, Matsushita Y, Ota DM, Cleary KR, Yamori T et al. (1989) Increased expression of sialyl-dimeric LeX antigen in liver metastases of human colorectal carcinoma. *Cancer Res* 49: 6883–6888.
- Nakamori S, Kameyama M, Imaoka S, Furukawa H, Ishikawa O et al. (1993) Increased expression of sialyl Lewisx antigen correlates with poor survival in patients with colorectal carcinoma: clinicopathological and immunohistochemical study. *Cancer Res* 53: 3632–3637.
- Ichikawa D, Kitamura K, Tani N, Nishida S, Tsurutome H et al. (2000) Molecular detection of disseminated cancer cells in the peripheral blood and expression of sialylated antigens in colon cancers. *J Surg Oncol* 75: 98–102.
- Sauter G, Simon R, Hillan K (2003) Tissue microarrays in drug discovery. *Nat Rev Drug Discov* 2: 962–972.
- Jass JR, Atkin WS, Cuzick J, Bussey HJ, Morson BC et al. (1986) The grading of rectal cancer: historical perspectives and a multivariate analysis of 447 cases. *Histopathology* 10: 437–459.
- Hampel H, Stephens JA, Pukkala E, Sankila R, Aaltonen LA et al. (2005) Cancer risk in hereditary nonpolyposis colorectal cancer syndrome: later age of onset. *Gastroenterology* 129: 415–421.
- Zlobec I, Minoo P, Baumhoer D, Baker K, Terracciano L et al. (2008) Multimarker phenotype predicts adverse survival in patients with lymph node-negative colorectal cancer. *Cancer* 112: 495–502.
- Zlobec I, Steele R, Terracciano L, Jass JR, Lugli A (2007) Selecting immunohistochemical cut-off scores for novel biomarkers of progression and survival in colorectal cancer. *J Clin Pathol* 60: 1112–1116.
- McShane LM, Altman DG, Sauerbrei W, Taube SE, Gion M et al. (2005) Reporting recommendations for tumor marker prognostic studies (REMARK). *J Natl Cancer Inst* 97: 1180–1184.
- Gabrilovich DI, Ostrand-Rosenberg S, Bronte V (2012) Coordinated regulation of myeloid cells by tumours. *Nat Rev Immunol* 12: 253–268.
- Condeelis JS, Pollard JW (2006) Macrophages: obligate partners for tumor cell migration, invasion, and metastasis. *Cell* 124: 263–266.
- Donskov F, von der MH (2006) Impact of immune parameters on long-term survival in metastatic renal cell carcinoma. *J Clin Oncol* 24: 1997–2005.
- Ilie M, Hofman V, Ortholan C, Bonnetaud C, Coelle C et al. (2012) Predictive clinical outcome of the intratumoral CD66b-positive neutrophil-to-CD8-positive T-cell ratio in patients with resectable non-small cell lung cancer. *Cancer* 118: 1726–1737.
- Jensen HK, Donskov F, Marcussen N, Nordmark M, Lundbeck F et al. (2009) Presence of intratumoral neutrophils is an independent prognostic factor in localized renal cell carcinoma. *J Clin Oncol* 27: 4709–4717.
- Li YW, Qiu SJ, Fan J, Zhou J, Gao Q et al. (2011) Intratumoral neutrophils: a poor prognostic factor for hepatocellular carcinoma following resection. *J Hepatol* 54: 497–505.
- Biswas SK, Mantovani A (2010) Macrophage plasticity and interaction with lymphocyte subsets: cancer as a paradigm. *Nat Immunol* 11: 889–896.
- Ladoire S, Martin F, Ghiringhelli F (2011) Prognostic role of FOXP3+ regulatory T cells infiltrating human carcinomas: the paradox of colorectal cancer. *Cancer Immunol Immunother* 60: 909–918.

50. Kang JC, Chen JS, Lee CH, Chang JJ, Shieh YS (2010) Intratumoral macrophage counts correlate with tumor progression in colorectal cancer. *J Surg Oncol* 102: 242–248.
51. Kinouchi M, Miura K, Mizoi T, Ishida K, Fujibuchi W et al. (2011) Infiltration of CD14-positive macrophages at the invasive front indicates a favorable prognosis in colorectal cancer patients with lymph node metastasis. *Hepatogastroenterology* 58: 352–358.
52. Ong SM, Tan YC, Beretta O, Jiang D, Yeap WH et al. (2011) Macrophages in human colorectal cancer are pro-inflammatory and prime T cells towards an anti-tumour type-1 inflammatory response. *Eur J Immunol* 42: 89–100.
53. Rigo A, Gottardi M, Zamo A, Mauri P, Bonifacio M et al. (2010) Macrophages may promote cancer growth via a GM-CSF/HB-EGF paracrine loop that is enhanced by CXCL12. *Mol Cancer* 9: 273.
54. Zhou Q, Peng RQ, Wu XJ, Xia Q, Hou JH et al. (2010) The density of macrophages in the invasive front is inversely correlated to liver metastasis in colon cancer. *J Transl Med* 8: 13.
55. McLean MH, Murray GI, Stewart KN, Norrie G, Mayer C et al. (2011) The inflammatory microenvironment in colorectal neoplasia. *PLoS One* 6: e15366.
56. Rao HL, Chen JW, Li M, Xiao YB, Fu J et al. (2012) Increased intratumoral neutrophil in colorectal carcinomas correlates closely with malignant phenotype and predicts patients' adverse prognosis. *PLoS One* 7: e30806.
57. Dransfield I, Buckle AM, Savill JS, McDowall A, Haslett C et al. (1994) Neutrophil apoptosis is associated with a reduction in CD16 (Fc gamma RIII) expression. *J Immunol* 153: 1254–1263.
58. Ueda E, Kinoshita T, Nojima J, Inoue K, Kitani T (1989) Different membrane anchors of Fc gamma RIII (CD16) on K/NK-lymphocytes and neutrophils. Protein- vs lipid-anchor. *J Immunol* 143: 1274–1277.
59. Zlobec I, Karamitopoulou E, Terracciano L, Piscuoglio S, Iezzi G et al. (2010) TIA-1 cytotoxic granule-associated RNA binding protein improves the prognostic performance of CD8 in mismatch repair-proficient colorectal cancer. *PLoS One* 5: e14282.
60. Trellakis S, Bruderek K, Dumitru CA, Gholaman H, Gu X et al. (2011) Polymorphonuclear granulocytes in human head and neck cancer: enhanced inflammatory activity, modulation by cancer cells and expansion in advanced disease. *Int J Cancer* 129: 2183–2193.
61. Theilgaard-Monch K, Jacobsen LC, Borup R, Rasmussen T, Bjerregaard MD et al. (2005) The transcriptional program of terminal granulocytic differentiation. *Blood* 105: 1785–1796.
62. Hoy A, Leininger-Muller B, Kutter D, Siest G, Visvikis S (2002) Growing significance of myeloperoxidase in non-infectious diseases. *Clin Chem Lab Med* 40: 2–8.
63. Silvo EI, Salminen JT, Rantanen TK, Ramo OJ, Ahotupa M et al. (2002) Oxidative stress has a role in malignant transformation in Barrett's oesophagus. *Int J Cancer* 102: 551–555.
64. Song M, Santanam N (2001) Increased myeloperoxidase and lipid peroxide-modified protein in gynecological malignancies. *Antioxid Redox Signal* 3: 1139–1146.
65. Samoszuk MK, Nguyen V, Gluzman I, Pham JH (1996) Occult deposition of eosinophil peroxidase in a subset of human breast carcinomas. *Am J Pathol* 148: 701–706.
66. Rainis T, Maor I, Lanir A, Shnizer S, Lavy A (2007) Enhanced oxidative stress and leucocyte activation in neoplastic tissues of the colon. *Dig Dis Sci* 52: 526–530.
67. Otamiri T, Sjodahl R (1989) Increased lipid peroxidation in malignant tissues of patients with colorectal cancer. *Cancer* 64: 422–425.
68. Clark RA, Klebanoff SJ (1975) Neutrophil-mediated tumor cell cytotoxicity: role of the peroxidase system. *J Exp Med* 141: 1442–1447.
69. Colombo MP, Ferrari G, Stoppacciaro A, Parenza M, Rodolfo M et al. (1991) Granulocyte colony-stimulating factor gene transfer suppresses tumorigenicity of a murine adenocarcinoma in vivo. *J Exp Med* 173: 889–897.
70. Abi Abdallah DS, Egan CE, Butcher BA, Denkers EY (2011) Mouse neutrophils are professional antigen-presenting cells programmed to instruct Th1 and Th17 T-cell differentiation. *Int Immunol* 23: 317–326.
71. Sandilands GP, McCrae J, Hill K, Perry M, Baxter D (2006) Major histocompatibility complex class II (DR) antigen and costimulatory molecules on in vitro and in vivo activated human polymorphonuclear neutrophils. *Immunology* 119: 562–571.
72. Ning Y, Manegold PC, Hong YK, Zhang W, Pohl A et al. (2011) Interleukin-8 is associated with proliferation, migration, angiogenesis and chemosensitivity in vitro and in vivo in colon cancer cell line models. *Int J Cancer* 128: 2038–2049.
73. Trutmann M, Terracciano L, Noppen C, Kloth J, Kaspar M et al. (1998) GM-CSF gene expression and protein production in human colorectal cancer cell lines and clinical tumor specimens. *Int J Cancer* 77: 378–385.
74. Urdinguio RG, Fernandez AF, Moncada-Pazos A, Huidobro C, Rodriguez RM et al. (2012) Immune dependent and independent anti-tumor activity of GM-CSF aberrantly expressed by mouse and human colorectal tumors. *Cancer Res* 73: 395–405.
75. Roxburgh CS, McMillan DC (2012) The role of the in situ local inflammatory response in predicting recurrence and survival in patients with primary operable colorectal cancer. *Cancer Treat Rev* 38: 451–466.
76. Paz-Ares LG, Gomez-Roca C, Delord JP, Cervantes A, Markman B et al. (2011) Phase I pharmacokinetic and pharmacodynamic dose-escalation study of RG7160 (GA201), the first glycoengineered monoclonal antibody against the epidermal growth factor receptor, in patients with advanced solid tumors. *J Clin Oncol* 29: 3783–3790.
77. Galon J, Franck P, Marincola FM, Angell HK, Thurin M et al. (2012) Cancer classification using the Immunoscore: a worldwide task force. *J Transl Med* 10: 205.

# Colorectal carcinoma infiltration by myeloperoxidase-expressing neutrophil granulocytes is associated with favorable prognosis

Christian Hirt<sup>1,2</sup>, Serenella Eppenberger-Castori<sup>3</sup>, Giuseppe Sconocchia<sup>4</sup>, Giandomenica Iezzi<sup>2</sup>, Luigi Tornillo<sup>3</sup>, Luigi Terracciano<sup>3</sup>, Giulio C Spagnoli<sup>2</sup>, and Raoul A Droeser<sup>1,2,\*</sup>

<sup>1</sup>Department of Surgery; University Hospital Basel; Basel, Switzerland;

<sup>2</sup>Institute of Surgical Research and Hospital Management (ICFS) and Department of Biomedicine; University of Basel; Basel, Switzerland;

<sup>3</sup>Institute of Pathology; University Hospital Basel; Basel, Switzerland; <sup>4</sup>Institute of Translational Pharmacology; National Research Council; Rome, Italy

**Keywords:** human colorectal cancer, CD15, myeloperoxidase, mismatch repair status, tissue microarray, prognosis

The prognostic relevance of innate immune cells infiltrating colorectal carcinoma lesions is highly debated. By evaluating the expression of myeloperoxidase (MPO) as a marker of neutrophil granulocytes in a large cohort of colorectal carcinoma specimens, we have observed that robust tumor-infiltration by MPO<sup>+</sup> cells correlates with improved patient survival independently of other histopathological parameters, including disease stage.

The clinical course of colorectal carcinoma (CRC) critically depends on cancer cell-intrinsic features, including specific mutations, microsatellite instability, and epigenetic alterations, as well as on the tumor microenvironment, as shaped by the interaction of malignant and non-transformed cells. Tumor infiltration by cellular components of the adaptive immune system has been shown to predict the survival of CRC patients more efficiently than the tumor-node-metastasis (TNM) staging.<sup>1</sup> However, the role of the innate immune system in CRC progression remains matter of debate.

We observed that the infiltration of CRC lesions by natural killer (NK) cells is infrequent and devoid of prognostic significance.<sup>2</sup> In contrast, tumor infiltration by CD33<sup>+</sup>HLA-DR<sup>-</sup>CD16<sup>+</sup> myeloid cells was associated with improved patient survival, independently of TNM stage.<sup>3</sup> Functionally active neutrophil granulocytes (NGs) express high amounts of CD16 (Fcγ receptor IIIB, FCGR3B), which decrease along with a progressive

functional decline that precedes apoptosis.<sup>4</sup> Based on these premises, we have recently addressed the prognostic significance of NG infiltration in CRC.<sup>5</sup>

NGs are the most abundant circulating white cells and are the most prominent component of the first-line mechanism of defense against infection. Nonetheless, NGs have been long neglected by tumor immunologists. Notably, high amounts of intratumoral myeloid cells are generally thought to promote tumor progression and hence to correlate with poor disease outcome. In particular, CRC infiltration by CD66B<sup>+</sup> granulocytes has been proposed as a marker of adverse prognosis.<sup>6</sup>

Recent studies, mostly based on pre-clinical tumor models, have promoted a resurgence in the interest of tumor immunologists for the role of NGs in cancer immunobiology.<sup>7</sup> In particular, it has been suggested that, similar to macrophages, NGs may undergo cytokine-driven differentiation toward an N1 and an N2 phenotype, which are associated with anti- and pro-tumor effects, respectively.<sup>7</sup>

Myeloperoxidase (MPO), a heme protein that generates cytotoxic oxidants from hydrogen peroxide, chloride anion and tyrosine, is abundantly expressed by NGs and has been proposed to serve as an autocrine regulator of their activation.<sup>8</sup> Therefore, MPO might represent a valuable biomarker for the identification and quantification of functionally active NGs in clinical specimens. Conversely, the use of CD15 may be associated with a limited specificity, as this protein is expressed not only on mature neutrophils but also on a variety of malignant cells.

By using a tissue microarray (TMA) including a large number (> 1400) of clinically annotated specimens, we observed a significantly higher amount of infiltration by MPO<sup>+</sup> and CD15<sup>+</sup> cells in CRC lesions than in the normal colonic mucosa. A strong (R = 0.75) correlation between MPO<sup>+</sup> and CD15<sup>+</sup> cell infiltration was detectable at the tumor site. Moreover, univariate Cox regression analyses revealed that a high density of MPO<sup>+</sup> or CD15<sup>+</sup> infiltrating cells, detectable in

\* Correspondence to: Raoul A Droeser; Email: Raoul.Droeser@usb.ch

Submitted: 07/30/2013; Accepted: 07/31/2013

Citation: Hirt C, Eppenberger-Castori S, Sconocchia G, Iezzi G, Tornillo L, Terracciano L, Spagnoli G, Droeser R. Colorectal cancer infiltration by myeloperoxidase positive neutrophil granulocytes is associated with favorable prognosis. *Oncoimmunology* 2013; 2:e25990; <http://dx.doi.org/10.4161/onci.25990>

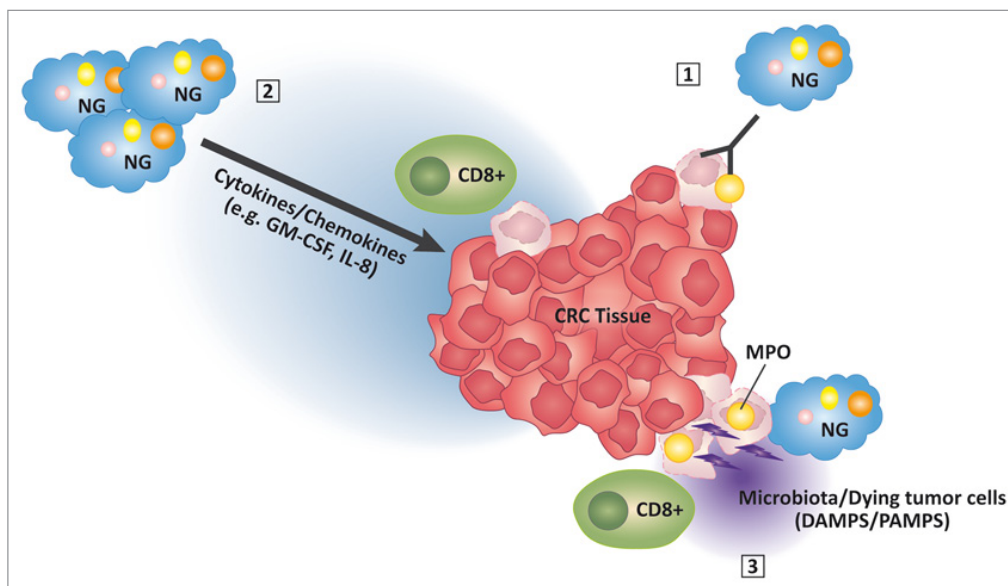


**Figure 1.** Molecular mechanisms potentially underlying the favorable effects of myeloperoxidase-expressing neutrophil granulocytes in colorectal carcinoma. Myeloperoxidase (MPO)-expressing neutrophil granulocytes (NGs) might exert direct antitumor effects on opsonized cancer cells (1), or they might be recruited to neoplastic lesions by the secretion of immunostimulatory cytokines including interleukin-8 (IL-8) and granulocyte macrophage colony-stimulating factor (GM-CSF) (2). The activation of MPO<sup>+</sup> NGs by danger-associated molecular patterns (DAMPs) released by dying tumor cells or by microbiota-derived pathogen-associated molecular patterns (PAMPs) might further promote the antitumor activity of these cells (3).

14.5% and 10.8% of CRC specimens, respectively, was significantly associated with early tumor stage (pT1–2), absence of local recurrence and increased 5-y survival rate. After adjusting for several known prognostic factors including age, sex, T stage, N stage, tumor grade, vascular invasion, tumor border configuration, and microsatellite stability, only the abundance of tumor-infiltrating MPO<sup>+</sup> cells retained a prognostic significance. Ex vivo analyses of MPO<sup>+</sup> cells infiltrating CRC lesions and the normal mucosa showed that a large majority of these cells also expressed CD15, CD16 and CD66B, consistent with the phenotype of the granulocytic lineage. However, a substantial percentage of CD66B<sup>+</sup> CRC-infiltrating cells was MPO<sup>-</sup>.<sup>6</sup>

To the best of our knowledge, we were the first to document a positive prognostic impact for tumor infiltration by NGs among CRC patients. Our analysis involved a large number of cases with

an extensive clinical annotation, further increasing its value. Future research is warranted to gain additional insights into the molecular mechanisms underlying our observations.

CRC-infiltrating NGs might exert direct antitumor effects, perhaps upon the release of cytokines, chlorinated oxidants or enzymes including MPO (Fig. 1). However, such a direct antitumor activity has rarely been ascribed to human NGs, and was near-to-invariably associated with the presence of tumor-specific opsonizing monoclonal antibodies.<sup>9</sup> Alternatively, NG infiltration might constitute an epiphenomenon of the release of chemokines and cytokines such as interleukin-8 (IL-8) and granulocyte macrophage colony-stimulating factor (GM-CSF) by malignant cells or tumor-infiltrating lymphocytes.<sup>10</sup> Thus, while devoid of intrinsic antitumor functions, NGs might constitute a marker of favorable microenvironmental features (Fig. 1).

These explanations are not necessarily mutually exclusive. NGs could be recruited to neoplastic lesions and activated by chemokines and lymphokines secreted by cells of the adaptive immune system in the context of their interaction with cancer cells.<sup>1</sup> It is tempting to speculate that products of commensal microorganisms might also play a role in the recruitment and activation of immune cells in the peculiar CRC microenvironment. Within this framework, it would be important to specifically investigate the functions of tumor-infiltrating NGs (Fig. 1).

In summary, the mobilization of granulocytes and their sustained activation at the tumor site might be of benefit for CRC patients, both as a natural process and in the context of monoclonal antibody-based immunotherapy.

#### Disclosure of Potential Conflicts of Interest

No potential conflicts of interest were disclosed.

## References

1. Galon J, Costes A, Sanchez-Cabo F, Kirilovsky A, Mlecnik B, Lagorce-Pagès C, Tosolini M, Camus M, Berger A, Wind P, et al. Type, density, and location of immune cells within human colorectal tumors predict clinical outcome. *Science* 2006; 313:1960-4; PMID:17008531; <http://dx.doi.org/10.1126/science.1129139>
2. Sconocchia G, Arriga R, Tornillo L, Terracciano L, Ferrone S, Spagnoli GC. Melanoma cells inhibit NK cell functions. *Cancer Res* 2012; 72:5428-9, author reply 5430; PMID:23047870; <http://dx.doi.org/10.1158/0008-5472.CAN-12-1181>
3. Sconocchia G, Zlobec I, Lugli A, Calabrese D, Iezzi G, Karamitopoulou E, Patsouris ES, Peros G, Horcic M, Tornillo L, et al. Tumor infiltration by FcγRIII (CD16)+ myeloid cells is associated with improved survival in patients with colorectal carcinoma. *Int J Cancer* 2011; 128:2663-72; PMID:20715106; <http://dx.doi.org/10.1002/ijc.25609>
4. Moulding DA, Hart CA, Edwards SW. Regulation of neutrophil FcγRIIIb (CD16) surface expression following delayed apoptosis in response to GM-CSF and sodium butyrate. *J Leukoc Biol* 1999; 65:875-82; PMID:10380913
5. Droeser RA, Hirt C, Eppenberger-Castori S, Zlobec I, Viehl CT, Frey DM, Nebiker CA, Rosso R, Zuber M, Amicarella F, et al. High myeloperoxidase positive cell infiltration in colorectal cancer is an independent favorable prognostic factor. *PLoS One* 2013; 8:e64814; PMID:23734221; <http://dx.doi.org/10.1371/journal.pone.0064814>
6. Rao H-L, Chen J-W, Li M, Xiao Y-B, Fu J, Zeng Y-X, Cai M-Y, Xie D. Increased intratumoral neutrophil in colorectal carcinomas correlates closely with malignant phenotype and predicts patients' adverse prognosis. *PLoS One* 2012; 7:e30806; PMID:22295111; <http://dx.doi.org/10.1371/journal.pone.0030806>
7. Mantovani A, Cassatella MA, Costantini C, Jaillon S. Neutrophils in the activation and regulation of innate and adaptive immunity. *Nat Rev Immunol* 2011; 11:519-31; PMID:21785456; <http://dx.doi.org/10.1038/nri3024>
8. Lau D, Mollnau H, Eiserich JP, Freeman BA, Daiber A, Gehling UM, Brümmer J, Rudolph V, Münzel T, Heitzer T, et al. Myeloperoxidase mediates neutrophil activation by association with CD11b/CD18 integrins. *Proc Natl Acad Sci U S A* 2005; 102:431-6; PMID:15625114; <http://dx.doi.org/10.1073/pnas.0405193102>
9. Valerius T, Repp R, de Wit TP, Berthold S, Platzer E, Kalden JR, Gramatzki M, van de Winkel JG. Involvement of the high-affinity receptor for IgG (Fc gamma RI; CD64) in enhanced tumor cell cytotoxicity of neutrophils during granulocyte colony-stimulating factor therapy. *Blood* 1993; 82:931-9; PMID:7687898
10. De Larco JE, Wuertz BRK, Furcht LT. The potential role of neutrophils in promoting the metastatic phenotype of tumors releasing interleukin-8. *Clin Cancer Res* 2004; 10:4895-900; PMID:15297389; <http://dx.doi.org/10.1158/1078-0432.CCR-03-0760>

Available at [www.sciencedirect.com](http://www.sciencedirect.com)

SciVerse ScienceDirect

journal homepage: [www.ejcancer.com](http://www.ejcancer.com)

## Clinical impact of programmed cell death ligand 1 expression in colorectal cancer

Raoul A. Droseser<sup>a,b,\*,h</sup>, Christian Hirt<sup>a,b,h</sup>, Carsten T. Viehl<sup>a</sup>, Daniel M. Frey<sup>a</sup>, Christian Nebiker<sup>a,b</sup>, Xaver Huber<sup>a</sup>, Inti Zlobec<sup>c</sup>, Serenella Eppenberger-Castori<sup>d</sup>, Alexander Tzankov<sup>d</sup>, Raffaele Rosso<sup>e</sup>, Markus Zuber<sup>f</sup>, Manuele Giuseppe Muraro<sup>b</sup>, Francesca Amicarella<sup>b</sup>, Eleonora Cremonesi<sup>b</sup>, Michael Heberer<sup>b</sup>, Giandomenica Iezzi<sup>b</sup>, Alessandro Lugli<sup>c</sup>, Luigi Terracciano<sup>d</sup>, Giuseppe Sconocchia<sup>g</sup>, Daniel Oertli<sup>a</sup>, Giulio C. Spagnoli<sup>b</sup>, Luigi Tornillo<sup>d</sup>

<sup>a</sup> Department of Surgery, University Hospital of Basel, Switzerland

<sup>b</sup> Institute for Surgical Research and Hospital Management ICFS, Department of Biomedicine, University of Basel, Switzerland

<sup>c</sup> Institute of Pathology, University of Bern, Switzerland

<sup>d</sup> Institute of Pathology, University of Basel, Switzerland

<sup>e</sup> Department of Surgery, Ospedale Regionale di Lugano, Switzerland

<sup>f</sup> Department of Surgery, Kantonsspital Olten, Switzerland

<sup>g</sup> Institute of Translational Pharmacology, National Council Research, Rome, Italy

Available online 13 March 2013

### KEYWORDS

Human colorectal cancer  
PD-L1  
Prognostic factors  
Overall survival  
Tissue microarrays

**Abstract Background:** Programmed cell death 1 (PD-1) receptor triggering by PD ligand 1 (PD-L1) inhibits T cell activation. PD-L1 expression was detected in different malignancies and associated with poor prognosis. Therapeutic antibodies inhibiting PD-1/PD-L1 interaction have been developed.

**Materials and methods:** A tissue microarray ( $n = 1491$ ) including healthy colon mucosa and clinically annotated colorectal cancer (CRC) specimens was stained with two PD-L1 specific antibody preparations. Surgically excised CRC specimens were enzymatically digested and analysed for cluster of differentiation 8 (CD8) and PD-1 expression.

**Results:** Strong PD-L1 expression was observed in 37% of mismatch repair (MMR)-proficient and in 29% of MMR-deficient CRC. In MMR-proficient CRC strong PD-L1 expression correlated with infiltration by CD8<sup>+</sup> lymphocytes ( $P = 0.0001$ ) which did not express PD-1. In univariate analysis, strong PD-L1 expression in MMR-proficient CRC was significantly associated with early T stage, absence of lymph node metastases, lower tumour grade, absence of

\* Corresponding author: Address: Department of Surgery, University of Basel, Spitalstrasse 21, CH-4031 Basel, Switzerland. Tel.: +41 61 265 25 25; fax: +41 61 265 72 50.

E-mail address: [rdroseser@uhbs.ch](mailto:rdroseser@uhbs.ch) (R.A. Droseser).

<sup>h</sup> These authors contributed equally to this work.

vascular invasion and significantly improved survival in training ( $P = 0.0001$ ) and validation ( $P = 0.03$ ) sets. A similar trend ( $P = 0.052$ ) was also detectable in multivariate analysis including age, sex, T stage, N stage, tumour grade, vascular invasion, invasive margin and MMR status. Interestingly, programmed death receptor ligand 1 (PDL-1) and interferon (IFN)- $\gamma$  gene expression, as detected by quantitative reverse transcriptase polymerase chain reaction (RT-PCR) in fresh frozen CRC specimens ( $n = 42$ ) were found to be significantly associated ( $r = 0.33$ ,  $P = 0.03$ ).

**Conclusion:** PD-L1 expression is paradoxically associated with improved survival in MMR-proficient CRC.

© 2013 Elsevier Ltd. All rights reserved.

## 1. Introduction

Tumour-infiltrating lymphocytes (TILs) are widely considered to reflect primary host immune response against solid tumours. Recent reports have demonstrated a direct correlation between colorectal cancer (CRC) patient survival and tumour infiltration by cluster of differentiation 8 (CD8) positive T lymphocytes expressing typical activation markers.<sup>1,2</sup> However, the immune system is characterised by the presence of a number of inhibitory mechanisms preventing ‘excessive’ lymphocyte activation.<sup>3</sup> In particular, programmed cell death receptor 1 (PD-1; CD279) is typically expressed by activated lymphocytes.<sup>4</sup> Its engagement by specific ligands, including PD ligand 1 (PD-L1; B7-H1; CD274) and PD ligand 2 (PD-L2; B7-DC; CD273), induces down-regulation of antigen-stimulated lymphocyte proliferation<sup>5,6</sup> and cytokine production,<sup>6,7</sup> ultimately resulting in lymphocyte ‘exhaustion’ and in the induction of immunological tolerance.<sup>6,8–10</sup>

PD-L1 is constitutively expressed by T and B cells, macrophages and dendritic cells (DC) and is up-regulated upon activation by interferons (IFN).<sup>8,9</sup> PD-L1 is also expressed on additional cell types including endothelial, pancreatic and muscle cells.<sup>4</sup> In contrast, PD-L2 expression is much more restricted and typically detectable in activated DC and macrophages.<sup>9</sup> Importantly, up-regulation of the expression of PD-1 ligands in malignant cells has been suggested to play a central role in tumour-immune system interaction<sup>5,11</sup> since, by triggering PD-1, cancer cells might shut down specific immune responses. Indeed, the expression of PD ligands on tumour cells was shown to suppress the cytolytic activity of CD8<sup>+</sup> T-cells.<sup>12,13</sup>

PD-L1 and, to a lesser extent, PD-L2, have been reported to be expressed by tumour cells of different origins, including glioblastoma, ovarian and renal cell carcinomas, squamous cell carcinoma of the head and neck, oesophageal and non-small cell lung cancers.<sup>5,14–18</sup> A strong correlation between expression of PD ligands on tumour cells and severe prognosis has been observed in oesophageal cancer and in renal cell carcinoma.<sup>15,17</sup> Capitalising on this background, PD-1/PD-L1 blockade by anti PD-1 or anti PD-L1 monoclonal antibodies has been envisaged as an appealing option to activate the

host immune system to eradicate tumours. Recently, promising results of phase I clinical trials involving patients bearing a variety of malignancies have been published.<sup>19–21</sup>

Expression of PD-L1 in human CRC has not been addressed so far. In this study we used a tissue microarray (TMA)<sup>22</sup> including 1420 well documented, clinically annotated CRC specimens<sup>23</sup> to investigate the expression of PD-L1 in CRC and its clinical significance.

## 2. Materials and methods

### 2.1. Tissue microarray construction

The TMA used for this study includes 1420 unselected, non-consecutive, primary, sporadic CRCs treated between 1987 and 1996, and 71 normal mucosa specimens from the Institute of Pathology of the University of Basel (Switzerland), the Institute of Clinical Pathology, Basel (Switzerland) and the Institute of Pathology of the Stadtspital Triemli, Zürich (Switzerland). TMA was constructed with materials collected from the Tissue Biobank of the Institute of Pathology, University Hospital Basel. This institution performs translational research with the approval of the EKBB (Ethics Committee Beider Basel) in compliance with ethical standards and patient confidentiality. Construction of this TMA has been previously described in detail.<sup>23</sup> Briefly, formalin-fixed, paraffin-embedded tissue blocks from resected CRC were obtained. Tissue cylinders with a 0.6 mm diameter were punched from representative tissue areas of each donor tissue block and brought into one recipient paraffin block (30 × 25 mm). Each TMA spot included at least 50% tumour cells.

### 2.2. Immunohistochemistry

Four micron sections of TMA blocks were transferred to an adhesive-coated slide system (Instrumedics Inc., Hackensack, NJ, United States of America (USA)). Standard indirect immunoperoxidase procedures were used for immunohistochemistry (IHC; ABC-Elite, Vector Laboratories, Burlingame, CA, USA). Briefly, slides were dewaxed and rehydrated in distilled water. Endogenous peroxidase activity was

blocked using 0.5% H<sub>2</sub>O<sub>2</sub>. The sections were treated with 10% normal goat serum (DakoCytomation, Carpinteria, CA, USA) for 20 min and incubated with primary antibodies at room temperature. Two primary PD-L1 (CD274) specific reagents were used: a monoclonal antibody (mAb, clone 27A2, MBL, Woburn, MA, USA)<sup>24</sup> and a polyclonal preparation (ab82059, Abcam, Cambridge, United Kingdom (UK)).<sup>25</sup> Subsequently, sections were incubated with peroxidase-labelled secondary antibody (DakoCytomation, Glostrup, Denmark) for 30 min at room temperature. For visualisation of the antigen, the sections were immersed in 3-amino-9-ethylcarbazole plus substrate-chromogen (DakoCytomation) for 30 min and counterstained with Gill's haematoxylin. Data used for the analysis of correlations with the expression of other immune markers such as CD8, PD-1, T-intracellular antigen-1 (TIA-1) and Fork Head box P3 (FOXP3) were in part available from previous studies.<sup>26,27</sup>

Two independent observers, blinded to any prior information on clinicopathological features of the patients' samples, examined the immunohistochemical slides. Percentages of PD-L1 positive tumour cells and staining intensity were evaluated for each punch. Staining intensity was scored as previously reported.<sup>24</sup> Outcome analysis was mainly based on staining intensity because in the case of PD-L1 positivity nearly all tumour cells were stained, and tumours with weak or moderate expression were collectively classified as 'low' PD-L1 positive (Fig. 1).<sup>24</sup>

### 2.3. Flow cytometric analyses

Following the Basel Institutional Review Board approval (63/07), tissues from surgically removed CRC and adjacent normal mucosa were minced, centrifuged, and resuspended in RPMI 1640 medium supplemented with 5% foetal calf serum, 2 mg/ml collagenase IV, 0.1 mg/ml hyaluronidase V and 0.2 mg/ml DNase I (Sigma–Aldrich, Basel, Switzerland). Following a 12-h digestion, cell suspensions were filtered and centrifuged. Mononuclear cells were isolated by Ficoll-Hypaque gradient separation, stained with CD8 (clone RPA-T8) and PD-1 (clone MIH4) specific fluorochrome-conjugated monoclonal antibodies (Becton–Dickinson, San Jose, CA, USA), and analysed by flow cytometry using a 2-laser BD FACSCalibur (Becton–Dickinson, San Jose, CA, USA). Propidium iodide (PI) positive cells were excluded from the analysis. Results were analysed by Cell Quest (Becton–Dickinson, San Jose, CA, USA) and Flow Jo (Tree Star, Ashland, OR, USA) computer softwares.

### 2.4. Clinicopathological features and mismatch repair status

Available clinicopathological data included age, sex, pathological tumour stage (pT) stage, pathological

lymph node stage (pN) stage, tumour grade, vascular invasion, tumour border configuration and disease-specific survival. Tumour border configuration was evaluated using the original H&E slides of the resection specimens corresponding to each tissue microarray punch. Any disagreement between the numbers of available tissue punches and clinicopathological features shown was due to the fact that occasionally specific clinicopathological data were not available. CRCs were stratified according to DNA mismatch repair (MMR) status as described elsewhere.<sup>28,29</sup> Briefly, MMR-proficient tumours were defined as those simultaneously expressing MutL homolog 1 (MLH1), mutS homolog 2 (MSH2) and mutS homolog 6 (MSH6), while MMR-deficient tumours were defined as those lacking expression of at least one of these markers. Based on these features, 1197 CRCs could be classified as MMR-proficient and 223 as MMR-deficient. 47.6% of the patients were male and 34.9% of them were bearing right-sided tumours. Rectal tumours accounted for 34.4% of the cases and the mean tumour diameter was 4.75 cm. The predominant tumour stage was pT3 (64.8%) with over 50% of the samples pN0 (52.2%) and G1 or G2 (87.2%). Vascular invasion was present in 27.7% of the tumours and the overall 5-year survival was 56.4%. Clinicopathological data of the different CRC subsets are summarised in Table 1.

### 2.5. Quantitative real-time PCR

Total cellular RNA was extracted from CRC surgical specimens ( $n = 42$ ) and reverse transcribed as previously described.<sup>30</sup> cDNAs were then amplified in the presence of primers and probes specific for glyceraldehyde 3-phosphate dehydrogenase (GAPDH) house-keeping gene,<sup>31</sup> IFN- $\gamma$ <sup>30</sup> or PD-L1 genes (Assays-on-demand, Applied Biosystems, Rotkreuz, Switzerland) by using a 7300 Real Time PCR system (Applied Biosystems) according to manufacturer's recommendation. Specific gene expression was quantified by using GAPDH gene as reference.<sup>32</sup>

### 2.6. Statistical analysis

Differences in clinic-pathological features between negative, low and strong intensity PD-L1 positive CRCs were analysed using  $\chi^2$  or Fisher's exact tests, while differences in the number of infiltrating immune cells were investigated by using the non-parametric Wilcoxon Rank Sum test. Correlation analyses were performed using Spearman's rank correlation coefficient and agreement was calculated by Cohen's kappa statistics. Survival analysis was performed using one third of the total MMR-proficient collective as training set and the remaining two thirds as validation set. PD-L1 expression levels had a dichotomous character: absent or low

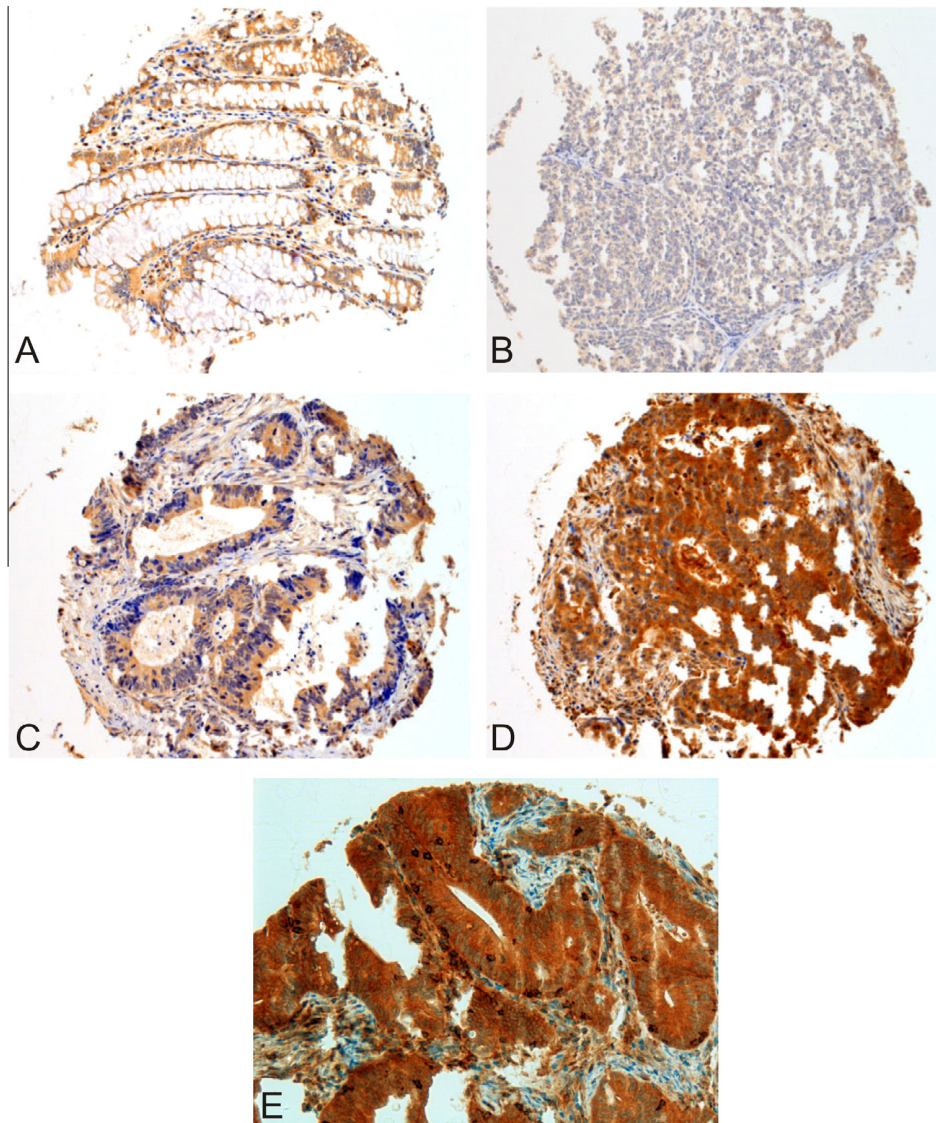


Fig. 1. Programmed cell death ligand 1 (PD-L1) staining in healthy colon mucosa and in colorectal cancer (CRC). Normal colon mucosa (panel A) and CRC samples (panels B–D) were stained with a PD-L1 specific monoclonal antibody (clone 27A2). Tumour punches are representative of negative (panel B), low (panel C) and high (panel D) PD-L1 specific staining intensities. Zoom (20 $\times$ ) of strong PD-L1 expression by tumour cells with high number of PDL-1 positive tumour infiltrating cells is shown in panel E.

or, high. The survival analysis was performed with the Kaplan–Meier method and the two curves were compared with the log rank test. Subsequently, the PD-L1 expression status was entered into uni- and multivariate Cox regression analysis. Hazard ratios (HR) and 95% confidence intervals (CI) were used to determine the prognostic effect of PD-L1 expression on survival time. The MMR-deficient CRC was analysed as a separate cohort.

Regarding tumour infiltrating cells detected as continuous variables, following proof of significant correlation with survival by univariate Cox regression, we used classification and regression trees analysis to calculate threshold values utilised to draw Kaplan–Meier curves.<sup>34</sup> Analyses were performed using SPlus software

(Version 6.1, Insightful Corporation, Seattle, WA, USA). Data reporting was performed according to the REMARK criteria.<sup>35</sup>

Correlations between the expression of different genes, as detected by quantitative reverse transcriptase polymerase chain reaction (RT-PCR) were evaluated by using Spearman's correlation coefficient ( $r$ ) and  $P$  values  $<0.05$  were considered statistically significant.

### 3. Results

#### 3.1. Immunohistochemical detection of PD-L1

Representative stainings of the tissues under investigation, as observed upon incubation with 27A2 mAb

specific for PD-L1, are shown in Fig. 1. PD-L1 was detectable in epithelial cells from normal colonic mucosa (Fig. 1A), and, importantly, in cancer cells (Fig. 1C–E).

In 433 MMR-proficient CRC (36%) a strong positivity (Fig. 1D) was observed, whereas in 723 and 41 cases, respectively, PD-L1 expression was low (Fig. 1C), or absent (Fig. 1B). Among the 223 MMR-deficient cases a strong positivity was observed in 62 cases (29%), whereas in 143 and 6 cases, respectively, PD-L1 expression was low or absent. Comparable stainings were also observed following incubation with polyclonal ab82059 antibody (Abcam, Cambridge, UK). This second staining was analysed by a second specialised investigator. The resulting combined inter-observer and inter-testing Kappa value of  $0.29 \pm 0.049$  indicated a fairly significant ( $P < 0.001$ ) agreement between experiments, antibodies and observers.

### 3.2. Correlation of PD-L1 expression with clinicopathological features

In univariate analysis, strong PD-L1 expression was associated with early T stage ( $P = 0.002$ ; OR = 2.14, CI = 0.87–5.22), absence of lymph node metastasis ( $P = 0.015$ ; OR = 2.29, CI = 1.16–4.54), lower tumour grade ( $P = 0.002$ ; OR = 2.33, CI = 0.91–5.98) and absence of vascular invasion ( $P = 0.017$ ; OR = 2.49, CI = 1.29–4.77) in MMR-proficient CRC (Table 2). Similar results were also observed upon TMA staining with the second reagent used in our study (data not shown).

### 3.3. PD-L1 expression correlates with high CD8<sup>+</sup> T-cell infiltration in MMR-proficient CRC

PD-L1 interaction with PD-1 expressed by activated T-cells has been shown to promote the induction of lymphocyte ‘exhaustion’.<sup>6,8,9</sup> Therefore, in order to evaluate the immunological context of PD-L1 expression, we analysed correlations with the expression of CD8, PD-1, TIA-1 and FOXP3 markers.<sup>26,27</sup>

Interestingly, in MMR-proficient CRC a direct correlation between PD-L1 expression in tumour cells and absolute numbers per punch of CD8<sup>+</sup> tumour-infiltrating lymphocytes, as detected in >1000 specimens,<sup>27</sup> was observed. In particular, CD8<sup>+</sup> infiltration was significantly ( $P = 0.0024$ ) higher in weakly to moderately (low) PD-L1 positive tumours than in negative cases and even higher ( $P = 0.0006$ ) in strongly positive tumours, as compared to low positivity CRC (Fig. 2A). Indeed, except for two cases, all CRCs with low PD-L1 expression displayed a CD8<sup>+</sup> infiltration by <10 cells per punch. In contrast, no significant correlation between PD-L1 expression and CRC infiltration by cells expressing TIA-1, a granule-associated cytotoxic protein typically detectable in activated cytotoxic T cells<sup>36</sup> or CRC infiltration by FOXP3<sup>+</sup> cells,<sup>26,27</sup> could

Table 1  
Summary of patient characteristics ( $n = 1420$ ).

| Clinicopathological features                | Frequency<br>N (%)  |
|---|---|
| Age ( $n = 1420$ )                          | Mean (range) 69.9 (30–96)   |
| Gender ( $n = 1414$ )                       | Female 741 (52.4)   |
|   | Male 673 (47.6)   |
| Tumour location ( $n = 1400$ )              | Left-sided 430 (30.7)   |
|   | Right-sided 488 (34.9)  |
|   | Rectum 482 (34.4)   |
| pT stage ( $n = 1387$ )                     | pT1 62 (4.5)  |
|   | pT2 203 (14.6)  |
|   | pT3 899 (64.8)  |
|   | pT4 223 (16.1)  |
| pN stage ( $n = 1363$ )                     | pN0 711 (52.2)  |
|   | pN1 358 (26.3)  |
|   | pN2 294 (21.6)  |
| Tumour grade ( $n = 1385$ )                 | G1 31 (2.2)   |
|   | G2 1177 (85.0)  |
|   | G3 177 (12.8)   |
| Histological subtype ( $n = 1420$ )         | Mucinous 119 (8.4)  |
|   | Other 1301 (91.6)   |
| Vascular invasion ( $n = 1385$ )            | Absent 1002 (72.4)  |
|   | Present 383 (27.7)  |
| Tumour border configuration ( $n = 1384$ )  | Pushing 513 (37.1)  |
|   | Infiltrating 871 (62.9)   |
| Mismatch repair (MMR) status ( $n = 1420$ ) | Proficient 1197 (84.3)  |
|   | Deficient 223 (15.7)  |
| Survival time (months) ( $n = 1379$ )       | Five-year survival rate (95% confidence interval (CI)) 56.4 (54–59) |

be observed (data not shown). Notably, PD-1 expression was detectable in small numbers of CRC infiltrating lymphocytes and in only 5% of all cases.<sup>27</sup> These data indicate that PD-L1 expression in MMR-proficient CRC cells is paradoxically associated with tumour infiltration by CD8<sup>+</sup> T cells which do not express the PD-1 co-receptor. No significant association was found between CD8<sup>+</sup> T cell infiltration and PD-L1 expression in MMR-deficient cases.

### 3.4. Ex vivo analysis of PD-1 expression on CD8 positive lymphocytes in CRC and normal colon mucosa

To further characterise CRC immune infiltrates we performed an *ex vivo* analysis of CD8<sup>+</sup> CRC infiltrating lymphocytes in freshly excised tumour tissues and corresponding normal mucosa ( $n = 7$ ). In accordance with TMA staining data (see above), this flow cytometry study confirmed that PD-1 expression in infiltrating CD8<sup>+</sup> lymphocytes is extremely limited in both CRC ( $3.5 \pm 2.4\%$ ) and normal mucosa ( $1.6 \pm 1\%$ ; Fig. 2B and C).

### 3.5. Prognostic significance of PD-L1 expression

Median overall survival was 32 and 23 months for patients with MMR-proficient tumours with high

Table 2

Association between programmed cell death ligand 1 (PD-L1) specific staining and clinico-pathological features in mismatch repair (MMR)-proficient colorectal cancer patients ( $n = 1197$ ).

|  |                                | Frequency $N$ (%) |              |                 | $P$ -value |
|--|--------------------------------|-------------------|--------------|-----------------|------------|
|  |                                | PD-L1<br>Negative | PD-L1<br>Low | PD-L1<br>Strong |            |
| Age ( $n = 1141$ ) (years)                 | Mean (min, max)                | 67.7 (40–83)      | 70.4 (30–96) | 69.6 (36–96)    | 0.201      |
| Tumour diameter ( $n = 1088$ ) (mm)        | Mean (min, max)                | 54.3 (4–100)      | 48.3 (5–150) | 45.5 (5–120)    | 0.008      |
| Gender ( $n = 1143$ )                      | Female                         | 22 (53.7)         | 335 (49.7)   | 217 (50.7)      | 0.858      |
|  | Male                           | 19 (46.3)         | 339 (50.3)   | 211 (49.3)      |            |
| Tumour location ( $n = 1129$ )             | Left-sided                     | 27 (65.9)         | 455 (68.3)   | 321 (76.1)      | 0.017      |
|  | Right-sided                    | 14 (34.2)         | 211 (31.7)   | 101 (23.9)      |            |
| Histologic type ( $n = 1197$ )             | Mucinous                       | 8 (19.5)          | 55 (7.6)     | 20 (4.6)        | <0.001     |
|  | Other                          | 33 (80.5)         | 668 (92.4)   | 413 (95.4)      |            |
| pT stage ( $n = 1117$ )                    | T1–2                           | 6 (14.6)          | 120 (18.3)   | 113 (26.8)      | 0.002      |
|  | T3–4                           | 35 (85.4)         | 535 (81.7)   | 308 (73.2)      |            |
| pN stage ( $n = 1098$ )                    | N0                             | 14 (35.9)         | 321 (49.8)   | 233 (56.3)      | 0.015      |
|  | N1–2                           | 25 (64.1)         | 324 (50.2)   | 181 (43.7)      |            |
| Tumour grade ( $n = 1117$ )                | G1–2                           | 35 (85.4)         | 565 (86.5)   | 394 (93.1)      | 0.002      |
|  | G3                             | 6 (14.6)          | 88 (13.5)    | 29 (6.9)        |            |
| Vascular invasion ( $n = 1118$ )           | Absent                         | 22 (53.7)         | 463 (70.8)   | 314 (74.2)      | 0.017      |
|  | Present                        | 19 (46.3)         | 191 (29.2)   | 109 (25.8)      |            |
| Tumour border configuration ( $n = 1118$ ) | Pushing                        | 32 (78.1)         | 521 (79.7)   | 337 (79.7)      | 0.969      |
|  | Infiltrating                   | 9 (21.9)          | 133 (20.3)   | 86 (20.3)       |            |
| Five-year survival rate ( $n = 1054$ )     | (95% confidence interval (CI)) | 35.6 (21–50)      | 49.7 (45–54) | 62.4 (57–67)    | <0.001     |

PD-L1 expression and no or low PD-L1 expression, respectively. This difference was significant in univariate analysis ( $P = 0.003$ ; HR = 0.84 (0.79–0.88); Table 3). A training set consisting of about 1/3 of the MMR-proficient CRC cases was also stained with the second polyclonal antibody preparation. With either staining high PD-L1 expression levels positively correlated with improved overall survival ( $P = 0.0001$  and  $P = 0.008$ , respectively; Fig. 3A and B). The remaining samples were stained with only one antibody. In this validation set, similar significant results were observed ( $P = 0.035$ ; Fig. 3C). Several randomisations of the overall MMR-proficient cohort were tested and all results were found to be comparable.

In MMR-deficient CRC no significant correlation between PD-L1 expression and survival could be observed (data not shown).

In multivariate Cox regression analysis including age, gender, T stage, N stage, tumour grade, vascular invasion, invasive margin and MMR status, a trend ( $P = 0.052$ ) suggesting a correlation between high PD-L1 expression in tumour cells and improved survival in CRC could still be observed (Table 3). These uni- and multivariate results indicate a significant, moderate correlation (HR = 0.85) between high expression of PD-L1 and good prognosis.

### 3.6. PD-L1 expression in tumour infiltrating cells

PD-L1 expression in non-cancerous interstitial cells was usually limited (cell/punch range: 0–44; median/mean: 0 cell/punch), as tested in a more restricted test

group of MMR-proficient CRC ( $n = 424$ ). However, classification and regression tree analysis<sup>33,34</sup> helped to define a cut-off (22 cells/punch) that identified a small (2.5%) percentage of cases with relatively high PD-L1 positive cell infiltration. Patients bearing these tumours also had a significantly ( $P = 0.006$ ) improved survival as compared with patients bearing tumours with lower interstitial numbers of PD-L1 positive cells (Figs. 1E and 3B). This correlation was confirmed by Cox regression analyses based on dichotomous values ( $P = 0.0001$ ; HR = 0.78, CI = 0.71–0.84) or on continuous values ( $P = 0.026$ ; HR = 0.97, CI = 0.96–0.98).

### 3.7. Correlation between IFN- $\gamma$ and PDL-1 gene expression in CRC

Detection of programmed death receptor ligand 1 (PDL-1) expression in melanoma cells has recently been suggested to mirror IFN- $\gamma$  gene expression by tumour infiltrating lymphocytes.<sup>37</sup> In order to verify whether a similar association could also be postulated in CRC, the expression of PDL-1 and IFN- $\gamma$  genes was quantitatively evaluated in surgically excised tumour specimens ( $n = 42$ ). Indeed, we found that expression of PDL-1 and IFN- $\gamma$  genes were significantly correlated ( $P = 0.03$ ,  $r = 0.33$ ).

## 4. Discussion

The aim of this study was to analyse the expression of PD-L1 in a large series of CRC samples and to evaluate its clinical relevance. Here we report that untransformed

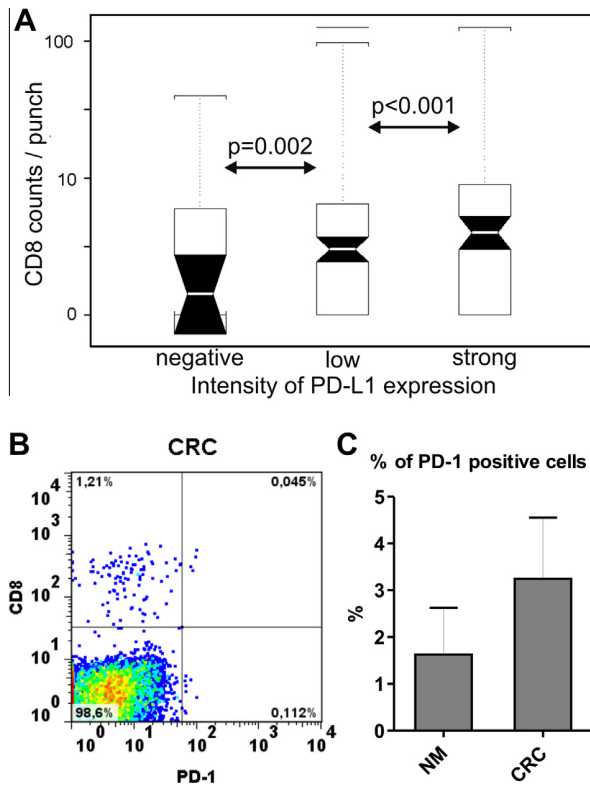


Fig. 2. CD8<sup>+</sup> T-cell infiltration in colorectal cancer (CRC): numbers and phenotype. (A) Absolute numbers of CD8<sup>+</sup> T-cells counted in individual CRC punches (*n* = 1082) were correlated with the intensity of programmed cell death ligand 1 (PD-L1) specific staining, as detectable in the same specimen. (B and C) CRC surgical specimens were enzymatically digested and immediately stained with fluorochrome labelled mAbs recognising CD8 and PD-1. Panel B reports one representative staining, whereas panel C summarises results from the seven freshly excised specimens investigated for PD-1 expression on CD8<sup>+</sup> cells in this study. Data in panel B are expressed as percentages of the total number of cells in the digested specimen, whereas data in panel C are expressed as percentages of CD8<sup>+</sup> cells showing evidence of PD-1 expression. NM = normal mucosa.

normal epithelial cells of colon mucosa do express PD-L1. More importantly, we have observed that PD-L1 expression is markedly enhanced in tumour cells in over 30% of CRC.

Unexpectedly, strong PD-L1 expression in MMR-proficient CRC was found to be associated with early tumour stage, absence of lymph node metastases, lower tumour grade, absence of vascular invasion and a significantly improved 5-year survival. More remarkably, a strong PD-L1 expression in CRC appeared to be paradoxically associated with high numbers of tumour infiltrating CD8<sup>+</sup> T cells. These cells however, did not express the PD-1 co-receptor. High PD-L1 expression in non-cancerous interstitial cells, as detectable in a small number of cases (2.5%), was also found to be associated with a more favourable prognosis.

Cancers are frequently infiltrated by lymphocytes and TILs are widely considered to reflect host immune response against malignancy.<sup>38</sup> In defined cancer types, tumour-infiltration by lymphocytes has been shown to be associated with improved prognosis. In particular, CRC infiltration by CD3<sup>+</sup> T cells or by CD8<sup>+</sup> lymphocytes expressing the CD45RO activation marker has been suggested to be endowed with high prognostic value.<sup>1</sup>

However, tumour-immune system interaction is highly dynamic. Cancer cells might escape from destruction by immunocompetent cells by taking advantage of a range of different mechanisms.<sup>39</sup> Down-regulation of the expression of HLA determinants or tumour associated antigens or alterations in the antigen processing machinery might prevent tumour cell recognition by specific T cells.<sup>40</sup> Alternatively, production of immunosuppressive factors or intratumoural recruitment of immunosuppressive cell populations, including regulatory T-cells and myeloid derived suppressor cells,<sup>39</sup> might contribute to the generation of a tumour microenvironment unfavourable to the elicitation of effective antitumour immune responses.

Notably, it has been shown that cancer cells from solid tumours are able to up-regulate the expression of PD-1 ligands, thereby providing inhibitory signals down-modulating T-cell activation and ultimately shutting down immune responses<sup>41</sup> and inducing specific tolerance.<sup>42</sup> Expression of PD-1 ligands on tumour cells was also shown to suppress the cytolytic activity of CD8<sup>+</sup> T cells.<sup>12,13</sup> Indeed, PD-L1 has been shown to

Table 3  
Uni- and multivariate Cox-regression analysis in all colorectal cancers (CRCs) (*n* = 1420).

| Features                               | Univariate                                       |                 | Multivariate     |                 |
|--|--|-----------------|------------------|-----------------|
|  | Hazard ratio (HR) (95% confidence interval (CI)) | <i>P</i> -value | HR (95% CI)      | <i>P</i> -value |
| Programmed cell death ligand 1 (PD-L1) | 0.85 (0.81–0.89)                                 | 0.0003          | 0.92 (0.88–0.96) | 0.052           |
| Age (continuous)                       | 1.02 (1.02–1.02)                                 | <0.0001         | 1.03 (1.02–1.04) | <0.0001         |
| Sex (men–women)                        | 1.16 (1.12–1.20)                                 | 0.0002          | 1.17 (1.13–1.21) | <0.0001         |
| pT (pT: 1, 2, 3, 4)                    | 3.14 (1.76–5.61)                                 | <0.0001         | 1.79 (1.71–1.87) | <0.0001         |
| Grade (1, 2, 3)                        | 1.78 (1.67–1.88)                                 | <0.0001         | 1.14 (1.02–1.26) | 0.29            |
| pN (pN: 0, 1, 2)                       | 2.41 (2.36–2.46)                                 | <0.0001         | 1.91 (1.85–1.97) | <0.0001         |
| Vascular invasion                      | 2.78 (2.69–2.86)                                 | <0.0001         | 1.45 (1.36–1.54) | <0.0001         |
| Invasive margins                       | 2.50 (2.41–2.59)                                 | <0.0001         | 1.63 (1.53–1.73) | <0.0001         |
| Mismatch repair (MMR) status           | 1.74 (1.61–1.87)                                 | <0.0001         | 1.72 (1.59–1.76) | <0.0001         |

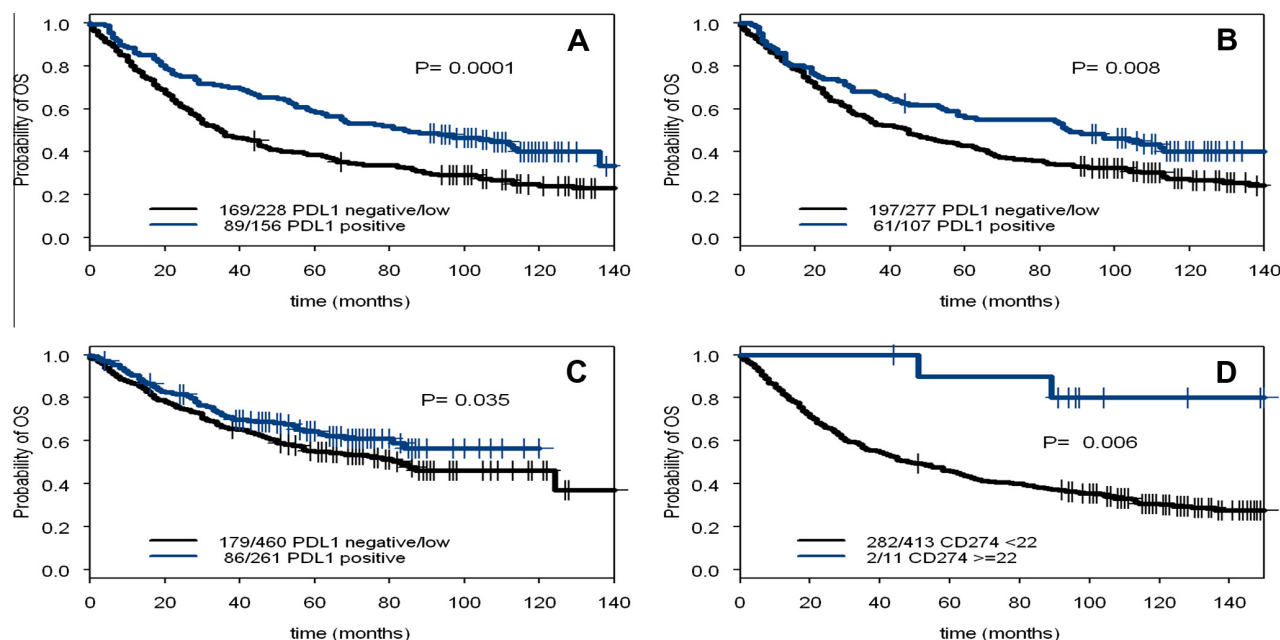


Fig. 3. Effect of programmed cell death ligand 1 (PD-L1) expression by cancer and tumour infiltrating cells on overall survival in patients with mismatch repair (MMR)-proficient colorectal cancer (CRC). Kaplan–Meier overall survival curves of patients bearing MMR-proficient CRC divided into training and validation set. Stratification occurs according to strong PD-L1 staining of tumour cells (blue line) and low to absent PD-L1 expression in tumour cells (black line). (A) Set 1, PD-L1 detection by monoclonal antibody. (B) Set 1, PD-L1 detection by polyclonal antibodies as scored by a second investigator. (C) Set 2: validation set. (D) Kaplan–Meier overall survival curves stratified according to PD-L1 expression in cancer infiltrating cells. Data refer to high (blue line) or low to absent (black line) infiltration by PD-L1+ cells. The threshold was defined at  $\geq 22$  cells per punch (see Section 2).

be expressed in different tumours, including glioblastoma, pancreas, ovarian, breast, renal cell carcinomas, head and neck squamous cell carcinomas as well as oesophageal, and non-small cell lung cancers.<sup>14–17,24,43,44</sup> Most importantly, a strong correlation between the expression of PD-1 ligands on tumour cells and severe prognosis has been observed.

Based on this background, the inhibition of PD-1/PD-L1 interaction has been proposed as a therapeutic target and PD-1 and PD-L1 specific monoclonal antibodies have been successfully developed and tested in phase I clinical trials.<sup>19–21</sup> In this context, our results are surprising and underline the specificities of tumour immune system interaction in CRC. Importantly however, no clinical responses have been observed to date in patients with CRC treated with therapeutic antibodies against PD-1 or PD-L1.<sup>20,21</sup>

What are the possible mechanisms underlying the favourable effect of PD-L1 over-expression in MMR-proficient CRC? Our data clearly indicate that CD8<sup>+</sup> T cell infiltration is unexpectedly increased in MMR-proficient CRC with high PD-L1 expression. These TILs do not express PD-1.

It is of note that in our study, overexpression of PD-L1 in tumour cells was not associated with an improved survival in MMR-deficient CRC. These tumours are known to be infiltrated by higher numbers of lymphocytes and to be characterised by a more favourable

prognosis as compared to MMR proficient tumours.<sup>26</sup> Thus, we might hypothesise that the association between PD-L1 expression in CRC cells and favourable prognosis in MMR proficient tumours could be related to the concomitant increase in CD8<sup>+</sup> T cell infiltration.

Interestingly, IFN- $\gamma$  gene expression in CRC tissues has been reported to be associated with a favourable prognosis.<sup>2</sup> This cytokine, typically produced by activated T cells has been shown to promote the expression of PD-1 ligands in different cell types, thus suggesting that the association of PD-L1 overexpression in MMR proficient CRC with a favourable prognosis might mirror tumour infiltration by IFN- $\gamma$  producing T cells.<sup>37</sup> Indeed, we found that PDL-1 and IFN- $\gamma$  gene expression are significantly ( $r = 0.33$ ,  $P = 0.03$ ) correlated in CRC. However, since PDL-1 gene expression was also observed in the absence of detectable IFN- $\gamma$  gene expression, other, presently undefined mechanisms are also likely to be involved in the elicitation of the favourable prognostic effects associated with PDL-1 expression by CRC cells.

On the other hand, the intestinal immune system is shaped by a continuous interaction with commensal microbiota.<sup>45</sup> Possibly, as a consequence of this specific microenvironment, CRC infiltration by immunocompetent cells is associated with paradoxically peculiar features.<sup>46</sup> Indeed, we and others<sup>26,47</sup> have previously demonstrated that, in contrast to a wide range of human

cancers, CRC infiltration by FOXP3<sup>+</sup> regulatory T cells, is associated with an improved prognosis. Furthermore, it has been observed that CRC infiltration by myeloid cells is also associated with a favourable prognosis.<sup>48,49</sup>

The results of this study contribute to the characterisation of the complex features inherent with gut micro-environment and with CRC-immune system interaction. Further research is warranted to clarify molecular mechanisms underlying increased CD8<sup>+</sup> T cell infiltration in PD-L1-high CRC. Nevertheless, PD-L1 expression in MMR-proficient CRC appears to play a conspicuously different role, as compared to a large variety of other solid tumours. Indeed, our data suggest that the role of immunological checkpoint markers could be different in different anatomical districts.

### Conflict of interest statement

None declared.

### Acknowledgements

Financial support was provided by the Swiss National Fund for scientific research (SNF) Grant No. PP00P3-133699 and 31003A-122235 and by the Italian Association for Cancer Research (AIRC) IG Grant No. 10555.

### References

- Galon J, Costes A, Sanchez-Cabo F, et al. Type, density, and location of immune cells within human colorectal tumors predict clinical outcome. *Science* 2006;**313**:1960–4.
- Pages F, Berger A, Camus M, et al. Effector memory T cells, early metastasis, and survival in colorectal cancer. *N Engl J Med* 2005;**353**:2654–66.
- Khoury SJ, Sayegh MH. The roles of the new negative T cell costimulatory pathways in regulating autoimmunity. *Immunity* 2004;**20**:529–38.
- Okazaki T, Honjo T. The PD-1–PD-L pathway in immunological tolerance. *Trends Immunol* 2006;**27**:195–201.
- Curiel TJ, Wei S, Dong H, et al. Blockade of B7-H1 improves myeloid dendritic cell-mediated antitumor immunity. *Nat Med* 2003;**9**:562–7.
- Freeman GJ, Long AJ, Iwai Y, et al. Engagement of the PD-1 immunoinhibitory receptor by a novel B7 family member leads to negative regulation of lymphocyte activation. *J Exp Med* 2000;**192**:1027–34.
- Latchman Y, Wood CR, Chernova T, et al. PD-L2 is a second ligand for PD-1 and inhibits T cell activation. *Nat Immunol* 2001;**2**:261–8.
- Keir ME, Liang SC, Guleria I, et al. Tissue expression of PD-L1 mediates peripheral T cell tolerance. *J Exp Med* 2006;**203**:883–95.
- Keir ME, Butte MJ, Freeman GJ, Sharpe AH. PD-1 and its ligands in tolerance and immunity. *Annu Rev Immunol* 2008;**26**:677–704.
- Shin T, Yoshimura K, Shin T, et al. In vivo costimulatory role of B7-DC in tuning T helper cell 1 and cytotoxic T lymphocyte responses. *J Exp Med* 2005;**201**:1531–41.
- Zhang L, Gajewski TF, Kline J. PD-1/PD-L1 interactions inhibit antitumor immune responses in a murine acute myeloid leukemia model. *Blood* 2009;**114**:1545–52.
- Hirano F, Kaneko K, Tamura H, et al. Blockade of B7-H1 and PD-1 by monoclonal antibodies potentiates cancer therapeutic immunity. *Cancer Res* 2005;**65**:1089–96.
- Iwai Y, Ishida M, Tanaka Y, Okazaki T, Honjo T, Minato N. Involvement of PD-L1 on tumor cells in the escape from host immune system and tumor immunotherapy by PD-L1 blockade. *Proc Natl Acad Sci U S A* 2002;**99**:12293–7.
- Konishi J, Yamazaki K, Azuma M, Kinoshita I, Dosaka-Akita H, Nishimura M. B7-H1 expression on non-small cell lung cancer cells and its relationship with tumor-infiltrating lymphocytes and their PD-1 expression. *Clin Cancer Res* 2004;**10**:5094–100.
- Ohgashi Y, Sho M, Yamada Y, et al. Clinical significance of programmed death-1 ligand-1 and programmed death-1 ligand-2 expression in human esophageal cancer. *Clin Cancer Res* 2005;**11**:2947–53.
- Strome SE, Dong H, Tamura H, et al. B7-H1 blockade augments adoptive T-cell immunotherapy for squamous cell carcinoma. *Cancer Res* 2003;**63**:6501–5.
- Thompson RH, Gillett MD, Chevillat JC, et al. Costimulatory B7-H1 in renal cell carcinoma patients: indicator of tumor aggressiveness and potential therapeutic target. *Proc Natl Acad Sci U S A* 2004;**101**:17174–9.
- Wintterle S, Schreiner B, Mitsdoerffer M, et al. Expression of the B7-related molecule B7-H1 by glioma cells: a potential mechanism of immune paralysis. *Cancer Res* 2003;**63**:7462–7.
- Brahmer JR, Drake CG, Wollner I, et al. Phase I study of single-agent anti-programmed death-1 (MDX-1106) in refractory solid tumors: safety, clinical activity, pharmacodynamics, and immunologic correlates. *J Clin Oncol* 2010;**28**:3167–75.
- Brahmer JR, Tykodi SS, Chow LQ, et al. Safety and activity of anti-PD-L1 antibody in patients with advanced cancer. *N Engl J Med* 2012;**366**:2455–65.
- Topalian SL, Hodi FS, Brahmer JR, et al. Safety, activity, and immune correlates of anti-PD-1 antibody in cancer. *N Engl J Med* 2012;**366**:2443–54.
- Kallioniemi OP, Wagner U, Kononen J, Sauter G. Tissue microarray technology for high-throughput molecular profiling of cancer. *Hum Mol Genet* 2001;**10**:657–62.
- Sauter G, Simon R, Hillan K. Tissue microarrays in drug discovery. *Nat Rev Drug Discov* 2003;**2**:962–72.
- Hamanishi J, Mandai M, Iwasaki M, et al. Programmed cell death 1 ligand 1 and tumor-infiltrating CD8<sup>+</sup> T lymphocytes are prognostic factors of human ovarian cancer. *Proc Natl Acad Sci U S A* 2007;**104**:3360–5.
- Loos M, Langer R, Schuster T, et al. Clinical significance of the costimulatory molecule B7-H1 in Barrett carcinoma. *Ann Thorac Surg* 2011;**91**:1025–31.
- Frey DM, Droezer RA, Viehl CT, et al. High frequency of tumor-infiltrating FOXP3(+) regulatory T cells predicts improved survival in mismatch repair-proficient colorectal cancer patients. *Int J Cancer* 2010;**126**:2635–43.
- Zlobec I, Karamitopoulou E, Terracciano L, et al. TIA-1 cytotoxic granule-associated RNA binding protein improves the prognostic performance of CD8 in mismatch repair-proficient colorectal cancer. *PLoS One* 2010;**5**:e14282.
- Lugli A, Zlobec I, Baker K, et al. Prognostic significance of mucins in colorectal cancer with different DNA mismatch-repair status. *J Clin Pathol* 2007;**60**:534–9.
- Baker K, Zlobec I, Tornillo L, Terracciano L, Jass JR, Lugli A. Differential significance of tumour infiltrating lymphocytes in sporadic mismatch repair deficient versus proficient colorectal cancers: a potential role for dysregulation of the transforming growth factor-beta pathway. *Eur J Cancer* 2007;**43**:624–31.
- Feder-Mengus C, Schultz-Thater E, Oertli D, et al. Nonreplicating recombinant vaccinia virus expressing CD40 ligand enhances APC capacity to stimulate specific CD4<sup>+</sup> and CD8<sup>+</sup> T cell responses. *Hum Gene Ther* 2005;**16**:348–60.

31. Martin I, Jakob M, Schafer D, Dick W, Spagnoli G, Heberer M. Quantitative analysis of gene expression in human articular cartilage from normal and osteoarthritic joints. *Osteoarthritis Cartilage* 2001;**9**:112–8.
32. Livak KJ, Schmittgen TD. Analysis of relative gene expression data using real-time quantitative PCR and the 2<sup>-</sup>(Delta Delta C(T)) method. *Methods* 2001;**25**:402–8.
33. Barlow RE, Bartholomew DJ, Bremner JM. *Statistical inference under order restrictions: theory and application of isotonic regression*. London: John Wiley & Sons Ltd.; 1972.
34. Breiman L, Friedman J, Stone CJ. *Classification and regression trees*. Chapman & Hall/CRC; 1984.
35. McShane LM, Altman DG, Sauerbrei W, Taube SE, Gion M, Clark GM. Reporting recommendations for tumor marker prognostic studies (REMARK). *J Natl Cancer Inst* 2005;**97**:1180–4.
36. Kanavaros P, Boulland ML, Petit B, Arnulf B, Gaulard P. Expression of cytotoxic proteins in peripheral T-cell and natural killer-cell (NK) lymphomas: association with extranodal site, NK or Tgammadelta phenotype, anaplastic morphology and CD30 expression. *Leuk Lymphoma* 2000;**38**:317–26.
37. Taube JM, Anders RA, Young GD, et al. Colocalization of inflammatory response with B7-h1 expression in human melanocytic lesions supports an adaptive resistance mechanism of immune escape. *Sci Transl Med* 2012;**4**:127ra37.
38. Mantovani A, Romero P, Palucka AK, Marincola FM. Tumour immunity: effector response to tumour and role of the microenvironment. *Lancet* 2008;**371**:771–83.
39. Schreiber RD, Old LJ, Smyth MJ. Cancer immunoeediting: integrating immunity's roles in cancer suppression and promotion. *Science* 2011;**331**:1565–70.
40. Ferris RL, Whiteside TL, Ferrone S. Immune escape associated with functional defects in antigen-processing machinery in head and neck cancer. *Clin Cancer Res* 2006;**12**:3890–5.
41. Zou W. Immunosuppressive networks in the tumour environment and their therapeutic relevance. *Nat Rev Cancer* 2005;**5**:263–74.
42. Francisco LM, Salinas VH, Brown KE, et al. PD-L1 regulates the development, maintenance, and function of induced regulatory T cells. *J Exp Med* 2009;**206**:3015–29.
43. Parsa AT, Waldron JS, Panner A, et al. Loss of tumor suppressor PTEN function increases B7-H1 expression and immunoresistance in glioma. *Nat Med* 2007;**13**:84–8.
44. Pardoll D, Drake C. Immunotherapy earns its spot in the ranks of cancer therapy. *J Exp Med* 2012;**209**:201–9.
45. Kau AL, Ahern PP, Griffin NW, Goodman AL, Gordon JI. Human nutrition, the gut microbiome and the immune system. *Nature* 2011;**474**:327–36.
46. Ladoire S, Martin F, Ghiringhelli F. Prognostic role of FOXP3+ regulatory T cells infiltrating human carcinomas: the paradox of colorectal cancer. *Cancer Immunol Immunother* 2011;**60**:909–18.
47. Salama P, Phillips M, Grieu F, et al. Tumor-infiltrating FOXP3+ T regulatory cells show strong prognostic significance in colorectal cancer. *J Clin Oncol* 2009;**27**:186–92.
48. Sconocchia G, Zlobec I, Lugli A, et al. Tumor infiltration by FcgammaRIII (CD16)+ myeloid cells is associated with improved survival in patients with colorectal carcinoma. *Int J Cancer* 2011;**128**:2663–72.
49. Roxburgh CS, McMillan DC. The role of the in situ local inflammatory response in predicting recurrence and survival in patients with primary operable colorectal cancer. *Cancer Treat Rev* 2012;**38**:451–66.



Contents lists available at ScienceDirect

## Advanced Drug Delivery Reviews

journal homepage: [www.elsevier.com/locate/addr](http://www.elsevier.com/locate/addr)

## “In vitro” 3D models of tumor-immune system interaction <sup>☆</sup>

Christian Hirt <sup>a,1</sup>, Adam Papadimitropoulos <sup>b,c,1</sup>, Valentina Mele <sup>a,1</sup>, Manuele G. Muraro <sup>a,1</sup>, Chantal Mengus <sup>a</sup>, Giandomenica Iezzi <sup>d</sup>, Luigi Terracciano <sup>e</sup>, Ivan Martin <sup>b,\*</sup>, Giulio C. Spagnoli <sup>a,\*</sup>

<sup>a</sup> “Oncology” lab., Department of Surgery and Department of Biomedicine, University Hospital Basel, University of Basel, Basel, Switzerland

<sup>b</sup> “Tissue Engineering” lab., Department of Surgery and Department of Biomedicine, University Hospital Basel, University of Basel, Basel, Switzerland

<sup>c</sup> Celtec Biotek, Basel, Switzerland

<sup>d</sup> “Cancer Immunotherapy” lab., Department of Surgery and Department of Biomedicine, University Hospital Basel, University of Basel, Basel, Switzerland

<sup>e</sup> Institute of Pathology, University of Basel, Basel, Switzerland

## ARTICLE INFO

Available online xxxx

## Keywords:

Cancer  
Immune system  
Three-dimensional cultures  
Hypoxia  
Perfusion bioreactors

## ABSTRACT

Interaction between cancer cells and immune system critically affects development, progression and treatment of human malignancies. Experimental animal models and conventional “in vitro” studies have provided a wealth of information on this interaction, currently used to develop immune-mediated therapies. Studies utilizing three-dimensional culture technologies have emphasized that tumor architecture dramatically influences cancer cell–immune system interaction by steering cytokine production and regulating differentiation patterns of myeloid cells, and decreasing the sensitivity of tumor cells to lymphocyte effector functions. Hypoxia and increased production of lactic acid by tumor cells cultured in 3D architectures appear to be mechanistically involved. 3D culture systems could be further developed to (i) include additional cell partners potentially influencing cancer cell–immune system interaction, (ii) enable improved control of hypoxia, and (iii) allow the use of freshly derived clinical cancer specimens. Such advanced models will represent new tools for cancer immunobiology studies and for pre-clinical assessment of innovative treatments.

© 2014 Elsevier B.V. All rights reserved.

## Contents

|  |   |
|--|---|
| 1. Introduction . . . . .  | 0 |
| 2. Tumor immune system interaction: basic concepts and clinical implications . . . . . | 0 |
| 3. Immune contexture of clinical human malignancies . . . . .                          | 0 |
| 4. A third dimension in tumor–immune system interaction . . . . .                      | 0 |
| 5. Challenges for the controlled analysis of tumor–immune system interaction . . . . . | 0 |
| 6. 3D tumor models including multiple cellular partners . . . . .                      | 0 |
| 7. Hypoxia and perfusion in 3D models . . . . .  | 0 |
| 8. Conclusions . . . . .   | 0 |
| Acknowledgments . . . . .  | 0 |
| References . . . . .   | 0 |

### 1. Introduction

The study of the interaction between tumor cells and the immune system represents a very active research field since more than a century

<sup>☆</sup> This review is part of the *Advanced Drug Delivery Reviews* theme issue on “Engineering of Tumor Microenvironments”.

\* Corresponding authors at: “Oncology” and “Tissue Engineering” labs, Institute of Surgical Research and Hospital Management and Department of Biomedicine, University of Basel, 20, Hebelstrasse, 4031, Basel, Switzerland.

E-mail addresses: [ivan.martin@usb.ch](mailto:ivan.martin@usb.ch) (I. Martin), [giulio.spagnoli@usb.ch](mailto:giulio.spagnoli@usb.ch) (G.C. Spagnoli).

<sup>1</sup> Equal contribution.

[1]. The past two decades have provided decisive advances in the understanding of basic cancer immunobiology concepts, which are presently leading to the development of novel immunotherapy treatments of potentially high clinical relevance.

Three dimensional (3D) “in vitro” models are increasingly being used to study cancer cell biology and the interaction of cancer cells with tumor microenvironment under conditions more similar to “in vivo” situation than standard bidimensional (2D) cultures. A number of studies in the last years do suggest that tumor–immune system interactions may also be productively investigated by using 3D culture models.

These technologies might provide an important link between “in vivo” experimental models, standard “in vitro” cultures and clinical

<http://dx.doi.org/10.1016/j.addr.2014.05.003>

0169-409X/© 2014 Elsevier B.V. All rights reserved.

Please cite this article as: C. Hirt, et al., “In vitro” 3D models of tumor-immune system interaction, *Adv. Drug Deliv. Rev.* (2014), <http://dx.doi.org/10.1016/j.addr.2014.05.003>

oncology, possibly accelerating and facilitating the translation of basic advances into innovative treatments.

In this paper, we summarize main concepts underlying the biology of tumor-immune system interactions and then review how they have been studied in 3D cell culture models. Finally, we discuss the possible use of novel 3D culture systems to address open questions in cancer immunobiology.

## 2. Tumor immune system interaction: basic concepts and clinical implications

The interaction with innate and adaptive immune system plays a critical role in cancer development, control and treatment (Fig. 1).

Inflammation is known to promote oncogenesis [2,3], as indicated by increased cancer risk in chronically inflamed organs. A typical example is represented by the higher incidence of colorectal cancers in patients with inflammatory bowel diseases (IBD) [4]. Prostate cancer outgrowth is also typically accompanied by elevated serum levels of IL-6 and other pro-inflammatory cytokines [5,6]. Indeed, aberrant expression and activation of NF- $\kappa$ B and STAT3 transcription factors have been detected in different types of cancer [2,7]. They might directly promote cancer development by a variety of mechanisms, including the inhibition of tumor cell apoptosis and the enhancement of their proliferative potential. Furthermore, STAT3 activity has been suggested to induce epithelial-to-mesenchymal transition (EMT) in cancer cells leading them to lose their cell-cell and cell-ECM interactions, to undergo cytoskeleton reorganization and to gain morphological and functional

characteristics of mesenchymal cells [8,9], ultimately resulting in increased cell motility and invasiveness [10]. Tumor promoting effects have been shown to be mediated by myeloid cells chemoattracted into inflamed areas. These cells might be polarized within the tumor microenvironment towards a tumor associated macrophage (TAM), phenotypic and functional M2 profile characterized by the production of pro-angiogenic factors and cytokines directly stimulating cancer cell proliferation and survival as well as inhibiting the generation of adaptive immune responses or the elicitation of effector functions [11]. Importantly, particularly in experimental models, powerful immunosuppression has also been shown to be exerted by myeloid cells at relatively early maturation stages, collectively referred to as myeloid derived suppressor cells (MDSC) attracted and activated within the tumor microenvironment [12].

Adaptive and innate immune responses including those mediated by natural killer (NK) cells have been shown in experimental models to play central roles in the control of cancer outgrowth. Seminal works by the Schreiber group [13,14] have popularized the notion of the three “Es” marking the different phases of the interaction between cancers and adaptive and innate immune systems within the “immunosurveillance” framework. An early phase characterized by the elimination of transformed cells would be followed by an “equilibrium” phase, prior to the escape of tumor cells from immunosurveillance preluding to clinically significant tumor outgrowth. Most obviously, this concept implies that tumor cells from clinically detectable human cancers may have undergone “immunoediting” and may have been selected based on their ability to evade immune responses. Indeed,

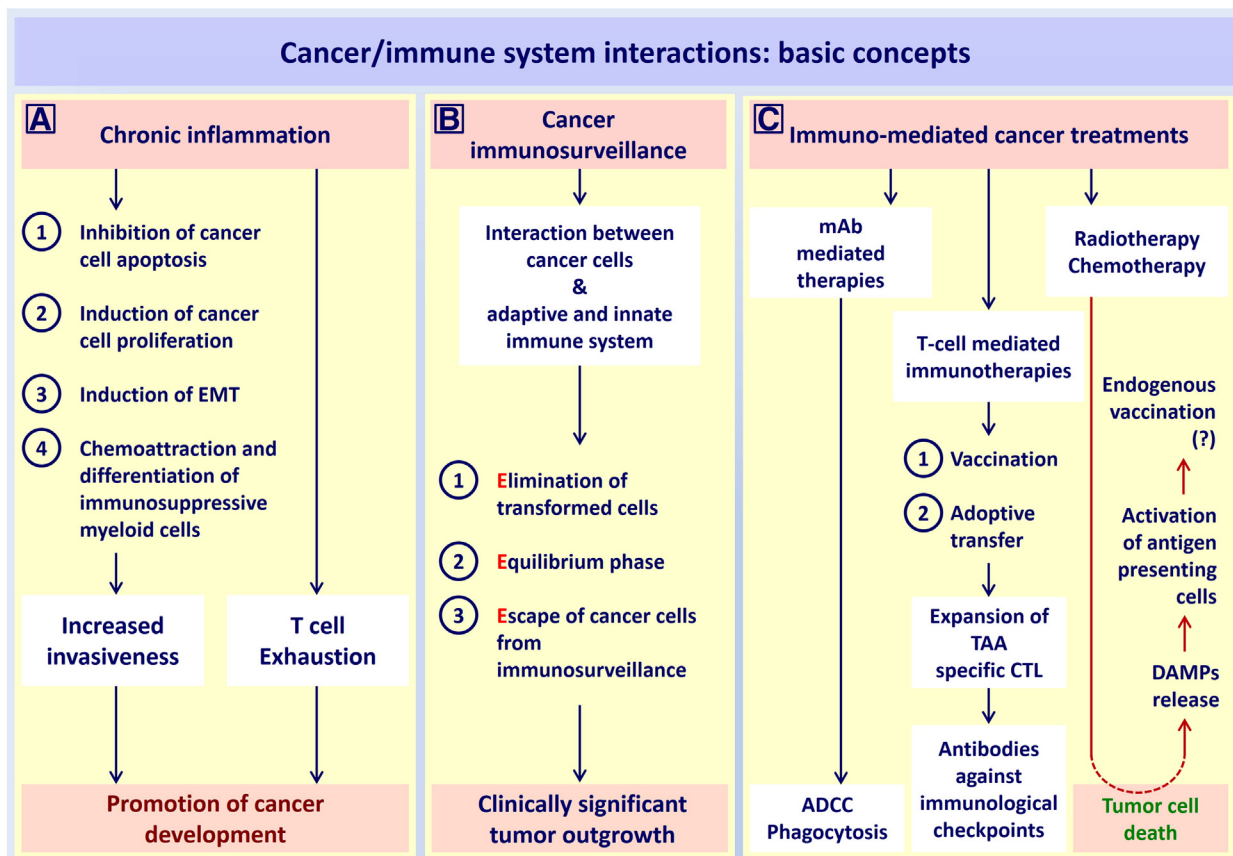


**Fig. 1.** Basic concepts underlying cancer/immune system interaction. Cancer/immune system interaction plays key roles in tumor development, progression and treatment. In particular (panel A), cancer related chronic inflammation is known to promote tumor cell growth and to attract macrophages and induce their differentiation towards a pro-tumoral functional profile also contributing to immunosuppression. Cancer immunosurveillance elicited by T lymphocytes and NK cells (panel B) is assumed to control tumor outgrowth prior to the escape of relatively poorly immunogenic cancer cells, promoting the generation of clinically detectable malignancies. A wide variety of immune-mediated cancer treatments (panel C) are currently used in clinical practice or undergoing clinical evaluation; furthermore, the immune system is supposed to play an important role in the outcome of a variety of conventional treatments, including chemo- and radio-therapy.

human cancers do induce specific T cell responses and may be targeted by effector T cells.

Following the molecular identification of the first human tumor associated antigen (TAA), MAGE-A1, a large number of human TAA expressed by cancer cells and mostly recognized, in MHC class I restricted form, by cytotoxic CD8 + T cells have been described [15, 16]. They include proteins overexpressed in cancer cells, but also detectable in their non transformed counterparts, so called differentiation antigens, and antigens expressed by viruses involved in specific oncogenic processes, such as human papilloma virus (HPV). Additional TAA, the so called cancer/testis antigens, such as those of the MAGE-A family and NY-ESO-1, are aberrantly expressed in cancer cells of diverse histological origin and in healthy spermatogonia or placental cells. Most importantly, mutated gene products of proven oncogenic relevance may also be recognized as antigens by specific T cells [15].

The identification of antigenic determinants expressed by virtually all cancer types has led to the development of a variety of immunization procedures and clinical immunotherapy trials. Antigenic peptides or entire proteins may be administered in the presence of adjuvants or upon pulsing of dendritic cells (DC) [17]. Alternative approaches include the administration of recombinant viruses as vaccines [18,19] and the use of “in vitro” expanded tumor specific T cells for re-infusion in the context of “adoptive” treatments [20]. More recently adoptive transfer of cells transfected with TAA specific T-cell receptor or chimeric antigen receptor (CAR) genes has also been used [21,22].

Regarding active, antigen specific, immunotherapies, it should be noted that specific T cells have been successfully expanded in patients immunized according to a variety of protocols. However, clinical results most frequently have not met expectations, thus suggesting the possibility of the existence of mechanisms blunting treatment effectiveness. Remarkably, tumor infiltrating, TAA specific T cells have also been characterized as functionally impaired or anergic [23]. Basic immunology studies indicate that chronic immunostimulation might lead to lymphocyte exhaustion, mediated by the interaction of markers expressed by activated lymphocytes, such as CTLA4 and PD1 with ligands expressed by antigen presenting cells, or also by tumor cells [24]. Active research in this area has led to the development of human monoclonal antibodies preventing this interaction and the resulting functional exhaustion of TAA specific T cells [25–27]. Based on this background innovative treatments aimed at preventing lymphocyte exhaustion have been recently successfully utilized in clinical oncology [25,27,28]. Although mechanisms of action are still debated [29], promising clinical results have been reported.

On the other hand, both innate and adaptive immune responses have also been suggested to impact on the outcome of conventional chemo and radiotherapy treatments. Malignant cells dying or damaged upon treatment have indeed been shown to release damage associated molecular patterns (DAMPs), including ATP and HMGB1, or expose calreticulin, collectively promoting macrophage activation and ultimately providing endogenous forms of anti-tumor vaccination [30]. Selected chemotherapeutic agents, and, in particular, anthracyclins, cisplatin and gemcitabine have been shown to induce “immunogenic” cell death, possibly leading to the development of tumor specific T cell responses.

Importantly, immunocompetent cells may also influence the effectiveness of antibody-based treatments. A large number of human or humanized monoclonal antibodies (mAbs) are now routinely used in cancer treatment [31]. While immunomodulating mAbs are also being used (see above), most of them were developed with the intent to inhibit the interaction between soluble factors of essential relevance for tumor cell biology, such as EGF or VEGF and their receptors. Their mechanisms of action however, are partially unclear, in that a full display of their therapeutic effectiveness might require Fc receptor expressing myeloid or NK cells and might be mediated by antibody dependent cellular cytotoxicity (ADCC), phagocytosis or by the induction of tumor specific T cells [31]. Based on this background, human mAbs characterized

by improved Fc receptor binding capacity are now being developed and tested in clinical oncology [32].

### 3. Immune contexture of clinical human malignancies

The clinical relevance of tumor infiltration by immunocompetent cells has been highlighted by a large number of studies addressing its prognostic significance [33].

With remarkable exceptions [34], tumor infiltration by myeloid cells indeed appears to be most frequently associated with poor prognosis [35], possibly related to pro-angiogenic activities of alternatively activated M2 macrophages [36] or to immunosuppression mediated by MDSC [12]. On the other hand, in sharp contrast to what anticipated by experimental models, NK cell infiltration of human tumors is usually poor and largely devoid of prognostic relevance [37,38]. Indeed, direct inhibition of NK cell functions by tumor cells has been described [39].

Regarding T cells, tumor infiltration by CD8 + cells, and, in particular, by CD45RO + has frequently been found to be associated with favorable prognosis in cancers of different histological origin [33,37,40]. Instead, the prognostic relevance of tumor infiltration by CD4 + lymphocytes is debated. In particular, CD4 + regulatory T cells (Treg) have been found to infiltrate a variety of cancers. However, whereas in ovarian and breast cancers, among others, Treg infiltration was reported to be associated with poor prognosis [41,42], in colorectal cancer a correlation with favorable clinical outcome was observed [43,44].

Taken together these data powerfully underline the critical relevance of tumor-immune system interaction in cancer outgrowth, control and treatment. Accordingly, they also emphasize the need for an improved understanding of underlying molecular mechanisms. However, particularly for cues emerging from large scale immunohistochemical analysis of clinical specimens, mechanistic insights are difficult to obtain and animal models may provide limited help.

### 4. A third dimension in tumor-immune system interaction

Most data available on tumor/immune system interactions in humans have been obtained by culturing immunocompetent cells isolated from peripheral blood or cancer tissues together with established cell lines in conventional bidimensional “in vitro” conditions. These technologies were essential for the discovery of human TAA or for the characterization of the antigen presenting potential of differentiated DC. However, they fail to account for critical aspects of tumor microenvironment likely playing decisive “in vivo” roles, as suggested, for example, by the frequently detected discrepancies between “in vitro” data and the outcome of clinical immunotherapies designed according to their indications [45]. On the other hand, murine models have emphasized the poor immunogenicity of cancer tissue fragments, as compared to single cell suspensions derived from the same tumor, thus suggesting a pro-tumoral role of tissue architectures [46].

Three-dimensional (3D) tumor spheroids were initially developed to address radio- and chemo-sensitivity of cancer cells “in vitro” under conditions putatively mimicking “in vivo” features more closely than standard culture monolayers [47,48]. The ability of spheroids to reproduce architectural characteristics of normal and cancerous tissues “in vitro” in controlled conditions has attracted the attention of cell biologists [49–51] and has suggested the possibility of integrating different cell types in the same spheroids, as tools to explore tumor microenvironment [52].

In spite of the high relevance of the role played by the interaction between cancer and immunocompetent cells in the tumor microenvironment, only a limited number of studies have used spheroid technologies to address these issues in 3D cultures. Pioneering research by Sutherland et al. [53] suggested that allospecific spleen cells could infiltrate murine cancer spheroids and kill tumor cells. Later studies, however, indicated that lysis of head and neck cancer cells included in multicellular spheroids by lymphokine activated killer (LAK) cells was only

detectable following three days co-culture, as opposed to 4 h for tumor cells cultured in single cell suspensions [54]. The elicitation of ADCC was also reported to be significantly improved by the disruption of spheroids by mAbs recognizing adhesion molecules [55]. Subsequent reports have addressed the activation of autologous tumor infiltrating lymphocytes or antigen specific CD8 + T cell clones by human bladder and lung cancer spheroids. Target cells cultured in 3D were characterized by a significantly lower ability to stimulate cytokine release by specific effector cells as compared to monolayer cultures [56,57], possibly due to inefficient antigen presentation, as related to down-regulation of heat-shock protein 70 [56].

Our group has mainly focused on spheroid formation by melanoma cells [58] and the reactivity of HLA class I restricted cytotoxic T lymphocyte (CTL) clones specific for melanoma differentiation antigens [59,60]. In keeping with studies with cells of different histological origin (see above), we found that, spheroid cultures of established melanoma are poor stimulators of cytokine release by Melan-A/MART-1 or gp100 melanoma differentiation antigen specific CTL clones, as compared to monolayer cultures (Fig. 2). Accordingly, we observed, that T cells specific for melanoma differentiation antigens appear to poorly infiltrate target cells cultured in spheroids (Fig. 3), thus reminding the “non brisk” infiltrate frequently observed in clinical tumor specimens [61].

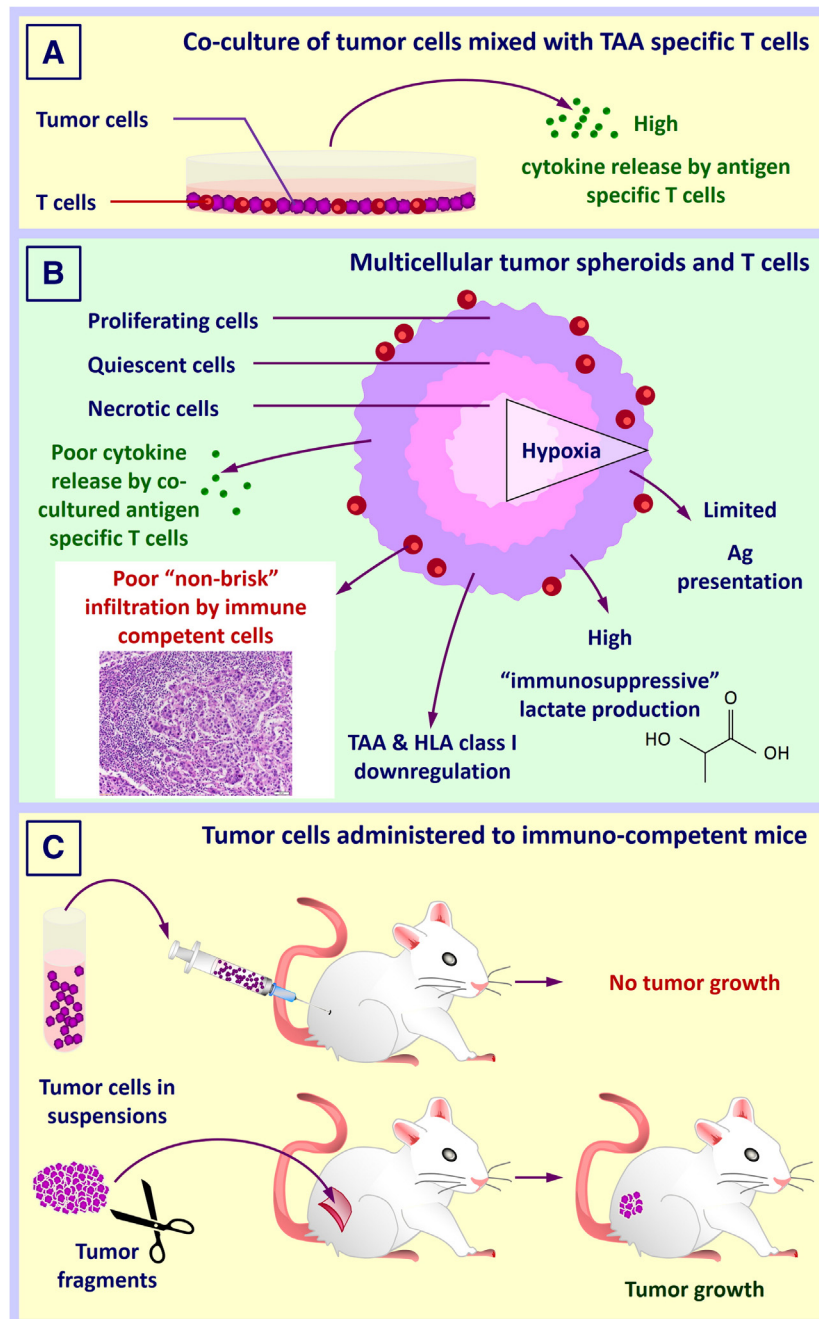


**Fig. 2.** Interaction of antigen specific T cells and cancer cells cultured in three-dimensional architectures. A: Co-culture of TAA specific T lymphocytes with cancer cells in conventional monolayers or in pellets stimulates a high production of “effector” cytokines, typically including IFN- $\gamma$ , and killing of target cells. B: In contrast, co-culture of TAA specific T cells with cancer cell spheroids is usually characterized by a poor infiltration and cytokine production. C: Murine models also suggest that cancer tissue fragments are significantly less immunogenic than corresponding cell suspensions and promote the outgrowth of solid malignancies in immunocompetent animals. While a variety of mechanisms have been proposed, high lactate production by tumor cells cultured in spheroids is generally considered to play a major role in the elicitation of these effects.

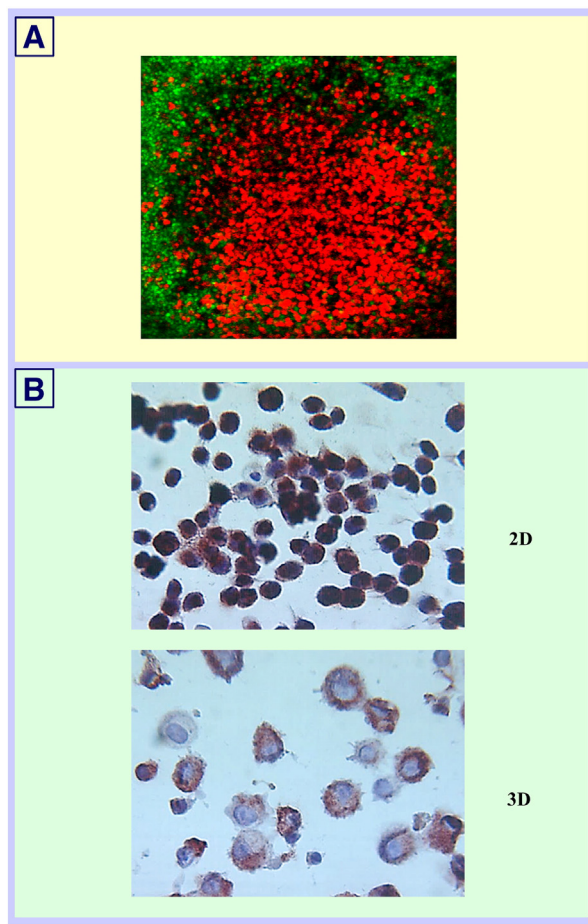


**Fig. 3.** Antigen specific T cells poorly infiltrate tumor spheroids: potential role of down-regulation of TAA expression. A: HLA-A0201 + HBL melanoma cells expressing Melan-A/MART-1 differentiation antigen (red fluorescence) were cultured as spheroids [59] and co-incubated overnight with a HLA-A0201 restricted cytotoxic T lymphocyte (CTL) clone recognizing Melan-A/MART-1<sub>27–35</sub> epitope (green fluorescence). T cells failed to infiltrate melanoma spheroid, consistent with a “non brisk” immunocontexture, as frequently detectable in clinical melanoma samples. B: HBL cells were cultured in conventional monolayers (2D) or in 3D. Spheroids were then mechanically disrupted and Melan-A/MART-1 expression was analyzed by immunocytochemistry by taking advantage of a specific monoclonal reagent in cells pre-cultured in 2D (upper panel) or 3D (lower panel).

Although spheroids generated by using tumor cells of different histological origin or different melanoma cell lines may be infiltrated by activated T cells, the defective T cell activation by putative target cells cultured in tridimensional architectures has been largely confirmed by other groups [62]. More recently, melanoma cells cultured in spheroids were also shown to be able to inhibit mitogen-dependent lymphocyte proliferation [63].

Tumor cells cultured in spheroids are also resistant to NK cell mediated killing, in the absence of therapeutic monoclonal antibodies or cytokine stimulation [64,65].

Other immune-competent cell types are also affected by co-culture with tumor spheroids. In particular, a variety of cells of the myeloid lineage, including monocytes, macrophages and dendritic cells, display altered phenotypic features, motility, cytokine production patterns and differentiation ability, upon culture with cancer cells in spheroids, as compared to monolayer cultures [66,67], ultimately resulting in reduced antigen presentation capacity or even in the promotion of tumor cell proliferation [68].

Depending on the histological origin of the cancer cells under investigation and on specificities inherent in individual cell lines, a variety of potential mechanisms of actions have been identified, including down-regulation of the expression of TAA (Fig. 3) and HLA class I determinants or heat shock proteins involved in antigen processing [56,59]. Importantly similar alterations may relatively frequently be observed in clinical cancer specimens [69,70]. Most interestingly, a number of studies concur in the identification of high lactate production as a unifying mechanism of action underlying the “immunosuppressive” effects of tumor cells cultured in tridimensional architectures [45,59,62,66].

High production of lactate resulting from increased glycolysis in aerobic conditions represents the hallmark of the so-called “Warburg effect” [71]. Indeed, high glucose uptake by cancer cells is routinely utilized for diagnosis and staging of human malignancies by positron-emission tomography (PET) technologies. Although it is now widely recognized that these peculiar respiration modalities are not causing cancer [72,73], and may be differentially detectable in different types of tumors [74,75], they do provide distinct advantages to tumor cells, possibly including the ability to inhibit discrete steps of innate and adaptive immune response.

Proliferating lymphocytes are also metabolically characterized by predominant aerobic glycolysis [76]. Furthermore, glucose availability plays critical roles in the elicitation of effector lymphocyte functions [77,78]. Competition for access to nutrients and low microenvironmental pH could then represent critical limitations for T cell activities and favor the induction of T cell anergy [79]. Remarkably, high tumor-derived lactate production has also been shown to inhibit NK cell function and to increase MDSC numbers “in vivo” [80].

Within this context, hypoxia, a condition frequently detectable in human cancers, appears to be critically involved in the regulation of glucose metabolism in tumor cells mainly through the production of hypoxia-inducible factor 1 (HIF1) [81]. It is thus reasonable to speculate that realistic “in vitro” models of tumor-immune system interaction should also include hypoxia induction.

### 5. Challenges for the controlled analysis of tumor-immune system interaction

Several reviews [82,83], capitalizing on advances in tissue engineering, have highlighted the possibility to generate advanced tissue engineered models providing higher cellular complexity and precise control of tumor surrounding environment.

The development of innovative technologies for the controlled analysis of tumor/immune system interactions is highly challenging but urgently required, particularly when the use of human cells from solid tumors is planned.

Indeed, this necessity largely stems from the poor performance of current “in vivo” models utilizing human cells. Heterotopic implantation of human cell lines derived from solid cancers in immunodeficient animals routinely results in the generation of tumors amenable to genetic, phenotypic and functional analyses. While these models are extremely useful for the evaluation of the tumorigenicity of defined cancer cell subsets, the lack of immune cells and the presence of murine stromal components hamper a systematic understanding of tumor/immune system interaction and of its impact on tumor progression. As a result, this technology may be of limited use, even for drug screening purposes [84,85].

Tumor cell lines, despite their essential relevance for basic biology studies, poorly reproduce the heterogeneity of tumor tissues “in vivo”, thus urging the use of cells or tissue fragments derived from freshly excised cancer specimens. Particularly for carcinomas, viability of tumor cells rapidly decreases upon culture in standard conditions and successful generation of “primary” cultures represents rather the exception than the rule. Implantation in immunodeficient animals frequently results in tumor cell growth and successful xenograft generation. However, human stromal cells are usually substituted by murine cells

thereby introducing additional confounding factors for the analysis of the interaction between tumors and human immune system.

Most obviously, no “in vitro” model could be able to reproduce the complexity of tumor microenvironment “in vivo”. Nevertheless, specific aspects could be productively investigated by using advanced technologies, mostly developed for regenerative medicine and tissue engineering purposes. In particular, we may anticipate that the use of tumor models under perfusion or with controlled levels of ischemia and including non transformed stromal cells might lead to important advances in the comprehension of tumor immune system interactions. Furthermore, the possibility of using viable freshly derived tumor fragments by taking advantage of innovative tissue engineering techniques should be specifically explored.

### 6. 3D tumor models including multiple cellular partners

A main component in the tumor microenvironment is represented by cancer associated fibroblasts (CAF), an activated form of fibroblasts with specific contractile and secretory characteristics [86,87]. CAFs may derive from resident fibroblasts through trans-differentiation promoted by cancer-derived factors, or by bone marrow-derived mesenchymal stromal cells (BM-MSCs) which are recruited at tumor sites by chemokines, cytokines and growth factors produced by tumor cells [87–89]. BM-MSC are known to possess immunosuppressive properties [90,91]. Furthermore, because CAFs are constantly exposed to immune cells and inflammatory cytokines/chemokines in the tumor microenvironment, they may acquire functions that are distinct from those of normal tissue stromal cells, and these unique functions may, in turn, play a role in modulating the tumor microenvironment and ultimately affect tumor progression.

Most interestingly, CAFs are also able to modulate the immune response due to the secretion of the pro-inflammatory cytokines interleukin-1,6,8 and tumor necrosis factor- $\alpha$  (TNF $\alpha$ ) as well as of monocyte chemoattractant protein 1 (MCP1/CCL2) [87]. It has been shown that TNF-activated MSCs promote faster growth of the B16 melanoma and the 4T1 mammary carcinoma. Via CCL2-CCR2 axis, MSCs are also able to recruit tumor associated macrophages (TAMs), a key element of cancer-related inflammation, and may induce a pro-tumorigenic M2-like phenotype [11]. Thus, macrophages and MSCs can engage in a bidirectional interaction resulting in tumor promotion [92,93].

Another important key factor produced by the stromal component is TGF $\beta$ . This cytokine plays a decisive role, in its soluble and membrane bound forms, in the activation of EMT in tumor cells [94,95]. Furthermore, it exerts a wide range of immunosuppressive effects, also related to cancer immunobiology [96,97] including the promotion of Treg generation and M2 macrophage differentiation [98]. Recent studies suggest the possibility of antitumor effects of neutrophils [99,100]. However, exposure of neutrophils to TGF $\beta$  may result in a pro-tumorigenic N2 neutrophil expression profile while inhibition of TGF $\beta$  signalling would switch this cellular phenotype to an anti-tumorigenic N1 phenotype [101]. N2 neutrophils are associated with the expression of pro-tumorigenic factors, such as MMP9, CXCL1, and ARG1. Taken together these data indicate that TGF $\beta$  signaling in the immune system may function as an antagonist suppressing the recognition and the clearance of tumor cells [102].

This scenario suggests that the inclusion of stromal cells in controlled tridimensional “in vitro” systems, as proposed by recent studies [103–105] could help to improve the characterization of the interplay between stromal cells and immunocompetent cells and to test, under controlled conditions, therapeutic strategies potentially counteracting inflammatory mechanisms promoting tumor progression. Importantly, the possibility to use stromal cells directly isolated from clinical specimens could further increase the potential significance of this strategy.

### 7. Hypoxia and perfusion in 3D models

Hypoxia represents a microenvironmental factor decisively contributing to tumor progression by affecting the behavior of tumor, stromal and infiltrating immunocompetent cells. Since three-dimensional cancer models should aim at reproducing, at least in part, the heterogeneity of in-vivo tumors in a controlled fashion, it would be of interest if hypoxic and necrotic areas could be represented. In-vivo, diffusion limited hypoxia occurs because of distance from vessels. “In-vitro” three dimensional culture of cell lines in spheroid architectures mimics the microenvironmental conditions of small avascular tumor regions and micrometastases [47,106]. Time controlled generation of spheroids of different sizes allows the generation of structures reproducibly characterized by normoxic, hypoxic and necrotic areas (Muraro et al, 2013, unpublished observations). Co-culture with immunocompetent cells might provide important information related to chemoattraction and activation of specific cell subsets and establish a relevant tool for the test of innovative anti-inflammatory compounds or immunostimulating agents of potential anti-tumoral significance.

The large majority of the studies cited so far rely on the spontaneous formation of spheroids under conditions preventing the attachment to culture plasticware and favoring cell–cell adhesion. A number of tumor models are also based on the use of scaffold technology, i.e. porous natural or synthetic materials with tailored biological, chemical and mechanical properties providing a 3D structure to cells for growth and tissue formation [107–109]. Recent studies have showed that using this technology it is possible to generate in vitro tumor tissue constructs sharing morphological and functional characteristics of in vivo analogs, as a possible approach to study cancer biology with higher pre-clinical relevance [83,110,111]. However, the major limitations of this technique, which are also common to spheroids and gel embedding systems, are (i) the limited mass transportation, i.e. the reduced and uncontrolled diffusion of oxygen and nutrients inside the newly formed tissue, compromising tissue growth and viability and (ii) the inefficient delivery of compounds in the innermost cells that may affect drug response. Additionally, manual operations associated to the seeding of the scaffolds with cells may profoundly affect subsequent uniform growth of tissue and assay reproducibility.

Perfusion bioreactors may force cell suspensions or culture media to flow through scaffold pores at predefined speed, thereby enhancing their cell seeding efficiency and uniformity as well as the viability of the resulting cell-laid tissue formation through proper delivery of nutrients and removal of waste cell/tissue-by-products [112–115]. This constrained perfusion is a key technological aspect, which is fundamentally different from the convective fluid flow around the scaffold of more conventional dynamic culture systems such as spinner flasks or rotating wall vessels. In this regard, perfusion flow may ideally suit for the efficient delivery of additional cell types or compounds/drugs, and, due to bioreactor configurations and working principles, continuous or intermittent schedules could be applied. Interestingly, the generated flows may mimic naturally occurring interstitial fluid flow and, based on tunable velocity profiles, they may confer mechanically stimulation to the cells in the form of shear stresses, known to alter tumor microenvironment and the metastatic potential of tumor cells [116,117].

In-line sensors able to non-invasively measure crucial culture parameters, including oxygen consumption, pH and CO<sub>2</sub> concentration, and allowing real-time monitoring of cell viability may be incorporated within bioreactor devices [115]. In the context of tumor/immune system interaction, previous studies have demonstrated the compatibility of a perfusion-based bioreactor device with several porous scaffold materials and cell preparations, including freshly isolated cells from clinically relevant sources [118,119]. Notably, the combined use of perfusion with scaffolds was instrumental for the maintenance in co-culture of low adherent cell populations such as hematopoietic and endothelial lineage cells, which are otherwise difficult to establish in scaffolds with manual seeding processes and static cultures [115,119].

Most importantly, the presence of endothelial cells under perfusion has been shown to result in the development of vascularized tissue structures [119]. These bioreactors could be productively combined with scaffold technologies enabling the interaction with defined extracellular matrix proteins and to guide vessel formation [120] to address the challenge of mimicking the irregular nature of tumor microvasculature [82]. Moreover, initial studies by our groups indicate that these systems thanks to the constrained perfusion, can achieve a higher grade of cellular complexity by allowing the seeding of further cell sources within an already formed tissue at different stages of maturation and culture time points, e.g. of hematopoietic [121] or immune competent progenitor cells [122].

Currently, fluid flow-based systems are mostly utilized in tumor immunology for small or large scale expansion of tumor-reactive T-cells for adoptive tumor immunotherapy [123–125]. Other systems are taking advantage of an overflow of 2D plated cells in micro channels [126,127] or using direct flow through over seeded scaffolds in micro-scale [128–130]. By utilizing a macro scale perfusion bioreactor device [115], we were able to rapidly generate large tumor-tissue like structures from the colorectal cancer cell line HT29 on a 3D porous scaffold (Fig. 4). The system can even be adapted for more heterogeneous tissue constructs using co-culture approaches consisting of tumor cells and MSC (Fig. 4).

A perfused culture system not only allows a homogenous distribution of tumor-tissue-structures throughout a scaffold, but also supports the generation of denser tissue structures as compared to static conditions possibly due to improved availability of nutrients and oxygen. Indeed, while tumor-tissue formation in non-perfused systems does

not exceed a few hundred micrometers size [110,131] perfusion reproducibly allows the generation of tissues in a size range of several millimeters. Moreover, oxygen levels can be maintained at specific levels throughout the tissue structures, thus supporting controlled establishment of defined conditions to investigate the role of hypoxia. Comparative evaluation of perfused and not perfused tissues will help to better understand molecular mechanisms underlying the beneficial effects of perfusion on tumor cell cultures.

On the other hand, perfused models could be productively utilized for short term culture and analysis of freshly excised cancer tissues, thereby at least partially bypassing the need of expansion as xenografts or as conventionally established cell cultures. Preliminary data indicate that this is possible, at least with colorectal cancer surgical specimens (Hirt et al., 2013, unpublished). The development of these technologies might allow “in situ” functional analyses of the tumor immune system interaction, as successfully attempted in the past, even by using static collagen gel matrix-supported organ cultures [132]. Importantly, such cultures could take at least partially into account the heterogeneity of both tumor cells and cancer microenvironment.

## 8. Conclusions

The rapid development of novel forms of cancer immunotherapy is urging the establishment of innovative more accurate “in vitro” models able to realistically capture the complexity of tumor microenvironment. “Engineered tumors” should obviously be of tridimensional nature, and include heterogeneous multicellular systems addressing metabolic specificities and the complex interplay of cell–cell and cell–ECM

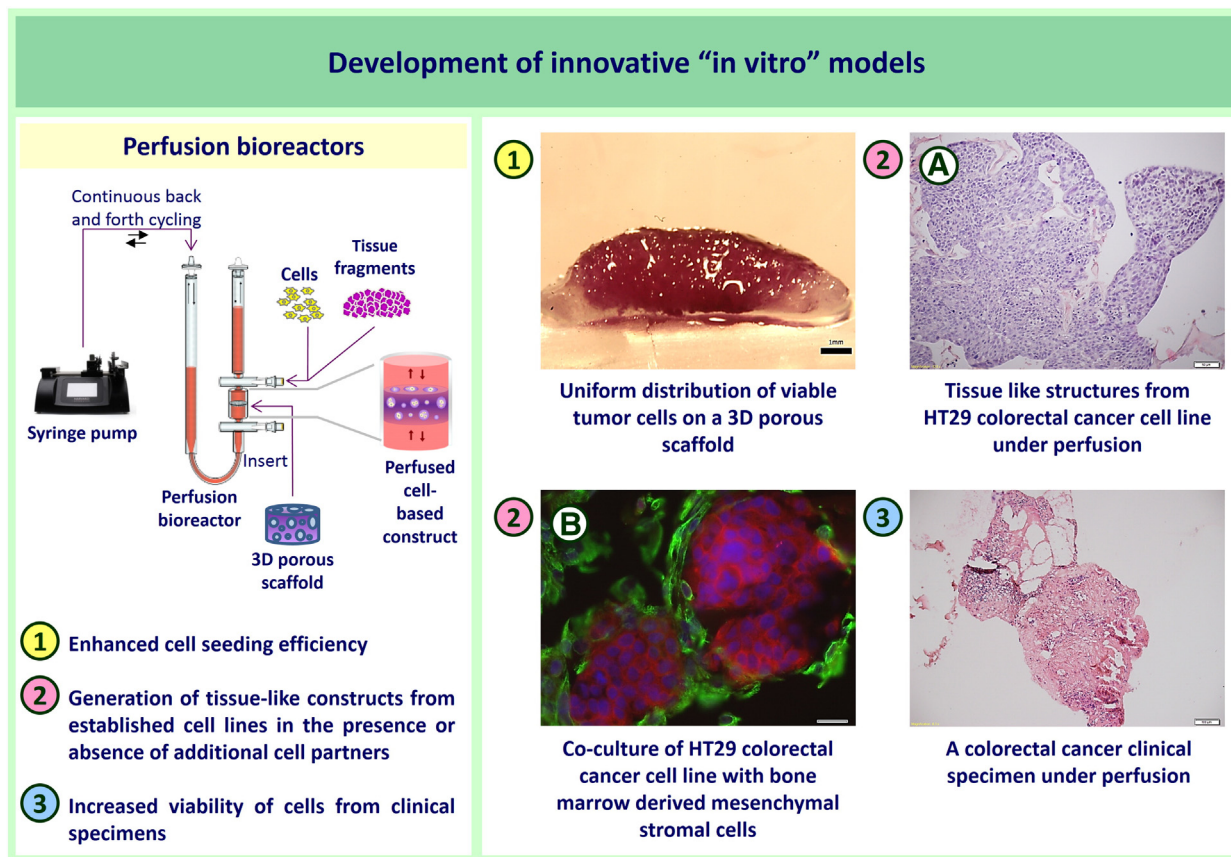


**Fig. 4.** Perfusion bioreactors in the generation and maintenance of tissue-like tumor structures. Perfused bioreactors (left panel) may be used in combination with scaffolds in innovative culture models. Perfusion warrants a uniform distribution of cells on scaffolds (right panel 1) and promotes the generation of relatively large tissue-like structures from established cell lines, in the presence or absence of additional, non transformed cell partners (right panels 2A and 2B, respectively). Furthermore perfused bioreactors may also be used to preserve cell viability and tissue structure in fragments derived from clinical cancer specimens (right panel 3). Bioreactor images are courtesy of Cellec Biotek AG ([www.cellecbiotek.com](http://www.cellecbiotek.com)).

interactions, possibly influencing the response of tumor cells to different subsets of immunocompetent cells.

Well established *in vitro* 3D culture techniques, have shown superiority to conventional monolayer cultures allowing an improved recapitulation of tumor phenotypes and behavior in response to drugs similar, to some extent, to those detectable “*in vivo*” [133]. These models have also started to provide important information regarding the interaction between cancer cells and the immune system [45]. It is tempting to speculate that in a near future culture models including multiple cellular partners and allowing a controlled manipulation of critical metabolic aspects could provide important insights in cancer immunobiology, as related to tumor development and immunotherapy.

In particular, they might be productively used to analyze in highly controlled conditions activation pathways stimulated by the interaction of cancer and myeloid cells, their effects on macrophage chemoattraction and differentiation and their functional outcome, as related to tumor promotion and immunosuppressive effects. The potential anti-tumor role of known or experimental anti-inflammatory compounds could also be pre-clinically evaluated accordingly.

Advanced “*in vitro*” technologies could also support the generation of knowledge towards innovative therapies. In particular optimization of adoptive treatments could be addressed by the analysis of defined steps of T cell extravasation into tumor tissues and pharmacological conditioning of tumor microenvironment in order to favor the elicitation of lymphocyte effector functions. Immunological checkpoint specific mAb might also be tested in these conditions.

These systems could also be utilized to evaluate the ability of chemotherapeutic compounds to induce immunogenic cell death and engineered or bispecific mAbs [131] could also be preliminarily evaluated in the presence of potential effector cells.

Most obviously, further applications of these methods might decisively take advantage of the development of innovative immune system engineering technologies. Successful engineering of secondary lymphoid organs [134,135] and lymphatic vessels [136], might set the stage for studies addressing the molecular background of metastatic progression and immune-system mediated strategies potentially counteracting it.

It is an exciting time for tumor immunology and immune response based treatments are finally exiting experimental phases and gaining the approval of regulatory bodies. Within this context the use of “*in vitro*” engineered tumor systems might accelerate the development of innovative treatment strategies and provide critical insights into cancer immunobiology.

## Acknowledgments

This work was supported by the Swiss National Science Foundation (SNF, 31003A-122235, 310030-127490, PMPD33-118653 and PP00P3-133699), Freiwillige Akademische Gesellschaft (FAG) of the University of Basel and the Kommission für Technologie und Innovation (KTI, Grant number 10761).

## References

- [1] W.B. Coley II, The influence of injury upon the development of sarcoma, *Ann. Surg.* 27 (1898) 259–284.
- [2] F. Colotta, P. Allavena, A. Sica, C. Garlanda, A. Mantovani, Cancer-related inflammation, the seventh hallmark of cancer: links to genetic instability, *Carcinogenesis* 30 (2009) 1073–1081.
- [3] D. Hanahan, R.A. Weinberg, Hallmarks of cancer: the next generation, *Cell* 144 (2011) 646–674.
- [4] T.T. Macdonald, I. Monteleone, M.C. Fantini, G. Monteleone, Regulation of homeostasis and inflammation in the intestine, *Gastroenterology* 140 (2011) 1768–1775.
- [5] Z. Culig, M. Pühr, Interleukin-6: a multifunctional targetable cytokine in human prostate cancer, *Mol. Cell. Endocrinol.* 360 (2012) 52–58.
- [6] C. Mengus, M.C. Le, E. Trella, K. Yousef, L. Bubendorf, M. Provenzano, A. Bachmann, M. Heberer, G.C. Spagnoli, S. Wyler, Elevated levels of circulating IL-7 and IL-15 in patients with early stage prostate cancer, *J. Transl. Med.* 9 (2011) 162.
- [7] M. Karin, Nuclear factor-kappaB in cancer development and progression, *Nature* 441 (2006) 431–436.
- [8] M.A. Nieto, A. Cano, The epithelial–mesenchymal transition under control: global programs to regulate epithelial plasticity, *Semin. Cancer Biol.* 22 (2012) 361–368.
- [9] S. Yamashita, C. Miyagi, T. Fukada, N. Kagara, Y.S. Che, T. Hirano, Zinc transporter LIV1 controls epithelial–mesenchymal transition in zebrafish gastrula organizer, *Nature* 429 (2004) 298–302.
- [10] N. Tiwari, A. Gheldof, M. Tatari, G. Christofori, EMT as the ultimate survival mechanism of cancer cells, *Semin. Cancer Biol.* 22 (2012) 194–207.
- [11] A. Mantovani, P. Allavena, A. Sica, F. Balkwill, Cancer-related inflammation, *Nature* 454 (2008) 436–444.
- [12] D.I. Gabrilovich, S. Ostrand-Rosenberg, V. Bronte, Coordinated regulation of myeloid cells by tumours, *Nat. Rev. Immunol.* 12 (2012) 253–268.
- [13] G.P. Dunn, L.J. Old, R.D. Schreiber, The three Es of cancer immunoeediting, *Annu. Rev. Immunol.* 22 (2004) 329–360.
- [14] R.D. Schreiber, L.J. Old, M.J. Smyth, Cancer immunoeediting: integrating immunity's roles in cancer suppression and promotion, *Science* 331 (2011) 1565–1570.
- [15] L. Novellino, C. Castelli, G. Parmiani, A listing of human tumor antigens recognized by T cells: March 2004 update, *Cancer Immunol. Immunother.* 54 (2005) 187–207.
- [16] P. Van der Bruggen, C. Traversari, P. Chomez, C. Lurquin, E. De Plaen, B. Van den Eynde, A. Knuth, T. Boon, A gene encoding an antigen recognized by cytolytic T lymphocytes on a human melanoma, *Science* 254 (1991) 1643–1647.
- [17] C.G. Figdor, I.J. de Vries, W.J. Lesterhuis, C.J. Melief, Dendritic cell immunotherapy: mapping the way, *Nat. Med.* 10 (2004) 475–480.
- [18] J. Schlom, Therapeutic cancer vaccines: current status and moving forward, *J. Natl. Cancer Inst.* 104 (2012) 599–613.
- [19] P. Zajac, D. Oertli, W. Marti, M. Adamina, M. Bolli, U. Guller, C. Noppen, E. Padovan, E. Schultz-Thater, M. Heberer, G. Spagnoli, Phase I/II clinical trial of a nonreplicative vaccinia virus expressing multiple HLA-A0201-restricted tumor-associated epitopes and costimulatory molecules in metastatic melanoma patients, *Hum. Gene Ther.* 14 (2003) 1497–1510.
- [20] S.A. Rosenberg, N.P. Restifo, J.C. Yang, R.A. Morgan, M.E. Dudley, Adoptive cell transfer: a clinical path to effective cancer immunotherapy, *Nat. Rev. Cancer* 8 (2008) 299–308.
- [21] N.P. Restifo, M.E. Dudley, S.A. Rosenberg, Adoptive immunotherapy for cancer: harnessing the T cell response, *Nat. Rev. Immunol.* 12 (2012) 269–281.
- [22] M. Sadelain, R. Brentjens, I. Riviere, The basic principles of chimeric antigen receptor design, *Cancer Discov.* 3 (2013) 388–398.
- [23] A. Zippelius, P. Batard, V. Rubio-Godoy, G. Bioley, D. Lienard, F. Lejeune, D. Rimoldi, P. Guillaume, N. Meidenbauer, A. Mackensen, N. Rufer, N. Lubenow, D. Speiser, J.C. Cerottini, P. Romero, M.J. Pittet, Effector function of human tumor-specific CD8 T cells in melanoma lesions: a state of local functional tolerance, *Cancer Res.* 64 (2004) 2865–2873.
- [24] R.A. Droeser, C. Hirt, C.T. Viehl, D.M. Frey, C. Nebiker, X. Huber, I. Zlobec, S. Eppenberger-Castori, A. Tzankov, R. Rosso, M. Zuber, M.G. Muraro, F. Amicarella, E. Cremonesi, M. Heberer, G. Iezzi, A. Lugli, L. Terracciano, G. Sconocchia, D. Oertli, G.C. Spagnoli, L. Tornillo, Clinical impact of programmed cell death ligand 1 expression in colorectal cancer, *Eur. J. Cancer* 49 (2013) 2233–2242.
- [25] A.J. Korman, K.S. Peggs, J.P. Allison, Checkpoint blockade in cancer immunotherapy, *Adv. Immunol.* 90 (2006) 297–339.
- [26] S.L. Topalian, C.G. Drake, D.M. Pardoll, Targeting the PD-1/B7-H1 (PD-L1) pathway to activate anti-tumor immunity, *Curr. Opin. Immunol.* 24 (2012) 207–212.
- [27] S.L. Topalian, F.S. Hodi, J.R. Brahmer, S.N. Gettinger, D.C. Smith, D.F. McDermott, J.D. Powderly, R.D. Carvajal, J.A. Sosman, M.B. Atkins, P.D. Leming, D.R. Spigel, S.J. Antonia, L. Horn, C.G. Drake, D.M. Pardoll, L. Chen, W.H. Sharfman, R.A. Anders, J.M. Taube, T.L. McMiller, H. Xu, A.J. Korman, M. Jure-Kunkel, S. Agrawal, D. McDonald, G.D. Kollia, A. Gupta, J.M. Wigginton, M. Sznol, Safety, activity, and immune correlates of anti-PD-1 antibody in cancer, *N. Engl. J. Med.* 366 (2012) 2443–2454.
- [28] J.R. Brahmer, S.S. Tykodi, L.Q. Chow, W.J. Hwu, S.L. Topalian, P. Hwu, C.G. Drake, L.H. Camacho, J. Kauh, K. Odunsi, H.C. Pitot, O. Hamid, S. Bhatia, R. Martins, K. Eaton, S. Chen, T.M. Salay, S. Alaparthi, J.F. Grosso, A.J. Korman, S.M. Parker, S. Agrawal, S.M. Goldberg, D.M. Pardoll, A. Gupta, J.M. Wigginton, Safety and activity of anti-PD-L1 antibody in patients with advanced cancer, *N. Engl. J. Med.* 366 (2012) 2455–2465.
- [29] Y. Bulliard, R. Jolicoeur, M. Windman, S.M. Rue, S. Ettenberg, D.A. Knee, N.S. Wilson, G. Dranoff, J.L. Brogdon, Activating Fc gamma receptors contribute to the antitumor activities of immunoregulatory receptor-targeting antibodies, *J. Exp. Med.* 210 (2013) 1685–1693.
- [30] L. Zitvogel, L. Galluzzi, M.J. Smyth, G. Kroemer, Mechanism of action of conventional and targeted anticancer therapies: reinstating immunosurveillance, *Immunity* 39 (2013) 74–88.
- [31] L.M. Weiner, R. Surana, S. Wang, Monoclonal antibodies: versatile platforms for cancer immunotherapy, *Nat. Rev. Immunol.* 10 (2010) 317–327.
- [32] C.A. Gerdes, V.G. Nicolini, S. Herter, E. van Puijnenbroek, S. Lang, M. Roemmele, E. Moessner, O. Freytag, T. Friess, C.H. Ries, B. Bossenmaier, H.J. Mueller, P. Umama, GA201 (RG7160): a novel, humanized, glycoengineered anti-EGFR antibody with enhanced ADCC and superior *in vivo* efficacy compared with cetuximab, *Clin. Cancer Res.* 19 (2013) 1126–1138.
- [33] W.H. Fridman, F. Pages, C. Sautes-Fridman, J. Galon, The immune contexture in human tumours: impact on clinical outcome, *Nat. Rev. Cancer* 12 (2012) 298–306.
- [34] G. Sconocchia, I. Zlobec, A. Lugli, D. Calabrese, G. Iezzi, E. Karamitopoulou, E.S. Patsouris, G. Peros, M. Horic, L. Tornillo, M. Zuber, R. Droeser, M.G. Muraro, C. Mengus, D. Oertli, S. Ferrone, L. Terracciano, G.C. Spagnoli, Tumor infiltration by FcgammaRIII (CD16)+ myeloid cells is associated with improved survival in patients with colorectal carcinoma, *Int. J. Cancer* 128 (2011) 2663–2672.

- [35] J. Condeelis, J.W. Pollard, Macrophages: obligate partners for tumor cell migration, invasion, and metastasis, *Cell* 124 (2006) 263–266.
- [36] S.K. Biswas, A. Mantovani, Macrophage plasticity and interaction with lymphocyte subsets: cancer as a paradigm, *Nat. Immunol.* 11 (2010) 889–896.
- [37] G. Erdag, J.T. Schaefer, M.E. Smolkin, D.H. Deacon, S.M. Shea, L.T. Dengel, J.W. Patterson, C.L. Slingluff Jr., Immunotype and immunohistologic characteristics of tumor-infiltrating immune cells are associated with clinical outcome in metastatic melanoma, *Cancer Res.* 72 (2012) 1070–1080.
- [38] G. Sconocchia, R. Arriga, L. Tornillo, L. Terracciano, S. Ferrone, G.C. Spagnoli, Melanoma cells inhibit NK cell functions, *Cancer Res.* 72 (2012) 5428–5429.
- [39] E. Mamessier, A. Sylvain, M.L. Thibult, G. Houvenaeghel, J. Jacquemier, R. Castellano, A. Goncalves, P. Andre, F. Romagne, G. Thibault, P. Viens, D. Birnbaum, F. Bertucci, A. Moretta, D. Olive, Human breast cancer cells enhance self tolerance by promoting evasion from NK cell antitumor immunity, *J. Clin. Invest.* 121 (2011) 3609–3622.
- [40] J. Galon, A. Costes, F. Sanchez-Cabo, A. Kirilovsky, B. Mlecnik, C. Lagorce-Page, M. Tosolini, M. Camus, A. Berger, P. Wind, F. Zinzindohoue, P. Bruneval, P.H. Cugnenc, Z. Trajanoski, W.H. Fridman, F. Pages, Type, density, and location of immune cells within human colorectal tumors predict clinical outcome, *Science* 313 (2006) 1960–1964.
- [41] G.J. Bates, S.B. Fox, C. Han, R.D. Leek, J.F. Garcia, A.L. Harris, A.H. Banham, Quantification of regulatory T cells enables the identification of high-risk breast cancer patients and those at risk of late relapse, *J. Clin. Oncol.* 24 (2006) 5373–5380.
- [42] T.J. Curiel, Tregs and rethinking cancer immunotherapy, *J. Clin. Invest.* 117 (2007) 1167–1174.
- [43] D.M. Frey, R.A. Droeser, C.T. Viehl, I. Zlobec, A. Lugli, U. Zingg, D. Oertli, C. Kettelhack, L. Terracciano, L. Tornillo, High frequency of tumor-infiltrating FOXP3(+) regulatory T cells predicts improved survival in mismatch repair-proficient colorectal cancer patients, *Int. J. Cancer* 126 (2010) 2635–2643.
- [44] P. Salama, M. Phillips, F. Griew, M. Morris, N. Zeps, D. Joseph, C. Platell, B. Iacopetta, Tumor-infiltrating FOXP3+ T regulatory cells show strong prognostic significance in colorectal cancer, *J. Clin. Oncol.* 27 (2009) 186–192.
- [45] C. Feder-Mengus, S. Ghosh, A. Reschner, I. Martin, G.C. Spagnoli, New dimensions in tumor immunology: what does 3D culture reveal? *Trends Mol. Med.* 14 (2008) 333–340.
- [46] A.F. Ochsenbein, P. Klenerman, U. Karrer, B. Ludewig, M. Pericin, H. Hengartner, R. M. Zinkernagel, Immune surveillance against a solid tumor fails because of immunological ignorance, *Proc. Natl. Acad. Sci. U. S. A.* 96 (1999) 2233–2238.
- [47] R.M. Sutherland, Cell and environment interactions in tumor microregions: the multicell spheroid model, *Science* 240 (1988) 177–184.
- [48] K.M. Yamada, E. Cukierman, Modeling tissue morphogenesis and cancer in 3D, *Cell* 130 (2007) 601–610.
- [49] J. Debnath, K.R. Mills, N.L. Collins, M.J. Reginato, S.K. Muthuswamy, J.S. Brugge, The role of apoptosis in creating and maintaining luminal space within normal and oncogene-expressing mammary acini, *Cell* 111 (2002) 29–40.
- [50] T. Jacks, R.A. Weinberg, Taking the study of cancer cell survival to a new dimension, *Cell* 111 (2002) 923–925.
- [51] V.M. Weaver, S. Lelievre, J.N. Lakin, M.A. Chrenek, J.C. Jones, F. Giaccanti, Z. Werb, M.J. Bissell, beta4 integrin-dependent formation of polarized three-dimensional architecture confers resistance to apoptosis in normal and malignant mammary epithelium, *Cancer Cell* 2 (2002) 205–216.
- [52] L.A. Kunz-Schughart, M. Kreutz, R. Knuechel, Multicellular spheroids: a three-dimensional in vitro culture system to study tumour biology, *Int. J. Exp. Pathol.* 79 (1998) 1–23.
- [53] R.M. Sutherland, H.R. Macdonald, R.L. Howell, Multicellular spheroids: a new model target for in vitro studies of immunity to solid tumor allografts, *J. Natl. Cancer Inst.* 58 (1977) 1849–1853.
- [54] P.G. Sacks, D.L. Taylor, T. Racz, T. Vasey, V. Oke, S.P. Schantz, A multicellular tumor spheroid model of cellular immunity against head and neck cancer, *Cancer Immunol. Immunother.* 32 (1990) 195–200.
- [55] S.K. Green, M.C. Karlsson, J.V. Ravetch, R.S. Kerbel, Disruption of cell-cell adhesion enhances antibody-dependent cellular cytotoxicity: implications for antibody-based therapeutics of cancer, *Cancer Res.* 62 (2002) 6891–6900.
- [56] V. Dangles-Marie, S. Richon, M. El-Behi, H. Echchakir, G. Dorothee, J. Thiery, P. Validire, I. Vergnon, J. Menez, M. Ladjimi, S. Chouaib, D. Bellet, F. Mami-Chouaib, A three-dimensional tumor cell defect in activating autologous CTLs is associated with inefficient antigen presentation correlated with heat shock protein-70 down-regulation, *Cancer Res.* 63 (2003) 3682–3687.
- [57] V. Dangles, P. Validire, M. Wertheimer, S. Richon, C. Bovin, D. Zeliszewski, G. Vallancien, D. Bellet, Impact of human bladder cancer cell architecture on autologous T-lymphocyte activation, *Int. J. Cancer* 98 (2002) 51–56.
- [58] S. Ghosh, G.C. Spagnoli, I. Martin, S. Ploegert, P. Demougin, M. Heberer, A. Reschner, Three-dimensional culture of melanoma cells profoundly affects gene expression profile: a high density oligonucleotide array study, *J. Cell. Physiol.* 204 (2005) 522–531.
- [59] C. Feder-Mengus, S. Ghosh, W.P. Weber, S. Wyler, P. Zajac, L. Terracciano, D. Oertli, M. Heberer, I. Martin, G.C. Spagnoli, A. Reschner, Multiple mechanisms underlie defective recognition of melanoma cells cultured in three-dimensional architectures by antigen-specific cytotoxic T lymphocytes, *Br. J. Cancer* 96 (2007) 1072–1082.
- [60] S. Ghosh, R. Rosenthal, P. Zajac, W.P. Weber, D. Oertli, M. Heberer, I. Martin, G.C. Spagnoli, A. Reschner, Culture of melanoma cells in 3-dimensional architectures results in impaired immunorecognition by cytotoxic T lymphocytes specific for Melan-A/MART-1 tumor-associated antigen, *Ann. Surg.* 242 (2005) 851–857 (discussion).
- [61] M.C. Mihm Jr., C.G. Clemente, N. Cascinelli, Tumor infiltrating lymphocytes in lymph node melanoma metastases: a histopathologic prognostic indicator and an expression of local immune response, *Lab. Invest.* 74 (1996) 43–47.
- [62] K. Fischer, P. Hoffmann, S. Voelkl, N. Meidenbauer, J. Ammer, M. Etinger, E. Gottfried, S. Schwarz, G. Rothe, S. Hoves, K. Renner, B. Timischl, A. Mackensen, L. Kunz-Schughart, R. Andreesen, S.W. Krause, M. Kreutz, Inhibitory effect of tumor cell-derived lactic acid on human T cells, *Blood* 109 (2007) 3812–3819.
- [63] K. Ramgolam, J. Lauriol, C. Lalou, L. Lauden, L. Michel, P. de la Grange, A.M. Khatib, F. Aoudjit, D. Charron, C. Alcaide-Loridan, R. Al-Daccac, Melanoma spheroids grown under neutral crest cell conditions are highly plastic migratory/invasive tumor cells endowed with immunomodulator function, *PLoS ONE* 6 (2011) e18784.
- [64] T.K. Hoffmann, K. Schirlau, E. Sonkoly, S. Brandau, S. Lang, A. Pivarcsi, V. Balz, A. Muller, B. Homey, E. Boelke, T. Reichert, U. Friebe-Hoffmann, J. Greve, P. Schuler, K. Scheckenbach, J. Schipper, M. Bas, T.L. Whiteside, H. Bier, A novel mechanism for anti-EGFR antibody action involves chemokine-mediated leukocyte infiltration, *Int. J. Cancer* 124 (2009) 2589–2596.
- [65] T.D. Holmes, Y.M. El-Sherbiny, A. Davison, S.L. Clough, G.E. Blair, G.P. Cook, A human NK cell activation/inhibition threshold allows small changes in the target cell surface phenotype to dramatically alter susceptibility to NK cells, *J. Immunol.* 186 (2011) 1538–1545.
- [66] K. Dietl, K. Renner, K. Dettmer, B. Timischl, K. Eberhart, C. Dorn, C. Hellerbrand, M. Kastenberg, L.A. Kunz-Schughart, P.J. Oefner, R. Andreesen, E. Gottfried, M.P. Kreutz, Lactic acid and acidification inhibit TNF secretion and glycolysis of human monocytes, *J. Immunol.* 184 (2010) 1200–1209.
- [67] E. Gottfried, L.A. Kunz-Schughart, S. Ebner, W. Mueller-Klieser, S. Hoves, R. Andreesen, A. Mackensen, M. Kreutz, Tumor-derived lactic acid modulates dendritic cell activation and antigen expression, *Blood* 107 (2006) 2013–2021.
- [68] S. Hauptmann, G. Zwadlo-Klarwasser, M. Jansen, B. Klosterhalfen, C.J. Kirkpatrick, Macrophages and multicellular tumor spheroids in co-culture: a three-dimensional model to study tumor–host interactions. Evidence for macrophage-mediated tumor cell proliferation and migration, *Am. J. Pathol.* 143 (1993) 1406–1415.
- [69] M. Campoli, S. Ferrone, HLA antigen and NK cell activating ligand expression in malignant cells: a story of loss or acquisition, *Semin. Immunopathol.* 33 (2011) 321–334.
- [70] D.S. Widmer, K.S. Hoek, P.F. Cheng, O.M. Eichhoff, T. Biedermann, M.I. Raaijmakers, S. Hemmi, R. Dummer, M.P. Levesque, Hypoxia contributes to melanoma heterogeneity by triggering HIF1alpha-dependent phenotype switching, *J. Invest. Dermatol.* 133 (2013) 2436–2443.
- [71] O. Warburg, On respiratory impairment in cancer cells, *Science* 124 (1956) 269–270.
- [72] S.Y. Lunt, M.G. Vander Heiden, Aerobic glycolysis: meeting the metabolic requirements of cell proliferation, *Annu. Rev. Cell Dev. Biol.* 27 (2011) 441–464.
- [73] M.G. Vander Heiden, L.C. Cantley, C.B. Thompson, Understanding the Warburg effect: the metabolic requirements of cell proliferation, *Science* 324 (2009) 1029–1033.
- [74] K. Dettmer, F.C. Vogl, A.P. Ritter, W. Zhu, N. Nummerger, M. Kreutz, P.J. Oefner, W. Gronwald, E. Gottfried, Distinct metabolic differences between various human cancer and primary cells, *Electrophoresis* 34 (2013) 2836–2847.
- [75] M.O. Yuneva, T.W. Fan, T.D. Allen, R.M. Higashi, D.V. Ferraris, T. Tsukamoto, J.M. Mates, F.J. Alonso, C. Wang, Y. Seo, X. Chen, J.M. Bishop, The metabolic profile of tumors depends on both the responsible genetic lesion and tissue type, *Cell Metab.* 15 (2012) 157–170.
- [76] N.J. MacIver, R.D. Michalek, J.C. Rathmell, Metabolic regulation of T lymphocytes, *Annu. Rev. Immunol.* 31 (2013) 259–283.
- [77] C.M. Cham, T.F. Gajewski, Glucose availability regulates IFN-gamma production and p70S6 kinase activation in CD8+ effector T cells, *J. Immunol.* 174 (2005) 4670–4677.
- [78] C.H. Chang, J.D. Curtis, L.B. Maggi Jr., B. Faubert, A.V. Villarino, D. O'Sullivan, S.C. Huang, G.J. van der Windt, J. Blagih, J. Qiu, J.D. Weber, E.J. Pearce, R.G. Jones, E.L. Pearce, Posttranscriptional control of T cell effector function by aerobic glycolysis, *Cell* 153 (2013) 1239–1251.
- [79] A. Calcinotto, P. Filippazzi, M. Groni, M. Iero, M.A. De, A. Ricupito, A. Cova, R. Canese, E. Jachetti, M. Rossetti, V. Huber, G. Parmiani, L. Generoso, M. Santinami, M. Borghi, S. Fais, M. Bellone, L. Rivoltini, Modulation of microenvironment acidity reverses energy in human and murine tumor-infiltrating T lymphocytes, *Cancer Res.* 72 (2012) 2746–2756.
- [80] Z. Husain, Y. Huang, P. Seth, V.P. Sukhatme, Tumor-derived lactate modifies antitumor immune response: effect on myeloid-derived suppressor cells and NK cells, *J. Immunol.* 191 (2013) 1486–1495.
- [81] N.C. Denko, Hypoxia, HIF1 and glucose metabolism in the solid tumour, *Nat. Rev. Cancer* 8 (2008) 705–713.
- [82] E. Burdett, F.K. Kasper, A.G. Mikos, J.A. Ludwig, Engineering tumors: a tissue engineering perspective in cancer biology, *Tissue Eng. B Rev.* 16 (2010) 351–359.
- [83] D.W. Hutmacher, R.E. Horch, D. Loessner, S. Rizzi, S. Sieh, J.C. Reichert, J.A. Clements, J.P. Beier, A. Arkudas, O. Bleiziffer, U. Kneser, Translating tissue engineering technology platforms into cancer research, *J. Cell. Mol. Med.* 13 (2009) 1417–1427.
- [84] M.R. Juntila, F.J. de Sauvage, Influence of tumour micro-environment heterogeneity on therapeutic response, *Nature* 501 (2013) 346–354.
- [85] M. Singh, N. Ferrara, Modeling and predicting clinical efficacy for drugs targeting the tumor milieu, *Nat. Biotechnol.* 30 (2012) 648–657.
- [86] R. Kalluri, M. Zeisberg, Fibroblasts in cancer, *Nat. Rev. Cancer* 6 (2006) 392–401.
- [87] M.L. Taddei, E. Giannoni, G. Comito, P. Chiarugi, Microenvironment and tumor cell plasticity: an easy way out, *Cancer Lett.* 341 (2013) 80–96.

- [88] R.M. Dwyer, S.M. Potter-Berirne, K.A. Harrington, A.J. Lowery, E. Hennessy, J.M. Murphy, F.P. Barry, T. O'Brien, M.J. Kerin, Monocyte chemotactic protein-1 secreted by primary breast tumors stimulates migration of mesenchymal stem cells, *Clin. Cancer Res.* 13 (2007) 5020–5027.
- [89] E. Spaeth, A. Klopp, J. Dembinski, M. Andreeff, F. Marini, Inflammation and tumor microenvironments: defining the migratory itinerary of mesenchymal stem cells, *Gene Ther.* 15 (2008) 730–738.
- [90] C. Bocelli-Tyndall, L. Bracci, G. Spagnoli, A. Braccini, M. Bouchenaki, R. Ceredig, V. Pistoia, I. Martin, A. Tyndall, Bone marrow mesenchymal stromal cells (BM-MSCs) from healthy donors and auto-immune disease patients reduce the proliferation of autologous- and allogeneic-stimulated lymphocytes in vitro, *Rheumatology (Oxford)* 46 (2007) 403–408.
- [91] A. Uccelli, L. Moretta, V. Pistoia, Mesenchymal stem cells in health and disease, *Nat. Rev. Immunol.* 8 (2008) 726–736.
- [92] R.H. Lee, N. Yoon, J.C. Reneau, D.J. Prockop, Preactivation of human MSCs with TNF- $\alpha$  enhances tumor-suppressive activity, *Cell Stem Cell* 11 (2012) 825–835.
- [93] G. Ren, X. Zhao, Y. Wang, X. Zhang, X. Chen, C. Xu, Z.R. Yuan, A.I. Roberts, L. Zhang, B. Zheng, T. Wen, Y. Han, A.B. Rabson, J.A. Tischfield, C. Shao, Y. Shi, CCR2-dependent recruitment of macrophages by tumor-educated mesenchymal stromal cells promotes tumor development and is mimicked by TNF $\alpha$ , *Cell Stem Cell* 11 (2012) 812–824.
- [94] V. Mele, M.G. Muraro, D. Calabrese, D. Pfaff, N. Amatruda, F. Amicarella, B. Kvinlaug, C. Bocelli-Tyndall, I. Martin, T.J. Resink, M. Heberer, D. Oertli, L. Terracciano, G.C. Spagnoli, G. Iezzi, Mesenchymal stromal cells induce epithelial-to-mesenchymal transition in human colorectal cancer cells through the expression of surface-bound TGF- $\beta$ , *Int. J. Cancer* 134 (2014) 2583–2594.
- [95] V.K. Tiwari Tiwari, L. Waldmeier, P.J. Balwierc, P. Arnold, M. Pachkov, N. Meyer-Schaller, D. Schubeler, E. van Nimwegen, G. Christofori, Sox4 is a master regulator of epithelial-mesenchymal transition by controlling Ezh2 expression and epigenetic reprogramming, *Cancer Cell* 23 (2013) 768–783.
- [96] J.J. Letterio, A.B. Roberts, TGF- $\beta$ : a critical modulator of immune cell function, *Clin. Immunol. Immunopathol.* 84 (1997) 244–250.
- [97] B.E. Lippitz, Cytokine patterns in patients with cancer: a systematic review, *Lancet Oncol.* 14 (2013) e218–e228.
- [98] R.A. Flavell, S. Sanjabi, S.H. Wrzesinski, P. Licona-Limon, The polarization of immune cells in the tumour environment by TGF $\beta$ , *Nat. Rev. Immunol.* 10 (2010) 554–567.
- [99] Z.G. Fridlender, S.M. Albelda, Tumor-associated neutrophils: friend or foe? *Carcinogenesis* 33 (2012) 949–955.
- [100] Z. Granot, E. Henke, E.A. Comen, T.A. King, L. Norton, R. Benezra, Tumor entrained neutrophils inhibit seeding in the premetastatic lung, *Cancer Cell* 20 (2011) 300–314.
- [101] Z.G. Fridlender, J. Sun, S. Kim, V. Kapoor, G. Cheng, L. Ling, G.S. Worthen, S.M. Albelda, Polarization of tumor-associated neutrophil phenotype by TGF- $\beta$ : "N1" versus "N2" TAN, *Cancer Cell* 16 (2009) 183–194.
- [102] M. Pickup, S. Novitskiy, H.L. Moses, The roles of TGF $\beta$  in the tumour microenvironment, *Nat. Rev. Cancer* 13 (2013) 788–799.
- [103] A.K. Clark, A.V. Taubenberger, R.A. Taylor, B. Niranjana, Z.Y. Chea, E. Zotenko, S. Sieh, J.S. Pedersen, S. Norden, M. Frydenberg, J.P. Grummet, D.W. Pook, C. Storzaker, S.J. Clark, M.G. Lawrence, S.J. Ellem, D.W. Huttmacher, G.P. Risbridger, A bioengineered microenvironment to quantitatively measure the tumorigenic properties of cancer-associated fibroblasts in human prostate cancer, *Biomaterials* 34 (2013) 4777–4785.
- [104] H. Dolznig, C. Rupp, C. Puri, C. Haslinger, N. Schweifer, E. Wieser, D. Kerjaschki, P. Garin-Chesa, Modeling colon adenocarcinomas in vitro a 3D co-culture system induces cancer-relevant pathways upon tumor cell and stromal fibroblast interaction, *Am. J. Pathol.* 179 (2011) 487–501.
- [105] K.D. Grugan, C.G. Miller, Y. Yao, C.Z. Michaylira, S. Ohashi, A.J. Klein-Szanto, J.A. Diehl, M. Herlyn, M. Han, H. Nakagawa, A.K. Rustgi, Fibroblast-secreted hepatocyte growth factor plays a functional role in esophageal squamous cell carcinoma invasion, *Proc. Natl. Acad. Sci. U. S. A.* 107 (2010) 11026–11031.
- [106] L.A. Kunz-Schughart, Multicellular tumor spheroids: intermediates between monolayer culture and in vivo tumor, *Cell Biol. Int.* 23 (1999) 157–161.
- [107] D.W. Huttmacher, M. Sittlinger, M.V. Risbud, Scaffold-based tissue engineering: rationale for computer-aided design and solid free-form fabrication systems, *Trends Biotechnol.* 22 (2004) 354–362.
- [108] J.D. Kretlow, A.G. Mikos, 2007 AIChE alpha chi sigma award: from material to tissue: biomaterial development, scaffold fabrication, and tissue engineering, *AIChE J.* 54 (2008) 3048–3067.
- [109] E.S. Place, N.D. Evans, M.M. Stevens, Complexity in biomaterials for tissue engineering, *Nat. Mater.* 8 (2009) 457–470.
- [110] C. Fischbach, R. Chen, T. Matsumoto, T. Schmelzle, J.S. Brugge, P.J. Polverini, D.J. Mooney, Engineering tumors with 3D scaffolds, *Nat. Methods* 4 (2007) 855–860.
- [111] E.L. Fong, S.E. Lamhamedi-Cherradi, E. Burdett, V. Ramamoorthy, A.J. Lazar, F.K. Kasper, M.C. Farach-Carson, D. Vishwamitra, E.G. Demicco, B.A. Menegaz, H.M. Amin, A.G. Mikos, J.A. Ludwig, Modeling Ewing sarcoma tumors in vitro with 3D scaffolds, *Proc. Natl. Acad. Sci. U. S. A.* 110 (2013) 6500–6505.
- [112] G.N. Bancroft, V.I. Sikavitsas, A.G. Mikos, Design of a flow perfusion bioreactor system for bone tissue-engineering applications, *Tissue Eng.* 9 (2003) 549–554.
- [113] W.L. Grayson, D. Marolt, S. Bhumiratana, M. Frohlich, X.E. Guo, G. Vunjak-Novakovic, Optimizing the medium perfusion rate in bone tissue engineering bioreactors, *Biotechnol. Bioeng.* 108 (2011) 1159–1170.
- [114] I. Martin, D. Wendt, M. Heberer, The role of bioreactors in tissue engineering, *Trends Biotechnol.* 22 (2004) 80–86.
- [115] D. Wendt, S. Stroebel, M. Jakob, G.T. John, I. Martin, Uniform tissues engineered by seeding and culturing cells in 3D scaffolds under perfusion at defined oxygen tensions, *Biorheology* 43 (2006) 481–488.
- [116] J.M. Munson, R.V. Bellamkonda, M.A. Swartz, Interstitial flow in a 3D microenvironment increases glioma invasion by a CXCR4-dependent mechanism, *Cancer Res.* 73 (2013) 1536–1546.
- [117] J.D. Shields, M.E. Fleury, C. Yong, A.A. Tomei, G.J. Randolph, M.A. Swartz, Autologous chemotaxis as a mechanism of tumor cell homing to lymphatics via interstitial flow and autocrine CCR7 signaling, *Cancer Cell* 11 (2007) 526–538.
- [118] A. Braccini, D. Wendt, C. Jaquierey, M. Jakob, M. Heberer, L. Kenins, A. Wodnar-Filipowicz, R. Quarto, I. Martin, Three-dimensional perfusion culture of human bone marrow cells and generation of osteoinductive grafts, *Stem Cells* 23 (2005) 1066–1072.
- [119] A. Scherberich, R. Galli, C. Jaquierey, J. Farhadi, I. Martin, Three-dimensional perfusion culture of human adipose tissue-derived endothelial and osteoblastic progenitors generates osteogenic constructs with intrinsic vascularization capacity, *Stem Cells* 25 (2007) 1823–1829.
- [120] Y. Liu, D.A. Markov, J.P. Wikswa, L.J. McCawley, Microfabricated scaffold-guided endothelial morphogenesis in three-dimensional culture, *Biomed. Microdevices* 13 (2011) 837–846.
- [121] M.N. Di, E. Piccinini, M. Jaworski, A. Trumpp, D.J. Wendt, I. Martin, Toward modeling the bone marrow niche using scaffold-based 3D culture systems, *Biomaterials* 32 (2011) 321–329.
- [122] A. Papadimitropoulos, A. Scherberich, S. Guven, N. Theilgaard, H.J. Crooijmans, F. Santini, K. Scheffler, A. Zallone, I. Martin, A 3D in vitro bone organ model using human progenitor cells, *Eur. Cell Mater.* 21 (2011) 445–458.
- [123] K.S. Carswell, E.T. Papoutsakis, Culture of human T cells in stirred bioreactors for cellular immunotherapy applications: shear, proliferation, and the IL-2 receptor, *Biotechnol. Bioeng.* 68 (2000) 328–338.
- [124] R.A. Knazek, Y.W. Wu, P.M. Aebersold, S.A. Rosenberg, Culture of human tumor infiltrating lymphocytes in hollow fiber bioreactors, *J. Immunol. Methods* 127 (1990) 29–37.
- [125] R.P. Somerville, L. Devillier, M.R. Parkhurst, S.A. Rosenberg, M.E. Dudley, Clinical scale rapid expansion of lymphocytes for adoptive cell transfer therapy in the WAVE(R) bioreactor, *J. Transl. Med.* 10 (2012) 69.
- [126] E. Gottwald, B. Lahni, D. Thiele, S. Giselsbrecht, A. Welle, K.F. Weibezahn, Chip-based three-dimensional cell culture in perfused micro-bioreactors, *J. Vis. Exp.* 136 (2008).
- [127] Z.T. Yu, K. Kamei, H. Takahashi, C.J. Shu, X. Wang, G.W. He, R. Silverman, C.G. Radu, O.N. Witte, K.B. Lee, H.R. Tseng, Integrated microfluidic devices for combinatorial cell-based assays, *Biomed. Microdevices* 11 (2009) 547–555.
- [128] M. Lagana, M.T. Raimondi, A miniaturized, optically accessible bioreactor for systematic 3D tissue engineering research, *Biomed. Microdevices* 14 (2012) 225–234.
- [129] K.F. Lei, M.H. Wu, C.W. Hsu, Y.D. Chen, Real-time and non-invasive impedimetric monitoring of cell proliferation and chemosensitivity in a perfusion 3D cell culture microfluidic chip, *Biosens. Bioelectron.* 51 (2014) 16–21.
- [130] L. Ma, J. Barker, C. Zhou, W. Li, J. Zhang, B. Lin, G. Foltz, J. Kublbeck, P. Honkakoski, Towards personalized medicine with a three-dimensional micro-scale perfusion-based two-chamber tissue model system, *Biomaterials* 33 (2012) 4353–4361.
- [131] F. Hirschhaeuser, S. Walenta, W. Mueller-Klieser, Efficacy of catumaxomab in tumor spheroid killing is mediated by its trifunctional mode of action, *Cancer Immunol. Immunother.* 59 (2010) 1675–1684.
- [132] V. Bronte, T. Kasic, G. Gri, K. Gallana, G. Borsellino, I. Marigo, L. Battistini, M. Iafraite, T. Prayer-Galetti, F. Pagano, A. Viola, Boosting antitumor responses of T lymphocytes infiltrating human prostate cancers, *J. Exp. Med.* 201 (2005) 1257–1268.
- [133] M.J. Bissell, D. Radisky, Putting tumours in context, *Nat. Rev. Cancer* 1 (2001) 46–54.
- [134] T. Cupedo, A. Stroock, M. Coles, Application of tissue engineering to the immune system: development of artificial lymph nodes, *Front. Immunol.* 3 (2012) 343.
- [135] T. Hitchcock, L. Niklason, Lymphatic tissue engineering: progress and prospects, *Ann. N. Y. Acad. Sci.* 1131 (2008) 44–49.
- [136] M. Wu, M. Swartz, Modeling tumor microenvironments in vitro, *J. Biomech. Eng.* 136 (2014).

## Research article. Cancer Therapy: Preclinical

### Bioreactor-engineered cancer tissues mimic phenotypes, gene expression profiles and drug resistance patterns observed in xenografts and clinical specimens

Christian Hirt<sup>1,2</sup>, Adam Papadimitropoulos<sup>1,2</sup>, Evangelos Panopoulos<sup>1,2</sup>, Eleonora Cremonesi<sup>1,2</sup>, Valentina Mele<sup>1,2</sup>, Manuele G. Muraro<sup>1,2</sup>, Robert Ivanek<sup>2</sup>, Elke Schultz-Thater<sup>1,2</sup>, Raoul A. Drosier<sup>1</sup>, Chantal Mengus<sup>1,2</sup>, Michael Heberer<sup>1,2</sup>, Daniel Oertli<sup>1</sup>, Giandomenica Iezzi<sup>1,2</sup>, Paul Zajac<sup>1,2</sup>, Serenella Eppenberger-Castori<sup>3</sup>, Luigi Tornillo<sup>3</sup>, Luigi Terracciano, Ivan Martin<sup>1,2</sup> and Giulio C. Spagnoli<sup>1,2</sup>

<sup>1</sup>Department of Surgery, University Hospital Basel, Switzerland; <sup>2</sup>Department of Biomedicine, University of Basel, Switzerland and <sup>3</sup>Institute of Pathology, University of Basel, Switzerland

*Christian Hirt, Adam Papadimitropoulos, Ivan Martin and Giulio C. Spagnoli contributed equally to this article.*

**Running title:** Culture of colorectal cancer cells in perfused bioreactors

**Keywords:** Bioreactors, tri-dimensional cultures, tumor tissue-like structures, colorectal cancer, drug resistance

**Corresponding authors:** Ivan Martin (ivan.martin@usb.ch) and Giulio C. Spagnoli (giulio.spagnoli@usb.ch), Departments of Surgery and Biomedicine, Basel University Hospital, ICFS, 20, Hebelstrasse, 4031, Basel, Switzerland

**Financial support:** Funding by the Lichtenstein-Stiftung of the University of Basel (CH), the Kommission für Technologie und Innovation (KTI, Bern, Switzerland) (GCS) and the Department of Surgery of the University Hospital Basel is gratefully acknowledged.

**Competing interests:** A.P., M.G.M, I.M. and G.C.S. are shareholders of Cellec Biotek AG.

**Statement of translational relevance (137 words)**

Effects of anticancer compounds on malignant cells are usually initially tested in bi-dimensional (2D) cultures and validated “in vivo” in immunodeficient mice prior to clinical trials. High attrition rates urge the investigation of novel technologies to reduce costs and accelerate clinical development. Tridimensional (3D) cultures were developed to generate structures mimicking “in vivo” features more efficiently than 2D cultures. However, resulting tumor tissue-like structures are small, non-uniform and with poor cell proliferation. Here we show that 3D culture of tumor cells in perfused bioreactors developed for tissue engineering purposes promotes the generation of tumor tissue-like structures displaying phenotypic, gene expression and drug sensitivity patterns highly similar to those observed in xenografted cells and in clinical specimens. This culture technology, efficiently mimicking clinically relevant “in vivo” traits, could be of help in pre-clinical screening of novel anticancer drugs.

## Abstract (250 words)

**Purpose:** Anticancer compound screening on bi-dimensional (2D) cell cultures poorly predicts “in vivo” performance and requires validation by xenografts. We addressed the generation of tri-dimensional (3D) tissue-like structures amenable to drug sensitivity testing from cultured cancer cells.

**Experimental design:** Tumor cell lines were cultured in 2D, on collagen scaffolds in static conditions or in perfused bioreactors, or injected subcutaneously in immunodeficient mice. Gene expression profiles were evaluated by whole genome RNA-sequencing. Drug sensitivity was comparatively analyzed “in vitro” and “in vivo” and drug resistance-related markers expression was explored in samples from patients undergoing neo-adjuvant chemotherapy.

**Results:** Perfused 3D (p3D) culture allowed more homogeneous scaffold seeding than static 3D (s3D) cultures and significantly higher cell ( $p < 0.0001$ ) proliferation. Using colorectal cancer (CRC) HT-29 cells as model, we observed that resulting tissue-like structures exhibited morphology and phenotypes similar to xenografts. Transcriptome analysis revealed a high correlation between xenografts and p3D cultures ( $r = 0.985$ ). 5-Fluorouracil (5-FU) treatment induced apoptosis and significant *BCL-2*, *TRAF1*, and *c-FLIP* genes down-regulation in monolayers, but only “nucleolar stress” in perfused cells and xenografts, and reduced by 55% cell numbers in 2D but not in p3D cultures or xenografts. Conversely, BCL-2 inhibitor ABT-199 induced cytotoxic effects in p3D but not in 2D cultures. Following neo-adjuvant 5-FU based chemotherapy, tumor cells from 14 of 26 unresponsive or partially responsive (Dworak 0-2) patients were found to express to variable extents BCL-2, consistent with the trend captured by p3D cultures.

**Conclusions:** p3D cultures efficiently mimic functional features observed in CRC xenografts and clinical specimens.

## Introduction

Established cell lines play a central role in tumor cell biology investigations and in the development of novel anticancer treatments [1, 2]. Their availability in large quantities and their relatively stable phenotypes, transcriptomes and functional characteristics represent obvious advantages. Screening of novel antitumor compounds is currently based on the assessment of their ability to inhibit proliferation or to induce cytotoxicity in human cancer cell lines cultured in high-throughput formats. Frequently however, “in vitro” behavior of established cell lines poorly mirrors “in vivo” cancer cell features [3].

Xenografts of human cells in immunodeficient mice are utilized to fill the gap between “in vitro” results and successful clinical studies. Limitations inherent in their use include high costs, latency time following engraftment and the interaction with murine extracellular matrix components and innate immune system [4, 5]. Therefore, the development of innovative, reliable and rapid “in vitro” assays is urgently required. Most obviously, their relevance might extend beyond drug screening purposes, and they might also play a decisive role to address basic issues in cancer biology in highly controlled conditions [6].

A series of studies have underlined that culture in bi-dimensional (2D) or in tri-dimensional (3D) systems differentially affects sensitivity of cancer cells to compounds used in cancer treatment [7-9] or to immune effector cells specific for human tumor associated antigens [10]. These findings have been related to a variety of mechanisms, including differential drug penetration and cell proliferation in different cell layers and differential modulation of defined signaling pathways, in 2D cultures and in 3D tumor structures.

3D cancer cell culture technologies include surface-contact-independent tumor cell spheroids generated by gravity [11, 12] and systems allowing cell attachment and integration in a soft matrix [13]. These techniques have been suggested to mimic, at least in part, defined tumor microenvironmental conditions such as cell-to-cell contact and cell-stroma interactions, or generation of hypoxic-necrotic areas, potentially playing a role in tumor metabolism and progression and in metastasis formation [14, 15]. Alternative models, based on seeding and culture of tumor cells within porous 3D scaffolds composed of different materials, have also been described [16, 17]. Although the generated tissue-like structures share morphological and biochemical features of “in vivo” growing tumors, they are usually characterized by poor cell proliferation and display only scattered areas of clustered tumor cells, with limited resemblance to xenografts and human malignant tissues [16, 17].

Bioreactors applying direct perfusion through the pores of 3D scaffolds and the resulting tissue structures, have been utilized in a variety of culture systems for tissue engineering [18, 19], but their potential for tumor tissue formation “in vitro” has not been explored so far.

Colorectal cancer (CRC) is the third most common malignancy worldwide both in women and men [20]. Despite major progress in the understanding of its molecular pathogenesis and the development of new therapies over the last decade, cure rates remain low [21].

In this study we comparatively analyzed morphology, cell phenotype, proliferation rates, gene expression profiles and sensitivity to drug treatment in CRC cells growing in 2D cell cultures, in tissue-like structures in perfused bioreactors or in xenografts in immunodeficient mice. We here report that culture of CRC cells in

perfused 3D (p3D) cultures results in the formation of tumor tissue-like structures characterized by high similarities with xenografts generated in immunodeficient mice and clinical specimens.

## Materials and Methods

### Cell lines and scaffolds

HT-29, SW480 and DLD-1 CRC cell lines and PC-3 (prostate cancer), A549 (non-small cell lung cancer) and BT474 (breast-cancer) cell lines were obtained and authenticated by short tandem repeat (STR) DNA profiles from the American Type Culture Collection (ATCC). The cell lines were passaged for fewer than 6 months after resuscitation. HT-29 cells were maintained in McCoy's 5A medium (Sigma-Aldrich) containing 10% heat-inactivated fetal calf serum, GlutaMAX-I, and Kanamycin sulphate (all from Gibco). All other cancer cell lines were cultured in RPMI-1640 (Sigma-Aldrich) containing 10% heat-inactivated fetal calf serum, 0.1% 2- $\beta$ -Mercaptoethanol (Sigma-Aldrich), GlutaMAX-I, MEM non-essential aminoacids (NEAA), Sodium Pyruvate, HEPES buffer and Kanamycin sulphate (all from Gibco). Collagen scaffolds (Ultrafoam, Avitene) obtained from Davol, were cut with 6-8mm biopsy punches prior to cultures. A non-woven polyethylene (PET, 185g/m<sup>2</sup>) scaffold mesh was obtained from Norafin Industries and silk scaffolds were a gift from Dr. Sourabh Ghosh, Indian Institute of Technology, Delhi, India [22]. Prior to use, PET and silk scaffolds were autoclaved and cut by a biopsy punch.

### Cell culture in 2D, and in static and perfused 3D conditions

For standard 2D cell cultures we used 75cm<sup>2</sup> culture flasks or 8-well-tissue chamber slides (Becton Dickinson) and 5x10<sup>5</sup>-10<sup>6</sup>/mL cell concentrations. For static 3D (s3D) cell cultures, 6-well-plates (Becton Dickinson) were coated with 1mL of 1.5% Agar in DMEM (Sigma-Aldrich) at least one day before use and kept at 4°C. Static seeding was achieved by resuspending 10<sup>6</sup> cells in 40 $\mu$ L of medium and letting them attach to scaffolds for 1 hour at 37°C. Culture medium (5mL) was then added. For perfused 3D (p3D) cultures, we used a commercially available (Cellec Biotek AG) perfusion bioreactor system [23]. Cells (10<sup>6</sup>) were seeded and perfused overnight at a superficial velocity of 400 $\mu$ m/sec. After a 24 hour cell seeding phase, superficial velocity was reduced to 100 $\mu$ m/sec.

Cell seeding efficiency on different scaffolds was determined by analyzing DNA content in constructs harvested after overnight culture. Briefly, samples were digested with proteinase K solution (Sigma-Aldrich) for 16h at 56°C, as previously described [23], and DNA quantity was evaluated by CyQUANT Cell Proliferation Assay (Invitrogen) according to manufacturer's protocols. Fluorescence was measured by a Spectra-Max Gemini XS Microplate Spectrofluorometer (Molecular Devices), at 485nm excitation and 538nm emission wavelengths. Seeding efficiencies were calculated as percentages of the original cell input detectable in cultured constructs.

Cell proliferation was determined in constructs harvested at various time points using an MTT assay (Sigma-Aldrich), as previously described [22], and pH levels in culture supernatants were measured by standard methods.

### **Immunofluorescence and cytofluorimetric analysis**

Constructs retrieved following 7 or 14 days cultures were fixed overnight in 1.5% paraformaldehyde at 4°C and paraffin embedded (TPC15 Medite). Sections (5µm) were deparaffinized, hydrated and stained with hematoxylin and eosin (H&E). Culture chamber slides used for 2D cultures were fixed with paraformaldehyde and directly stained with H&E.

Immunofluorescence analyses were performed following deparaffinization, re-hydration and antigen retrieval at 95°C for 30min with ready-to-use S1700 solution (DAKO). Proliferating cells were identified using a Ki67 specific rabbit monoclonal antibody (mAb) (ab27619, AbCAM,) and apoptotic cells were identified using a cleaved caspase 3 specific rabbit mAb (cCl3, Asp175, rabbit mAb #9664, Cell Signaling) [24]. As secondary reagent, we used an Alexa-Fluor 488 labelled goat-anti-rabbit polyclonal antibody (A-11034, Invitrogen) at a 1:400 final dilution. Nuclei were counterstained with DAPI (Invitrogen). Histological and immunofluorescence sections were analyzed using a BX-61 microscope (Olympus).

Alternatively, for cytofluorimetric analysis, cells were extracted from scaffolds by treatment with TrypLE (Gibco) for 10 min, followed by incubation in 0.3% collagenase (Worthington) for 30 min at 37°C, as previously described [25], and stained with Annexin V FITC/PI according to manufacturer's protocol (Becton Dickinson) or with a Ki67 specific mAb (see above). Cells were analyzed by flow cytometry (FACScalibur, BD).

### **Quantification of gene expression by quantitative Real-Time PCR**

Total cellular RNA was extracted by using NucleoSpin RNA II kit (Macherey-Nagel) and reverse transcribed, as previously described [26]. Quantitative Real-Time PCR (qRT-PCR) assays were performed in the presence of primers and probes specific for the indicated genes (Assays-on-demand, Applied Biosystems). Normalization of gene expression was performed using GAPDH as reference gene [27].

### **RNA-sequencing and analysis**

Purity of total cellular RNA was evaluated by a 2100 Bioanalyzer (Agilent Technologies). Non-stranded RNA libraries were prepared by using the Illumina TruSeq sample preparation kit and sequenced on Illumina HiSeq 2000 sequencer (Illumina).

Single-end RNA-seq reads (50-mers) were mapped to the human genome assembly, version hg19, with SpliceMap [28], implemented in Bioconductor's package QuasR. By using RefSeq mRNA coordinates from UCSC (genome.ucsc.edu, downloaded in January 2014) and the qCount function, we quantified gene expression as the number of reads that started within any annotated exon of a gene. Nucleotide sequences are deposited in the NCBI at GSE57961.

After quality control, we excluded from analysis a single sample from 2D cultures due to degraded RNA (reads obtained only at the end of transcripts) and poor correlation to other samples. Differentially expressed genes were identified using the edgeR package (version 3.4.2) [29]. Multidimensional scaling was used to visualize the relation between different cultures conditions. Differentially expressed genes, defined as having FDR  $\leq 0.05$  in any pairwise comparison, were clustered into 13 clusters using PAM algorithm. Individual clusters were tested for enrichment in

functional annotations using DAVID and REVIGO bioinformatics resources, as previously described [30, 31].

### **”In vitro” and “in vivo” drug-sensitivity assays**

Chemotherapeutic agents were used at the following concentrations in “in vitro” assays: 5-Fluoruracil (5-FU, Teva Pharma), 1 µg/ml and 10 µg/mL; Oxaliplatin (Sanofi-Aventis), 1 µg/mL and 10 µg/mL; Irinotecan (Pfizer), 10 µg/mL and 100 µg/mL; Sunitinib (LC Laboratories), 0.8 µg/mL and 8 µg/mL; ABT-199 (Active Biochemicals), 2.2 µg/mL.

“In vitro” tests were performed in standard 2D in 96 or 12 flat bottom wells trays (Falcon) following a one day pre-culture or in 3D perfused bioreactors following a four days pre-culture. In all conditions, a  $10^5$  cells/mL concentration was used. Effects of chemotherapeutic agents were assessed after 48 or 96 hours by DNA content analysis, as described above. Flow cytometric, histological and immunofluorescence studies were performed at the same times.

“In vivo” assays were performed at Oncotest GmbH. Briefly, NMRI-mice were injected with 400'000 HT-29 cells in Matrigel (Becton Dickinson). After reaching a tumor volume of 6mm<sup>3</sup>, usually after 21 days, a 5-FU bolus (50 µg/Kg) was administered and animals were sacrificed after 48 or 96 hours. Xenografts were explanted and further analyses were performed in Basel, as for the “in vitro” conditions. In each experiment, four mice per time point and condition were used.

### **Immunohistochemistry staining of BCL-2, CDX2 and Cytokeratin 20**

Standard procedures (ABC-Elite, Vector Laboratories) were used for immunohistochemical analysis of paraffin embedded sections from clinical specimens. Briefly, 5 µm slides were dewaxed and rehydrated in distilled water. Endogenous peroxidase activity was blocked using 0.5% H<sub>2</sub>O<sub>2</sub>. Sections were treated with 10% normal goat serum (DakoCytomation) for 20 min and incubated with a monoclonal mouse anti-human BCL-2 (clone 124, DAKO) primary antibody for one hour at room temperature. Subsequently, sections were incubated with peroxidase-labelled secondary antibody (DakoCytomation) for 30 min at room temperature. For antigen visualization, sections were immersed in 3-amino-9-ethylcarbazole plus substrate-chromogen (DakoCytomation) for 30 min, and counterstained with Gill’s hematoxylin. Immunohistochemical detection of CDX2 (clone AMT28, 1:50, Abcam) and Cytokeratin 20 (clone Ks20.8, 1:50, DAKO) was similarly performed.

Two independent observers examined immunohistochemical slides without any prior information on clinical pathological features of the patient samples. Percentages of BCL-2 positive tumor cells and staining intensities were evaluated for each slide.

### **Clinical pathological feature analysis**

Clinical pathological data from 29 patients with CRC treated with neoadjuvant regimen, including 5-FU, were collected retrospectively from the Tissue Biobank of the Institute of Pathology, University Hospital Basel, performing translational research with the approval of the Ethical Committee Beider Basel (EKBB), in compliance with ethical standards and patient confidentiality. All patients were treated at the University Hospital Basel, Switzerland. Clinical annotation included patient age, location, pT/pN stage, grade, Dworak regression grading [32], relapse and disease-specific survival.

## Statistical Analysis

Data are presented as mean values±standard deviations (SD). Statistical comparisons between groups were performed by one or two-way analysis of variance (ANOVA) followed by post-hoc Tukey or Bonferroni tests. BCL-2 levels in paired biopsies from patients with CRC before and after neoadjuvant treatment were compared by paired Wilcoxon tests. In all cases,  $p$  values  $\leq 0.05$  were considered statistically significant. GraphPad Prism (Software Inc.) and R version 3.0.2 (<http://www.R-project.org>) softwares were used for statistical analysis.

## Results

### Generation of tumor tissue-like structures on tri-dimensional scaffolds in perfused bioreactors

To evaluate the possibility of efficiently “in vitro” engineering cancer tissue-like structures, we seeded cells from established tumor cell lines onto scaffolds located within previously described perfused bioreactor chambers (Fig. 1A) [19, 25]. Different types of scaffolds were initially tested (Supplementary Fig. S1A). However, PET scaffolds were difficult to process for histological analysis and silk scaffolds underwent substantial shrinkage upon perfusion. Therefore, a collagen-based sponge (Ultrafoam) was used for the rest of our study, because of its natural composition, fiber structure, and simplicity of histological processing and cell retrieval by using commercially available enzymes.

Since we are particularly interested in the investigation of colorectal cancer (CRC) cell biology and microenvironmental features [33-35], we addressed in detail the generation of tissue-like structures upon 3D culture of cells from established CRC cell lines in p3D. HT-29, DLD-1 and SW480 CRC cell lines could be maintained in culture for over 7 days in the bioreactor system under investigation and developed tissue-like structures (Supplementary Fig. S1B). Mismatch repair proficient HT-29 cell line, yielding high-density tissue-constructs upon p3D culture (see below), was selected for additional studies.

The p3D cultures were characterized by a clearly more homogeneous cell seeding as compared to s3D ones, and by a higher cell density, as detectable by whole scaffold MTT uptake after a 7 days culture (Fig. 1B, upper and lower panels, respectively). Growth curves of cells cultured in 2D, s3D or p3D, or displayed markedly different patterns (Fig. 1C). Standard monolayers reached a plateau after 3 days, whereas cells in p3D cultures displayed a significantly slower proliferation (Fig. 1C). Remarkably however, the lowest proliferation rate was observed in s3D cultures. These growth patterns were mirrored by decreasing pH values over time (Supplementary Fig. S2).

H&E staining showed that perfusion promoted the generation of high density, homogeneous tissue-like structures (Fig. 1D, upper left panel). In contrast, and consistent with previous studies [16, 17], in s3D cultures small tumor clumps were only detectable on the outer rims of the scaffolds while inner parts were largely free of tumor cells (Fig. 1D, lower left panel). Cross-sectional areas covered by tumor tissues in p3D cultures were usually over tenfold larger than those measured in s3D conditions (Fig. 1D right panel).

To address the broad applicability of p3D tumor cell culture, we tested a variety of cell lines of different histological origin, including PC-3 (prostate cancer), A549 (non-small cell lung cancer) and BT474 (breast cancer), in the bioreactor system under investigation. In all cases, p3D cultures resulted in the expansion of higher cell numbers, as compared to s3D cultures, and in the generation of larger tissue-like structures (Supplementary Fig. S3).

### **Histological and transcriptional profiles of p3D tumor cultures**

Histological characteristics of HT-29 CRC cells cultured in monolayers and of tissue-like 3D structures generated in p3D or s3D were then evaluated in comparison with xenografts obtained “in vivo” upon subcutaneous (s.c.) injection in immunodeficient mice (Fig. 2A). HT-29 cells cultured in 2D showed homogeneous cell shape and nodular-like growth upon H&E staining. Culture in s3D conditions resulted in the generation of small tissue nodules (Fig. 2A). HT-29 cell culture in p3D conditions promoted the formation of large, anaplastic tumor structures integrating into the collagen scaffold. Interestingly, HT-29 cells from p3D cultures and xenografts displayed a high grade of mitotic figures and atypical mitoses, as well as signet ring cells and acini-like structures (Supplementary Fig. S4A, B).

Cytokeratin 20 (CK20) was consistently expressed through all culture conditions and in xenografts, whereas CDX2 [36] was undetectable in cells from 2D cultures and expressed to different extents in HT-29 cells from s3D and p3D cultures and xenografts (Fig. 2A).

In agreement with the observed proliferation rates (Fig. 2B), Ki67 positive cells were ubiquitously detectable in monolayer cultures, rare in s3D cultures and detectable to higher extents in both p3D cultures and xenografts (Fig. 2A). Conversely, cC13 positive, apoptotic HT-29 cells were rare in monolayer cultures, but detectable to significantly higher extents in tissue-like structures from s3D than in p3D cultures or xenografts (Fig. 2A, C).

Transcriptional profiles of cells cultured in the different conditions under investigation and growing in xenografts were investigated by RNA sequencing. A comparative analysis revealed clear differences between culture conditions. In particular, gene expression profiles of 2D cultures significantly differed from those detectable in 3D cultures or xenografts (Fig. 3A). Transcriptomes from s3D and p3D cultures were highly similar. However, pairwise correlation analysis of averaged expression profiles indicates that the gene expression profile bearing the highest similarity to “in vivo” xenografts was that of HT-29 cells cultured in p3D conditions ( $r=0.985$ ).

Distinct gene clusters appeared to be differentially expressed in 2D, s3D and p3D cultures and xenografts (Fig. 3B). In particular, expression of cluster 2 and 12 genes regulating cell cycle, and DNA transcription and repair was detectable to higher extents in 3D cultures and xenografts, as compared to 2D cultures. Instead, cluster 10 and 4 genes, regulating, among other processes, apoptosis and response to hypoxia, were differentially expressed in p3D cultures and xenografts, as compared to 2D and s3D cultures. Yet, cluster 1 and 11 genes, regulating cell adhesion and migration, and immune response were expressed to uniquely high extents in xenografts.

Taken together, these data clearly indicate that p3D culture of HT-29 CRC cells promotes the formation of relatively large tumor tissue-like structures,

characterized by proliferation, apoptotic rates and gene expression profiles similar to “in vivo” growing cells.

### **Response of HT-29 p3D culture to chemotherapeutic treatment**

We then asked whether responsiveness to current chemotherapy treatments was also similar in p3D cultures and xenografts, using, as control, currently utilized, standard, monolayer cultures. As s3D cultures failed to induce the generation of tissue-like structures of sizes amenable to drug testing and were characterized by negligible cell proliferation and high apoptotic rates, they were not further considered as experimental group.

We treated p3D cultured cells and xenografts with 5-Fluoruracil (5-FU), which is included in standard neo-adjuvant and adjuvant protocols for CRC treatment. For “in vitro” studies, 5-FU was used at a 1 µg/mL concentration, whereas for xenograft treatment we chose a 50 µg/kg dose, which has been reported to produce plasma levels similar to those used “in vitro” [37].

Following a 48 hours treatment, signs of cellular “stress” were detectable to different extents in all cultures and in xenografts (Fig. 4A) [38]. In 2D cultures, nucleoli became prominently visible in all cells, whereas in p3D cultures and xenografts this effect was significantly reduced (Fig. 4B, left panel).

Remarkably, in 2D cultures total cell number was decreased by about 50% following a 48 or 96 hours exposure to 5-FU (Fig. 4B, middle panel). In contrast, in p3D cultures and xenografts no significant reduction of total cell numbers or tumor volumes could be observed (Fig. 4B). Similar trends were also observed by using other drugs commonly utilized in CRC treatment (Supplementary Fig. S5). In keeping with these data, a significant increase in apoptotic cell numbers upon treatment was observed in 2D, but not in p3D cultures or xenografts after 96h of treatment (Fig. 4B, left panel).

To obtain a more detailed insight into the effects of 5-FU treatment on cells cultured in different conditions and in xenografts, we analyzed by qRT-PCR the expression of a large panel of genes potentially regulating defined tumor environmental features, cell cycle and apoptosis induction. Expression of PD-L1 [39] and CCL22 chemokine genes was similarly increased upon 5-FU treatment in 2D, p3D cultures and in xenografts (Supplementary Fig. S6A, B). In contrast, IL-8 gene expression was exclusively increased in 5-FU treated HT-29 cells cultured in 2D, but not in p3D cultures or xenografts (Supplementary Fig. S6C). Most importantly, the expression of genes associated to anti-apoptotic effects, such as BCL-2, TRAF-1 and c-FLIP was significantly down regulated upon 5-FU treatment in 2D but was unaffected in p3D cultures or xenografts (Fig. 4C). Thus, responsiveness to 5-FU treatment appears to be similar in p3D cultures and xenografts.

Based on data emerging from 5-FU treatment of HT-29 cells, we reasoned that inhibition of anti-apoptotic proteins could potentially represent a viable treatment strategy in CRC. Interestingly, a BCL-2 inhibitor (ABT-199) has recently been developed for leukemia treatment [40]. This drug had no effect on HT-29 cells cultured in 2D, whereas a significant reduction in the number of HT-29 cells cultured in p3D was detectable upon 48 hours treatment (Fig. 5A). Annexin V-PI staining showed that ABT-199 treatment led to a two-fold (46.6% vs. 22.4%) increase in the percentage of HT-29 cells undergoing apoptosis, as compared to untreated or 5-FU treated cells. Accordingly, H&E staining of ABT-199 treated p3D cultures documented a marked reduction in size of HT-29 tissue-like structures (Fig. 5B).

### **BCL-2 expression in human specimens pre- and post-neoadjuvant treatment**

Data from “in vitro” cultures and xenografts urged us to explore their potential clinical relevance. Indeed, BCL-2 expression in CRC specimens has been reported to be associated with improved survival in untreated patients [41]. However, its association with responsiveness to standard chemotherapy treatments has not been analyzed yet.

Therefore, we investigated BCL-2 expression in a cohort of 29 patients with CRC undergoing neoadjuvant 5-FU treatment (Fig. 6A). Responsiveness to chemotherapy was evaluated according to Dworak index, ranging between 0 and 4 [32]. For 13 patients we had access to the corresponding initial tumor biopsy and we could therefore evaluate modulation of BCL-2 expression induced by chemotherapy in (Fig. 6B). A significant increase in BCL-2 expression upon treatment was detectable in tumor cells ( $p=0.009$ ) while BCL-2 expression in stromal cells was significantly decreased ( $p=0.025$ ) (Fig. 6C).

Interestingly, tumor cells obtained post-treatment from 14 of 26 patients who did not respond or only showed partial responsiveness to chemotherapy (Dworak regression grade 0-2, Figure 6D), were found to express BCL-2 to different extents.

## **Discussion**

The initial screening of novel anticancer compounds traditionally utilizes human established tumor cell lines in “in vitro” assays [2]. This approach has led to the identification of a large variety of drug classes, with high therapeutic impact. However, results from conventional “in vitro” tests frequently fail to be confirmed by clinical investigation [3, 42]. To enhance the predictive relevance of pre-clinical studies, established human cell lines are xenografted in immunodeficient mice to allow “in vivo” assessment of the effectiveness of potential antitumor drugs. These models, of essential relevance for target validation, have a number of limitations, including role of murine stroma and innate immune system in response to treatment, latency time after engraftment, and high costs [2, 5].

Based on this background, a variety of innovative “tumor engineering” technologies are currently being developed to provide the scientific community with advanced models potentially overcoming limitations of current assays and eventually improving their predictive performance [43, 44]. Indeed, a large body of literature supports the concept that human established tumor cell lines cultured in conventional 2D conditions exhibit functional and drug sensitivity profiles significantly differing from those detectable in 3D cultures or “in vivo” [9, 45, 46].

In this study we have used a perfused bioreactor system successfully utilized for the culture of mesenchymal cells [19], to address the generation of tissue-like structures from established cancer cell lines and to explore their functional characteristics.

We observed that p3D culture of established human tumor cell lines resulted in the rapid generation of tissue-like structures characterized by homogeneous architectures and significantly higher cell yields, as compared to s3D cultures. Different cell lines showed slightly different growth patterns in p3D cultures. Whereas HT-29 cells were growing as tumor nodules, DLD-1 cells formed tissue-like structures oriented by the scaffold-fibers. Most importantly however, apoptosis and proliferation

rates in p3D cultures closely matched those detectable in xenografts of the same cells in immunodeficient mice.

We have studied in detail, HT-29 CRC cell line cultured in p3D. Perfused culture of these cells resulted in the generation of acini-like formations, reminding histological features of differentiated colorectal mucosa. Interestingly, the formation of these structures was previously attributed to cellular polarization associated with modifications of culture medium and, possibly, related to glutamine deprivation [47].

CDX2 homeobox gene has been shown to be highly expressed in colonic adenocarcinomas, typically displaying a high intensity specific staining in 90% of cases [36]. In our study HT-29 cells cultured in monolayers did not express CDX2. However, specific staining was readily observed, to different intensities, upon culture in 3D, irrespective of perfusion, or upon injection in immunodeficient animals, thereby further supporting the notion of the high similarity between 3D cultures of established cancer cell lines and clinical specimens.

These data prompted us to perform a comparative analysis by next generation sequencing of the whole transcriptome of HT-29 cells cultured in different conditions or growing as xenografts. This study, one of the first of its kind, clearly demonstrated, by cluster analysis, that although p3D and s3D cultures were highly similar, gene expression profiles of HT-29 cells in xenografts and p3D cultures were characterized by the highest similarity to each other.

On the other hand, at difference with s3D, p3D culture promoted the formation of large tissue-like structures characterized by a significantly higher tumor cell proliferation, thus suggesting that it could effectively complement or partially replace “in vivo” studies. In particular, it is remarkable that the clusters of genes regulating apoptotic process and response to hypoxia appeared to be similarly expressed in p3D cultures and in xenografts.

We then addressed the sensitivity to drug treatment of tumor tissue-like structures generated in p3D, in comparison with xenografts, and conventional HT-29 monolayers, the current standard. Our data show that while HT-29 cells in 2D cultures were highly sensitive to 5-FU treatment, p3D cultures and xenografts were similarly characterized by a partial sensitivity, as indicated by cell “stress” signs in the absence of significant cytotoxicity. These effects were accompanied by typical gene signatures. In particular, 5-FU induces BCL-2, c-FLIP and TRAF-1 gene down-regulation in treated HT-29 cell monolayers. However, the expression of these genes was not affected in “stressed” HT-29 cells from treated xenografts or p3D cultures.

Our results underline that CRC cells cultured in p3D and xenografts not only share similar functional, phenotypic and gene expression profiles, but are also characterized by a similar unresponsiveness to drug treatment.

To assess the potential clinical relevance of these findings, we investigated CRC tissues from patients undergoing neo-adjuvant cytoreductive treatment based on 5-FU administration to attempt tumor re-staging prior to radical surgery. We found that BCL-2 expression was frequently detectable to variable extents in tumor cells from post-treatment clinical specimens from patients showing no responsiveness or partial responsiveness (Dworak 0-2) to neo-adjuvant chemotherapy. This finding is consistent with the detection of high BCL-2 expression following 5-FU treatment in cells from p3D but not 2D cultures. Further studies including larger numbers of patients and additional time points during and shortly after neoadjuvant treatment are warranted to obtain further insights into the modulation of BCL-2 expression by neo-adjuvant chemotherapy.

These data, concurrently underlining the major role potentially played by the expression of anti-apoptotic genes in the resistance to 5-FU treatment, have urged us to investigate the effects of newly developed anti BCL-2 pharmacological treatments. Interestingly, by using ABT-199, a promising BCL-2 inhibitor currently being tested in clinical trials for chronic lymphocytic leukemia (41), we did not observe any effect on standard HT-29 monolayers, whereas treatment of p3D cultures led to substantial decreases in total cell numbers. Collectively, these findings indicated that standard 2D assays not only overestimated the antitumor effectiveness of 5-FU, but dramatically underestimated the therapeutic potential of unrelated compounds (53), which was, instead, revealed by p3D cultures.

Thus, p3D cultures may represent “in vitro” models of CRC of potentially high significance in drug screening and to address drug resistance mechanisms or basic tumor biology issues in highly controlled conditions by taking advantage of human cells. Moreover, the p3D culture system described here may be used to efficiently mimic phenotypic and functional features observed in animal models and clinical specimens. Similar technologies could also be used to generate primary tumor cultures from clinical specimens for personalized treatment assessment.

Our study has several limitations. In particular, molecular mechanisms underlying differential phenotypic, transcriptional and functional profiles detectable in monolayers, 3D static and 3D perfusion cultures are largely unclear. Furthermore, most obviously, p3D cultures fail to account for the huge complexity of cancer microenvironment and for tumor cell heterogeneity. In order to partially address the latter issues, the p3D culture system could also be extended to include the co-culture of a variety of tumor cells with additional, non-transformed cell types such as mesenchymal stromal cells, tumor-associated fibroblasts or endothelial and immunocompetent cells, in order to explore tumor specific microenvironmental features [48].

On the other hand, the use of tumor tissue-like structures in p3D could also help to overcome limitations inherent in the use of human cell lines xenografts for drug screening, particularly regarding costs, time requirements and confounding effects of murine stromal and innate immune system cells.

### Reference List

- [1] Garnett MJ, Edelman EJ, Heidorn SJ, et al. Systematic identification of genomic markers of drug sensitivity in cancer cells. *Nature* 2012;483:570-5.
- [2] Wilding JL, Bodmer WF. Cancer cell lines for drug discovery and development. *Cancer Res* 2014;74:2377-84.
- [3] Lieu CH, Tan AC, Leong S, Diamond JR, Eckhardt SG. From bench to bedside: lessons learned in translating preclinical studies in cancer drug development. *J Natl Cancer Inst* 2013;105:1441-56.
- [4] Kopetz S, Lemos R, Powis G. The promise of patient-derived xenografts: the best laid plans of mice and men. *Clin Cancer Res* 2012;18:5160-2.
- [5] Siolas D, Hannon GJ. Patient-derived tumor xenografts: transforming clinical samples into mouse models. *Cancer Res* 2013;73:5315-9.
- [6] Horch RE, Boos AM, Quan Y, et al. Cancer research by means of tissue engineering--is there a rationale? *J Cell Mol Med* 2013;17:1197-206.
- [7] Bissell MJ, Radisky D. Putting tumours in context. *Nat Rev Cancer* 2001;1:46-54.
- [8] Herrmann D, Conway JR, Vennin C, et al. Three-dimensional cancer models mimic cell-matrix interactions in the tumour microenvironment. *Carcinogenesis* 2014;35:1671-9.
- [9] Yamada KM, Cukierman E. Modeling tissue morphogenesis and cancer in 3D. *Cell* 2007;130:601-10.
- [10] Feder-Mengus C, Ghosh S, Reschner A, Martin I, Spagnoli GC. New dimensions in tumor immunology: what does 3D culture reveal? *Trends Mol Med* 2008;14:333-40.
- [11] Friedrich J, Seidel C, Ebner R, Kunz-Schughart LA. Spheroid-based drug screen: considerations and practical approach. *Nat Protoc* 2009;4:309-24.
- [12] Sharma SV, Haber DA, Settleman J. Cell line-based platforms to evaluate the therapeutic efficacy of candidate anticancer agents. *Nat Rev Cancer* 2010;10:241-53.
- [13] Szot CS, Buchanan CF, Freeman JW, Rylander MN. 3D in vitro bioengineered tumors based on collagen I hydrogels. *Biomaterials* 2011;32:7905-12.
- [14] Cairns RA, Harris IS, Mak TW. Regulation of cancer cell metabolism. *Nat Rev Cancer* 2011;11:85-95.
- [15] Joyce JA, Pollard JW. Microenvironmental regulation of metastasis. *Nat Rev Cancer* 2009;9:239-52.
- [16] Fischbach C, Chen R, Matsumoto T, et al. Engineering tumors with 3D scaffolds. *Nat Methods* 2007;4:855-60.
- [17] Fong EL, Lamhamedi-Cherradi SE, Burdett E, et al. Modeling Ewing sarcoma tumors in vitro with 3D scaffolds. *Proc Natl Acad Sci U S A* 2013;110:6500-5.
- [18] Martin I, Wendt D, Heberer M. The role of bioreactors in tissue engineering. *Trends Biotechnol* 2004;22:80-6.

- [19] Wendt D, Marsano A, Jakob M, Heberer M, Martin I. Oscillating perfusion of cell suspensions through three-dimensional scaffolds enhances cell seeding efficiency and uniformity. *Biotechnol Bioeng* 2003;84:205-14.
- [20] Parkin DM, Bray F, Ferlay J, Pisani P. Global cancer statistics, 2002. *CA Cancer J Clin* 2005;55:74-108.
- [21] Cunningham D, Atkin W, Lenz HJ, et al. Colorectal cancer. *Lancet* 2010;375:1030-47.
- [22] Bhattacharjee M, Miot S, Gorecka A, et al. Oriented lamellar silk fibrous scaffolds to drive cartilage matrix orientation: towards annulus fibrosus tissue engineering. *Acta Biomater* 2012;8:3313-25.
- [23] Sadr N, Pippenger BE, Scherberich A, et al. Enhancing the biological performance of synthetic polymeric materials by decoration with engineered, decellularized extracellular matrix. *Biomaterials* 2012;33:5085-93.
- [24] Mazumder S, Plesca D, Almasan A. Caspase-3 activation is a critical determinant of genotoxic stress-induced apoptosis. *Methods Mol Biol* 2008;414:13-21.
- [25] Braccini A, Wendt D, Jaquiere C, et al. Three-dimensional perfusion culture of human bone marrow cells and generation of osteoinductive grafts. *Stem Cells* 2005;23:1066-72.
- [26] Schultz-Thater E, Frey DM, Margelli D, et al. Whole blood assessment of antigen specific cellular immune response by real time quantitative PCR: a versatile monitoring and discovery tool. *J Transl Med* 2008;6:58.
- [27] Livak KJ, Schmittgen TD. Analysis of relative gene expression data using real-time quantitative PCR and the 2<sup>-</sup>(Delta Delta C(T)) Method. *Methods* 2001;25:402-8.
- [28] Au KF, Jiang H, Lin L, Xing Y, Wong WH. Detection of splice junctions from paired-end RNA-seq data by SpliceMap. *Nucleic Acids Res* 2010;38:4570-8.
- [29] Robinson MD, McCarthy DJ, Smyth GK. edgeR: a Bioconductor package for differential expression analysis of digital gene expression data. *Bioinformatics* 2010;26:139-40.
- [30] Huang dW, Sherman BT, Tan Q, et al. DAVID Bioinformatics Resources: expanded annotation database and novel algorithms to better extract biology from large gene lists. *Nucleic Acids Res* 2007;35:W169-W175.
- [31] Supek F, Bosnjak M, Skunca N, Smuc T. REVIGO summarizes and visualizes long lists of gene ontology terms. *PLoS One* 2011;6:e21800.
- [32] Dworak O, Keilholz L, Hoffmann A. Pathological features of rectal cancer after preoperative radiochemotherapy. *Int J Colorectal Dis* 1997;12:19-23.
- [33] Drosier RA, Hirt C, Viehl CT, et al. Clinical impact of programmed cell death ligand 1 expression in colorectal cancer. *Eur J Cancer* 2013.
- [34] Mele V, Muraro MG, Calabrese D, et al. Mesenchymal stromal cells induce epithelial-to-mesenchymal transition in human colorectal cancer cells through the expression of surface-bound TGF-beta. *Int J Cancer* 2013.
- [35] Nebiker CA, Han J, Eppenberger-Castori S, et al. GM-CSF Production by Tumor Cells Is Associated with Improved Survival in Colorectal Cancer. *Clin Cancer Res* 2014;20:3094-106.
- [36] Moskaluk CA, Zhang H, Powell SM, Cerilli LA, Hampton GM, Frierson HF, Jr. Cdx2 protein expression in normal and malignant human tissues: an immunohistochemical survey using tissue microarrays. *Mod Pathol* 2003;16:913-9.

- [37] Codacci-Pisanelli G, van der Wilt CL, Pinedo HM, et al. Antitumour activity, toxicity and inhibition of thymidylate synthase of prolonged administration of 5-fluorouracil in mice. *Eur J Cancer* 1995;31A:1517-25.
- [38] Boulon S, Westman BJ, Hutten S, Boisvert FM, Lamond AI. The nucleolus under stress. *Mol Cell* 2010;40:216-27.
- [39] Zhang P, Su DM, Liang M, Fu J. Chemopreventive agents induce programmed death-1-ligand 1 (PD-L1) surface expression in breast cancer cells and promote PD-L1-mediated T cell apoptosis. *Mol Immunol* 2008;45:1470-6.
- [40] Souers AJ, Levenson JD, Boghaert ER, et al. ABT-199, a potent and selective BCL-2 inhibitor, achieves antitumor activity while sparing platelets. *Nat Med* 2013;19:202-8.
- [41] Tornillo L, Lugli A, Zlobec I, et al. Prognostic value of cell cycle and apoptosis regulatory proteins in mismatch repair-proficient colorectal cancer: a tissue microarray-based approach. *Am J Clin Pathol* 2007;127:114-23.
- [42] Phillips RM, Bibby MC, Double JA. A critical appraisal of the predictive value of in vitro chemosensitivity assays. *J Natl Cancer Inst* 1990;82:1457-68.
- [43] Hutmacher DW, Horch RE, Loessner D, et al. Translating tissue engineering technology platforms into cancer research. *J Cell Mol Med* 2009;13:1417-27.
- [44] Wu M, Swartz M. Modeling tumor microenvironments in vitro. *J Biomech Eng* 2014.
- [45] Jacks T, Weinberg RA. Taking the study of cancer cell survival to a new dimension. *Cell* 2002;111:923-5.
- [46] Weaver VM, Lelievre S, Lakins JN, et al. beta4 integrin-dependent formation of polarized three-dimensional architecture confers resistance to apoptosis in normal and malignant mammary epithelium. *Cancer Cell* 2002;2:205-16.
- [47] Gout S, Marie C, Laine M, Tavernier G, Block MR, Jacquier-Sarlin M. Early enterocytic differentiation of HT-29 cells: biochemical changes and strength increases of adherens junctions. *Exp Cell Res* 2004;299:498-510.
- [48] Hirt C, Papadimitropoulos A, Mele V, et al. "In vitro" 3D models of tumor-immune system interaction. *Adv Drug Deliv Rev* 2014.

## Figures

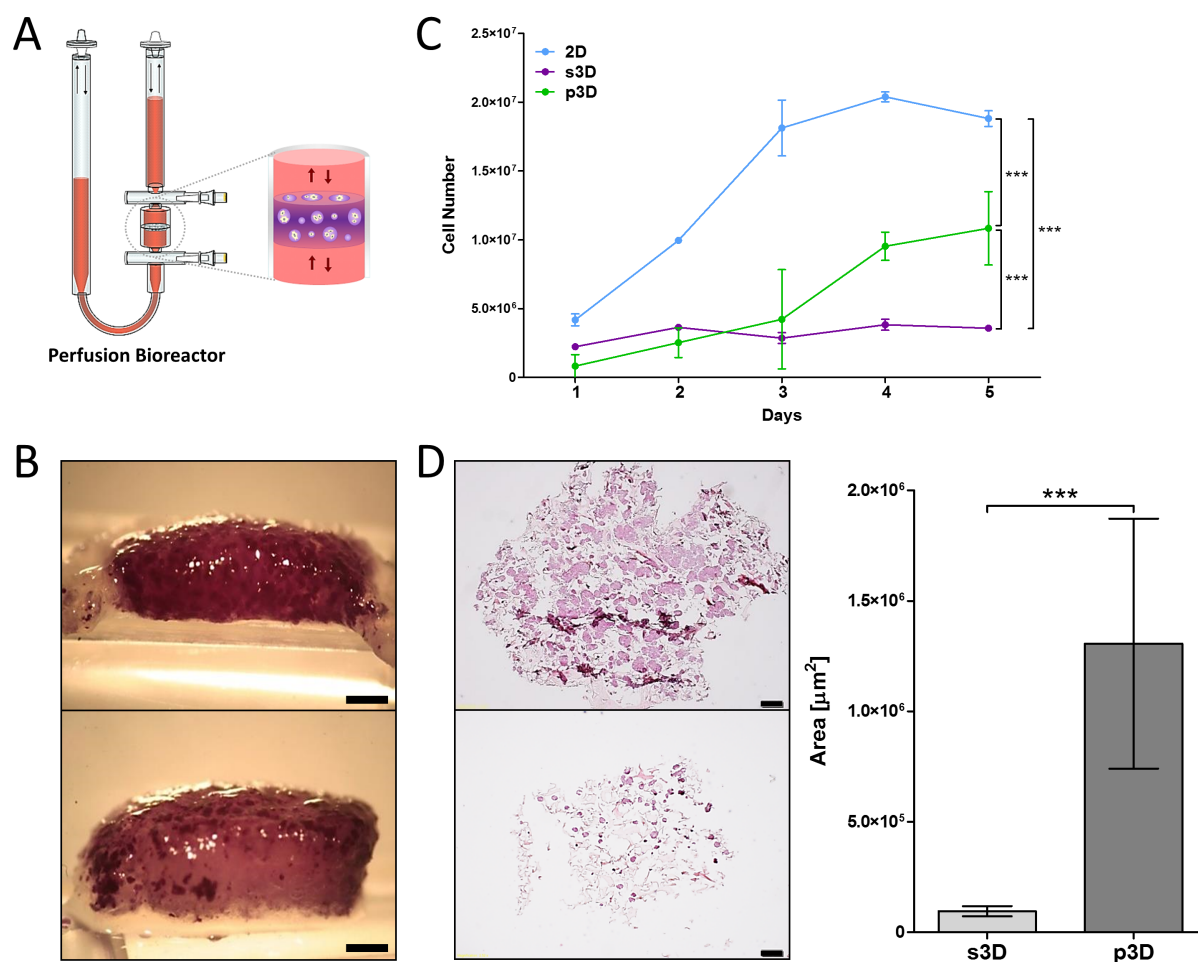


**Figure 1. Growth characteristics of perfused and static tridimensional cultures.**

A: A schematic view of the scaffold-based bioreactor utilized for the culture of tumor cells in perfused tridimensional (p3D) conditions. B: MTT staining of collagen scaffolds seeded with HT-29 cells in p3D (upper panel) or in s3D (lower panel) conditions, following a 7 days culture (scale bar: 1mm). C: Growth kinetics of HT-29 cells under different culture conditions. D: H&E staining of whole scaffold sections from p3D (upper left panel) or s3D (lower left panel) cultures (scale bar: 200 μm). Histomorphometric assessment of tumor tissue areas in whole scaffold sections from p3D and s3D cultures of HT-29 cells (right panel) (\*\*\*: p<0.001).

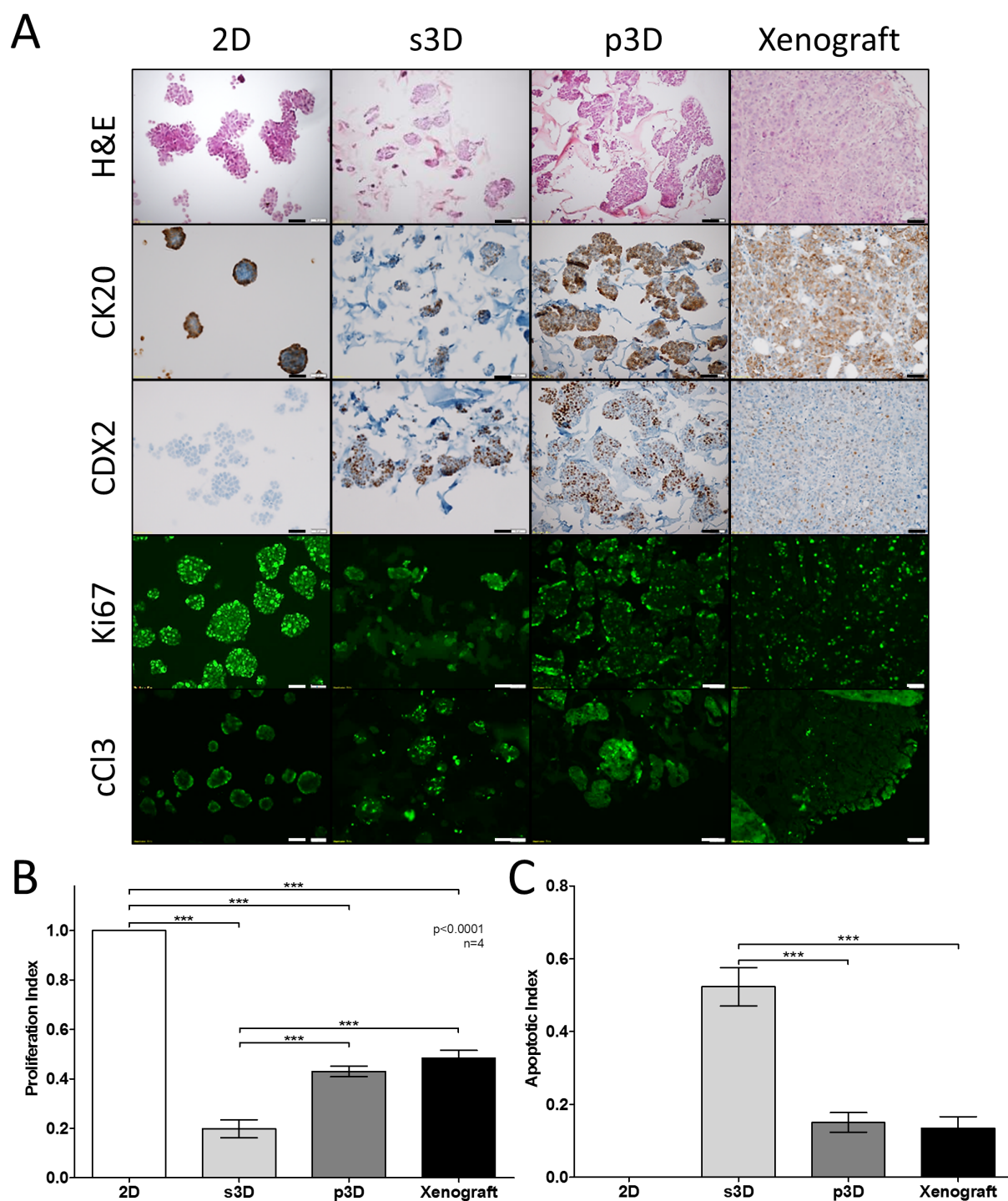


**Figure 2. Comparative analysis of phenotype and proliferation potential of HT-29 cells cultured in different conditions.**

A: HT-29 cells cultured in the indicated conditions or injected subcutaneously in NMRI-mice (xenografts) were stained by H&E or by Cytokeratin 20 (CK20) or CDX2 specific mAbs. Specific binding was visualized by standard immunohistochemical techniques. In parallel experiments, cells were stained by using fluorochrome labeled Ki67 and Cleaved Caspase 3 (cCl3) specific mAbs (scale bar: 50 $\mu$ m). B: Proliferation index was calculated as ratio of Ki67+ cells to total cell number. C: Apoptotic index was calculated as ratio of cCl3+ cells to total cell number. (\*\*\*:  $p < 0.001$ ).

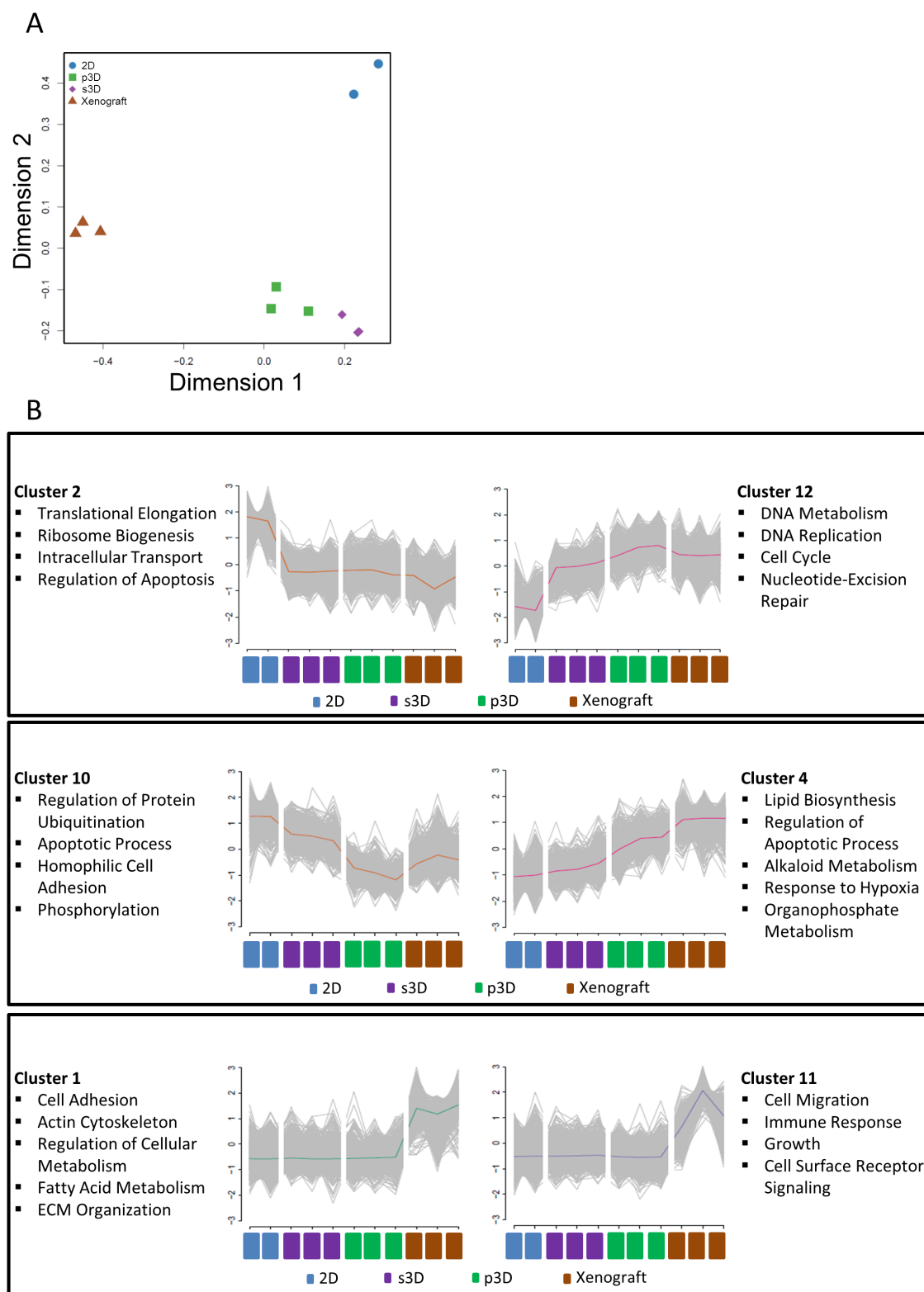


**Figure 3. Next generation sequencing transcriptome analysis of HT-29 cells cultured in 2D, s3D and p3D conditions or growing as xenografts.**

Total cellular RNA was extracted from cells cultured according to the indicated conditions or growing as xenografts. A: Multi-Dimensional Scaling plot showing the relations occurring between individual samples. Distances on the plot represent coefficient of variation of expression between samples for the whole transcriptome. B: Expression profiles and enriched pathways in selected gene clusters based on DAVID Functional Annotation and REVIGO using GO Biological Processes.

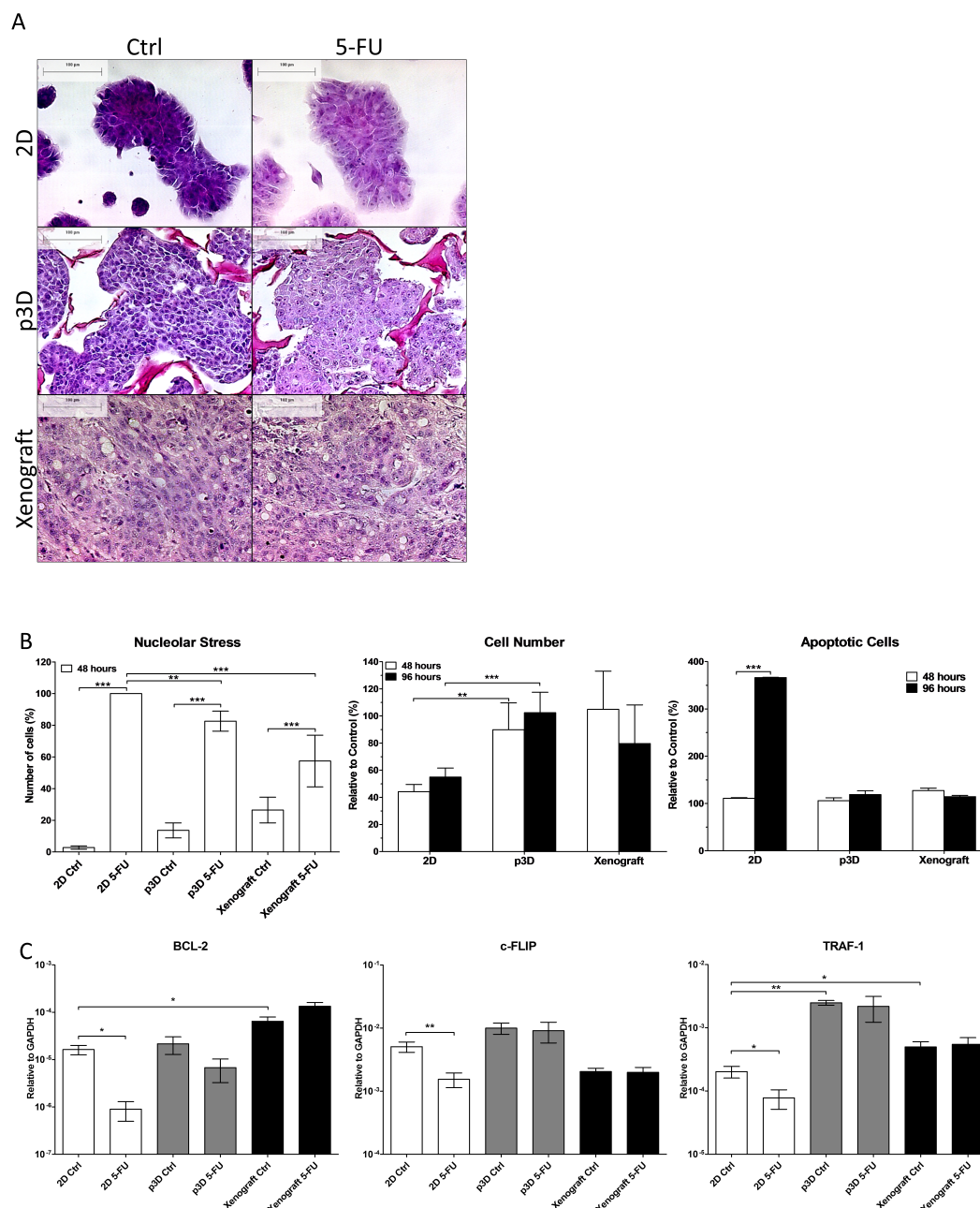


**Figure 4. Response of HT-29 cells cultured in different conditions to 5-FU treatment.**

A: HT-29 cells were cultured in the indicated conditions or injected subcutaneously in NMRI-mice. Cultures and experimental animals were then treated by 5-FU ( $1\mu\text{g}/\text{mL}$  and  $50\mu\text{g}/\text{Kg}$ , respectively), for 48 hours, as detailed in “Materials and methods”. Cells and tissue sections were stained by H&E according to standard methods (scale bar:  $100\mu\text{m}$ ). B: Percentages of cells showing evidence of nucleolar stress in untreated cultures and animals or following a 48 hours 5-FU treatment (left panel). Effects of 48 and 96 hours 5-FU treatment on total tumor cell number or tumor volume as assessed by DNA staining, as compared to untreated controls. (middle panel). Increases in apoptotic tumor cell percentages upon 5-FU treatment in comparison to untreated controls, as measured by Annexin V-PI staining. (right panel). C: Total cellular RNA was also extracted from HT-29 cells cultured according to the indicated conditions or growing as xenografts in NMRI-mice following a 24 hour treatment with 5-FU, and reverse transcribed. Expression of BCL-2 (left panel), c-FLIP (middle panel) and TRAF-1 (right panel) genes was measured by qRT-PCR, using GAPDH gene expression as reference. (\*:  $p < 0.05$ ; \*\*:  $p < 0.01$ ; \*\*\*:  $p < 0.001$ ).

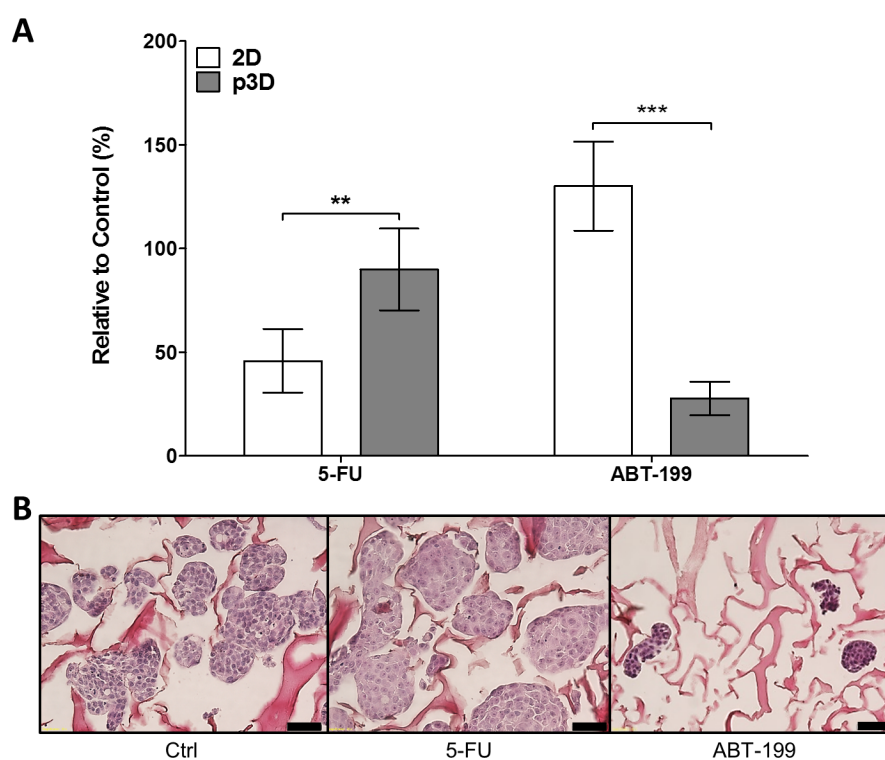
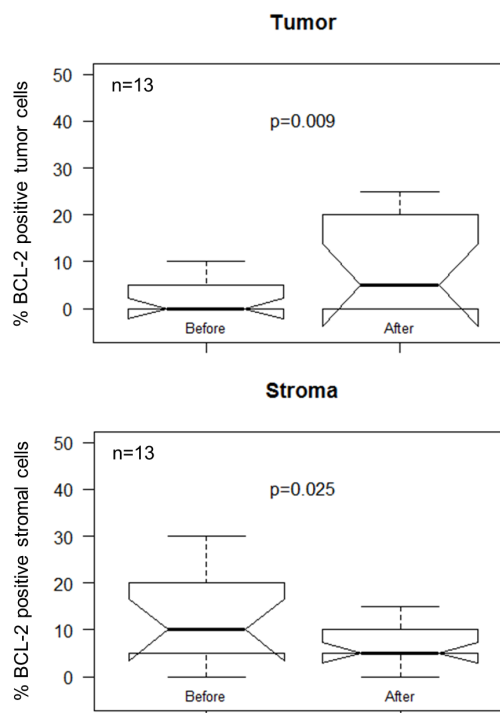


**Figure 5. Differential responsiveness to 5-FU and BCL-2 inhibition by HT-29 cells in 2D and p3D cultures.**

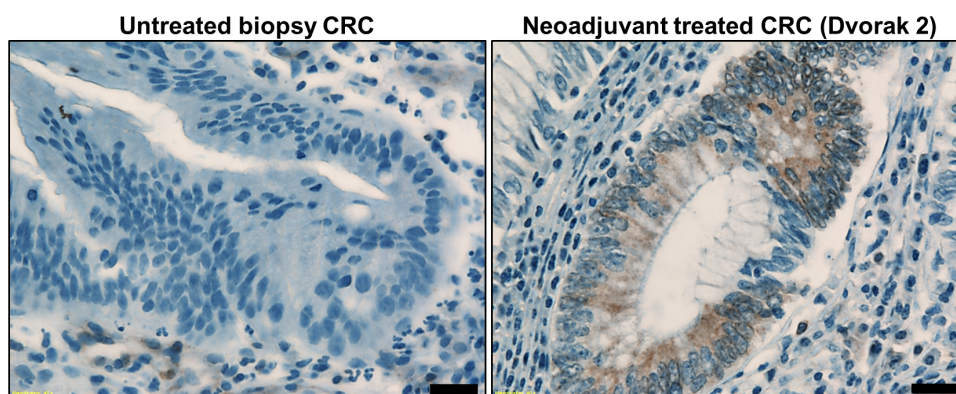
A: Effects of 48 hours treatment with 5-FU or ABT-199 on total numbers of HT-29 cells cultured in 2D or in p3D cultures, as measured by DNA dye staining. B: H&E staining of p3D cultures of HT-29 cells untreated (Ctrl) or following treatment with 5-FU or ABT-199. Scale bar: 50 $\mu$ m. (\*\*:  $p < 0.01$ ; \*\*\*:  $p < 0.001$ ).

**A**

|              |    |
|--------------|----|
| Total number | 29 |
| Sigma        | 3  |
| Coecum       | 1  |
| Rectum       | 25 |
| T =1         | 1  |
| T =2         | 5  |
| T =3         | 16 |
| T =4         | 6  |
| N =0         | 9  |
| N =1         | 16 |
| N =2         | 4  |
| M = 0        | 22 |
| M =1         | 7  |
| Dworak 0     | 5  |
| Dworak 1     | 10 |
| Dworak 2     | 11 |
| Dworak 3     | 1  |
| Dworak 4     | 2  |



**B**



**D**

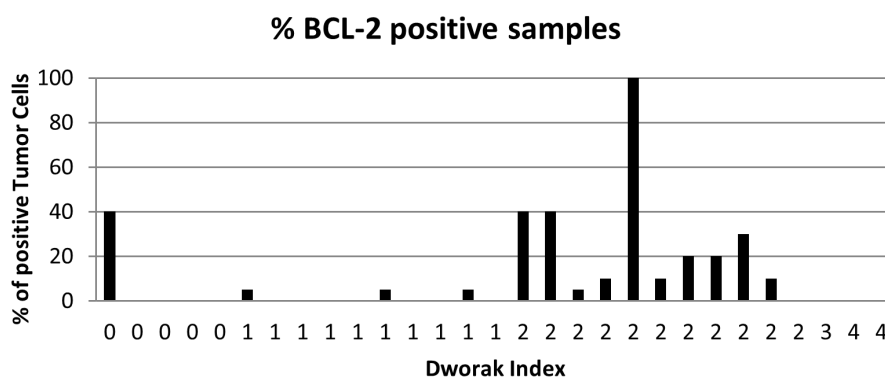


**Figure 6. BCL-2 expression in colorectal cancer specimens from patients undergoing neoadjuvant treatment.**

A: Clinical pathological characteristic of patients with CRC undergoing neoadjuvant treatment. B: Representative BCL-2 specific immunohistochemical staining of CRC pre- and post-treatment specimens from a patient showing evidence of partial (Dworak 2) responsiveness to neoadjuvant therapy (scale bar: 20µm). C: Effect of neoadjuvant treatment on percentages of BCL-2+ cells in tumor and stroma in tissue specimens from patients undergoing neoadjuvant treatment.. D: Percentages of BCL-2+ tumor cells in post-treatment specimens from patients with different degrees of responsiveness to neoadjuvant treatment, as assessed by Dworak grading.

## Supplementary figures

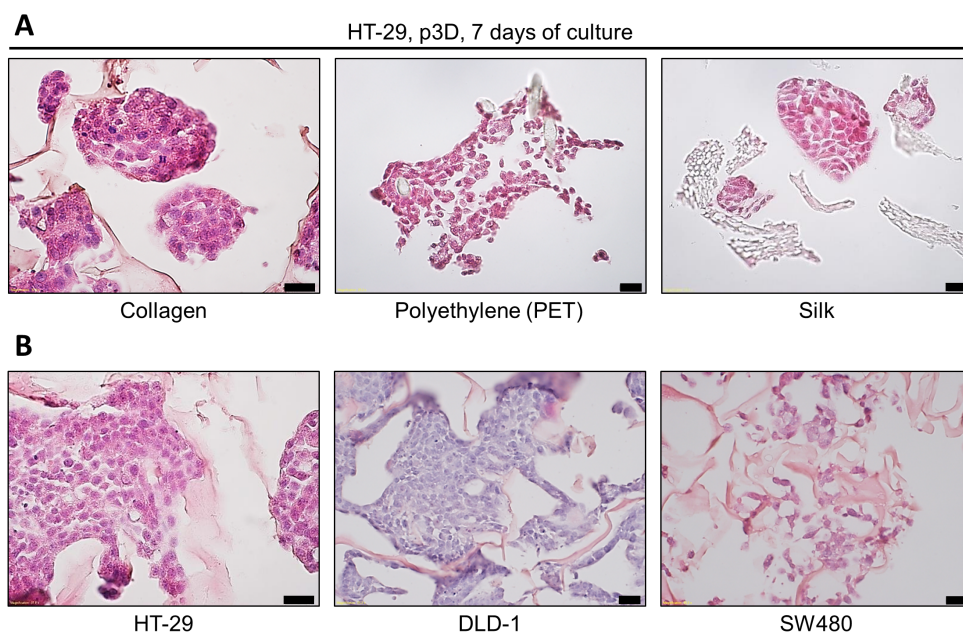


**Figure S1. Colorectal cancer cell lines and scaffolds used in p3D cultures.**

A: Collagen, polyethylene and silk scaffolds were used as substrates for 3D culture of HT-29 CRC cells over 7 days (scale bar: 20 $\mu$ m). B: H&E staining of HT-29, DLD-1 and SW480 CRC cells cultured for 7 days in perfused bioreactors.

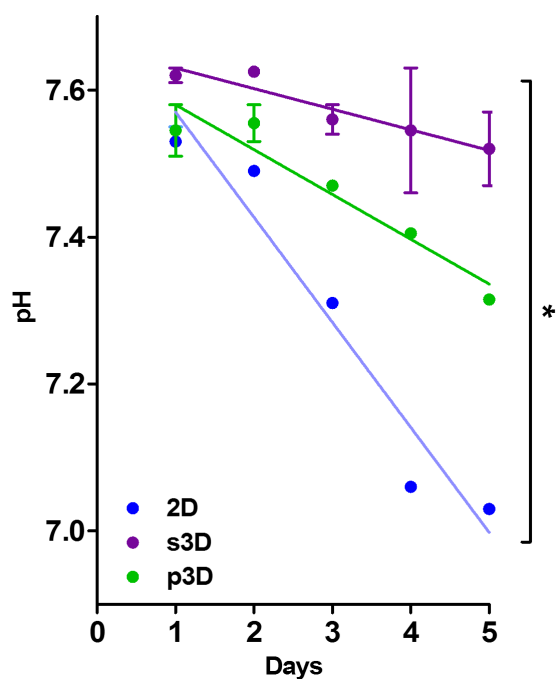


**Figure S2. pH monitoring in supernatants from HT-29 cells cultured in different conditions.**

Supernatants from HT-29 cells cultured in the indicated conditions were used for pH assessment reflecting ongoing cell proliferation. (\*:  $p < 0.05$ ).

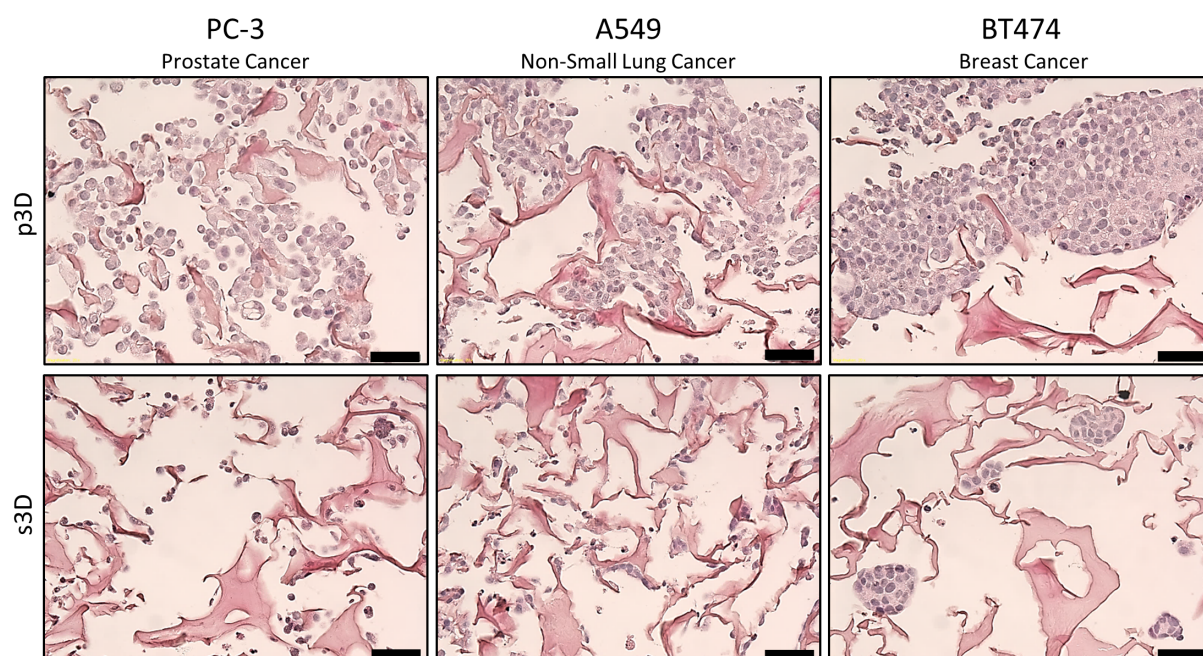


**Figure S3. Generation of tissue-like structures in p3D cultures of cell lines of different histological origin.**

H&E staining of PC-3 (prostate cancer), A547 (non-small lung cancer) and BT474 (breast cancer) cells cultured in p3D and s3D conditions (scale bar: 50 $\mu$ m).

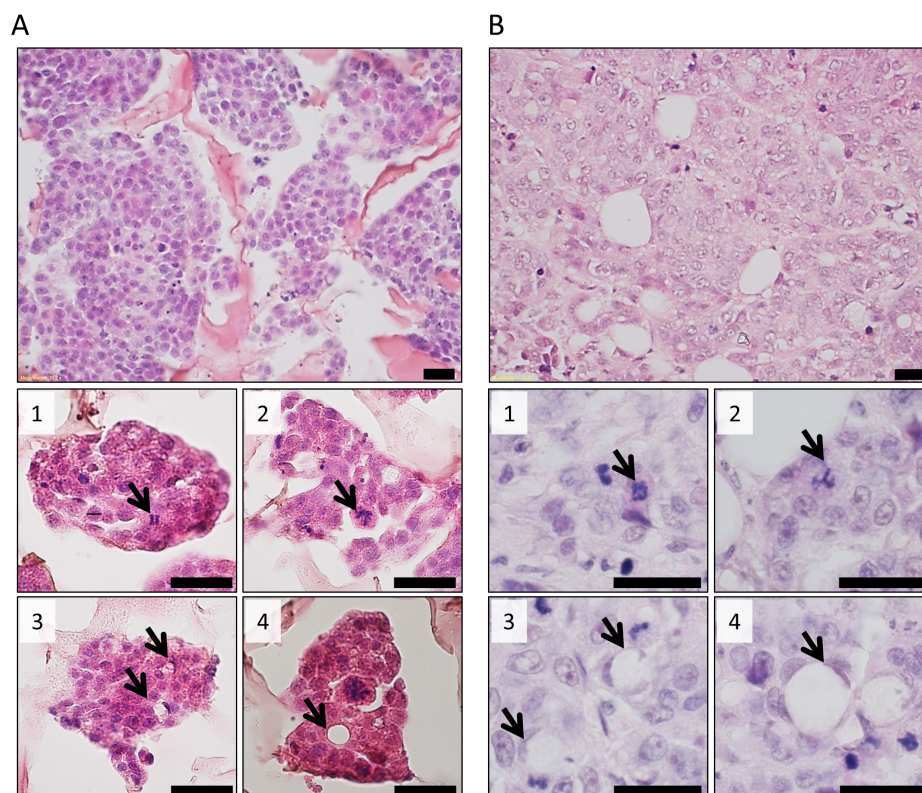


**Figure S4. Morphological analysis of HT-29 cells cultured in p3D or growing as xenografts upon subcutaneous injection in NMRI-mice.**

H&E staining of sections derived from p3D HT-29 cell cultures (A) and xenografts obtained upon subcutaneous injection of the same cells in NMRI-mice (B) (20x). Higher magnification pictures displayed in the bottom panels show the presence in both specimens of mitosis figures (1), atypical mitoses (2), signet ring cells (3) and acini-like formations (4) (scale bar: 20 $\mu$ m).

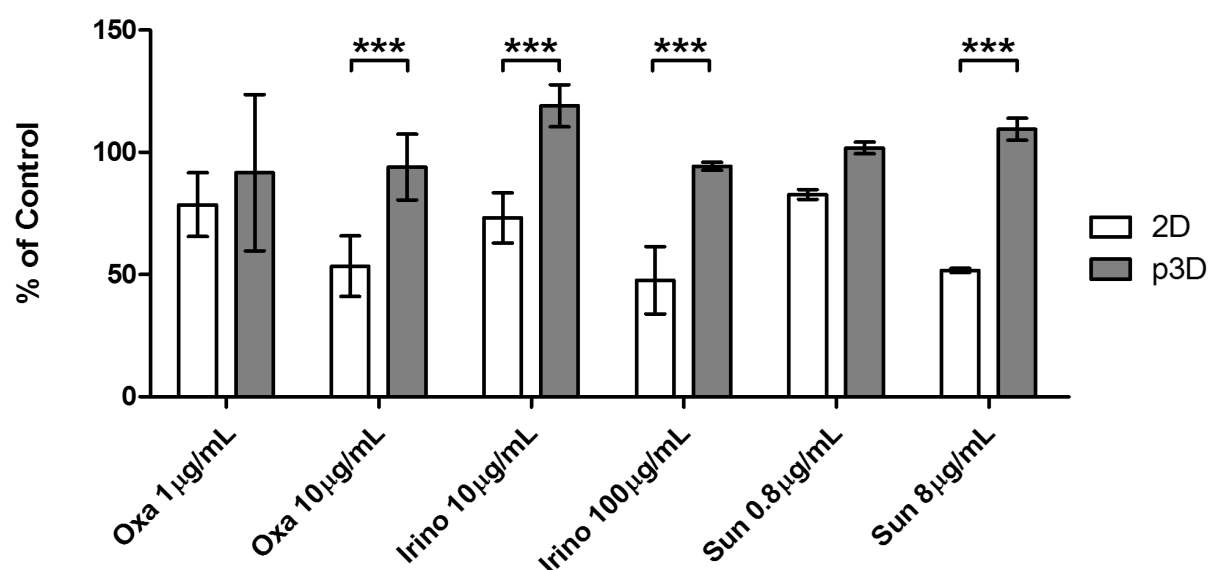


**Figure S5. Effects of standard chemotherapeutic agents commonly used in colorectal cancer treatment on 2D and p3D cultures.**

Effects of different concentrations of chemotherapeutic compounds used in CRC treatment on total numbers of HT-29 cells cultured in 2D or p3D cultures, as assessed by DNA staining following a 24 hour treatment. Oxa=Oxaliplatin, Irino=Irinotecan, Sun=Sunitinib. (\*\*\*:  $p < 0.001$ )

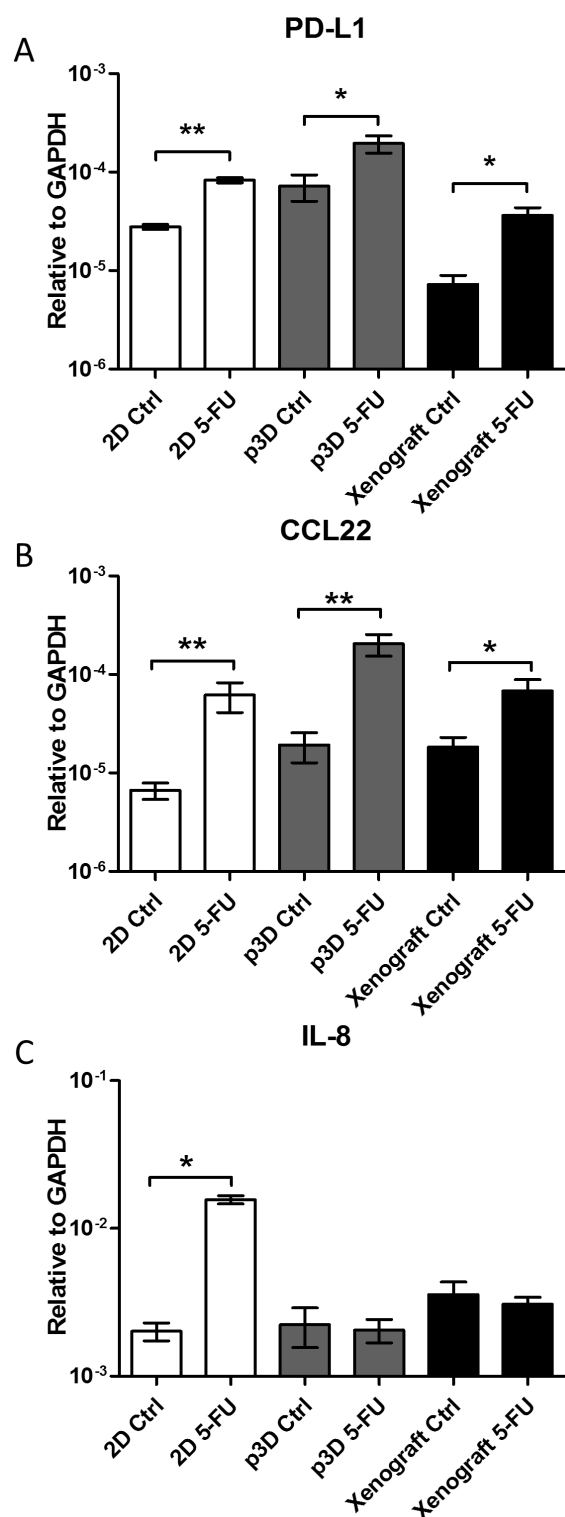


**Figure S6. Expression of PD-L1, CCL22 and IL-8 genes upon 5-FU treatment of HT-29 cells cultured in different conditions or growing as xenografts.**

HT-29 cells cultured in the indicated conditions were left untreated (Ctrl) or incubated in the presence of 5-FU. Immunodeficient animals carrying HT-29 xenografts were also left untreated or were administered 5-FU as indicated in “materials and methods”. Total cellular RNA was then extracted from tumor specimens and reverse transcribed. The expression of the indicated genes was then assessed by qRT-PCR, using *GAPDH* gene expression as reference. (\*p: <0.05; \*\*p: <0.01).

## **Perfused primary tumor culture in a bioreactor enables preservation of initial tumor microenvironment in vitro for several tumor entities**

Christian Hirt<sup>1,2</sup>, Francesca Amicarella<sup>2</sup>, Eleonora Cremonesi<sup>2</sup>, Savas Soysal<sup>1,2</sup>, Simone Münt Soysal<sup>3</sup>, Luigi Mariani<sup>1,4</sup>, Christoph Kettelhack<sup>1</sup>, Michael Heberer<sup>1</sup>, Giulio Spagnoli<sup>2</sup>, Ivan Martin<sup>5</sup>, Giandomenica Iezzi<sup>2</sup> and Adam Papadimitropoulos<sup>5</sup>

*Departement of Surgery, University Hospital Basel, Switzerland<sup>1</sup>*

*ICFS Oncology Group, Department of Biomedicine, University of Basel, Switzerland<sup>2</sup>*

*Institute of Pathology, University of Basel, Switzerland<sup>3</sup>*

*Brain Tumor Biology Group, Department of Biomedicine, University of Basel, Switzerland<sup>4</sup>*

*ICFS Tissue Engineering Group, Department of Biomedicine, University of Basel, Switzerland<sup>5</sup>*

### **Key words:**

Primary tumor specimens – tissue engineering – 3D tumor culture – perfusion bioreactor – collagen scaffold

### **Notes:**

1) Financial support was provided by the Lichtenstein-Stiftung of the university Basel, the KTI grant and the department of surgery university hospital Basel, Switzerland

2) Corresponding Authors:

Adam Papadimitropoulos, Tissue Engineering lab, Institute of Surgical Research and Hospital Management and Department of Biomedicine, University of Basel, 20, Hebelstrasse, 4031, Basel, Switzerland. Mail: adam.papadimitropoulos@usb.ch

Giandomenica Iezzi, Cancer Immunotherapy, Institute of Surgical Research and Hospital Management and Department of Biomedicine, University of Basel, 20, Hebelstrasse, 4031, Basel, Switzerland. Mail: giandomenica.iezzi@usb.ch

3) A.P., I.M. and G.C.S. are shareholders of Celtec Biotek AG.

4) Word count: 6455

5) Total number of figures/tables: 13/2

### **Category:**

Original report

### **Abbreviations:**

CRC, colorectal cancer; UF, ultrafoam (collagen); PET, polyethylen; HS, Human Serum; HP, Human Plasma;

## Abstract

Statical in vitro culture of tumor specimens from epithelial tumor's like colorectal cancer have a limited survival efficiency and expansion of tissue remains low. Nutrient availability and oxygen delivery could be increased by using a 3D perfused bioreactor system.

Fresh colorectal cancer specimens were minced and enzymatically predigested to generate tissue chunks of 1-2mm size. After carefully washing and Octenisept treatment of the chunks, they were placed between to collagen scaffolds to generate a kind of "sandwich-construct". This was then placed in the chamber of the perfusion bioreactor and directly perfused over 10-20 days.

Collagen scaffolds were strongly remodeled over time presenting with nodular structures visible by eye. Efficiency of tissue generation after 10 days was 66.6% (10/15). 3 samples (20%) were contaminated and in 2 samples (13.3%) we did not found any tissue. For both fresh and frozen tumor chunks it was possible to generate tissue. Compared to only slight expansion of tissue in liquid-overlay technique or statical 3D culture we could obtain up to 13 fold increase in tissue formation due to perfusion 3D culture. The generated tissues were of a heterogeneous phenotype: besides epithelial structures, as stained by EPCAM, many Vimentin positive tumor stroma cells were visible. Additionally some CD4 and CD8 T-cells consisted within the preserved tissue. Both parts, tumor and stromal cells were alive and proliferating. By using autologous patient-derived plasma or allogeneic human serum in the medium instead of supplements or fetal-calf-serum much larger and denser tissue was generated. Splitting of tumor tissue and expansion to over 20 days was possible for both epithelial and stromal parts. Additionally EPCAM positive and negative living cells were found in suspension over 20 days culture period.

The established protocol could easily be adapted to other tumor entities with a high efficiency of tissue formation as tested for primary breast-cancer, glioblastoma, sarcomas and melanomas. In none of them contamination was a problem, therefore antibiotic in culture medium could be reduced.

Taken together, our results show that primary tumor cultures can be successfully performed within a perfusion bioreactor device, by maintaining and expanding a tissue of mixed epithelial and stromal phenotype over a short-time period in a reproducible manner. These ex-vivo generated tissues could better mirror features of the original tumor, in particular with regard to treatment sensitivity, and may therefore be a useful tool to evaluate standard chemotherapies or new targeted treatments.

## Introduction

Cancer Cell lines are widely used for preclinical studies but only marginally reflect the heterogeneity of tumor tissue where they derive from. They are mostly genetically homogenous with some limited morphological heterogeneity and adapted to plastic dishes through decades of in vitro cultures<sup>1</sup>. A recent study compared copy-number changes, mutations and mRNA expression profiles of commonly used ovarian cancer cell lines and high-grade serous ovarian cancer tumor samples. Alarmingly, rarely used cell lines in this case resembled more closely the cognate tumor profiles than commonly used cell lines<sup>2</sup>. Because of this reasons the translation to their patient-counterparts is from cell line studies not always simple to perform. Culture of primary tumor cells in vitro could therefore represent an optimal tool for not only studying tumor biology but as well to as use for drug screening purposes.

The tumor microenvironment consist on cellular, e.g. stromal and immune cells, and non-cellular, e.g. extracellular matrix, components. Even characterized for their malignant invasive cell growth in vivo most cancer cells depend strongly on this factors for sustained growth not only in the patient but as well in vitro. Stromal and immune cells strongly influence tumor growth patterns and angiogenesis due to endothelial cells is crucial to overcome the limitation by otherwise reduced nutrient and oxygen availability<sup>3,4</sup>.

In the context of colorectal cancer it has been shown that retaining cell-cell contact increases the efficiency of spheroid-generation from primary colorectal cancer specimens<sup>5</sup>. Providing niche-dependent signals can be critical for tumor cells. Only recently, with the establishment of the liquid-overlay culture from not completely digested colorectal cancer tissue, in up to 30% of primary tumors so-called organoids could be generated<sup>6</sup>. First growth can be estimated after few days in culture. Expansion of such organoids is low and several passages needed to obtain enough material for serial testing.

On the other hand patient-derived xenograft models, where tumor tissue is injected subcutaneously, have been proposed to overcome the limitations of tumor material availability<sup>7</sup>. The efficiency reported here is depending on tumor type and reaches for colorectal cancer 68%<sup>8</sup>. Tumor growth can be seen after 1-2 months. Studies have shown that the generated xenograft tumor is corresponding more to the metastatic lesion than to the primary tumor it was derived from<sup>9</sup>. For both organoid cell culture but as well patient derived xenografts the initial tumor microenvironment get's replaced by the epithelial tumor cells over time. In the case of the PDX human stromal cells are replaced by mouse stromal cells<sup>10</sup>. The initial composition is therefore drastically changed.

As older studies have shown the possibility to culture whole tumor tissue over time with some efficiency but low expansive capacity<sup>11</sup>, more advanced 3D culture techniques could help to further increase nutrient and oxygen availability leading to survival of both stromal and epithelial parts of the initial tumors. We have seen that we can increase several fold the tumor-tissue generation of a colorectal cancer cell line by direct perfusion in a 3D bioreactor system (Hirt et al., submitted). The generated tissue-like structures where not only based on morphological features and whole genome expression more similar to in-vivo generated tumors, but corresponded in response and resistance mechanisms to 5-fluorourail similar to

xenografts and even neoadjuvant treated colorectal cancer samples. A 3D perfused culture device could therefore preserve important functions of the initial tumor tissue. We wanted therefore to adapt this culture technique for primary tumor culture in general. We established a new culture method by initially using primary colorectal cancer specimens which are because of the high commensal load difficult to culture and extended then the protocol to other tumor entities. By using small tissue-chunks we aimed to sustain the initial tumor microenvironment composition and allowing the integration of the tissue in the surrounding collagen-scaffold.

## **Material and Methods**

### ***Medium, supplements and scaffolds***

Tissue specimens were maintained up to 20 days in RPMI (SIGMA-Aldrich®) or DMEM/F12 (Gibco®) containing 1% GlutaMAX™-I 100x (Gibco®), 1% Kanamycin sulphate 100x (Gibco®), Metronidazol (250x; 200mg/ml, Braun), Cefuroxim (250x; 15mg/ml, Braun), 1% Fungizol (Sigma-Aldrich), 1% HEPES 1 M (Gibco®), N-Acetyl-Cysteine 1mM (NAC, 500x, stock 500mM, Sigma-Aldrich), Nicotinamid 10mM (Nic, 100x, stock 1M, Sigma-Aldrich). Additional supplements were Prostaglandin E<sub>2</sub> 0.1ug/ml (Tocris Bioscience) and Epidermal Growth Factor 25ng/ml (Stem Cell Technologies, Grenoble, France).

For blood-derived culture conditions either patient derived plasma, pooled human serum (Blood Bank, University Hospital Basel, Switzerland) or fetal calf serum (Gibco®) in a 10% concentration was used. For serum-free culture standard organoid culture supplements B27 2% (Invitrogen) and N2 1% (Invitrogen) were used.

Collagen (UF) Scaffolds (Ultrafoam Avitene Collagen Hemostat®, UF) were obtained from Davol Inc., Warwick, USA. A non-woven polyethylene (185g/m<sup>2</sup>, needlepunch, cat. N. 72.185.503, PET) scaffold mesh was obtained from Norafin Industries, Mildenau, Germany. Collagen-crosslinked scaffolds (Optimaix) were obtained from Matricel GmbH, Germany. The scaffolds were cut by a biopsy punch for 8mm for the collagen-sandwich-assay.

### ***Human Tissue Materials***

Fresh surgically resected colorectal cancer (n=15), glioblastoma (n=3), sarcoma (n=2), melanoma (n=1) or breast cancer specimen's (n=3) samples were obtained from patients operated at the University Hospital Basel, Regional Hospital Olten or regional Hospital Lugano. All patients gave informed consent. Initial tissue samples were 3-5mm in diameter and excised by a pathologist from the tumor center. The tissue was carefully washed in 4° C phosphate buffered saline (PBS, Sigma-Aldrich).

### ***Preparation of minced and chunked tissues***

The tissue is washed 3 times with PBS and minced in pieces with a scalpel. Minced tissue is then enzymatically pre-digested in DMEM (GIBCO) with collagenase IV (100x, stock 20kU/ml; Worthington CLSS-4), DNase I (100x, stock 50mg/ml; Sigma-Aldrich D5025), HEPES (100x, stock 1M, GIBCO 15630-056), Kanamycin (100x; GIBCO 15160-047), Amphotericin B (100x, stock 250ug/ml; Sigma-Aldrich A9528), Metronidazol (250x; stock 200mg/ml, Braun), Cefuroxim (250x; stock 15mg/ml, Braun) for 1 hour at 37° at continuously smooth rotation on a MACSmix tube rotator (Miltenyi Biotec). The generated chunk tissue was washed once with

PBS including EDTA 1:250 & 10% pooled Human Serum (Blood Bank, University Hospital Basel, Switzerland), and treated afterwards for 5 min with a 2.5% Octenisept (Schülke&Mayr, Germany)-10% Human Serum-PBS solution. To remove the Octenisept completely an additional wash with EDTA-HS-PBS was performed.

### ***3D perfused culture in collagen-sandwich assay***

To culture tissue chunks in 3D under perfusion we used the previously developed perfusion bioreactor system for cell seeding and culture of 3D scaffolds<sup>12</sup>. The predigested tissue fragments (chunks) were therefore placed on the scaffold together with the remaining cell digest. 2-3 larger tissue fragments (0.5mm in size) could be placed. Scaffolds were then transferred to the scaffold holder and another scaffold was applied to obtain the collagen-sandwich assay. A grid was used on top and bottom of the collagen-scaffold and the scaffolds held fixed by a teflonring. This construct was then placed in the culture chamber of the perfusion bioreactor. A flow rate of 0.3ml/min was chosen for perfusion culture.

Medium change was performed twice a week. Constructs were harvested at either 10 or 20 days. DNA quantification, histological and immunofluorescence analysis were performed for those time points.

### ***Organoid cell culture of chunked tissues***

For organoid cell culture of chunk tissues the previous method from Sato et al. was used<sup>6</sup>. Briefly fragments, measuring 0.5-1mm, were cultured on coated Matrigel (growth-factor reduced, phenol red free, BD Bioscience, Switzerland) 24-well plates. Culture medium with supplements was overlaid and tissue fragments cultured for the same culture period as 3D perfused cultures.

### ***DNA quantification***

Collected samples as described above were further digested with proteinase K solution (1 mg/ml proteinase K, 50 mM TRIS, 1 mM EDTA, 1 mM iodoacetamide, and 10 µg/ml pepstatin-A; Sigma–Aldrich, USA) in double distilled water or potassium phosphate buffer for 16 h at 56 °C as previously described.

DNA quantification was performed by means of a commercially available fluorescence based kit, namely CyQUANT® Cell Proliferation Assay (Invitrogen, USA). Working solutions were prepared according to the manufacturer's protocols. The analyses were carried out measuring fluorescence with a Spectra Max Gemini XS Microplate Spectrofluorometer (Molecular Devices, USA). Excitation and emission wavelengths were respectively 485 nm and 538 nm. Samples in each plate included a calibration curve. Each sample was measured in triplicate.

### ***Histological staining and immunofluorescence***

Tumor-Collagen tissues after 3D perfusion culture were fixed overnight in 1.5% paraformaldehyde at 4°C, paraffin embedded (TPC15 Medite, Switzerland) and sectioned (5 µm-thick) by means of a microtome (Leica, Switzerland). Paraffin sections were deparaffinized, hydrated and stained with hematoxylin and eosin (H&E), followed by observation under light microscopy.

Immunofluorescence analyses on paraffin embedded sections were performed after antigen retrieval at 95° for 30min with target retrieval solution ready-to-use (DAKO, S1700). To characterize the proliferating cell population a Ki67 monoclonal antibody 1:100 (Rb mAb FITC, AbCAM, ab27619) was used<sup>13</sup>. For visualization of stromal

cells Vimentin monoclonal antibody (Rabbit mAb, Cell Signaling 5741), for epithelial cells EPCAM monoclonal antibody (Mouse mAb, Cell Signaling 2929) and for immune cells CD4 (Mouse mAb) or CD8 (Rabbit mAb) were applied. To improve the signal strength a secondary monoclonal antibody goat-anti-rabbit, Alexa-Fluor 488 1:400 (IgG, Invitrogen), resp. monoclonal antibody goat-anti-mouse Alexa-Fluor 546 1:400 (IgG, Invitrogen) was applied. Nuclei were stained with DAPI 1:100 (Invitrogen). Histological and immunohistochemical sections were analyzed using a BX-61 microscope (Olympus, Germany).

### ***Quantification of gene expression by quantitative Real-Time PCR***

Total cellular RNA was extracted by using NucleoSpin RNA II kit (Macherey-Nagel) and reverse transcribed by standard methods<sup>14</sup>. qRT-PCR assays were performed in the presence of primers and probes specific for the indicated genes (Assays-on-demand, Applied Biosystems). Normalization of gene expression was performed using GAPDH as reference gene<sup>15</sup>.

### ***Flow cytofluorometric analysis***

Supernatant of cultured primary samples was stained with EPCAM-APC (ab27619, clone SP6, Abcam, Cambridge, UK) and Propidium Iodid (Sigma-Aldrich). Analyses were performed using a FACSCalibur flow cytometer (BD Biosciences, Germany). Gates were adjusted according to isotype control reps. unstained sample.

### ***Statistical Analysis***

Statistical Analysis was performed as previously described (Flis et al. Anticancer Res 2009). The data is presented as mean values±standard deviation (SD).

## **Results**

### ***Establishment of a primary perfused tumor culture of colorectal cancer***

To culture primary colorectal cancer specimens for in-vitro 3D culture we took advantage of a previously described perfusion bioreactor and adapted it to our needs (Fig.1)<sup>16</sup>. As earlier reports mentioned the critical dependence of primary tumor cells on niche-signals, cellular heterogeneity and 3D architecture<sup>17</sup>, we used either pre-digested minced tissue or tissue fragments for perfusion culture. Enzymatic pre-treatment of tissue fragments enhanced their tissue forming capacity (Fig.1.1), as previously reported<sup>6</sup>.

Commensal microorganisms heavily contaminate CRC tissue specimens. Therefore, an initial wash with PBS-EDTA supplemented with 10% HS and a short treatment with 2.5% Octenisept was performed to reduce bacterial load.

Following preparation and pre-treatment tumor fragments were placed between two collagen scaffolds, e.g. in a “scaffold-sandwich”. This step is necessary not only to keep tissue specimens in place after static loading under perfusion but also to allow expansion and remodeling of the tumor in the surrounding scaffold. A 10 days perfusion culture results in a profound restructuring of collagen scaffolds as compared to their empty counterparts (Fig.2). Other scaffolds tested, like polyethylene or crosslinked collagen scaffolds were unsuitable for the generation of tissue-like structures (Fig.1.3, Sup Fig 1).

Initial studies have shown the superiority of autologous human plasma over fetal calf serum with denser and larger tissue formation by H&E stainings (Sup. Fig. 2). As availability of autologous human plasma is usually limited, we used pooled human serum for tissue culture and could obtain similar tissue structures over time<sup>18</sup>. Expression of genes regulating apoptosis (BCL-2) and proliferation (Ki67) were similar for both autologous human serum and human plasma. EPCAM gene expression similar to pre-expansion values using pooled human serum and stromal marker Thy1 was slightly increased (Sup. Fig. 6). Pooled human serum showed a trend in superior tissue yield and quality as compared to conventional serum-free approaches using B27/N2 as evaluated by organoid (Sup.Fig.1) and perfusion cell culture (Sup.Fig.3). As described for static 3D cultures addition of Prostaglandin E 2 (PGE2) and epidermal growth factor (EGF) could help to further increase tissue formation<sup>19</sup>. Measured by the total DNA-amount (Sup.Fig.1) and evaluated histologically (Sup.Fig.3), we found a similar trend and therefore used for our perfusion culture medium supplemented with commercially available pooled human serum together with EGF and PGE2.

***Perfused primary tumor culture enables formation of proliferating tumor-stroma nodules over short-term culture periods***

Using the above-described approach for tumor culture we observed after 10 days culture a strong remodeling of collagen scaffolds. Large tumor-nodules ranging up to one millimeter in diameter were clearly visible in all cases tested. The remodeling capacity depended on the individual patient and tissue status, e.g. fresh or frozen, prior to culture. Interestingly, RPMI1640 medium appeared to induce a stronger restructuring of the collagen scaffold as compared to DMEM/F12 Medium (Fig. 2A).

Upon histological evaluation, we could observe a heterogeneous tissue formation with both epithelial and stromal parts, as detectable by EPCAM or Vimentin specific staining, respectively (Fig.3.B/C). In some cases infiltration by lymphocytes could be observed (Fig. 3.D/E & Sup.Fig.4). RPMI1640 Medium promoted stromal proliferation to a slightly higher extent than DMEM, as visible by macroscopic view and histological evaluation (Fig. 2B). Interestingly, epithelial cells formed barriers or acini structures and eventually lead to maintenance of villi-like protrusions (Fig.2 C/D), recapitulating gut morphology. Nevertheless, the epithelial structure still displayed a highly dysmorphic and anaplastic phenotype consistent with its origin from the initial tumor mass (Fig. 2B, Sup. Fig. 5 A)

Immunofluorescence evaluation by staining for EPCAM, showed that nodular structures were largely, albeit not exclusively, of epithelial nature. Tissue was viable and proliferating, as stained with the proliferation marker Ki67 (Fig. 3A). Proliferation could be seen on both stromal and epithelial parts. The frequency of proliferating cells was similar to that observed in the initial tumor biopsies (Sup. Fig. 5 C).

Regarding gene expression analysis EPCAM was slightly reduced and stromal marker Thy1 increased by using a perfused tumor culture with pooled human serum (Sup. Fig. 7 A/B). Proliferation measured by Ki67 was reduced compared to the pre-expansion sample and apoptotic gene expression BCL-2 were similar (Sup. Fig. 7 C/D). As the prognosis of colorectal cancer is largely influenced by immune cell infiltration<sup>20-22</sup>, we assessed expression of CD8, FOXP3 and CD16. This genes were reduced compared to the initial values but still detectable (Sup. Fig. 7 E-G). Without

perfusion respectively in 2D cultures no gene expression could be measured (GAPDH > 35).

### ***Slight tissue expansion through organoid culture resp. tissue lysis in static conditions compare to several fold tissue expansion under perfusion***

To evaluate the use of perfusion in primary tumor culture, we compared our 3D perfused cultures to the culture of tissue chunks by the organoid culture technique. Macroscopically, as above mentioned, after 10 days perfusion culture large tumor nodules were visible measuring up to 2 millimeter, where in organoid static cultures only slight size differences and evasion of single cells could be observed (Fig 4A).

Depending on samples after 10 days an up to 13 fold increase (+/- 7.3) in total DNA-amount was reached in perfused, as compared to static cultures. The difference after 20 days culture was reduced but remained at 2.2 fold (Fig.4B). Indeed, if tumor specimens were cultured within the scaffold-sandwich in static conditions, only a small sample was recovered after 10 days culture and the surrounding collagen scaffold was mostly digested. In the perfused culture a scaffold remodeling took place. In addition, in the absence of perfusion tissues were largely degraded and signs of tissue lysis were visible.

### ***Preservation of co-culture of epithelial and mesenchymal parts over 20 days of culture***

As we could keep tumor tissue for 10 days under perfusion culture alive and proliferating, we wondered whether tumor tissue could be expanded through longer time. We therefore cultured tumor tissue either for 10 or 20 days and performed a histological analysis (Fig.5A/B). Compared to the initial tumor fragment we could observe an expansion of the tissue and maturation over time reaching a compact tissue at day 20. Both stromal and epithelial cells could be preserved over time.

### ***3D passaging of tumor tissue under perfusion***

To study the potential of our 3D perfused culture technique we cultured tumor tissue for 12 days and re-cultured afterwards half of the tumor-tissue for additional 9 days. The collagen scaffold showed at the first time point several tumor-nodules and at the later one a higher central density with slight remodeling. Histologically epithelial and stromal cells could be observed at both time points integrating in the collagen scaffolds.

As tumor tissue is shedding cells in the circulation during the growth, tumor cells can be detected as circulating tumor cells in the blood stream<sup>23</sup>. The number of circulating tumor cells is correlating with prognosis and correlating as well with treatment response<sup>24</sup>. Interestingly by FACS analysis of the perfused medium we could detect over time living tumor cells, as evaluated by with EPCAM and PI (Sup.Fig. 7). Shed viable tumor cells were detected over 20 days and the percentage varied from tumor. A substantial number of cells were of non-epithelial nature as well.

### ***Evaluation of culture conditions for other tumor entities***

As with the established method it was possible to culture primary colorectal cancer specimens with a high efficiency, we wondered if this could be adapted to other tumor types. Therefore we cultured similarly sarcomas, glioblastomas, breast cancer and melanoma primary samples directly coming from the operating room (Tab. 2 and Fig. 6). Compared to static plain culture and static perfusion culture much

more cells could be preserved over time. No contamination was detectable and as antibiotics have some anti-proliferative capacity, they could be reduced to one (Kanamycin). Sarcomas were most similar after perfusion culture to pre-expansion samples. Glioblastomas showed only reduced tissue preservation. Breast-cancer perfusion culture seem to be dependend to some extend on the supplementation with estrogen as supplementation increased the tissue yield. Tissue quality after perfusion culture strongly depends on the initial tissue quality, as evident in the neoadjuvant pretreated melanoma samples where necrotic tissue was repopulated by the infiltration with single macrophages.

## Discussion

Primary epithelial tumor culture from patient biopsies or surgical specimens in vitro have been a long time goal in science since decades. Despite the significant efforts performed in the past, primary culture remained very difficult to be established. For many types of cancer, it is far easier to grow the normal cells than the cancer cells<sup>25</sup>. Even for cancers that are relatively easy to grow, such as melanomas, only the metastatic cancers can be established as immortal cell lines<sup>26</sup>. Previous studies showed that primary tumors strongly depend on signals from the tumor microenvironment for successful in vitro culture<sup>5,17</sup>, Preservation of the tumor microenvironment consisting of both benign and malign cells remains even with this organoid cell culture technique difficult to achieve

In our study we established a new protocol to prepare and directly culture in vitro fresh tumor specimens for a high efficient in vitro culture using a perfused bioreactor system. As single cells digest of tumor tissue are in most cases leading to an in vitro cell-death due to missing micro environmental signals<sup>5</sup>, we use mechanically and enzymatically pre-treated colorectal cancer specimens leading to cell clumps and tissue fragments of hundreds of cells. For the first time this helps not only to prevent cell death in vitro but as well keeps the initial heterogeneous tumor microenvironment consisting of epithelial, stromal and immune cells together. This stays in the context of the work by Sato et al. where enzymatically pre-digestion of murine intestinal tissue increases significantly the efficiency of organoid formation<sup>6</sup>. We assume that this mechanical and enzymatical stress leads to the initiation of tissue healing process, which could be of help to in tissue generation in vitro.

Colorectal specimens are heavily overgrown by commensals a reduction and inhibition of the bacterial growth is in this context essential<sup>27</sup>. Bacterial growth in best conditions, as a perfused 37° mediums offers, exceeds cellular growth several fold. Addition of a cocktail of antibiotics is besides this successful pretreatment necessary. For other tumor's where the interaction with commensals is less pronounced fewer antibiotics can be used, as this additives lead as well to a reduction in proliferative capacity of the cells itself.

Interestingly we have seen that the culture with autologous patient derived plasma or pooled human serum is superior to fetal calf serum, where only few fragments of tissue are surviving. It has been shown that fetal calf serum-sensitized human lymphoid cells were active in cytotoxicity assays against a wide variety of cultured human tumor and normal target cells<sup>28</sup>. As in our culture conditions lymphoid cells will be present, non-specific activation due to FCS could lead to tissue destruction. In our hands serum-based medium is still superior to serum-free

approaches. Further additives like EGF or PGE2 could be helpful to increase tissue-regeneration capacity depending on individual tumor properties.

By using direct perfusion of tumor-constructs in a collagen-sandwich assay we were able to observe not only a survival of the heterogeneous tumor tissue but as well a strong remodeling and integration into the scaffold. For general tissue engineering purposes scaffolds are besides cells and growth factors one of the main important parts and are crucial to build up a physiological architecture<sup>29</sup>. Collagen scaffolds have a high compatibility for supporting growth of different cell types and have been shown to enhance the histogenesis under perfusion in bioreactor systems<sup>30</sup>.

Compared to the established organoid cell culture where epithelial cells are selected during the culture phase we were able to observe stromal survival 20 days and longer in the perfused bioreactor. This is important in the context, that tumor-stromal interactions are crucial in modifying drug responses<sup>31</sup>. Without flow, tissue degraded in static conditions possible due to limitations in oxygen and nutrient availability. A flow culture of tumor tissue can lead to a several fold higher tissue amount in regard to static assays. Flow is able to mimic to some extent vascularity resp. the natural occurring interstitial flow with additional mechanical stimulation of the cells through shear stress.

Tissue formation under perfusion for primary colorectal cancer specimens was possible in 66% of all cases and even higher if contaminated samples were excluded as commensals are a major problem for colorectal cancer in vitro culture. This exceeds significantly the reported 30% efficiency for primary colorectal cancer organoid culture<sup>6</sup> and places it similar to patient derived xenograft (PDX) with an efficiency for successful tumor generation of 66%<sup>8</sup>. As for PDX-models up to two months are necessary to grow a 6-8mm measuring tumor (own experience), perfusion culture in bioreactor is able to integrate tumor tissue in scaffold in much shorter time.

The tissue quality and composition was varying from patient to patient and there was some heterogeneity from culture to culture even coming from the same patients, as the starting tissue was not homogenous. Proper selection of initial tissue specimens is important to obtain successful cultures. The standardization is a major limitation of general tissue resp. organoid-like cultures and future studies are necessary to reduce the heterogeneity in tissue-forming capacity from same starting material. Stringent selection criteria for tissue prior culture (size, form, pathological assessment) or increase in parallel bioreactor culture could be used to circumvent this issue – nevertheless starting material is generally limited. In some cases starting material from operation could be necrotic and fibrotic as the case for our neoadjuvant treated melanoma sample.

This culture techniques can be adapted for to other tumor types like breast-cancer, melanoma, bladder-cancer, prostate-cancer, glioblastoma etc. Different supplemental could be of need as for example in breast-cancer with estrogen.

In our perfused 3D culture the tumor microenvironment is preserved over time, therefore drug testing in individualized manner could be possible. This opens new fields in personalized drug screening. One of the major limitations is still the amount of tumor material available. As we were able to show as well tumor tissue growth from frozen tissue specimens, screening could be done in centers and tumor tissue transported in freezing medium. Future studies are necessary to both expand tumor tissue in its initial composition and on the same time preserve initial composition and

functionality. Markers for treatment response must be found and implemented for such screenings. In this context, by using colorectal cancer cell lines, we have recently shown that anti-apoptotic genes like c-Flip, Traf-1 and Bcl-2 could be markers for treatment response similar to neoadjuvant treated rectal cancer patient samples (Hirt et al. submitted).

Culturing of the whole tumor microenvironment *in vitro* could help further to better understand effects of it on the tumor growth. This could open the screening of drug-ability of new targets, which are difficult to assess by using tumor cell lines alone. New physiological phenotypic screenings integrating the complex microenvironment are in context of tumor research of great potential.

Additionally tumor infiltrating lymphocytes (TIL) in the tumor microenvironment contribute significantly to survival of patients. Expansion of this population and re-transfusion during adoptive cellular therapy has been highly efficient. Systems to expand specifically TIL population and/or methods to select for tumor specificity could be of great value in this context. Our technique for primary tumor culture could be of importance in this regard.

## **Conclusions**

Perfused 3D culture in a bioreactor device is able to maintain fresh and frozen tissue specimens of different tumor entities alive and proliferating. The sandwich-collagen scaffold is strongly remodeled in few days. The tumor microenvironment consisting of epithelial, stromal and immune cells is preserved. The method is applicable to other tumor entities with slight adaptations. This culture technique could therefore be a useful tool to study not only biological questions concerning the tumor microenvironment but as well lead to a new phenotypical drug screening tool.

## **Acknowledgements**

The research leading to these results has received funding from the Lichtenstein-Stiftung of the university Basel, from KTI grant (Kommission für Technologie und Innovation, Bern, Switzerland) and the department of surgery university hospital Basel. Tumor digestions of CRC specimens was performed by Valentina Mele and Manuele G. Muraro, Oncology Surgery ICFS Basel

## Reference List

1. Marusyk, A. & Polyak, K. Tumor heterogeneity: causes and consequences. *Biochim. Biophys. Acta* **1805**, 105–17 (2010).
2. Domcke, S., Sinha, R., Levine, D. A., Sander, C. & Schultz, N. Evaluating cell lines as tumour models by comparison of genomic profiles. *Nat. Commun.* **4**, 2126 (2013).
3. Whiteside, T. L. The tumor microenvironment and its role in promoting tumor growth. *Oncogene* **27**, 5904–5912 (2008).
4. Giaccia, A. J. & Schipani, E. Role of carcinoma-associated fibroblasts and hypoxia in tumor progression. *Curr. Top. Microbiol. Immunol.* **345**, 31–45 (2010).
5. Kondo, J. *et al.* Retaining cell-cell contact enables preparation and culture of spheroids composed of pure primary cancer cells from colorectal cancer. *Proc. Natl. Acad. Sci. U. S. A.* **108**, 6235–40 (2011).
6. Sato, T. *et al.* Long-term Expansion of Epithelial Organoids From Human Colon, Adenoma, Adenocarcinoma, and Barrett's Epithelium. *Gastroenterology* **141**, 1762–1772 (2011).
7. Siolas, D. & Hannon, G. J. Patient-derived tumor xenografts: transforming clinical samples into mouse models. *Cancer Res.* **73**, 5315–9 (2013).
8. Williams, S. A., Anderson, W. C., Santaguida, M. T. & Dylla, S. J. Patient-derived xenografts, the cancer stem cell paradigm, and cancer pathobiology in the 21st century. *Lab. Invest.* **93**, 970–82 (2013).
9. Ding, L. *et al.* Genome remodelling in a basal-like breast cancer metastasis and xenograft. *Nature* **464**, 999–1005 (2010).
10. Kopetz, S., Lemos, R. & Powis, G. The promise of patient-derived xenografts: the best laid plans of mice and men. *Clin. Cancer Res.* **18**, 5160–2 (2012).
11. Freeman, A. E. & Hoffman, R. M. In vivo-like growth of human tumors in vitro. *Proc. Natl. Acad. Sci. U. S. A.* **83**, 2694–8 (1986).
12. Sadr, N. *et al.* Enhancing the biological performance of synthetic polymeric materials by decoration with engineered, decellularized extracellular matrix. *Biomaterials* **33**, 5085–93 (2012).
13. Simony, J. *et al.* Characterization of proliferative cells in malignant melanomas and their inflammatory infiltrates. *Cancer Detect. Prev.* **15**, 183–7 (1991).
14. Schultz-Thater, E. *et al.* Whole blood assessment of antigen specific cellular immune response by real time quantitative PCR: a versatile monitoring and discovery tool. *J. Transl. Med.* **6**, 58 (2008).
15. Livak, K. J. & Schmittgen, T. D. Analysis of relative gene expression data using real-time quantitative PCR and the 2(-Delta Delta C(T)) Method. *Methods* **25**, 402–8 (2001).

16. Wendt, D., Marsano, A., Jakob, M., Heberer, M. & Martin, I. Oscillating perfusion of cell suspensions through three-dimensional scaffolds enhances cell seeding efficiency and uniformity. *Biotechnol. Bioeng.* **84**, 205–14 (2003).
17. Sato, T. *et al.* Paneth cells constitute the niche for Lgr5 stem cells in intestinal crypts. *Nature* **469**, 415–8 (2011).
18. Gospodarowicz, D. & Ili, C. R. Do plasma and serum have different abilities to promote cell growth? *Proc. Natl. Acad. Sci. U. S. A.* **77**, 2726–30 (1980).
19. Pierzchalska, M., Grabacka, M., Michalik, M., Zyla, K. & Pierzchalski, P. Prostaglandin E2 supports growth of chicken embryo intestinal organoids in Matrigel matrix. *Biotechniques* **52**, 307–15 (2012).
20. Frey, D. M. *et al.* High frequency of tumor-infiltrating FOXP3(+) regulatory T cells predicts improved survival in mismatch repair-proficient colorectal cancer patients. *Int. J. Cancer* **126**, 2635–43 (2010).
21. Sconocchia, G. *et al.* Tumor infiltration by FcγRIII (CD16)+ myeloid cells is associated with improved survival in patients with colorectal carcinoma. *Int. J. Cancer* **128**, 2663–72 (2011).
22. Galon, J. *et al.* Type, density, and location of immune cells within human colorectal tumors predict clinical outcome. *Science* **313**, 1960–4 (2006).
23. Paterlini-Brechot, P. & Benali, N. L. Circulating tumor cells (CTC) detection: clinical impact and future directions. *Cancer Lett.* **253**, 180–204 (2007).
24. Cohen, S. J. *et al.* Prognostic significance of circulating tumor cells in patients with metastatic colorectal cancer. *Ann. Oncol.* **20**, 1223–9 (2009).
25. *Human Cancer in Primary Culture, A Handbook.* (Springer Netherlands, 1991). doi:10.1007/978-94-011-3304-3
26. *Human Cell Culture.* **1**, (Kluwer Academic Publishers, 2002).
27. Belkaid, Y. & Naik, S. Compartmentalized and systemic control of tissue immunity by commensals. *Nat. Immunol.* **14**, 646–53 (2013).
28. Zielske, J. V & Golub, S. H. Fetal calf serum-induced blastogenic and cytotoxic responses of human lymphocytes. *Cancer Res.* **36**, 3842–6 (1976).
29. Chan, B. P. & Leong, K. W. Scaffolding in tissue engineering: general approaches and tissue-specific considerations. *Eur. Spine J.* **17 Suppl 4**, 467–79 (2008).
30. Glowacki, J. & Mizuno, S. Collagen scaffolds for tissue engineering. *Biopolymers* **89**, 338–44 (2008).
31. McMillin, D. W., Negri, J. M. & Mitsiades, C. S. The role of tumour-stromal interactions in modifying drug response: challenges and opportunities. *Nat. Rev. Drug Discov.* **12**, 217–28 (2013).

## Figures

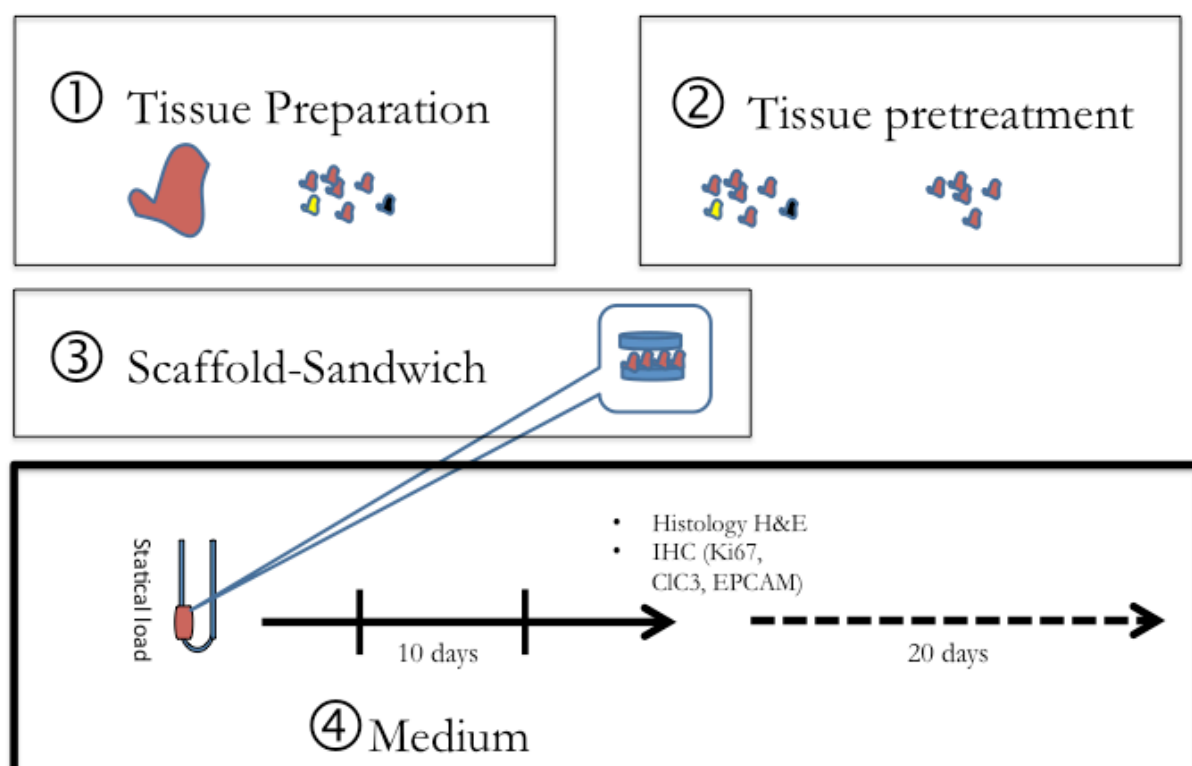


**Figure 1**

### Primary Perfusion culture of CRC specimens

Schematic view's of steps involved in primary CRC culture. 1: Tissue preparation by mincing. 2: Tissue pretreatment with washing steps and octenisept pretreatment. 3: Mounting tissue fragments between collagen scaffolds (sandwich-assay). 4: Culture in perfusion bioreactor.

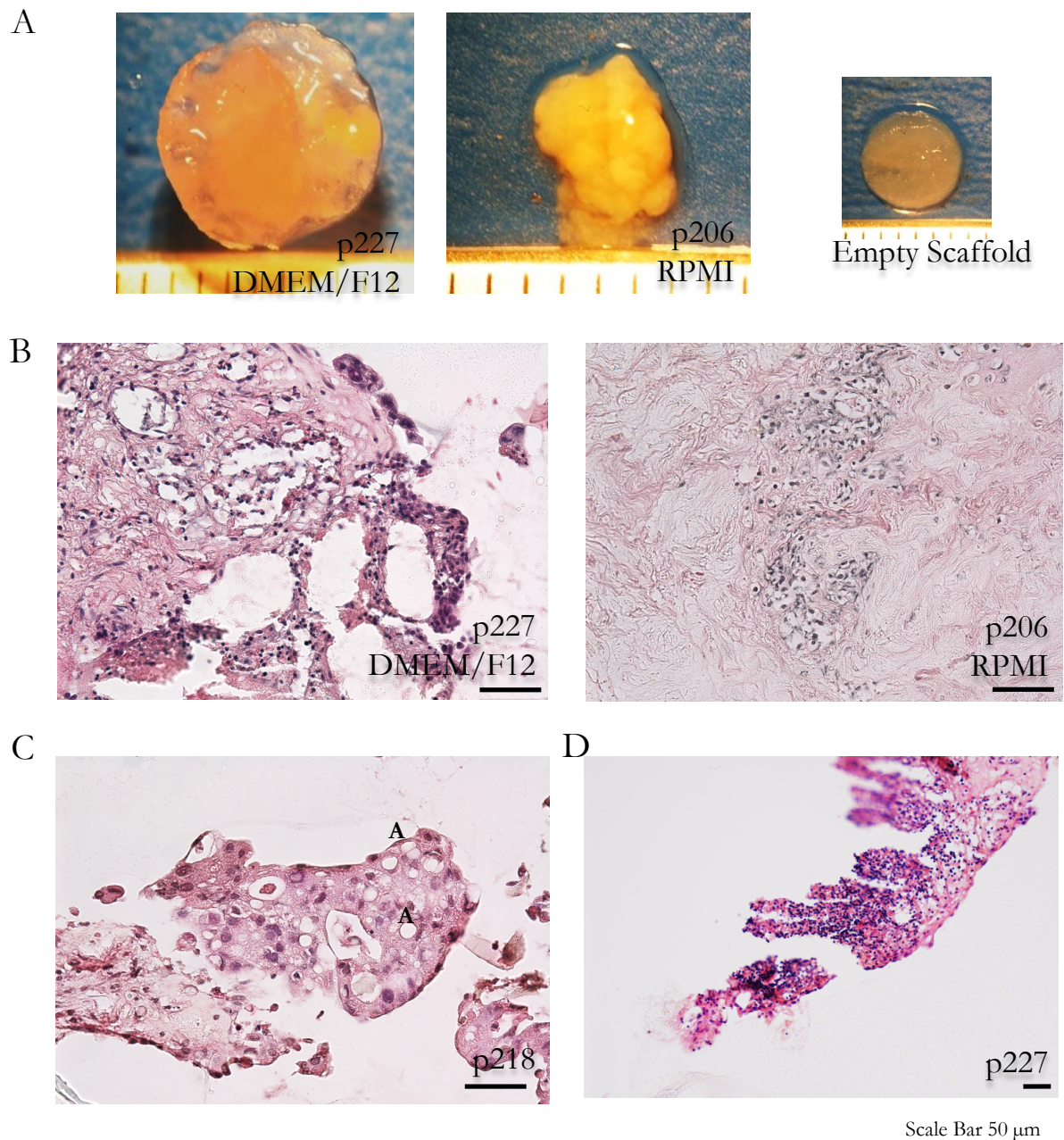


**Figure 2**  
**Tissue forming capacity under perfusion culture for different patients and several media.**

A: Fresh tumor specimens cultured in collagen sandwich-scaffolds cultured with human serum for 10 days in a perfusion bioreactor with RPMI1640 or DMEM/F12 Medium in comparison to empty scaffold. B: Tissue phenotype assessed by H&E staining after 10 days perfusion culture C: Highly dysmorphic tumor tissue with acini-structures after perfusion culture (H&E). D: H&E staining of tumor specimens after 10 days culture with villi-like structures.

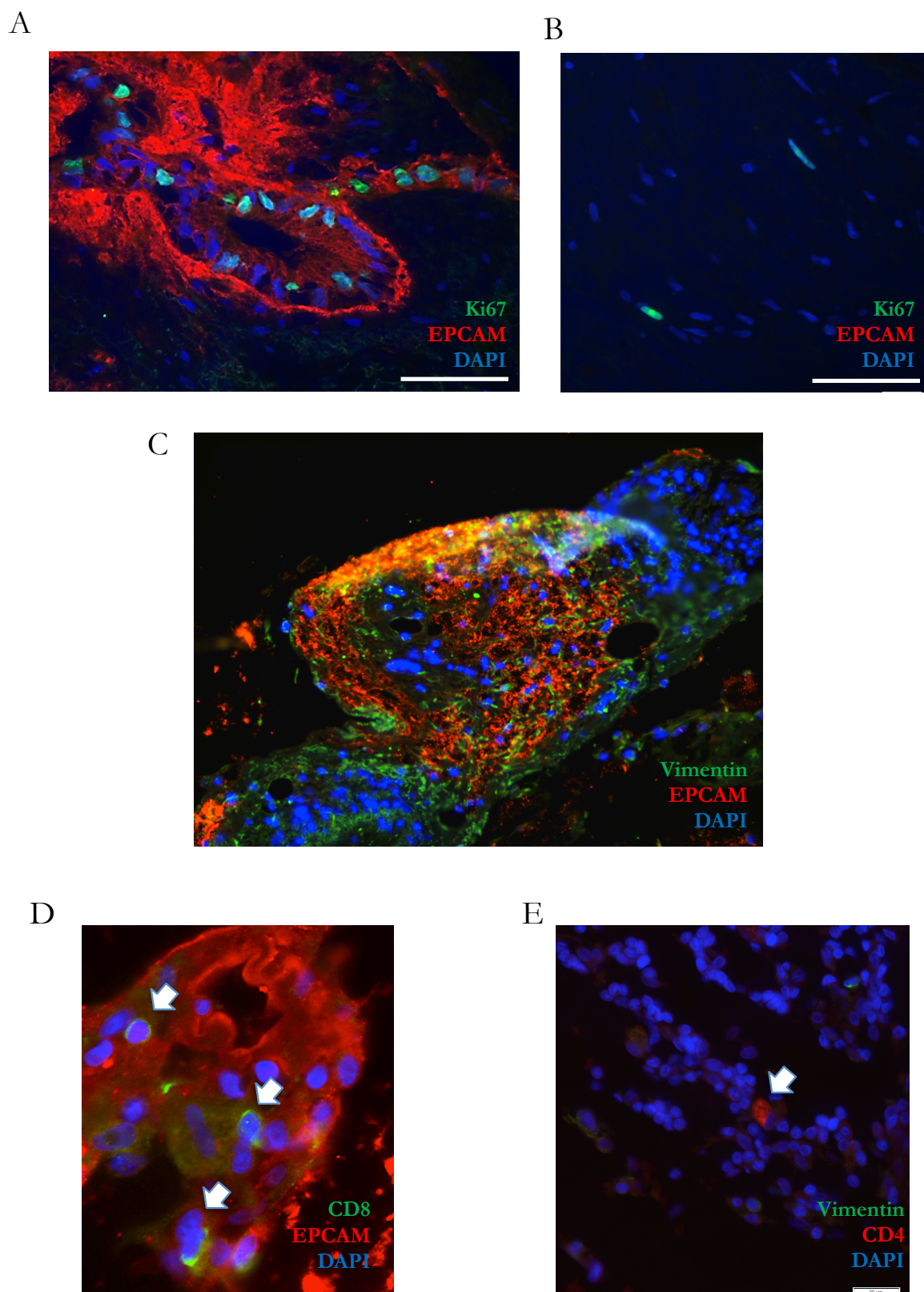


**Figure 3**  
**Immunofluorescence stainings for epithelial, stromal, immune and proliferation markers**

A/B: Tissue sample stained for proliferation marker Ki67 after perfusion culture with proliferating epithelial (A) and stromal cells (B). C: Interaction of stromal and epithelial cells after 10 days and (IF with Vimentin and EPCAM). D&E: Preservation of infiltrating CD8 and CD4-T-cells.

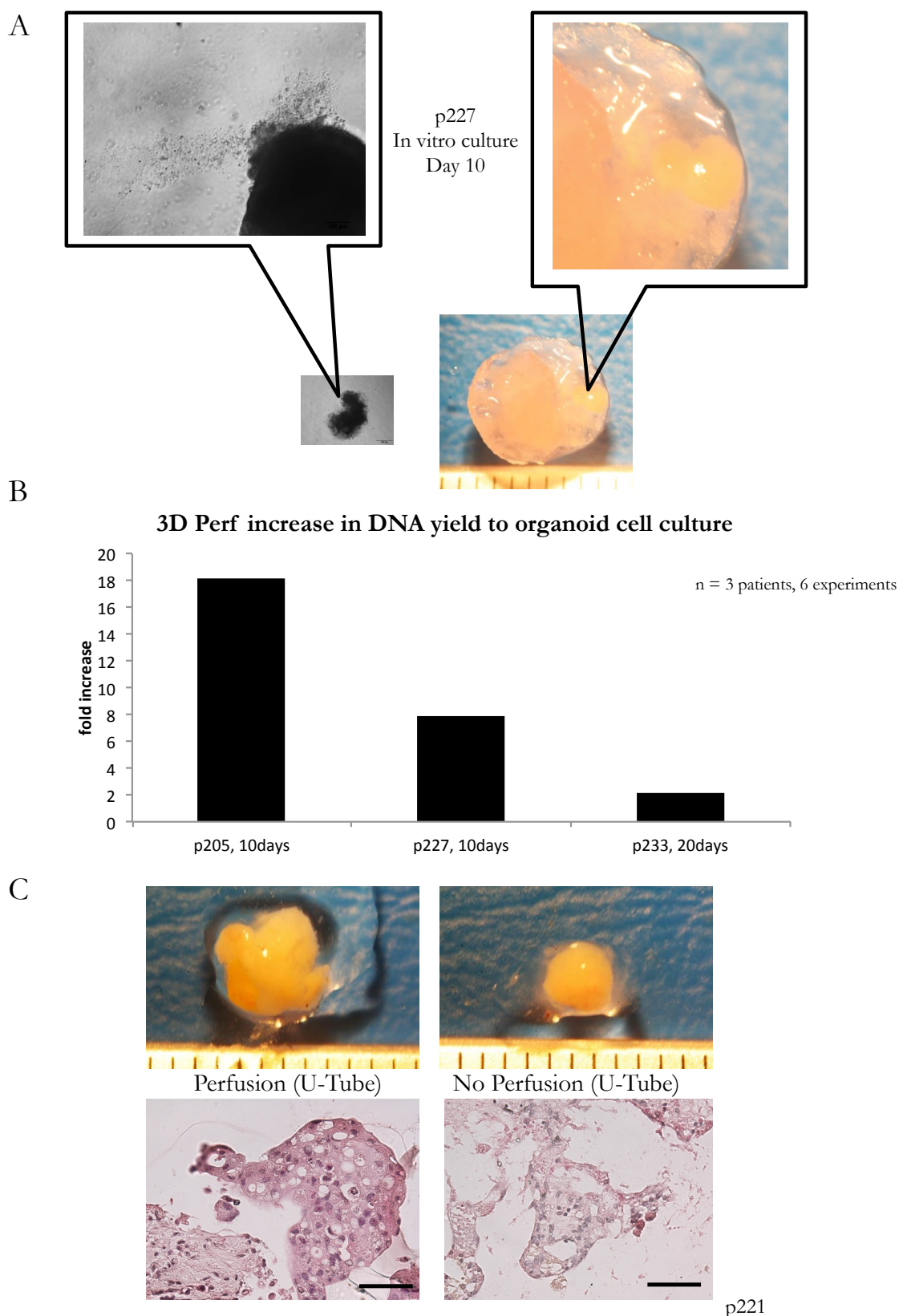


**Figure 4**  
**Effect of flow on tissue growth**

A: Comparison of organoid cell culture on matrigel to perfused tumor tissue culture by high magnification. B: Increase of DNA-quantity on collagen scaffold by perfusion at 10 days and 20 days for different samples. C: Culturing of tumor specimens with or without flow in culture chamber. Macroscopically significant larger construct and dense tissue by H&E staining, compared to small tissue and tissue lysis.

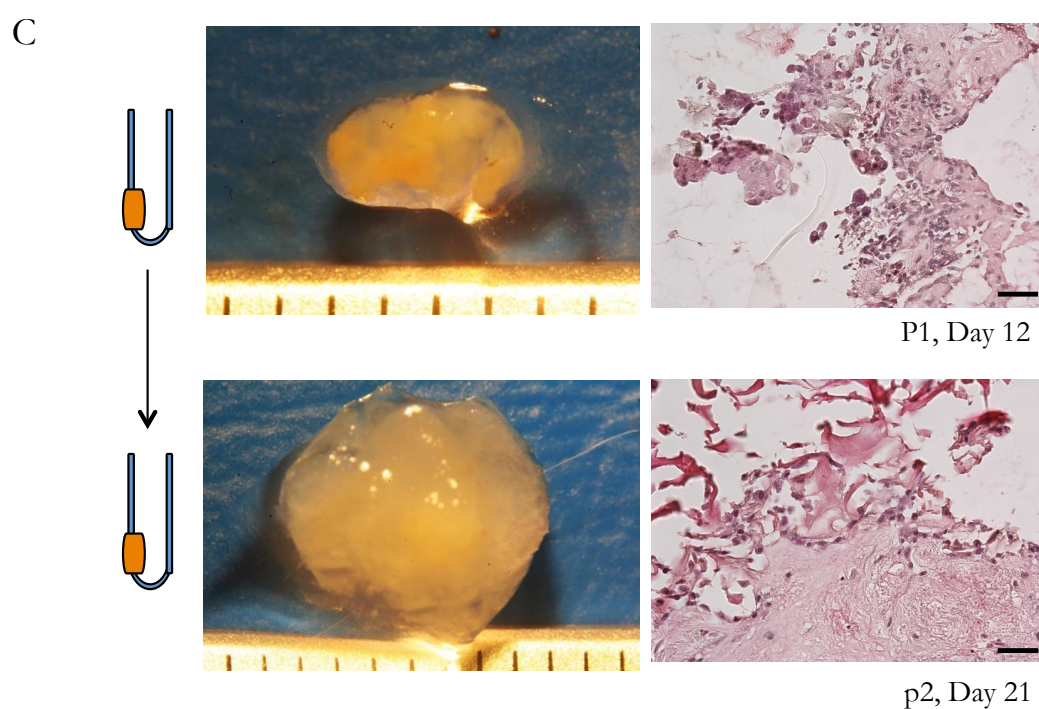
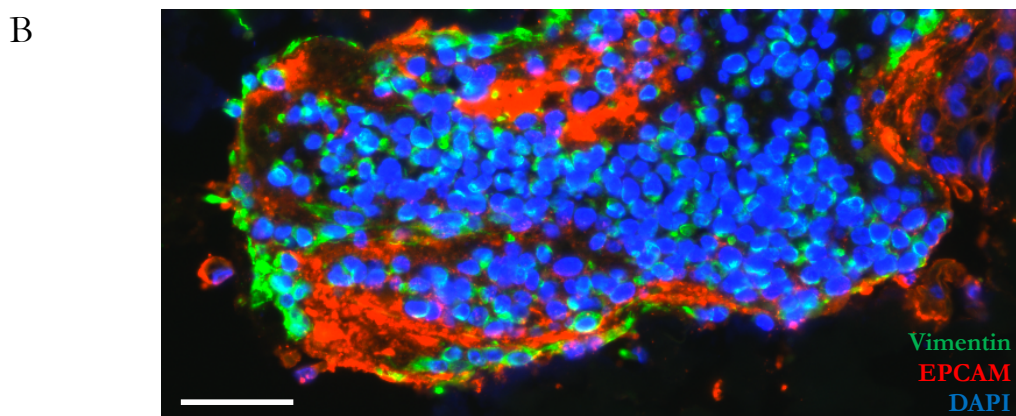
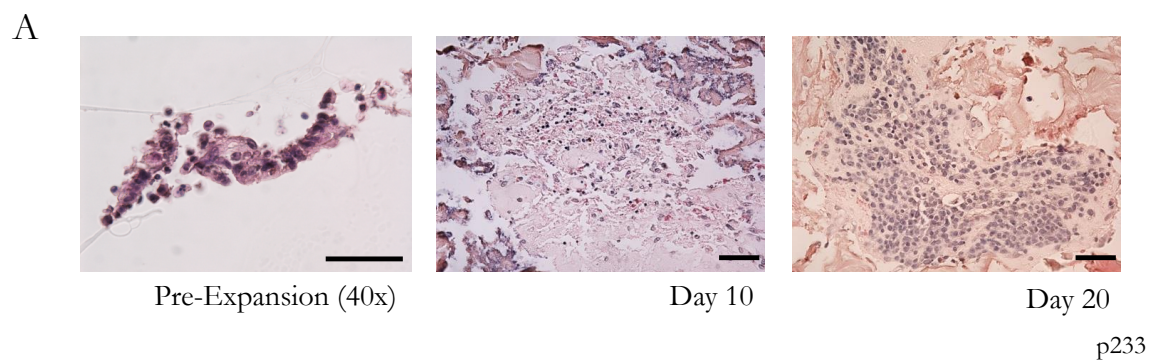
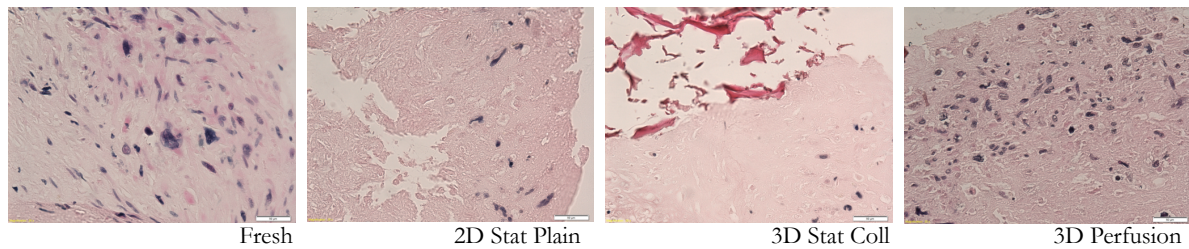


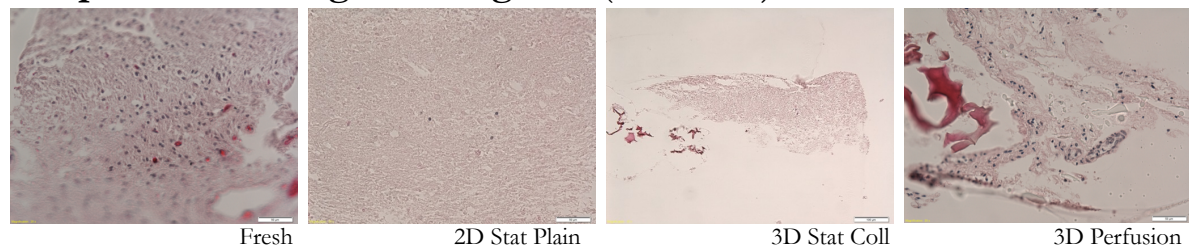
**Figure 5**  
**Expansion of tissue over 20 days culture**

A: H&E stainings of tumor tissue prior-expansion, after 10 days and after 20 days of perfusion culture in a collagen-sandwich. B: Immunofluorescenc of epithelial (EPCAMpos) and stromal (VIMENTINpos) cells in tumor tissue after 20 days of perfusion cultures. C: Splitting of tumor tissue after 12 days culture and further expansion in new bioreactor for up to 21 days total culture time.

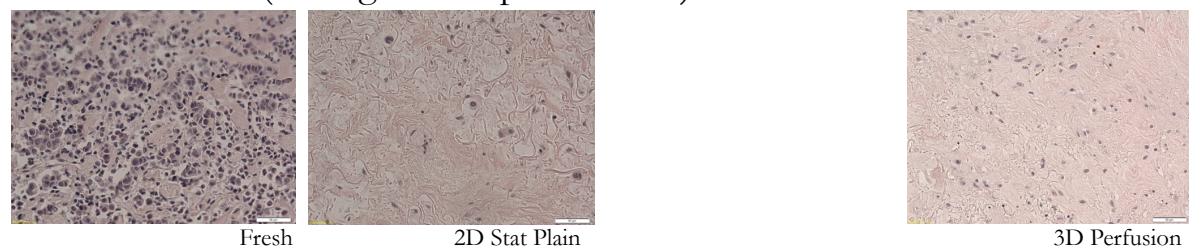
### A Dermatofibrosarkoma



### B Anaplastisches Oligodendrogliom (WHO III)



### C Breast-Cancer (Estrogen Receptor Positiv)



### D Melanom (neoadjuvant pretreated)

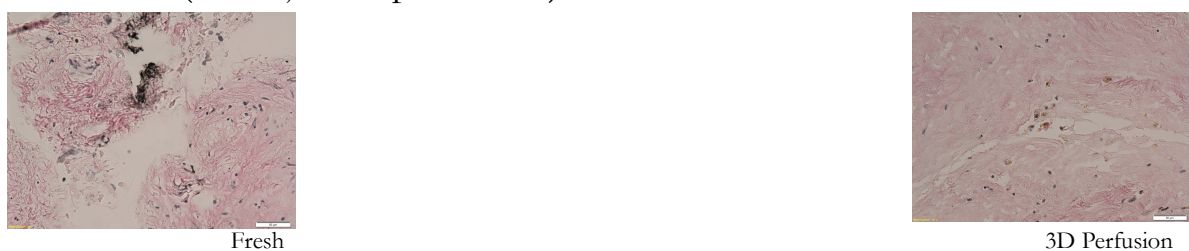


**Figure 6**  
**Preservation of tissue-like structure in 3D perfusion cultures of primary tumor tissue of different histological origin.**

HE staining of dermatofibrosarcoma (A), anaplastic oligodendroglioma WHO III (B), breast cancer (C) and neoadjuvant pretreated melanoma (D) samples before and after either 2D static plain, 2D static collagen and 3D perfusion culture for 9 days. Scale bar: 50µm.

## Tables

| Nr | Patient | Tissue Type  | Tissue Prep     | Medium        | Suppl.  | Scaffold | Culture time | Outcome   |
|----|---------|--------------|-----------------|---------------|---------|----------|--------------|-----------|
| 1  | P191    | Fresh        | Chunk           | RPMI          | aHP/FCS | UF       | 10           | Tissue    |
| 2  | P192    | Fresh        | Chunk           | RPMI          | aHP/FCS | UF       | 10           | No tissue |
| 3  | P193    | Fresh        | Chunk           | RPMI          | aHP/FCS | UF       | 10           | Tissue    |
| 4  | P202    | Fresh        | Chunk/<br>Mince | RPMI          | aHP/HS  | UF       | 10           | Infection |
| 5  | P205    | Fresh/Frozen | Chunk           | RPMI/<br>DMEM | aHP/HS  | UF       | 10           | Tissue    |
| 6  | P206    | Fresh        | Chunk           | RPMI          | aHP/HS  | UF       | 10           | Tissue    |
| 7  | P207    | Fresh        | Chunk/<br>Mince | RPMI          | HS      | UF       | 10           | Infection |
| 8  | P208    | Fresh        | Chunk/<br>Mince | RPMI          | HS      | UF       | 10           | Tissue    |
| 9  | P217    | Fresh        | Chunk           | RPMI          | HS      | UF       | 7(-34)       | Tissue    |
| 10 | P218    | Fresh        | Chunk           | RPMI          | HS      | UF       | 12-21        | Tissue    |
| 11 | P220    | Fresh        | Chunk           | RPMI          | HS      | UF       | 6-16         | No tissue |
| 12 | P221    | Fresh        | Chunk           | RPMI          | HS      | UF       | 9            | Tissue    |
| 13 | P227    | Frozen       | Chunk           | DMEM          | HS/B12  | UF/PET   | 10           | Tissue    |
| 14 | P233    | Fresh        | Chunk           | DMEM          | HS/B12  | UF       | 10-20        | Tissue    |
| 15 | P234    | Fresh/Frozen | Chunk           | DMEM          | HS/B12  | UF       | 3-12         | Infection |

**Tabl 1**

**Tissue generation for primary colorectal cancer specimens**

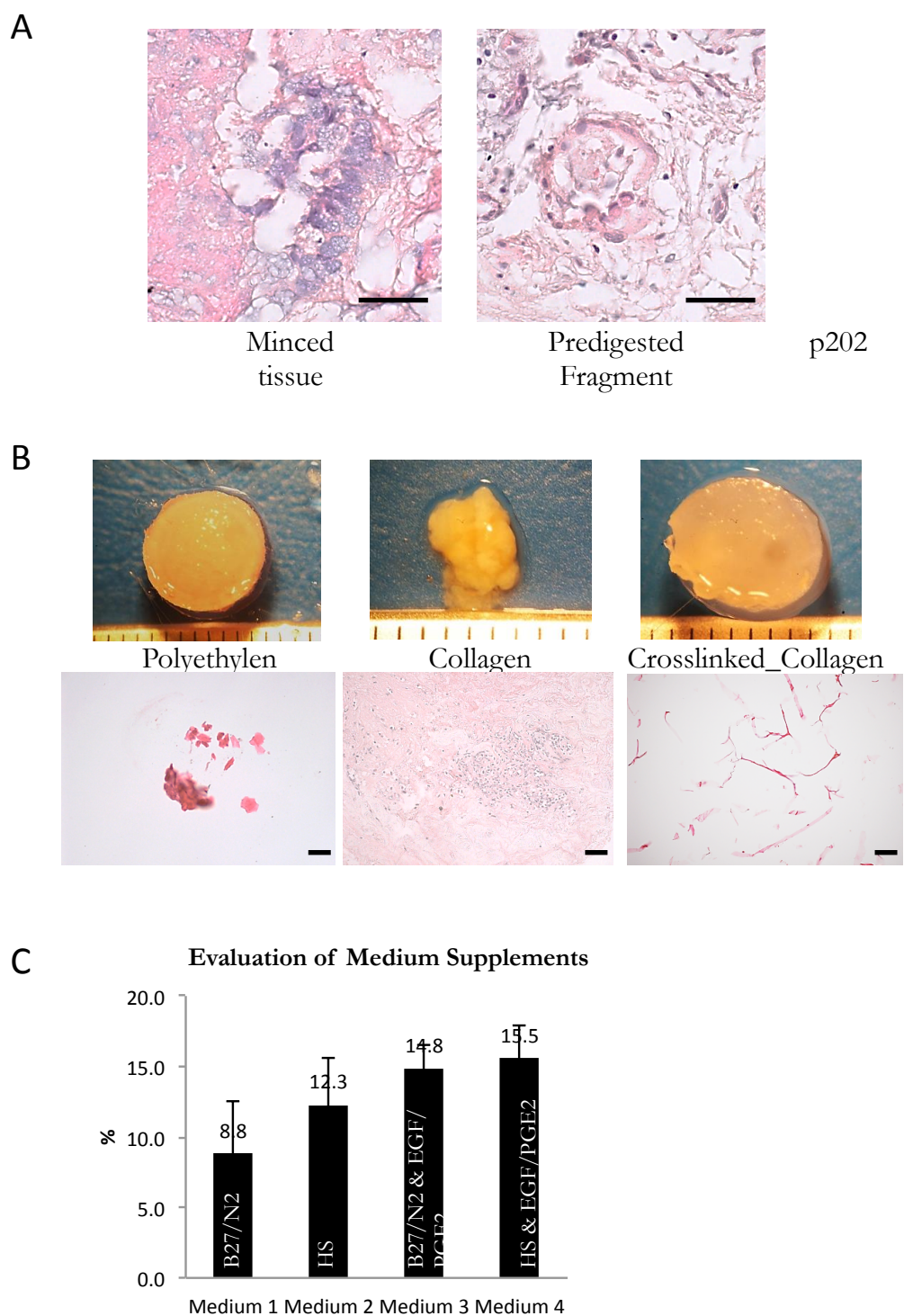
Tumor specimens of colorectal cancer cultured under perfusion and with different conditions and resulting tissue

| Nr                   | Clinical Data                             | Tissue Type | Tissue Prep | Medium | Suppl. | Scaffold | Culture time | Outcome         |
|----------------------|---|-------------|-------------|--------|--------|----------|--------------|-----------------|
| <b>Glioblastoma</b>  |   |             |             |        |        |          |              |                 |
| 01                   | Glioblastoma multiforme (WHO IV)          | Fresh       | Chunks      | DMEM   | HS     | UF       | 9 days       | Necrotic PreExp |
| 02                   | Anaplastisches Oligodendrogliom (WHO III) | Fresh       | Chunks      | DMEM   | HS     | UF       | 9 days       | Tissue          |
| 03                   | Glioblastoma multiforme (WHO IV)          | Fresh       | Chunks      | DMEM   | HS     | UF       | 9 days       | ?               |
| <b>Breast-Cancer</b> |   |             |             |        |        |          |              |                 |
| 01                   | Male Breast-Ca (ER pos)                   | Fresh       | Chunks      | DMEM   | HS     | UF       | 9 days       | Tissue          |
| 02                   | Female Breast-Ca (ER pos)                 | Fresh       | Chunks      | DMEM   | HS &E  | UF       | 9 days       | Tissue          |
| 03                   | Female Breast-Ca (Triplenegativ)          | Fresh       | Chunks      | DMEM   | HS &E  | UF       | 11 days      | Tissue          |
| <b>Sarcoma</b>       |   |             |             |        |        |          |              |                 |
| 01                   | Dermatofibrosarcoma                       | Fresh       | Chunks      | DMEM   | HS     | UF       | 15 days      | Tissue          |
| 02                   | Chondrosarcoma                            | Fresh       | Chunks      | DMEM   | HS     | UF       | 9 days       | Tissue          |
| <b>Melanoma</b>      |   |             |             |        |        |          |              |                 |
| 01                   | Neoadjuvant treated melanoma              | Fresh       | Chunks      | DMEM   | HS     | UF       | 11 days      | Necrotic PreExp |

**Tabl 2****Overview of tissue generation under perfusion for other tumor entities**

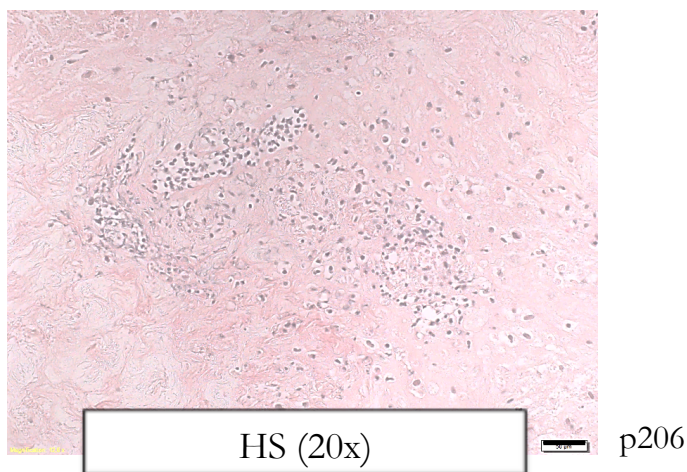
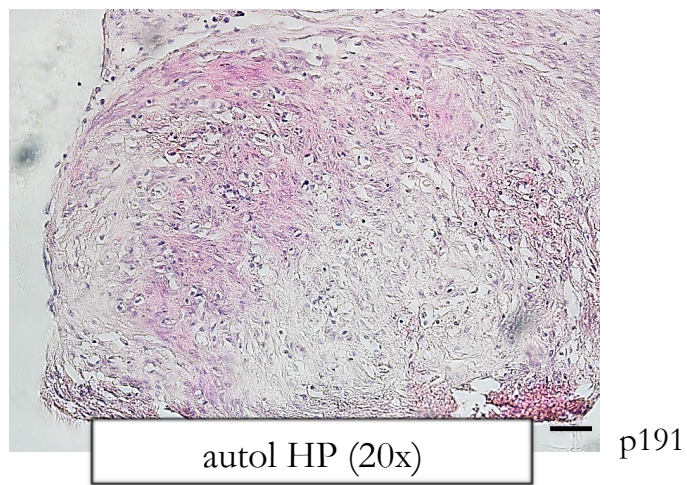
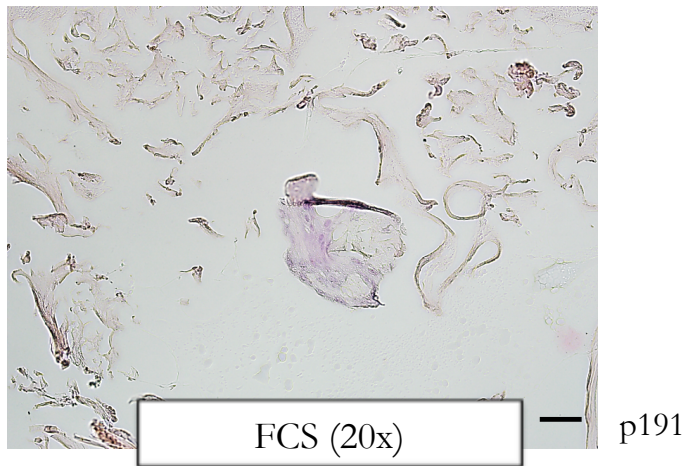
Specimens of other freshly excised tumor entities cultured under perfusion and with different conditions and resulting tissue

## Supplementary Figures



### Sup. Figure 1 Set up of perfusion culture

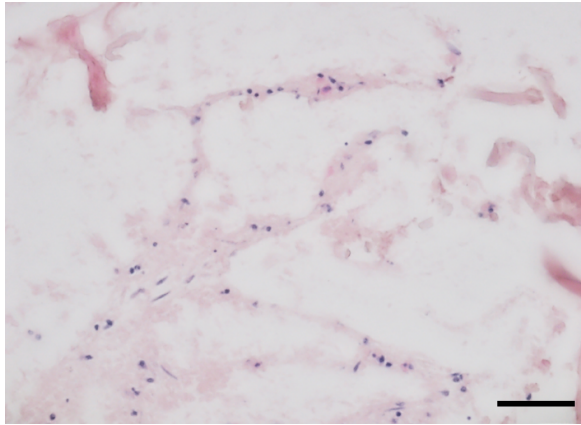
A: Tissue preparation of colorectal cancer specimens showing H&E stainings of either mechanically (Mince) or mechanically&enzymatically (Chunk) dissociated tumors. B: Scaffold-sandwich assay using either collagen, cross-linked collagen or synthetic (polyethylene) scaffold after 10 days perfusion culture. C: Effect of different medium supplements on organoid cell growth.



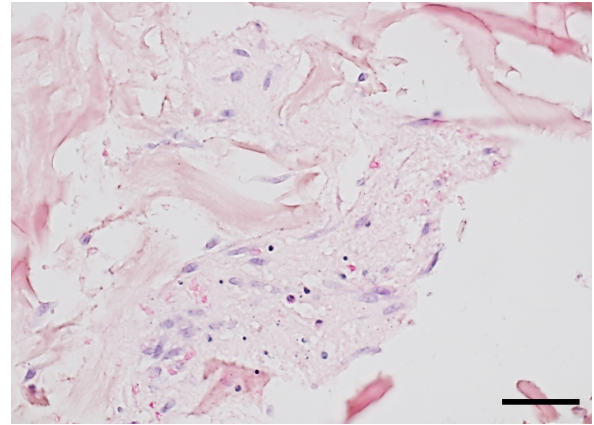
**Sup. Figure 2**

**Autologous Human Plasma (HP), Fetal Calf Serum (FCS), Human Serum (HS) for perfused tumor culture**

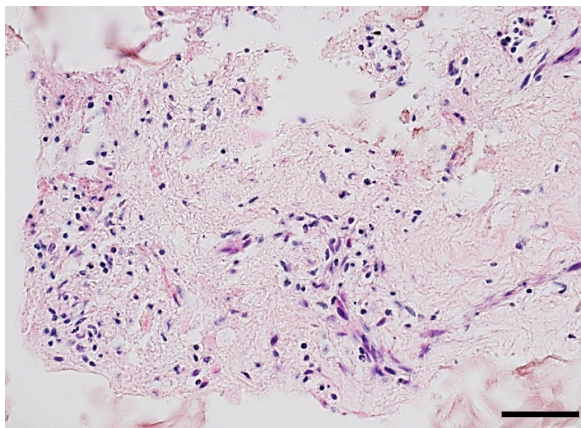
Superiority of autologous human plasma (HP) over fetal calf serum (FCS) in perfused 3D tumor culture. Similar tissue formation capacity by using human serum (HS) in representative sample. H&E stainings.



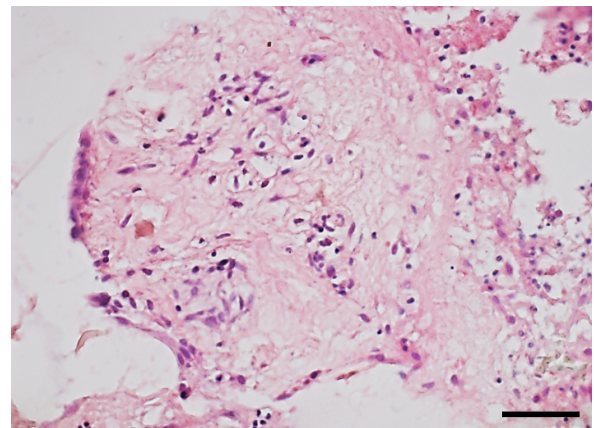
Medium 1  
(no HS, no EGF/  
PGE2)



Medium 2  
(HS, no EGF/PGE2)



Medium 3  
(no HS, EGF/PGE2)

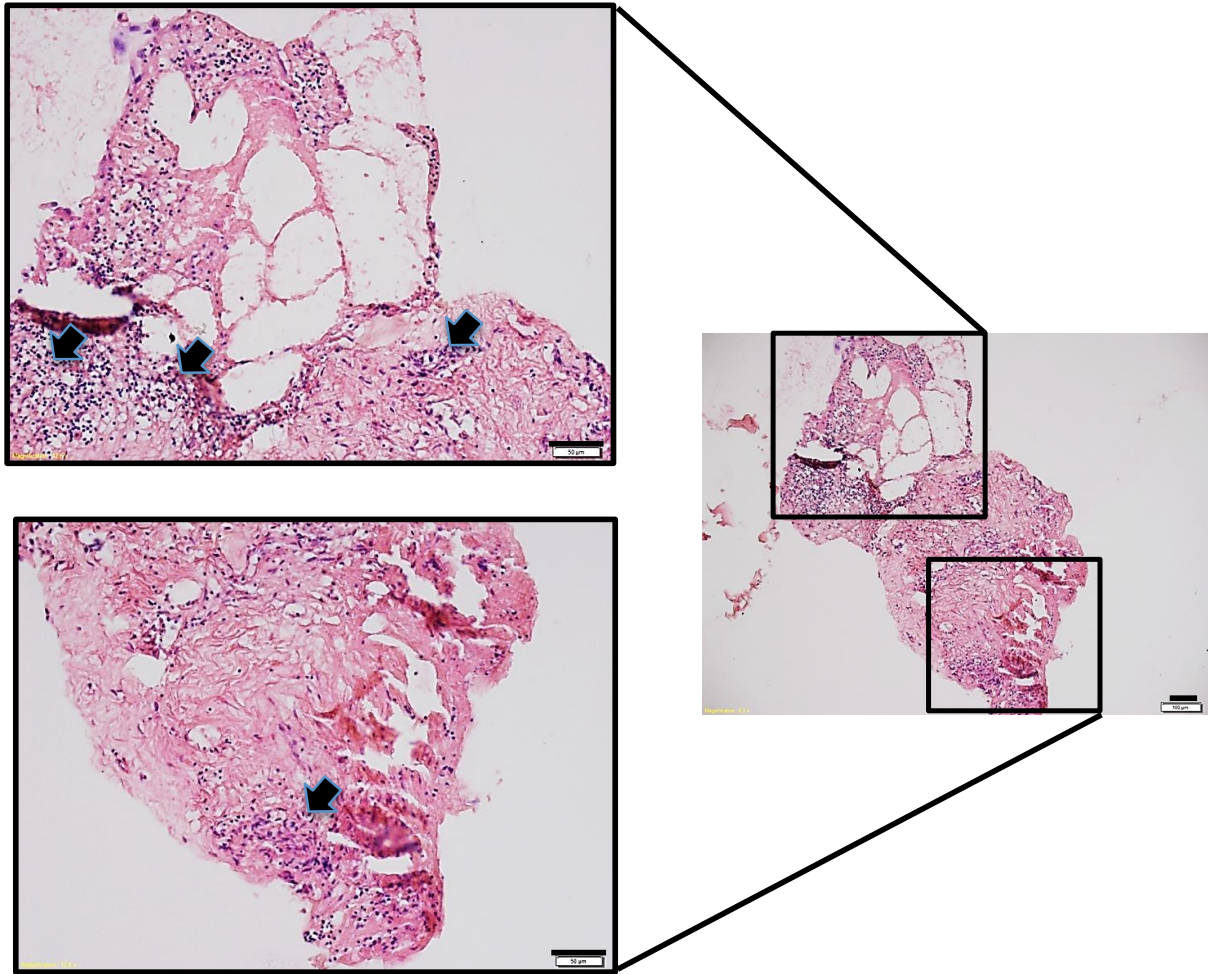


Medium 4  
(HS, EGF/PGE2)

**Sup. Figure 3**

**Advantage of use of HS and EGF/PG2 over serum free plus supplements.**

A: Collagen-sandwich after 10 days culture period with different culture conditions. B H&E stainings of conditions with superiority of HS & EGF/PGE2.

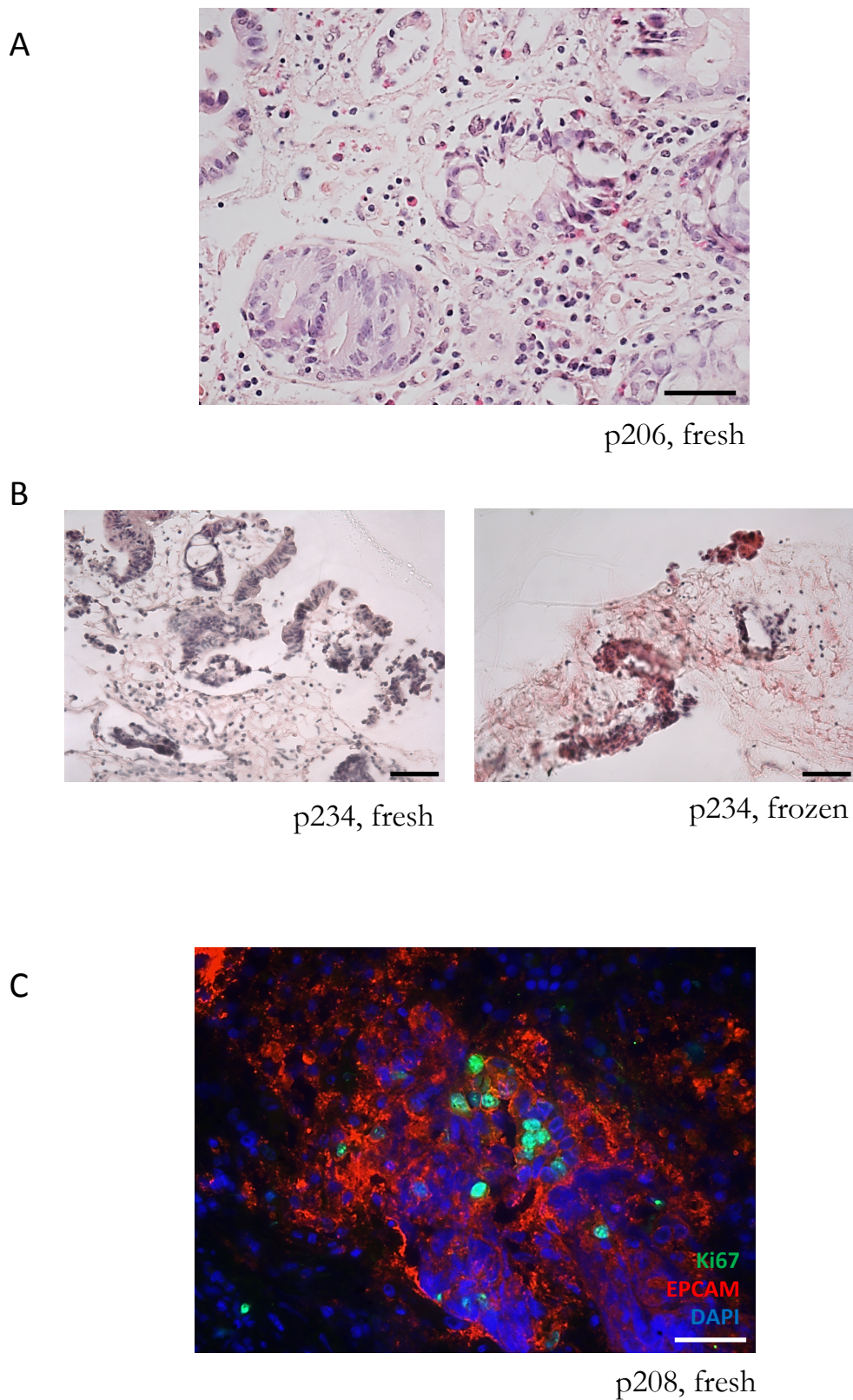


p227 Perf 3D Culture  
Frozen tissue  
10 days

**Sup. Figure 4**

**Heterogeneity of generated tumor tissue**

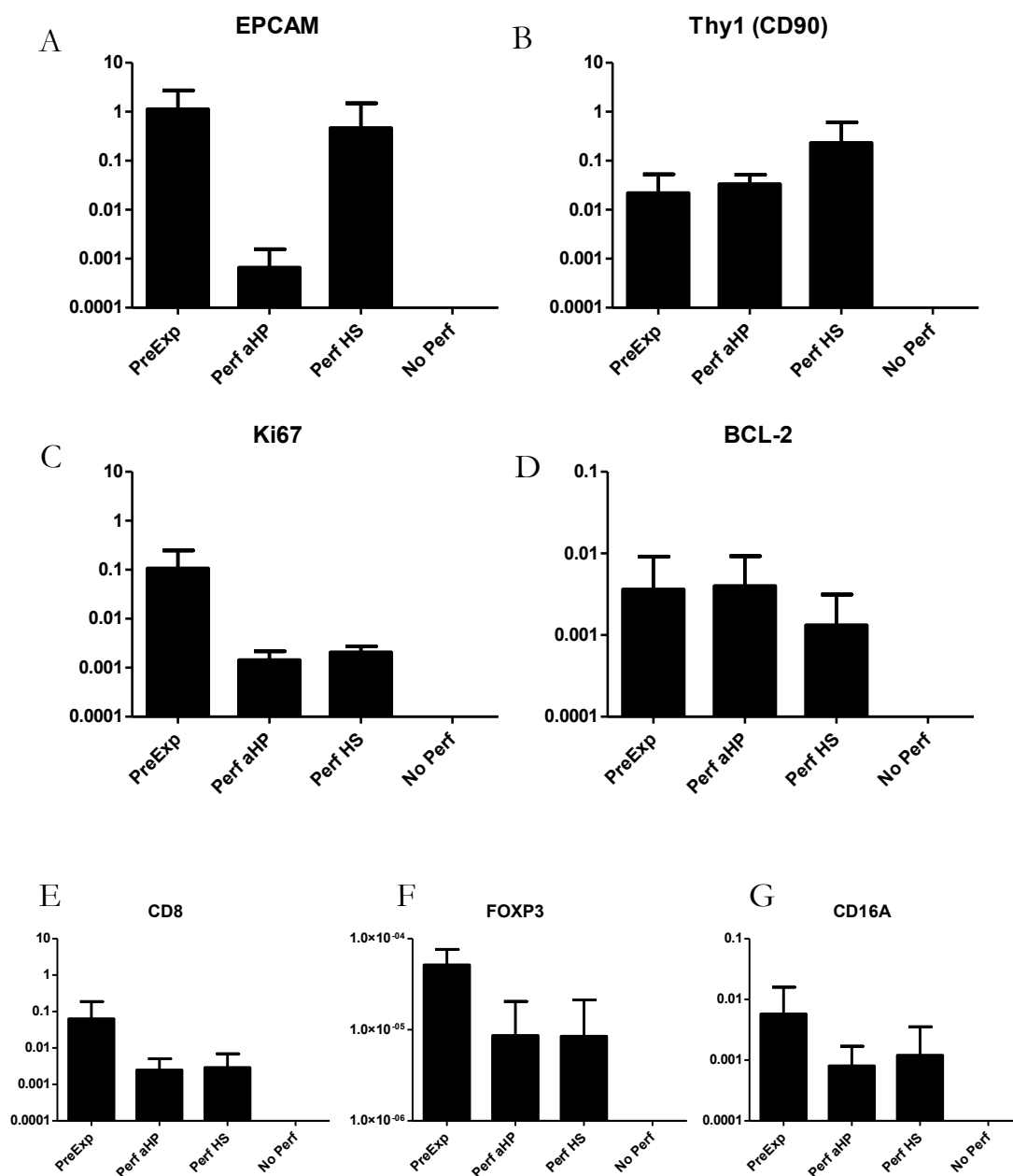
H&E staining of cultured tumor tissue with high magnification of region with interstitial cells, epithelial cells and large stromal parts. Immune cell infiltrates indicated by arrows.



### Sup. Figure 5

#### Histology of tissue prior culture

A: H&E staining of tumor tissue specimens prior perfusion culture. B: fresh and frozen tissue specimens of one patient sample (H&E) C: Ki67 proliferation assessment by immunofluorescence on pre-cultured specimen.

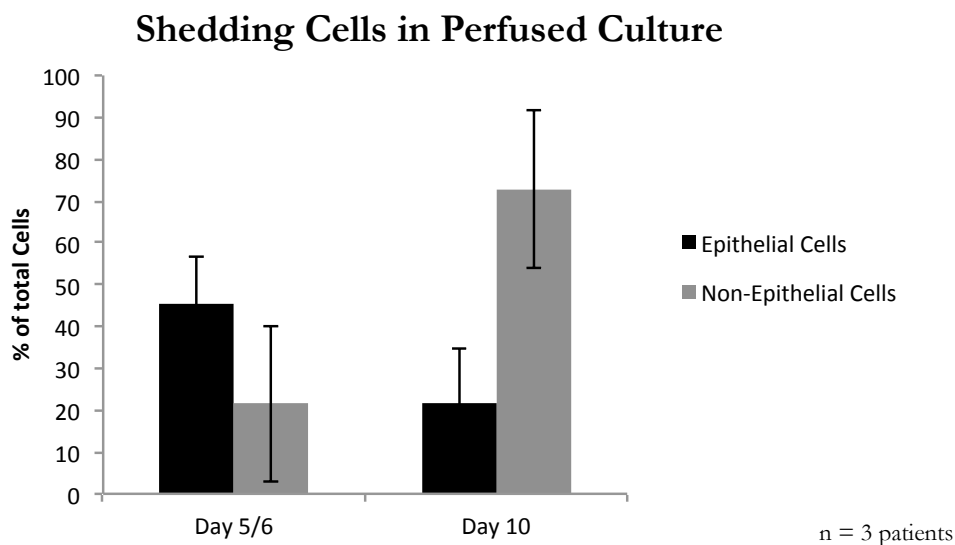


### Sup. Figure 6

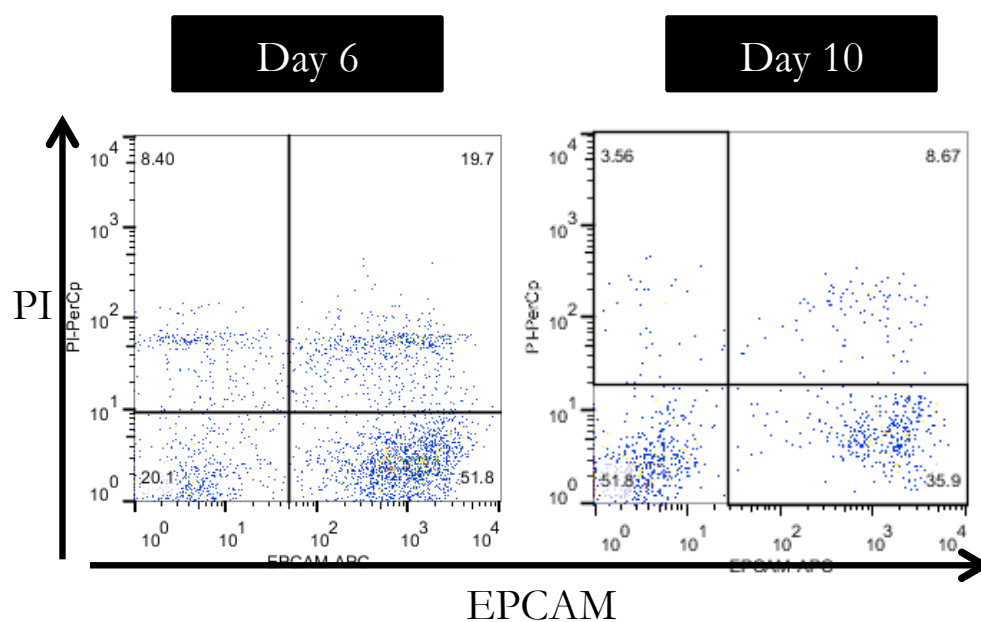
#### Expression of EPCAM, Thy1, BCL-2 and Ki67 together with immune cell genes in primary CRC tissue before and after in vitro culture in different conditions.

Total cellular RNA was extracted from primary CRC tissue before and after culture according to the indicated conditions and reverse transcribed. Expression of EPCAM (A), Thy1 (B), Ki67 (C), BCL-2 (D), CD8 (E), FOXP3 (F) and CD16A (C) genes was measured by RT-PCR, using GAPDH gene as reference.

A



B

**Sup. Figure 7****Survival of cells under suspension**

A: Shedding living cells of epithelial and non-epithelial origin based on different experiments assessed by FACS analysis. B: Representative FACS-plots for cells in supernatant stained by Propidium Iodid (PI) and EPCAM after 6, 10 and 20 days of culture

## Discussion and Conclusions

### ***A. Innate immunity in the tumor microenvironment – neutrophils the unknown players***

Innate immune cells are the most abundant immune cells of the human body. Nevertheless their role in human cancer is still unclear. NK cells have been proposed as possible tumor killer cells in leukemia and lymphatic tumors, but a role in solid tumors has still to be proven<sup>1</sup>. In CRC, NK cell infiltration has no significance in patient survival<sup>2,3</sup>. On the other hand, murine myeloid derived suppressor cells (MDSCs) have been related to a shorter overall survival<sup>4</sup>. MDSCs can be divided into monocytic or neutrophil subtypes based on different surface expression markers. In humans, this phenotypic characterization is less characterized and prognostic significance of the different subpopulations is unclear<sup>5</sup>. Monocytic MDSCs have been shown to be quite plastic in their effects on tumors; subpopulations based on specific phenotypic markers are either pro- (M2) or anti-tumoral (M1)<sup>6</sup>. Direct or indirect factors contributing to the tumor microenvironment appear to be related to their plasticity. Neutrophils are less well characterized, even though they are the central phagocytic effectors of the immune system<sup>7</sup>. Their survival *in vitro* is short, therefore studies *in vitro* are difficult to perform<sup>8</sup>.

In our study we addressed the prognostic role of MPO positive cell infiltration in CRC. Phenotypic characterization of surgical specimens revealed a neutrophilic phenotype (HLA-DR-, CD16+, CD66b+, CD15+). Interestingly the infiltration of tumor tissue by cells expressing a neutrophil phenotype with high MPO positivity was associated with a favorable prognosis in multivariate analysis. This was in contrast to previous reports where infiltration by cells expressing CD66b, a general marker, correlated with worse overall survival<sup>9</sup>. We observed in CRC a substantial percentage of cells positive for CD66 but negative for MPO-, which may explain the different results between our findings and the previous report<sup>10</sup>.

As we mentioned previously we see this with regard to a different activation pattern of neutrophils either towards a pro- (N2) or anti-tumoral (N1) phenotype<sup>11</sup>. Factors from the TME could strongly influence neutrophil functions. In this regard, work from Fridlender and others demonstrated that in murine models neutrophils are inhibited by Tgf-beta released from tumor cells and therefore acquiring an N1-phenotype<sup>12</sup>. Preliminary *in vitro* experiments of co-culture of human neutrophils with colorectal cancer cell lines showed a tumor stimulating effect (personal observation).

Besides the direct and indirect effects of factors released from tumor cells, other immune and interstitial cells in the TME could exert profound effects on neutrophilic functions. Type 1 IFN has been shown to prolong survival of neutrophils *in vitro*<sup>13</sup>. Additional release of chemokines like GM-CSF, CXCL1 and CXCL2 or cytokines such as TNF- $\alpha$  and IFN- $\gamma$  from tumor-stimulated activated CD8 T-cells might lead to an accumulation of neutrophils in the tissue<sup>14</sup>. Th17 cells, responsible for tissue homeostasis, can similarly attract neutrophils by release of CXCL8<sup>15</sup>. Stimulated Treg cells lead to apoptosis of neutrophils and inhibit their function<sup>16</sup>. Besides this adaptive immune regulation other innate immune cells like macrophages could play additional roles in the migration and survival of neutrophils in the TME. On the same time they are influenced by cytokines released from neutrophils<sup>17,18</sup>.

Most probably interplay of these “immune-cytokines” together with other factors is needed for an activation of neutrophils towards an anti-tumoral phenotype. TLR-agonists, like LPS, CPGs and others, induce an activation of neutrophils, but alone are insufficient to induce cytotoxicity towards surrounding tumor cells (personal observation). Whole, living or dead microbiota could give a much stronger stimulus than single TLR-agonists as has been shown recently<sup>19</sup>. It remains to be demonstrated if different commensals microbiota strains are important in the activation or inhibition of neutrophils and may therefore contribute to the pathogenesis of CRC<sup>20,21</sup>. Further studies will reveal if different microbiota strains, associated with healthy mucosa or CRC lesions, could differentially activate neutrophilic populations.

Could our findings be translated to other tumor types? In head and neck cancer an infiltration by polymorphonuclear granulocytes was associated with enhanced inflammation and poorer overall survival similar to the CD66+ cell infiltration in CRC<sup>22</sup>. It can be speculated that by staining activation markers like MPO, other anti-tumor neutrophilic subpopulations could be better evaluated. Attraction of innate immune cells into the TME could therefore be harmful, but re-education with factors from the TME could shift this towards an anti-tumor effect as we have observed in CRC.

### ***B. Adaptive immunity in the tumor microenvironment – the immune regulatory checkpoint PD-1 – PD-L1***

Cancer cells *in vivo* are largely influenced by the immune system. Whereas early cancer cells are detected and eliminated through a process called immunosurveillance, more advanced stages escape the destruction through immune cells. This process has been called immunoediting and consists of the elimination, equilibrium and escape phases (the three “E”)<sup>23</sup>. During immunoediting an immune-suppressive TME is frequently established through several mechanisms including 1) release of immune-suppressive factors like Tgf-Beta<sup>24,25</sup>, 2) expansion of Tregs, which suppress adaptive immune responses, and are attracted into TME by chemokines<sup>26,27</sup> and 3) shifting of the immune response towards a Th2 response, which prevents tumor rejection<sup>28</sup>. Additionally, the tumor escapes immune detection by downregulation of HLA class I expression<sup>29</sup>. Activated antigen presenting cells, but also some malignant cells are able to upregulate ligands leading to an activation of immunoinhibitory pathways on T-cells over their receptors PD-1, CTLA-4, TIM-3, and others<sup>30</sup>. This mechanism is a part of a natural tissue homeostasis. Upregulation of PD-L1 on tumor cells is induced by IFN- $\gamma$ , a cytokine mainly released by activated T-cells<sup>31</sup>.

In our study we evaluated the expression of PD-L1 (CD 274) on a tissue microarray of 1491 patient samples. Interestingly, we found that strong PD-L1 expression in MMR- proficient CRC was associated with early tumour stage, absence of lymph node metastases, lower tumour grade, absence of vascular invasion and a significantly improved 5-year overall survival. Additionally, we found a strong correlation with infiltration by CD8+ T cells, which were mostly PD-1neg. This was in agreement with a significant correlation of IFN- $\gamma$  and PD-L1 expression in the TME as measured by gene expression analysis. Therefore, activated CD8 infiltration in CRC specimens may partially contribute to the expression of PD-L1 on malignant cells as part of an ongoing immune response.

Our findings are in contrast to other studies for esophageal cancer and renal cancer where PD-L1 expression in cancer cells is associated with worse overall survival<sup>32,33</sup>, but similar to head and neck cancer where it is associated with a good prognosis<sup>34</sup>. Why do we see these discrepancies? The composition of the TME could be contributing to these findings. In head and neck cancer and colorectal cancer as well, there is a strong interplay of the immune system with the local microbiota<sup>35</sup>. In TME, where there is a high interaction with commensals it is crucial that tissue-regeneration processes are initiated rapidly. Therefore, signs of immune suppressive mechanisms may appear much earlier and could represent signs of an ongoing immune response against malignant cells.

There are now new antibodies in clinical trials which inhibit peripheral-immune-tolerance mechanism<sup>36</sup>. Peripheral immune tolerance is a process of tissue homeostasis where activated T-cells are suppressed through engagement of immune inhibitory receptors on healthy and specially tumor tissues. Ipilimumab anti CTLA-4 specific mAb is the first agent associated with an improved overall survival benefit in advanced melanoma. An important feature of CTLA-4 blockade is the durability of objective responses, leading to a possible cure for some advanced melanoma patients<sup>37</sup>. But, the CTLA-4 antibodies induce adverse side effects in approximately 64% of cases – mostly characterized by autoimmune reactions of different severity<sup>38</sup>. The side effects of PD-1/PD-L1 interaction blocking mAbs are much less pronounced, as proposed by the milder phenotype of PD-1 knockout mice<sup>30</sup>. Studies were performed to determine if ligand expression on tumour cells, PD-L1 in melanoma, could represent potential biomarkers predictive of response to treatment<sup>39</sup>. In this context our study showed that PD-L1 expression in CRC appeared to be restricted to an early tumor stage – therefore it could be speculated that treatment with a PD-L1 antibody could be of higher effectiveness in these stages than in the later stages where it is much more difficult to obtain a tumor response. Our data are in agreement with recent findings evaluating the response to anti-PD-L1 in different tumor types where no treatment response could be observed for CRC-patients<sup>40</sup>. In future, it will be necessary to study more patients and their corresponding pathology both before and after treatment with PD-L1 antibody.

As the PD-1/PD-L1 and CTLA-4-CD80 are only two immuno-checkpoints, others, such as TIM-3 and LAG-3 could be more specific for the TME and less associated with side effects in healthy tissue<sup>41</sup>. Additionally, breaking immune-tolerance mechanism could be helpful in combination immune-therapy as recently demonstrated in tumor-vaccination protocols<sup>42</sup>. Therefore more studies are necessary to not only understand better the clinical relevance of expression of immune-inhibitory checkpoints but effects related with their inhibition as well. New *in vitro* tools better representing the TME could help addressing these questions.

### **C. Microenvironment engineering through perfused tumor culture – moving to personalized medicine**

The TME is a complex structure and contributes significantly to patient survival. Standard *in vitro* culture conditions, where cancer cell lines are studied in plastic dishes and treatments are assessed for efficiency later *in vivo*, do not adequately represent the *in vivo* environment. Several studies have proposed that 3D tumor models may improve the efficiency of drug screening<sup>43–45</sup>. These models have still major limitations as other components like the ECM and interstitial non-malignant cells are not present. Depending on the tumor type, the TME varies from tumor to tumor. For example, in desmoplastic tumors, such as several carcinomas of the breast, stomach and pancreas, up to 90% or more of the total tumor mass consists of stroma. At the other extreme, there are tumors, such as medullary and lobular carcinomas of the breast and many lymphomas, in which only minimal stroma is deposited<sup>46</sup>.

Adding additional factors besides the tumor cells *in vitro*, exponentially increases the complexity of the system. High-throughput methods are needed for initial screenings, but improvements could be made by a second round of screening in more “physiological” *in vitro* models before going to *in vivo* models. There are several static 3D *in vitro* tumor models available consisting of either only cell line based (e.g. spheroids) approaches<sup>43,47</sup> or including natural or synthetic scaffold structures<sup>48,49</sup>. More complex models making use of tissue engineering techniques have been recently developed and were partially characterized in comparison to standard techniques and/or drug screening purposes<sup>50,51</sup>.

In our study we wanted to evaluate in depth a tissue engineered tumor model using a previously established u-tube-perfusion bioreactor<sup>52</sup>. By using established colorectal cancer cell lines, included in the NCI-60 cancer panel, we evaluated their ability to generate tumor-tissue-like structures in 3D statical or 3D perfused cultures using a collagen scaffold. Phenotype and functionality of tissue were compared to the xenografts obtained upon injection of the same cells in immunodeficient mice. In addition, the transcriptional profiles in the different culture conditions were compared with a next-generation-sequencing approach and pathway analysis was performed.

Perfused tumor cultures were much more effective in generating homogenous-tissue like structures similar to xenografts than 3D statical cultures. Comparing the expression of all exons throughout the genome, the highest correlation was observed between 3D perfused cultures and xenografts. Using standard chemotherapies we observed a higher resistance in 3D perfused tumor cultures as compared to standard cell cultures similarly to 5-Fluoruracil (5-FU) treated xenograft cells. Expression of genes regulating cell cycle, apoptosis and interaction with the TME from 3D perfused cells were similar to xenograft cultures. Expression of the anti-apoptotic gene Bcl-2 could represent a possible predictive marker for responses to neoadjuvant treatment in rectal cancer patients. Targeting BCL-2 with abt-199, a specific BCL-2 inhibitor, significantly reduced tumor cell number and increased apoptosis in the 3D perfused cultures compared to 2D cell cultures. We therefore concluded that this approach may be effective in patients with CRC where there is a limited response to 5-FU.

Our study on cancer cell lines, cultured in a perfused bioreactor, has similarities to the *in vivo* situation and may help discovering new chemotherapeutic resistance targets. As our model is easy to establish and tumor-tissue formation

quickly occurs, it may be a useful tool not only for drug screening purposes, but as a model to study fundamental biological questions *in vitro*.

Recent reviews on drug discovery have been claiming that after switching in the previous decade to target-based screening approaches, with limited success, the trend is now to shift back to tumor phenotype screenings, where treatments are evaluated based on the apoptosis or proliferation of tumor-tissue<sup>53,54</sup>. Therefore new models representing improved tumor-tissue structures *in vivo* are needed<sup>55</sup>. Tumor-tissue engineering, as we have shown in this study, may be used as a suitable approach where less animal studies would be needed.

In our review in *Advanced Drug Discovery* we discussed in depth *in vitro* 3D models for the examination of tumor-immune system interactions. The immune system contributes to the eradication of tumors as discussed and evaluated above. Standard *in vitro* cultures are based on co-incubation of immune cells on 2D cell layers of cancer cell lines. *In vivo* models fail to some extent in answering questions specifically addressing the role of the human immune system in cancer defense, as the human and murine immune systems differ significantly<sup>56</sup>. To circumvent these limitations *in vivo* a new humanized tumor mice model has been proposed, generated by concurrent transplantation of human hematopoietic stem cells (HSCs) and human breast cancer cells in neonatal NOD-scid IL2Rcnnull mice<sup>57</sup>. Still the model has its limitations and additional *in vitro* studies are necessary. Therefore, we recently started to explore the possibility to use our perfused 3D tumor model of CRC to study the migration potential of T cell subpopulation in a more physiological assay than the traditional Boyden chamber (Figure 2). An advantage of such a system would be to obtain beside quantitative measurements qualitative data related to cellular location and interactions within engineered tissues.

As studies on cancer cell lines have their limitations due to multiple mutations acquired over decades we ultimately wanted to evaluate our 3D perfused culture systems for primary tumor culture. The success rate of culturing primary tumors *in vitro* is limited, even though new techniques have been established<sup>58,59</sup>. Organoid cell culture induces growth of epithelial cells through Wnt-stimulators and is therefore able to sustain cancer tissue *in vitro* over long periods<sup>60</sup>. Stromal and other components of the TME are unable to survive. We therefore used tissue fragments, small pre-digested tumor pieces, for tissue culture under perfusion, to sustain the interaction between the interstitium and tumor cells. Interestingly, we were able to keep both the stromal and epithelial parts alive and proliferating for more than 20 days. The tumor-tissue was able to expand in the surrounding collagen scaffold. The use of perfusion was crucial as the tissue devoid of any nutrients (provided by the the flow apparatus) would degrade over time. As the rate of proliferation of the commensals expand faster under perfusion than the tissue itself, meticulous dissecting of the tissue-chunks combined with antibiotics was required. Growth of the cultures resulted in an efficiency of over 60%, including samples with contamination by the local microbiota. If we excluded these samples we obtained a growth success rate of 13 out of 15 tumor samples (87%).

Interestingly we found that the use of the patient's serum was crucial for tissue survival. Fetal calf serum led to very little tissue growth which was mostly of epithelial origin, whereas with human serum we could obtain much larger tissue constructs. Nevertheless, the best tissue-formation capacity we observed was through the use of patient-derived plasma added to the tissue culture medium. However, as it is difficult to obtain blood samples together with tumor tissue, we used pooled human sera for

perfusion of the primary tumor culture. Additives, such as prostaglandin E2 and epidermal growth factor, further improved tissue formation in our cultures as these factors had been previously demonstrated to be effective in chicken embryo intestinal organoid cultures<sup>61</sup>.

As we could successfully culture the initial components of the tumor tissue *in vitro* our goal was to study drug treatments on these cultures with the ultimate goal of providing a tool for drug screening on primary cultures. This might lead to innovative personalized medicine approaches similar to chemograms and antibiograms which are widely used in clinics to evaluate antibiotic efficiency on bacterial strains<sup>62</sup>. It remains to be proven if such *in vitro* screenings could predict the *in vivo* TME.

## Perspectives

As some of these projects have led to additional questions concerning the engineering and TME of colorectal cancer, as well as other tumors, I will present a short summary of future studies. As we previously demonstrated, neutrophilic subpopulations, as characterized by MPO+HLA-DR-CD15+CD16+CD66b, can contribute significantly to the overall survival of colorectal patients. Future studies will aim to elucidate the mechanisms underlying our findings. In addition, future studies will aim to clarify the mechanisms supporting the attraction of neutrophils and/or to modify residual tissue neutrophils towards an anti-tumoral phenotype. It is hoped that these studies will lead to a better understanding of key factors of the immune system in its interaction with cancer.

On the other hand, peripheral tolerance towards tumor cells is widely considered to influence clinical outcome in cancer patients. PD-L1 ligand expression in CRC patients was correlated with overall patient survival and CD8 infiltration. Few CD8-T-cells were positive for the corresponding receptor PD-1. This could help to distinguish tumor reactive T-cells from unspecific T-cells. Nowadays, there are only few tumor-specific TCRs known, which could be of use to transduce T-cells to target specifically tumor tissue<sup>63</sup>. In collaboration with Ton Schumacher's lab in Amsterdam, we are currently evaluating if single cell sorting of T-cells from the TME of CRC-patients and RT-PCR amplification of the TCR-sequence can help to identify additional tumor-specific TCR. Based on our study, we would sort PD-1+ and PD-1-CD8 cells and evaluate the population with the highest tumor specificity. From our data and other studies we speculate to find tumor reactive T-cells in the PD-1+ cell population<sup>64</sup>. This work could help to develop a protocol for individualized TCR-engineering and adoptive therapy.

As we have previously demonstrated, our engineered *in vitro* tumor model closely mirrors morphology, functions and transcriptional activities xenografts and that we are currently using it to evaluate tumor immune interactions. Therefore, we are trying to use this model to engineer tumor tissue with resident lymphocyte populations and to study the attraction of other immune cell populations through their activation. Compared to only quantitative read-outs from traditional *in vitro* migration assays like the Boyden chamber, we are able to additionally visualize the interaction in the tumor tissue itself by histological evaluation.

Furthermore, the similarities of our *in vitro* tumor tissue upon standard drug treatments and the induction of resistance mechanisms suggest that it might represent a suitable tool for drug screening purposes. In addition, our primary tumor cultures from CRC specimens could be used for individualized drug screenings as discussed above.

We are currently evaluating whether our culture technique could be used for other tumor types like Breast-Carcinoma, Glioblastoma, Sarcoma and Melanoma.

## References Discussion and Conclusions, Perspectives

1. Zamai, L. *et al.* NK cells and cancer. *J. Immunol.* **178**, 4011–6 (2007).
2. Sconocchia, G. *et al.* Tumor infiltration by FcγRIII (CD16)+ myeloid cells is associated with improved survival in patients with colorectal carcinoma. *Int. J. Cancer* **128**, 2663–72 (2011).
3. Zlobec, I. *et al.* TIA-1 cytotoxic granule-associated RNA binding protein improves the prognostic performance of CD8 in mismatch repair-proficient colorectal cancer. *PLoS One* **5**, e14282 (2010).
4. Marigo, I., Dolcetti, L., Serafini, P., Zanovello, P. & Bronte, V. Tumor-induced tolerance and immune suppression by myeloid derived suppressor cells. *Immunol. Rev.* **222**, 162–79 (2008).
5. Talmadge, J. E. & Gabrilovich, D. I. History of myeloid-derived suppressor cells. *Nat. Rev. Cancer* **13**, 739–52 (2013).
6. Yang, W.-C., Ma, G., Chen, S.-H. & Pan, P.-Y. Polarization and reprogramming of myeloid-derived suppressor cells. *J. Mol. Cell Biol.* **5**, 207–9 (2013).
7. Gregory, A. D. & Houghton, A. M. Tumor-associated neutrophils: new targets for cancer therapy. *Cancer Res.* **71**, 2411–6 (2011).
8. Nathan, C. Neutrophils and immunity: challenges and opportunities. *Nat. Rev. Immunol.* **6**, 173–82 (2006).
9. Rao, H.-L. *et al.* Increased intratumoral neutrophil in colorectal carcinomas correlates closely with malignant phenotype and predicts patients' adverse prognosis. *PLoS One* **7**, e30806 (2012).
10. Rao, H.-L. *et al.* Increased intratumoral neutrophil in colorectal carcinomas correlates closely with malignant phenotype and predicts patients' adverse prognosis. *PLoS One* **7**, e30806 (2012).
11. Mantovani, A., Cassatella, M. A., Costantini, C. & Jaillon, S. Neutrophils in the activation and regulation of innate and adaptive immunity. *Nat. Rev. Immunol.* **11**, 519–31 (2011).
12. Fridlender, Z. G. *et al.* Polarization of tumor-associated neutrophil phenotype by TGF-beta: "N1" versus "N2" TAN. *Cancer Cell* **16**, 183–94 (2009).
13. Wang, K. *et al.* Inhibition of neutrophil apoptosis by type 1 IFN depends on cross-talk between phosphoinositol 3-kinase, protein kinase C-delta, and NF-kappa B signaling pathways. *J. Immunol.* **171**, 1035–41 (2003).
14. Fridlender, Z. G. & Albelda, S. M. Tumor-associated neutrophils: friend or foe? *Carcinogenesis* **33**, 949–55 (2012).
15. Pelletier, M. *et al.* Evidence for a cross-talk between human neutrophils and Th17 cells. *Blood* **115**, 335–43 (2010).

16. Lewkowicz, N., Klink, M., Mycko, M. P. & Lewkowicz, P. Neutrophil-CD4+CD25+ T regulatory cell interactions: a possible new mechanism of infectious tolerance. *Immunobiology* **218**, 455–64 (2013).
17. Lefkowitz, D. L. & Lefkowitz, S. S. Macrophage-neutrophil interaction: a paradigm for chronic inflammation revisited. *Immunol. Cell Biol.* **79**, 502–6 (2001).
18. Silva, M. T. When two is better than one: macrophages and neutrophils work in concert in innate immunity as complementary and cooperative partners of a myeloid phagocyte system. *J. Leukoc. Biol.* **87**, 93–106 (2009).
19. Kanther, M. *et al.* Commensal microbiota stimulate systemic neutrophil migration through induction of Serum amyloid A. *Cell. Microbiol.* (2013). doi:10.1111/cmi.12257
20. Castellarin, M. *et al.* Fusobacterium nucleatum infection is prevalent in human colorectal carcinoma. *Genome Res.* **22**, 299–306 (2012).
21. Kostic, A. D. *et al.* Genomic analysis identifies association of Fusobacterium with colorectal carcinoma. *Genome Res.* **22**, 292–8 (2012).
22. Trellakis, S. *et al.* Polymorphonuclear granulocytes in human head and neck cancer: enhanced inflammatory activity, modulation by cancer cells and expansion in advanced disease. *Int. J. Cancer* **129**, 2183–93 (2011).
23. Dunn, G. P., Old, L. J. & Schreiber, R. D. The three Es of cancer immunoediting. *Annu. Rev. Immunol.* **22**, 329–60 (2004).
24. Yang, L. TGFβ, a potent regulator of tumor microenvironment and host immune response, implication for therapy. *Curr. Mol. Med.* **10**, 374–80 (2010).
25. Yoshimura, A. & Muto, G. TGF-β function in immune suppression. *Curr. Top. Microbiol. Immunol.* **350**, 127–47 (2011).
26. Curiel, T. J. *et al.* Specific recruitment of regulatory T cells in ovarian carcinoma fosters immune privilege and predicts reduced survival. *Nat. Med.* **10**, 942–9 (2004).
27. Beyer, M. & Schultze, J. L. Regulatory T cells in cancer. *Blood* **108**, 804–11 (2006).
28. Shurin, M. R., Lu, L., Kalinski, P., Stewart-Akers, A. M. & Lotze, M. T. Th1/Th2 balance in cancer, transplantation and pregnancy. *Springer Semin. Immunopathol.* **21**, 339–359 (1999).
29. Hicklin, D. J., Marincola, F. M. & Ferrone, S. HLA class I antigen downregulation in human cancers: T-cell immunotherapy revives an old story. *Mol. Med. Today* **5**, 178–186 (1999).
30. Pardoll, D. M. The blockade of immune checkpoints in cancer immunotherapy. *Nat. Rev. Cancer* **12**, 252–64 (2012).
31. Spranger, S. *et al.* Up-regulation of PD-L1, IDO, and T(regs) in the melanoma tumor microenvironment is driven by CD8(+) T cells. *Sci. Transl. Med.* **5**, 200ra116 (2013).

32. Thompson, R. H. *et al.* Costimulatory B7-H1 in renal cell carcinoma patients: Indicator of tumor aggressiveness and potential therapeutic target. *Proc. Natl. Acad. Sci. U. S. A.* **101**, 17174–9 (2004).
33. Ohigashi, Y. *et al.* Clinical significance of programmed death-1 ligand-1 and programmed death-1 ligand-2 expression in human esophageal cancer. *Clin. Cancer Res.* **11**, 2947–53 (2005).
34. Lyford-Pike, S. *et al.* Evidence for a role of the PD-1:PD-L1 pathway in immune resistance of HPV-associated head and neck squamous cell carcinoma. *Cancer Res.* **73**, 1733–41 (2013).
35. Belkaid, Y. & Naik, S. Compartmentalized and systemic control of tissue immunity by commensals. *Nat. Immunol.* **14**, 646–53 (2013).
36. Callahan, M. K. & Wolchok, J. D. At the bedside: CTLA-4- and PD-1-blocking antibodies in cancer immunotherapy. *J. Leukoc. Biol.* **94**, 41–53 (2013).
37. Ott, P. A., Hodi, F. S. & Robert, C. CTLA-4 and PD-1/PD-L1 blockade: new immunotherapeutic modalities with durable clinical benefit in melanoma patients. *Clin. Cancer Res.* **19**, 5300–9 (2013).
38. Voskens, C. J. *et al.* The price of tumor control: an analysis of rare side effects of anti-CTLA-4 therapy in metastatic melanoma from the ipilimumab network. *PLoS One* **8**, e53745 (2013).
39. Topalian, S. L. *et al.* Safety, activity, and immune correlates of anti-PD-1 antibody in cancer. *N. Engl. J. Med.* **366**, 2443–54 (2012).
40. Brahmer, J. R. *et al.* Safety and activity of anti-PD-L1 antibody in patients with advanced cancer. *N. Engl. J. Med.* **366**, 2455–65 (2012).
41. Sakuishi, K. *et al.* Targeting Tim-3 and PD-1 pathways to reverse T cell exhaustion and restore anti-tumor immunity. *J. Exp. Med.* **207**, 2187–94 (2010).
42. Duraiswamy, J., Kaluza, K. M., Freeman, G. J. & Coukos, G. Dual blockade of PD-1 and CTLA-4 combined with tumor vaccine effectively restores T-cell rejection function in tumors. *Cancer Res.* **73**, 3591–603 (2013).
43. Friedrich, J., Seidel, C., Ebner, R. & Kunz-Schughart, L. a. Spheroid-based drug screen: considerations and practical approach. *Nat. Protoc.* **4**, 309–24 (2009).
44. Lee, J. M. *et al.* A three-dimensional microenvironment alters protein expression and chemosensitivity of epithelial ovarian cancer cells in vitro. *Lab. Invest.* **93**, 528–42 (2013).
45. Begley, C. G. & Ellis, L. M. Drug development: Raise standards for preclinical cancer research. *Nature* **483**, 531–3 (2012).
46. Tumor Structure and Tumor Stroma Generation. (2003). at <<http://www.ncbi.nlm.nih.gov/books/NBK13447/>>

47. Hirschhaeuser, F. *et al.* Multicellular tumor spheroids: an underestimated tool is catching up again. *J. Biotechnol.* **148**, 3–15 (2010).
48. Fischbach, C. *et al.* Engineering tumors with 3D scaffolds. *Nat. Methods* **4**, 855–60 (2007).
49. Chen, L. *et al.* The enhancement of cancer stem cell properties of MCF-7 cells in 3D collagen scaffolds for modeling of cancer and anti-cancer drugs. *Biomaterials* **33**, 1437–44 (2012).
50. Ma, L. *et al.* Towards personalized medicine with a three-dimensional micro-scale perfusion-based two-chamber tissue model system. *Biomaterials* **33**, 4353–61 (2012).
51. Wen, Y., Zhang, X. & Yang, S.-T. Microplate-reader compatible perfusion microbio reactor array for modular tissue culture and cytotoxicity assays. *Biotechnol. Prog.* **26**, 1135–44
52. Wendt, D., Marsano, A., Jakob, M., Heberer, M. & Martin, I. Oscillating perfusion of cell suspensions through three-dimensional scaffolds enhances cell seeding efficiency and uniformity. *Biotechnol. Bioeng.* **84**, 205–14 (2003).
53. Barretina, J. *et al.* The Cancer Cell Line Encyclopedia enables predictive modelling of anticancer drug sensitivity. *Nature* **483**, 603–7 (2012).
54. Swinney, D. C. & Anthony, J. How were new medicines discovered? *Nat. Rev. Drug Discov.* **10**, 507–19 (2011).
55. Laggner, C. *et al.* Chemical informatics and target identification in a zebrafish phenotypic screen. *Nat. Chem. Biol.* **8**, 144–6 (2012).
56. Mestas, J. & Hughes, C. C. W. Of mice and not men: differences between mouse and human immunology. *J. Immunol.* **172**, 2731–8 (2004).
57. Wege, A. K. *et al.* Humanized tumor mice--a new model to study and manipulate the immune response in advanced cancer therapy. *Int. J. Cancer* **129**, 2194–206 (2011).
58. Masters, J. R. Human cancer cell lines: fact and fantasy. *Nat. Rev. Mol. Cell Biol.* **1**, 233–6 (2000).
59. Kondo, J. *et al.* Retaining cell-cell contact enables preparation and culture of spheroids composed of pure primary cancer cells from colorectal cancer. *Proc. Natl. Acad. Sci. U. S. A.* **108**, 6235–40 (2011).
60. Sato, T. *et al.* Long-term Expansion of Epithelial Organoids From Human Colon, Adenoma, Adenocarcinoma, and Barrett's Epithelium. *Gastroenterology* **141**, 1762–1772 (2011).
61. Pierzchalska, M., Grabacka, M., Michalik, M., Zyla, K. & Pierzchalski, P. Prostaglandin E2 supports growth of chicken embryo intestinal organoids in Matrigel matrix. *Biotechniques* **52**, 307–15 (2012).

62. Boehme, M. S., Somsel, P. A. & Downes, F. P. Systematic review of antibiograms: A National Laboratory System approach for improving antimicrobial susceptibility testing practices in Michigan. *Public Health Rep.* **125 Suppl** , 63–72
63. Restifo, N. P., Dudley, M. E. & Rosenberg, S. A. Adoptive immunotherapy for cancer: harnessing the T cell response. *Nat. Rev. Immunol.* **12**, 269–81 (2012).
64. Inozume, T. *et al.* Selection of CD8+PD-1+ lymphocytes in fresh human melanomas enriches for tumor-reactive T cells. *J. Immunother.* **33**, 956–64